P-glycoprotein transport cycle: 'cross-talk' between multiple binding sites and the catalytic domains

Thesis

UNRESTRICTED.

P-glycoprotein transport cycle: 'cross-talk' between multiple binding sites and the catalytic domains

Submitted by

Catherine Anne Martin (B.Sc., M.Sc.)

In fulfilment of the requirements for the degree of

Doctor of Philosophy

in

Biochemical Pharmacology

submitted July 23rd, 2001

The Open University,
Institute of Molecular Medicine,
University of Oxford,
John Radcliffe Hospital,
Oxford.

ProQuest LLC.
789 East Eisenhower Parkway
P.O. Box 1346
Ann Arbor, MI 48106 – 1346

Abstract

Elucidation of the mechanism by which P-gp can interact with multiple drugs, and harness the energy from hydrolysis of ATP to mediate transbilayer movement of drug, has been the goal of this thesis. Using radioligand binding studies, four distinct binding sites for drug have been identified on P-gp, explaining the molecular basis of its broad 'substrate' specificity. Two of the sites have been classified as transport sites and have been assigned the sites of interaction for vinblastine and paclitaxel respectively. A third site identified was capable of binding both drugs that are transported (Hoechst 33342) by P-gp, and those that are modulatory only (XR9576 and XR9051). The fourth binding site has been classified as a modulatory site, and has been assigned to the modulators nicardipine and GF120918. The existence of a negative heterotropic allosteric network between the sites, suggests that P-gp does not simultaneously bind multiple drugs. In order for transport of drug to occur, the drug binding site must undergo 're-orientation', switching from a high to a low affinity conformation. This transition must be associated with ATP hydrolysis, given the ATP dependency of P-gp transport function. Therefore, binding of vinblastine was measured at discrete steps of the catalytic cycle of P-gp, to ascertain when changes are wrought on the drug binding site. Binding of ATP, prior to hydrolysis, triggered a shift in the high affinity site to a single class of low affinity site. The low affinity conformation for the vinblastine binding site persisted immediately post-hydrolysis of nucleotide. Release of Pi from the P-gp.Mg.ADP.Pi complex, fully restored the drug binding site to high affinity once more. This has provided the first evidence to show that the binding of ATP is sufficient to instigate a transport event. Hydrolysis of ATP is most likely necessary to restore the drug binding site to high affinity in order to complete a transport cycle.

Dedication

I dedicate this work to working mothers and their daughters.

The greater the obstacle, the more glory there is in over-coming it.

Molière

Acknowledgements

This has been the most daunting page to compose of the entire thesis. I am deeply indebted to so many people for their willing assistance, generous contributions and unstinting support in making this thesis come to fruition. Apologies in advance for omissions that are bound to happen...

...To Dr. Callaghan, my director of studies and mentor, despite the unorthodoxy of your ways, I have over the years come to realise that there is method there!! Thank you for your constant encouragement, endless patience and for the inspiration imparted by your 'gritty, no nonsense, go out there and just do it' approach to science.

Thanks also to Chris Higgins, who first provided me with the opportunity to work in Oxford all those years ago, for withstanding 'flippant quips' and for his continued input and interest in my research.

A very special thank you is due to George, my much missed colleague and original member of the Callaghan crew, for her friendship and also her generous help, both intellectually and technically, over the years with many aspects of this thesis.

All of my colleagues both past; Gail, Rits, Kenny, Driver, Farmhouse, Tshepo, Blotty and present; Taylor, Kerry, Janet, Rothers, Shells, Alison, Szabolcs and my fellow 'brother in Arms' Marco, have been a constant source of provocation, fun and stimulation, making the good times possible and the bad days better. Thank you to all the other staff and students within the department, for creating a fun environment in which to work.

Special mention is due to Café Direct for providing much needed respite, sustenance, and excuses for early morning exchange of ideas; to my CD player for getting me through those long hours of writing in the loft and to Arthur Guinness for inspiring many interesting 'collaborative' projects over the years!!

To Meister for kindly proof-reading my thesis and yes, dinner is on the cards.

Many thanks to the Cancer Research Campaign who have generously funded the research reported in this thesis. I am grateful also to Ruth Peat & Co at the ICRF Tissue Culture Facility, Clare Hall Laboratories for the weekly supply of the cells used in this thesis. Thanks also to Xenova Ltd., for donation of many of the drugs used in this work.

And last but not least my family.....

To Mother and Dad, my heartfelt thanks to you both for the sacrifices you made to get me to where I am today.

Gearoid, your encouragement and support throughout, has always been there in plenty, thank you.

But most of all I want to say to my daughters Clíona and Maeve, that although Mummy has at times been consumed by her work, you have always been uppermost in my thoughts. I hope my endeavours will inspire you both in the future.

Table of contents

Chapter 1

Chapter 2

Chapter 3

Chapter 4

Chapter 5

Chapter 6

Appendices

List of figures

Chapter 1

Chapter 3

Chapter 4

Chapter 5

Chapter 6

List of tables

Chapter 1

Chapter 3

Chapter 4

Chapter 5

Abbreviations

[^{125}I]-IAAP	*[^{125}I]-iodoarylazidoprazosin*
[^{125}I]-INA	*5-[^{125}I]-iodonaphthalene-1-azide*
ABC	*ATP Binding Cassette*
ALDP	*adrenoleukodydstrophy*
AM	*acetoxy-methyl*
AMP-PNP	*5'-adenylimidodiphosphate*
ASM	*alanine-scanning mutagenesis*
ATP-γ-S	adenosine 5'-O-(3-thiotriphosphate)
CFTR	*Cystic fibrosis transmembrane conductance regulator*
CsA	*cyclosporin A*
CSM	*cysteine-scanning mutagenesis*
dBBn	*dibromobimane*
DR	dose ratio
F.R.E.T.	*fluorescence resonance energy transfer*
GF120918	*(N-{4-[2-(1,2,3,4-tetrahydro-6,7-dimethoxy-2-isoquinolinyl)-ethyl]-phenyl}-9,10-dihydro-5-methoxy-9-oxo-4-acridine carboximide)*
HisP	*nucleotide binding subunit of Histidine Permease transporter in prokaryotes*
k_{cat}	*turnover number for an enzyme*
Kir	*potassium inwardly rectifying channel*
LmrA	*multidrug resistance transporter of Lactococcus. lactis*
LRP	*lung resistance protein*
MalK	*nucleotide binding subunit of the prokaryotic maltose transporter*
MDR	*multidrug resistance*
MIANS	*2-(4-maleimidoanilino)naphthalene-6-sulfonic acid*
MRP	*multidrug resistance associated protein*
NBD	*nucleotide binding domain*
NBD-C6-HPC	*2-[6-(7-nitrobenzo-2-oxa-1,3-diazol-4-yl)amino]hexanoyl-sn-lycero-3-phosphocholine*

NBD-Cl	*7-chloro-4-nitrobenzo-2-Oxa-1,3-Diazole*
NEM	*N-ethylmaleimide*
nsb	*non-specific binding*
PC	*phosphatidylcholine*
PE	*phosphatidylethanolamine*
P-gp	*P-glycoprotein*
pH_i	*intracellular pH*
SUR	*sulfonylurea receptor*
TAP	*transporter associated with antigen presentation*
TM	*transmembrane*
TMD	*transmembrane domain*
TMR	*tetramethylrosamine*
Vi	*vanadate ion*
XR9051	*(N-(4-(2-(6,7-Dimethoxy-1,2,3,4,-tetrahydro-2-isoquinoyl)ethyl)phenyl)-3-((3Z,6Z)-6-benzylidene-1-methyl-2,5-dioxo-3-piperazinylidene) methylbenzamide)*
XR9576	*Quinoline-3-carboxylic acid (2-{4-[2-(6,7-dimethoxy-3,4-dihydro-1H-isoquinolin-2-yl)-ethyl]-phenylcarbamoyl}-4,5-dimethoxy-phenyl)-amide*

Chapter 1

General Introduction

1.1 Cancer chemotherapy

Chemotherapy as a treatment modality in cancer has been in use since 1942 when nitrogen mustard was first administered to a lymphoma patient. The goal of this anticancer treatment strategy is to use cytotoxic drugs to target rapidly proliferating cells, thereby arresting tumour growth and metastasis. Malignancies of the type presented in Hodgkin's disease, acute myeloid leukaemia in children and testicular cancer have been particularly amenable to treatment and cure using chemotherapeutic regimens. However, chemotherapy is quite often used as an adjuvant treatment being administered in conjunction with surgery and radiotherapy, or as a palliative measure in advanced cancers.

There has been a rapid expansion in the range of anticancer agents used in the treatment of cancer and in most cases many have been designed to work around the cell cycle. Anticancer agents are broadly classified according to their *modus operandi* as summarised in figure 1.1. Alkylating agents such as nitrogen mustards and cyclophosphamide generate highly reactive positively charged intermediates that form cross-links with nucleophilic groups on biological molecules, particularly the nucleotide bases of DNA. Drugs of this class have been shown to be maximally effective as cells proceed from G2 phase of cell cycle to mitosis, and at the transition from G1 to S-phase, or the DNA synthesis stage of the cell cycle. The antimetabolites are anticancer drugs that block DNA synthesis. Antimetabolites such as the purine analogue 5-fluorouracil do so through a direct interaction. On the other hand, the folic acid analogue methotrexate indirectly affects DNA synthesis through competitive inhibition of the enzyme dihydrofolate reductase, which is required in the conversion of dUMP to dTMP and in the synthesis of purines. Drugs in this category are cell cycle specific and are most active against cells in S-phase. A third classification incorporates agents that disrupt

microtubule function. These include the vinca alkaloids e.g vinblastine, also classified as natural product cytotoxics, which bind to tubulin and prevent microtubule formation thus interfering with mitosis. These agents have been shown to be most efficacious during the S-phase of the cell cycle as microtubule formation may be initiated at this stage. Taxanes, e.g. paclitaxel, also bind tubulin but at an alternative site to the vinca alkaloids resulting in stabilisation of microtubules formed and disruption of mitosis. There are also a number of anticancer drugs (many of them natural product compounds) that specifically target different aspects of the DNA replication process. For instance, camptothecin inhibits topoisomerase I activity. Topoisomerase II activity is blocked by the epipodophylotoxin etoposide which first results in single and then double strand breaks thus blocking DNA replication. These agents are specific to cells within S-phase.

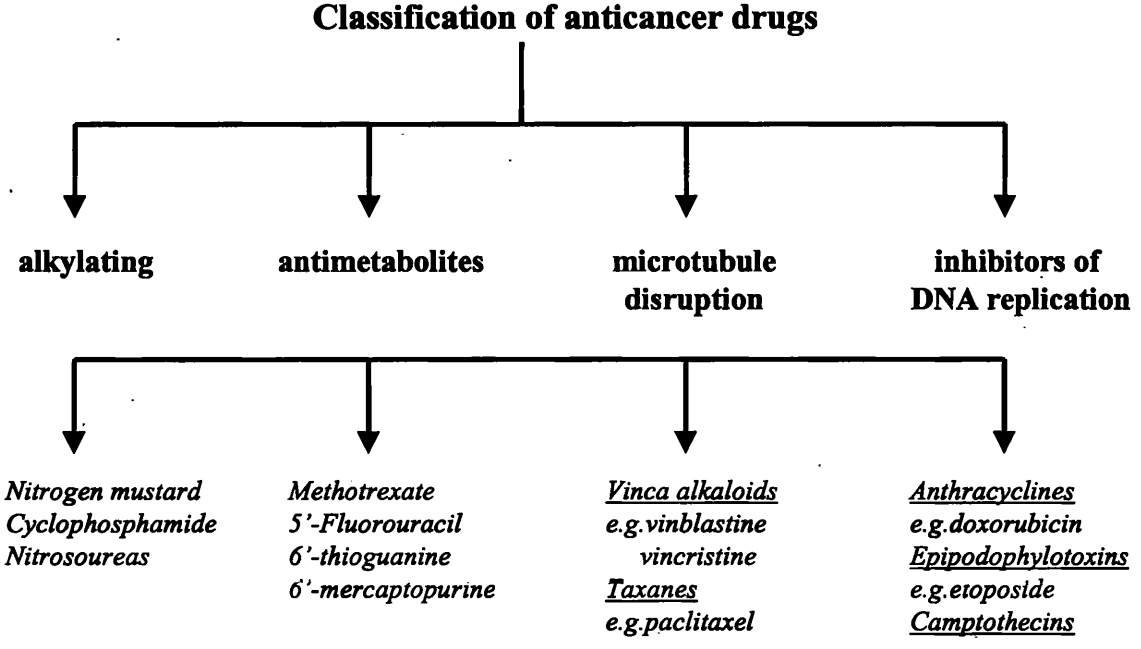

Figure 1.1 Classification of anticancer agents commonly used in chemotherapy

1.2 Drug resistance in cancer chemotherapy

A significant problem associated with using chemotherapy in the treatment of cancer is the resistance of tumour cells to the anticancer agents administered. Resistance of

cancers to cytotoxic drug can be classified as *unicellular* or *multicellular*. *Unicellular* resistance arises from mechanisms within individual tumour cells that prevent anticancer agents from effecting their cytotoxic action. *Multicellular* resistance is a phenomenon often associated with tumour populations because of the physical barrier posed by the three-dimensional arrangement of cells and the heterogeneity of layers that comprise a tumour mass. Some malignancies (e.g. colorectal and renal) are constitutively resistant to chemotherapeutic drugs during the first treatment course and are described as having *intrinsic* resistance to chemotherapy. Other cancers that respond initially to treatment with cytotoxics, but later develop resistance to anticancer agents, are said to have *acquired* resistance, as is the case in leukaemias, lymphomas, myeloma and breast and ovarian carcinomas (133).

1.2.1 Mechanisms of unicellular drug resistance

There are many ways by which cells can impede the efficacy of anticancer agents as outlined in figure 1.2. Cellular mechanisms leading to drug resistance are varied and include decreased uptake mechanisms, increased drug metabolism pathways, increase in DNA repair systems, reduced activation of drug and increased drug efflux processes (68). Some of these mechanisms, for example efflux pumps and altered topoisomerase II activity, can mediate cross-resistance to a variety of chemically and functionally different anticancer drugs. Cross-resistance of tumours to cytotoxics mediated by drug efflux pumps has been recognised as an important mechanism impeding chemotherapeutic efficacy in the clinic. A number of efflux pumps have been identified as mediators of resistance to a variety of anticancer agents. These proteins include P-glycoprotein (P-gp) or MDR1, Multidrug Associated Protein (MRP) and Lung Resistance Protein (LRP). P-glycoprotein (P-gp) is the most extensively studied of the efflux pumps and at present

there is more evidence supporting a role for P-gp in drug resistance in cancer chemotherapy than either MRP or LRP.

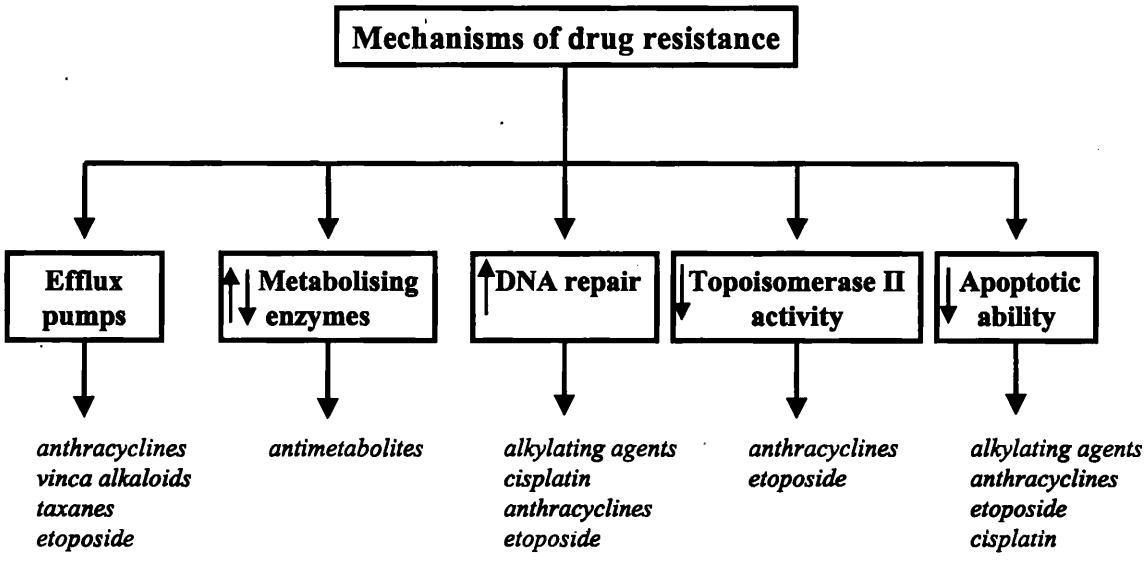

Figure 1.2 Different mechanisms by which tumour cells develop resistance to anticancer drugs

1.3 P-gp and the MDR phenomenon

To understand the role of efflux mechanisms in mediating resistance to chemotherapy, numerous *in vitro* studies were conducted in the late 1970s in cell lines that were grown in the presence of increasing concentrations of a single cytotoxic agent. A common feature of these cells was cross-resistance to a broad spectrum of dissimilar drugs with distinct cellular targets. Some of these agents included commonly used chemotherapeutic agents such as the vinca alkaloids and anthracyclines. Initial analysis of resistant cell lines revealed over-expression of a 170-180KDa membrane glycoprotein termed P-glycoprotein, as identified by Juliano and Ling (59). It was soon established that over-expression of P-glycoprotein was associated with an ATP-dependent decrease in the accumulation of a range of cytotoxics. This was thought to be due to an increase in drug efflux rates rather than a decrease in drug uptake. Although it appeared that P-gp was capable of transporting a diverse range of drugs, they all shared common physico

chemical features such as lipophilicity, the presence of a complex ring structure and a positively charged nitrogen group (refer to table 1.1). The term multi-drug resistance (MDR) has been devised to describe the resistance phenomenon attributable to P-gp.

Table 1.1 Compounds involved in P-gp mediated MDR and other ligands for P-gp transport

Physico-chemical properties of P-gp ligands	
Lipophilic weak bases	***Neutral polycyclic compounds***
Doxorubicin	paclitaxel
vinblastine	colchicine
verapamil	progesterone
nicardipine	***Amphiphiles***
trifluoperazine	Triton-X-100
tamoxifen	***Hydrophobic peptides***
Lipophilic cations	Gramicidin C
Rhodamine 123	valinomycin
Hoechst 33342	Cyclosporin A
	PSC 833

1.3.1 Relevance of P-gp to the clinical resistance problem

Despite evidence from studies conducted with drug resistant cell lines, there has been considerable debate over the precise contribution of P-gp to the clinical problem of cross-resistance, due primarily to difficulties experienced in relating resistance levels in tumours to P-gp expression (for detailed review (13)). In more recent years better detection methods have allowed quantitation of the proportion of P-gp positive cells in clinical samples. High levels of P-gp expression have been associated with tumours derived from tissues that normally express P-gp. These included tumours of adrenal glands, colon, kidney, liver and acute myelogenous lymphoma. There are now numerous studies that have showed a direct correlation between P-gp expression and prognostic outcome in chemotherapy (14, 112, 160). Other studies of patients with multiple myeloma have demonstrated high levels of P-gp expression thought to be specifically related to drug resistance (136, 149) and another which showed that P-gp

expression is frequently acquired following exposure to chemotherapeutic agents such as vincristine and doxorubicin (43).

1.3.2 Reversal of MDR through blockade of P-gp activity

One of the approaches adopted to circumvent the clinical problem posed by P-gp mediated multidrug resistance has been the development of inhibitors of drug efflux. This approach made use of P-gp's broad ligand specificity and involved co-administration of known pharmacological agents, which might block P-gp anticancer drug efflux activity, in combination with cytotoxic drugs in the hope that this would re-sensitise resistant cells. Early screening for potential reversal agents involved *in vitro* cytotoxicity assays, conducted in cell lines that over-expressed P-gp and displayed high levels of resistance to many different types of chemotherapeutic agents. The efficacy of a range of known pharmacological agents to inhibit P-gp transport activity was assessed by looking at the increased ability of cytotoxics to kill cells over-expressing P-gp. A diverse range of structurally and functionally distinct compounds, capable of reversing P-gp mediated MDR, was identified in these kinds of assays and have been termed chemosensitisers or modulators. These include calcium channel blockers (verapamil, nifedipine), calmodulin antagonists, steroids such as progesterone and immunosuppressive agents such as cyclosporin A (refer to table 1.2). The mechanism(s) underlying the ability of such a diverse range of functionally distinct compounds to block the efflux activity of P-gp is not understood. However, given the broad range of reversal agents identified it is quite probable that various aspects of P-gp function are targeted.

Some of these early reversal agents, also termed first generation, did enter phase I clinical trials to assess maximum dosages tolerated and to investigate the pharmacokinetics of drug behaviour when added in combination with anticancer agents

in humans. What emerged was that most of the reversal agents could not be administered in doses high enough to resensitise cells due to toxic side effects associated with their administration. For instance, verapamil was identified by Tsuro *et al.* (143) and was the first modulatory compound to be used in the clinic. However, it was not possible to administer verapamil at doses high enough to bring about complete reversal of MDR because of the level of cardiac toxicity associated with its administration (9, 23).

In light of the toxicities associated with administration of first generation modulators, a second generation of reversal agent was developed in which many of the compounds that emerged were analogues of the first generation modulatory compounds, but lacked the normal cellular role of the parent compound. For example, SDZ PSC833 is an analogue of cyclosporin A but lacks immunosuppressive activity, rendering its administration less toxic (10). It is currently undergoing clinical evaluation in phase I and II trials (11, 31). Many of these newer second generation agents were efficacious in the low micro-molar range and displayed fewer limiting side-effects.

However, application of modulators such as dexverapamil and PSC 833 to the reversal of MDR in the clinic has also been limited due to their effect on the pharmacokinetics of cytotoxics, e.g. paclitaxel, leading to increases in toxicity and necessitating reduction in the dose of cytotoxic drug administered (32, 107). Since the first and second generation reversal agents have not been specifically designed to reverse P-gp mediated MDR, a third generation of modulator compound has emerged. This generation of agent was born from systematic modifications of prototype MDR inhibitors in medicinal chemistry programmes, in the hope of developing greater selectivity for P-gp. One of the first compounds to emerge from such programmes was the acridone-carboxamide derivative GF120918 (GG918). This compound was shown to potently re-sensitise

Table 1.2 Compounds used to resensitise MDR cells through inhibition of P-gp

Modulator	*Chemical class*	*Pharmacological role*	*Reference*
1st Generation			
verapamil	*phenylalkylamine*	Ca^{2+} channel blocker	Tsuro *et al.*, 1981
nicardipine	*1,4 dihydropyridine*	Ca^{2+} antagonist	Tsuro *et al.*, 1983
trifluoperazine		calmodulin antagonist	Ford *et al.*, 1989
Cyclosporin A	*cyclic peptide*	immunosuppressive	Spoelstra *et al.*, 1991
2nd Generation			
dexverapamil	*R-enantiomer of verapamil*		Nawrath & Raschack (1997)
PSC 833	*analogue of cyclosporin A*		Watanabe *et al.*, 1996
3rd Generation			
LY 335979	*cyclopropyldibenzosuberone*	P-gp inhibition	Dantzig *et al.*, 1996
GF120918	*acridonecarboxamide*	P-gp inhibition	Hyafil *et al.*, 1993
XR9051	*diketopiperazine*	P-gp inhibition	Dale *et al.*, 1998
XR9576	*anthranilic acid*	P-gp inhibition	Mistry *et al.*, 1998

(EC_{50} = 0.02μM) the P-gp positive cell lines $CH^{r}C5$, OV1/DXR and MCF7/ADR to the cytotoxics doxorubicin and vincristine. GF120918 also effectively restored *in vivo* sensitivity to doxorubicin in a mouse model where mice were implanted with MDR P388/DOX tumour cells (57). Cells from acute myeloid leukaemia patients were re-sensitised to daunorubicin at low μM concentrations of GF120918 (100% samples tested) whereas verapamil at 100-fold higher concentrations could only restore drug sensitivity to 50% of samples (160). It has been shown that GF120918 has a longer duration of

action as compared to verapamil, which is effluxed by P-gp, and may help account for the more potent reversing activity of the former(57).

Many more compounds have emerged that also display greater potency (100-200 times) than earlier modulators such as verapamil and cyclosporin A. Reversal agents that hold great promise to potently and specifically block P-gp activity have been systematically developed, based on compounds such as GF120918, by the Medicinal Chemistry department of Xenova Ltd., Slough (see figure 1.3). These include the diketopiperazine derivative XR9051 (22) and the anthranilic acid derivative XR9576 (88, 140). In fact, XR9576 was developed through systematic modification of the physico-chemical properties of XR9051 that included the introduction of an anthranilamide nucleus. XR9051 was shown *in vitro* to reverse resistance to a number of MDR cytotoxics including doxorubicin, etoposide and vincristine using low μM concentrations in a number of murine and human cell lines. Co-administration of XR9051 with MDR cytotoxics *in vivo,* in murine and human tumour models, potentiated their anti-tumour activity (88).

This re-sensitisation was shown to be due to a direct interaction with P-gp as XR9051 could displace the binding of [^{3}H]-azidopine and [^{3}H]-vinblastine to P-gp (EC_{50} in nM range) (22). XR9576 was also shown to modulate resistance specific to P-gp for a number of cytotoxics (doxorubicin, paclitaxel, etoposide and vincristine) at low nM concentrations in cell lines derived from different tumour types (140). The potency of XR9576 to modify MDR was 15 times greater than PSC 833 and several fold greater than verapamil and CsA (89). This compound exhibited a long duration of action, displaying activity up to 24 hours post removal of excess XR9576 from the medium. This is in contrast to verapamil and CsA, which lose their activity within 60 minutes post

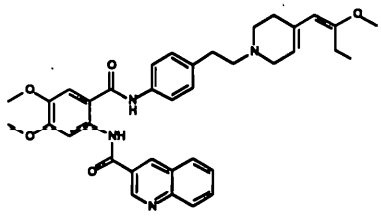

XR9576

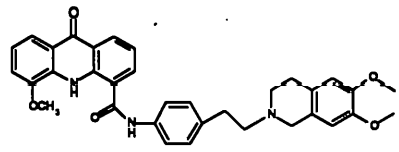

GF120918

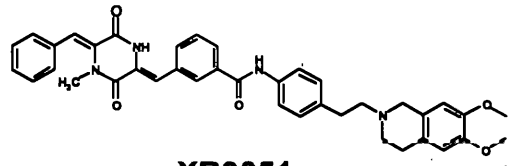

XR9051

Figure 1.3 Third generation modulators of P-gp mediated MDR

administration (89). The difference in the duration of activity of these modulators may be due to the fact that verapamil and CsA may be transported by P-gp whereas XR9576 may not. XR9567 is one of the most potent MDR reversers reported on to date and is currently undergoing Phase I clinical trials in healthy volunteers. It would seem that compounds such as XR9576 hold great promise for the treatment of P-gp mediated MDR and it is hoped that as more information is obtained concerning the mechanistics of P-gp's drug efflux activity more potent and selective modulators will be designed.

In fact the compounds XR9576, XR9051 and GF120918 were donated by Xenova Ltd., to enable study of the molecular pharmacology of these agents with P-gp and forms a substantial proportion of the studies reported in chapters 3 and 4 of this thesis.

1.4. P-glycoprotein: product of a multigene family

Over-expression of P-gp has been correlated with cross-resistance of tumours to diverse classes of anticancer drug, thus leading to poor chemotherapeutic outcome. There is considerable evidence to show that P-gp functions as a membrane bound transporter that actively translocates drugs out of cancer cells, preventing their intracellular accumulation. Therefore, blockade of P-gp drug efflux activity has been a strategy commonly adopted to overcome MDR in the clinic. However, little was known regarding the characteristics or the mechanism underlying the transport activity of P-gp. The first step towards elucidating the function of P-gp was to sequence the gene

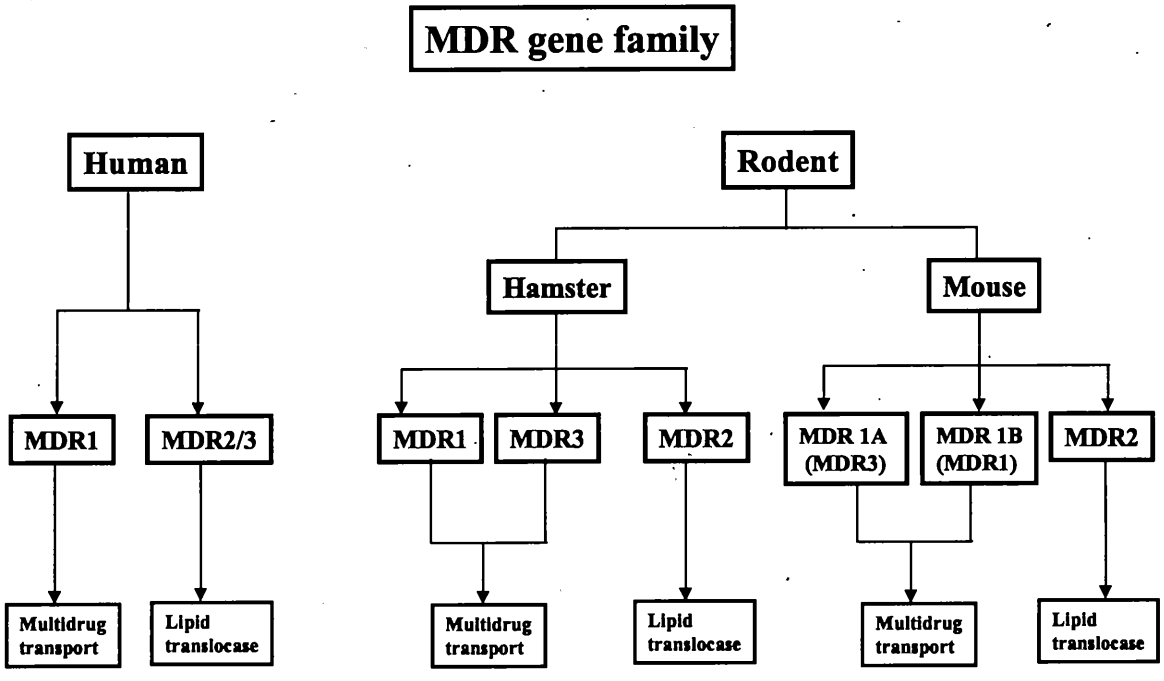

Figure 1.4 Nomenclature and function of P-glycoprotein family in humans and rodents

encoding P-gp in both human (MDR1) (18) and mouse (MDR3) (44). P-gp is a member of a multigene family encoded by variants of the multidrug resistance (MDR) gene (refer to figure 1.4). There are two classes of P-gp protein in humans, Class I (MDR1) and Class III (MDR2/3) (18). Rodents on the other hand, have three classes of P-gp (44).

Class I & II in rodents and Class I in humans confer multidrug resistance. Class III P-gp has been shown to display flippase activity in transporting phosphatidylcholine from inner to outer leaflets of the plasma membrane (108, 134). The P-glycoproteins are a highly conserved family and there is a high level of amino acid similarity, particularly between mammalian P-gps (69%-94%) (21).

1.5 P-glycoprotein, a member of the ABC superfamily of membrane transporters

Alignment studies of the primary amino acid sequence of P-gp classified it as a member of the ATP Binding Cassette (ABC) superfamily of transport proteins. This broad family of proteins is made up of a diverse spectrum of prokaryotic and eukaryotic transporters (47). There is high sequence similarity amongst the entire family particularly within the nucleotide binding domains (NBDs) that display an overall amino acid identity of 30% or more. Some of the conservation is made up of functional units located in the ATP binding pockets and are known as the Walker A (G-X-X-G-X-G-K-S-S/T) and B (h-h-h-h-D) motifs, necessary in ATP binding and hydrolysis (153). An additional important sequence, diagnostic of ABC proteins, is the 'signature' motif (L-S-G-G-Q-(Q/R/K)-Q-R) located upstream of the Walker B motif which can be up to 15 residues in length. It is the most highly conserved sequence amongst the entire ABC family. This sequence is critical to the functioning of ABC proteins as mutations of any of the residues results in a complete disruption of protein function. The precise role for the signature sequence in the functioning of P-gp is not known. It is speculated that it may play a role in communication between the NBDs during catalysis, as the NBDs of P-gp have been shown to interact with a high degree of co-operativity as discussed in later sections.

Most ABC proteins are plasma membrane transporters and have been found in a variety of organisms from microbes to man (see (49) for review) and translocate a wide

spectrum of ligand. The minimal functional requirement for an active ABC protein comprises two transmembrane domains (TMDs), each one usually composed of six membrane-spanning segments, and two NBDs $[TMD\text{-}NBD]_2$ (47). However, there is diversity within this family of transporters in the modular organisation of the domains that comprise each protein (as illustrated in figure 1.5). For instance, the [TMD-NBD] repeat can be made up of a single fused polypeptide as is the case for P-gp, MRP1 and the Cystic Fibrosis Transmembrane Conductance Regulator (CFTR) or from oligomers of different polypeptides, e.g. heterodimers in the TAP transporter of humans and the tetrameric prokaryotic histidine uptake transporter. Indeed, there is further diversification amongst the transporters whose domains arise from a single polypeptide. For example, CFTR contains an R domain (not found in any other ABC protein) that links the first NBD with the TMD of the second [TMD-NBD] repeat. The R domain when phosphorylated, modulates the influence of nucleotide on the gating of the chloride channel (35). MRP1 is distinguished by the presence of an additional TMD (TMD0) located N-terminal of the first [TMD-NBD] repeat.

The diversity in the modular composition of ABC proteins accommodates the presence of a range of transporter types within one family. Some proteins are involved in ion transport such as CFTR, which is a chloride channel, or the sulfonyl-urea receptor (SUR) that actively modulates K^+ ion flux through the associated channel Kir6.1. Some ABC proteins display specificity for a single ligand for transport, whereas there are other members of this superfamily that are poly-specific. Many prokaryotic ABC proteins function as importers such as the Histidine permease and Maltose transporters, involved in the import of histidine and maltose respectively. These transporters are generally specific for a single ligand for transport. Many prokaryotic importers contain an

additional feature, which are called accessory proteins, and they are involved in ligand presentation. There are however, no known importers amongst eukaryotic ABC proteins.

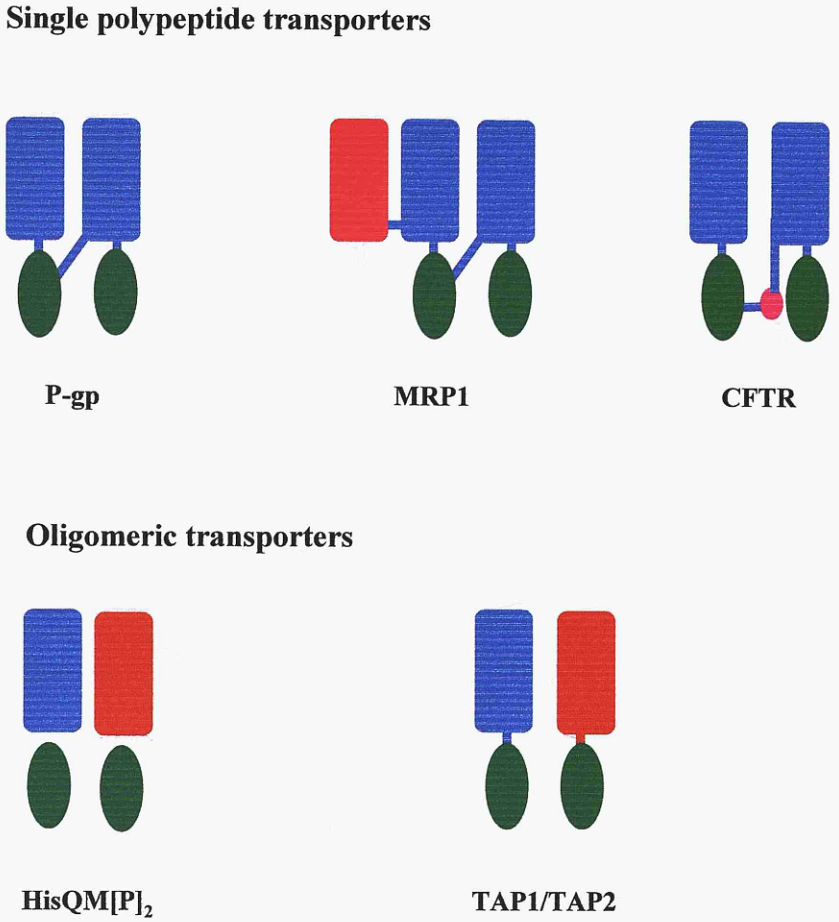

Figure 1.5 Diversity in domain composition amongst members of the ABC family of transporters.

All ABC proteins in eukaryotes, and many in prokaryotes, are involved in export processes such as anticancer drugs by P-gp and MRP1, antigenic peptides by TAP1 and 2 and multiple drugs by LmrA. The poly-specificity exhibited by the multi-drug transporting proteins P-gp and LmrA contrasts with more specific proteins such as TAP1/2 and CFTR.

In recent years there has been an explosion in the number of ABC proteins reported, and interest stems from the fact that some have been implicated in diseases such as cystic fibrosis (CFTR), adrenoleukodystrophy (ALDP) and hyperinsulinemia hypoglycemia

(SUR1). In general, the TMDs of ABC proteins confer specificity for ligand recognition and binding. Hydrolysis of ATP at the NBDs drives the transmembrane movement of ligand, although the mechanisms co-ordinating ligand binding with ATP hydrolysis to effect translocation, remain to be elucidated.

1.6 Structural studies of P-gp

1.6.1 Low resolution structure of P-gp

Determining the three-dimensional structure of any membrane bound protein is the holy grail of all studies concerned with elucidation of plasma membrane transport processes.

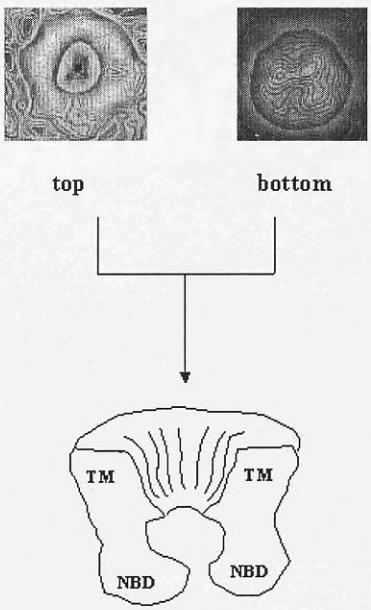

Figure 1.6 Electron microscopy and single particle analysis of purified reconstituted P-gp. (Top panel) Images produced from 3D reconstructions of single particle analysis and Fourier projection maps of small 2D crystalline arrays. Top, represents view from above the plane of the bilayer. Bottom, the protein as viewed from below the plane of the bilayer. A cartoon representation of 'goblet' like P-gp molecule has been derived from low resolution structure (adapted from Rosenberg *et al.*, 1997).

This is also the case with P-gp as our understanding of the mechanistics of the transport function of this protein will not be complete without full knowledge of its structure. The only solid structural information on P-gp available to date is a low resolution structure for hamster P-gp, the fruits of an on-going collaborative project between our laboratory in Oxford and Dr Robert Ford's group at UMIST in Manchester. The structure for P-gp has been determined to low (2.5nm) resolution by electron microscopy and single particle analysis of both detergent solubilized and reconstituted protein. This was further refined by three-dimensional reconstructions from single particle analysis and Fourier projection maps of small two-dimensional crystalline arrays (104). When the image produced is viewed from above the plane of the membrane a toroidal protein shape is visible (figure 1.6) that has 6-fold symmetry and a diameter of 10nm. A large central aqueous pore of diameter 5nm spans the membrane but narrows towards the cytoplasmic face of the membrane. Projection maps perpendicular to the membrane surface revealed two 3nm lobe like structures purported to be the NBDs.

1.6.2 Arrangement of TM segments of P-gp

This is the most detailed structural information for any ABC protein to date and accommodates P-gp as having a structure of 6 + 6 TMs arranged around a central pore that has been adopted as a working model for the study of other ABC proteins. Loo and Clarke have used cysteine-scanning mutagenesis (CSM) to directly look at packing of TM spanning elements in P-gp. They found that the topology of P-gp was consistent with six TM segments in each homologous half of P-gp (77) a finding that was also confirmed in a study conducted by Kast *et al.*, (63-65) where a small antigenic peptide epitope was inserted at various positions within mouse P-gp. Loo and Clarke extended their cross-linking studies to show that TM6 and TM12 are in close proximity as shown by formation of disulfide cross-links between residues located towards the cytoplasmic

end of the TMs. A model was proposed where TM arrangement in P-gp forms a mirror symmetry and this fitted in with the toroidal model proposed based on the low resolution structure of Rosenberg *et al.* But this was later refuted in a more recent crosslinking study that looked at the ability of a single cysteine residue in TM12 to crosslink with single cysteines in TM1-6 or cysteine in TM6 to crosslink to single cysteines in TM7-12. From the results of this study, a cyclone model depicting arrangement of TM segments in the membrane has been proposed (79). This model suggests that TM12 is in close proximity to TM 4,5 and 6 whereas TM6 is close to TM12, 11 and 10 (see figure 1.7(c)). The authors claim that no crosslinks could be formed between TM6 and TM7, 8 and 9 or TM12 and TM1,2,3. However, crosslinking agents of differing lengths were not employed in these studies, which is an important consideration given that any particular TM segment may not be equidistant from all other TM segments. The cyclone model is based on the fact that no crosslinks were formed with TM1-3 or 7-9. However, a mirror symmetry model may also be applied to the data produced as suggested in figure 1.7(b).

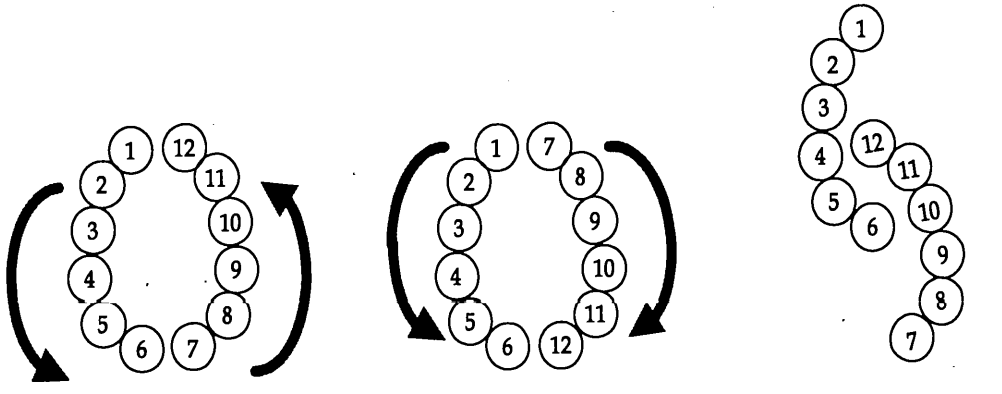

Figure 1.7 Proposed models depicting proximity and arrangement of TM spanning segments around aqueous pore of P-gp.

Crosslinking studies do pose a useful tool in determining intra- and inter-domain arrangements within multimeric proteins. However, in order to obtain a complete picture of the structural arrangement of domains it is necessary to systematically conduct an exhaustive range of crosslinks employing agents of differing lengths and flexibilities.

An alternative interpretation of the low resolution data produced has been proffered. This model proposes that the 12 membrane spanning segments of P-gp fold as 2 X β barrels that are arranged back to back in the membrane and are attached by short loops to bundles of α-helices formed by the large cytoplasmic loops connecting the TM segments (58). These cytoplasmically located loops are purported to form the ligand binding sites and move into the β barrel during ATP dependent translocation. These authors have not provided firm experimental evidence supporting their interpretation of P-gp studies, and have based their model on hydropathy analysis and algorithms for predicting secondary structural features. They have also cited work conducted by Sonveaux *et al.* (137) who used an infra-red spectroscopy technique to look at secondary and tertiary structure of P-gp. These authors report a high percentage of β barrel structure in the overall structure of P-gp, but a significant contribution is also made by α-helical components sufficient to support an α-helical TM model for P-gp. However, this issue cannot be truly resolved without higher resolution structure or until the periodicity of the membrane spanning segments has been determined.

1.6.3 Structure of isolated NBDs of ABC proteins

There have been many attempts to express and purify the NBDs of P-gp in order to determine their structure and have a closer look at the function of each. This has proved to be a difficult task due to the lack of solubility of the NBDs of ABC proteins and their propensity to aggregate in inclusion bodies when expressed without the membrane

domain. An additional difficulty arises in attempting to assess the functionality of expressed NBD proteins due to the requirement of two NBDs to hydrolyse ATP. However, high resolution crystal structures of the NBDs of at least three different bacterial ABC proteins have been achieved, and may help contribute to our understanding of NBD structure, and particularly the location of the catalytic pocket within the 3D structure.

The crystal structure of the catalytic subunit of the maltose transporter of *Thermococcus litoralis*, MalK, was obtained in the presence of bound MgADP (figure 1.8) (26). The MalK subunit is described as an ellipsoidal planeconvex lens and is proposed to form an asymmetric dimer subunit (figure 1.9). The monomeric subunit is described as having three layers.

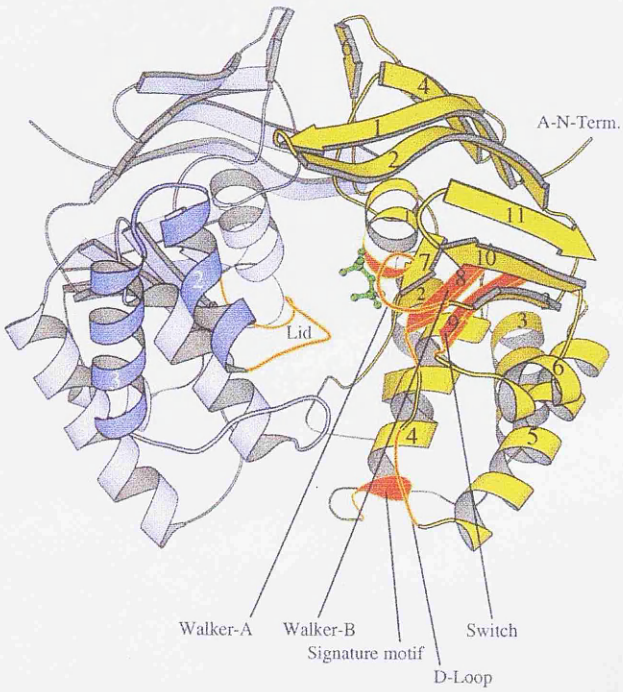

Figure 1.8 Crystal structure of the catalytic subunit of the maltose transporter (MalK) of *Thermococcus litoralis* (from Diederichs *et al.*, 2000).

The top layer comprises anti-parallel β sheets and the middle layer is made up of mixed sheets and includes the P-loop, which contains the Walker A motif necessary for ATP binding. A third layer contains the signature sequence and D-loop (which contains the Walker B motif) and is thought to form an interface with the translocation pore MalFG. Two of the four helices in this layer may also form an interface between the monomeric subunits.

The crystal structure of the ATP binding subunit of the histidine uptake system of *S.typhimurium,* His P, was derived from crystals produced in the presence of ATP but lacking Mg^{2+} ion. As shown in figure 1.9, the His P dimer is proposed to comprise back to back L-shaped monomers (56). 'Arm I' is proposed to form the interface with the cytoplasmic face of the membrane domain whilst 'Arm II' of each monomer unit forms the dimer interface.

Finally, a third dimerisation model has emerged from high resolution crystal structure of the DNA repair protein Rad50 (52). This protein comprises a single catalytic domain but functions as a dimer where the ATPase domains are joined by a coiled coil. The crystallisation studies revealed a unique feature of the Rad50 catalytic domain (Rad50cd) that showed it was comprised of two separate polypeptides. The ATP and AMP-PNP bound crystal forms showed that two Rad50cd domains dimerise in a head to tail orientation (figure 1.9). In this model, both ATP molecules are buried in the dimer interface, sandwiched between the P-loop (Walker A motif) and the signature motif of the opposing Rad50 catalytic domain. Mutational analysis revealed that ATP and an intact signature motif were essential for dimerisation. The requirement for ATP in dimer formation is suggestive of allosteric changes in the Rad50 catalytic domain due to ATP binding and the model proposed here may help explain the co-operativity and close

cross-talk that takes place between the NBDs of P-gp. This model also suggests a crucial role for the signature sequence in NBD:NBD interaction.

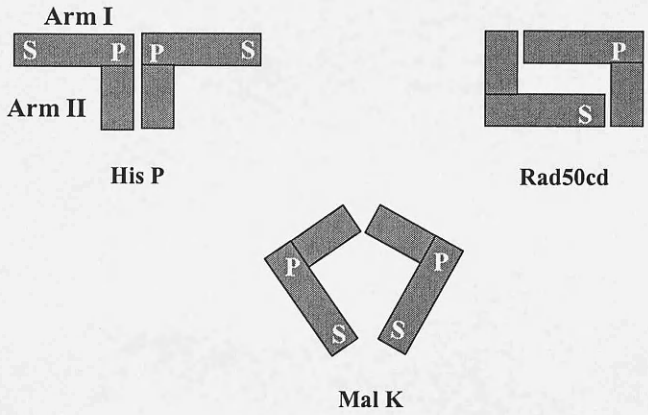

Figure 1.9 Cartoon representation of the different dimerisation models for bacterial NBDs arising from purification and crystallisation trials. 'S' signifies signature sequence and 'P' denotes P-loop.

The publication of three different models depicting possible dimerisation of the NBDs of ABC transporters has excited the imagination of all those concerned with elucidating the function of this family of transporters. All of the models produced have come from crystallization trials where different conditions have been used. However, in light of the extensive biochemical data produced to date regarding NBD:NBD interaction, the MalK and Rad50cd dimer models seem more plausible. These models portray a more intimate association of the catalytic pockets of each NBD (figure 1.9), which fits in with the high degree of co-operativity shown to exist between the NBDs of P-gp, for instance. Recently, Sharom *et al.*, (131) used a fluorescence resonance energy transfer (F.R.E.T) technique to show that the catalytic sites of P-gp are in close proximity, which would also favour the Rad50cd or Mal K dimer structure over that of HisP.

However, a high resolution structure of P-gp is required to elucidate the disposition of the NBDs with respect to the membrane domain and help determine whether additional

structural elements such as the cytoplasmic loops are involved in signal transduction between the NBDs and TMDs on P-gp. Higher resolution will also help to clarify how membrane spanning elements are arranged around the pore observed in the low resolution structure. More detailed structural information may help to pin-point location(s) of drug interaction sites within the membrane domain and help clarify ongoing uncertainty over the mode of ligand translocation.

1.7 Location of drug binding sites within the membrane domains of P-gp.

Given that the TMDs of ABC transporters contain elements involved in determining substrate specificity, efforts have focussed on identifying regions within the TMDs of P-gp that may be involved in the binding of ligand. Early studies employed the technique of photoaffinity labelling to detect membrane regions involved in binding. This procedure uses analogues of known transported ligands and modulators of P-gp that have a photoactivatable group (e.g. azido) attached. Following equilibration of drug with protein, the photoactive moiety, upon exposure to U.V. light, covalently attaches close to the drug binding site. Initial studies of Bruggeman *et al.*, (15) used [^{3}H]-azidopine, a 1,4-dihydropyridine photoactive derivative, to label P-gp. Azidopine labelled protein was subjected to protease digestion and labelled regions identified by antibody mapping of digested fragments. Azidopine labelled TM regions in both halves of the P-gp molecule and it was proposed that the two halves of the protein come together to form the drug binding site. Additional photoaffinity labelling studies have refined the findings of this study to implicate specific TM spanning segments in drug binding. For example, labelling of P-gp with the prazosin analogue ^{125}I-iodoarylazidoprazosin ([^{125}I]-IAAP), identified a TM region in each half of the molecule comprising TM segments 6 and 12 (refer to topology of P-gp in figure 1.10) (42). An analogue of forskolin only labelled TM segments 5 and 6 located in the N-terminal region of the protein (91).

The use of chimeric P-gp molecules supported and augmented the findings of the photo-affinity labelling studies of P-gp. Chimeric molecules have been constructed where the C-terminal membrane region of human MDR1 P-gp was systematically replaced from TM10 onwards with equivalent residues from the MDR3 isoform of human P-gp that does not confer MDR. The effect of these changes on drug specificity and resistance was assessed in *in vitro* cytotoxicity assays and by photolabelling studies. Replacement of TM12 reduced labelling with [^{125}I]-IAAP and abrogated resistance to a range of drugs such as doxorubicin and vincristine. Re-introduction of TM12 and the intracellular loop connecting TM segments 11 and 12 into the MDR1 molecule restored binding and drug sensitivity (157). In a similar study, TM segments of the MDR conferring P-gp (MDR1) were introduced into the backbone of MDR2 P-gp that is involved in phospholipid transport and does not mediate MDR. Introduction of TM6 and TM segments 11 and 12, allowed the MDR2 protein to transport drugs normally effluxed by MDR1 P-gp. Therefore, the results from photolabelling of intact MDR1 protein and study of chimeric P-gp molecules have suggested a role for TM segments 5, 6, 11 and 12 in drug recognition.

These studies have provided a good starting point for investigation of residues within the TMDs that may be important in conferring ligand specificity. The main approach adopted to identify residues important in ligand recognition has been site-directed mutagenesis. This allows the introduction of changes at precise locations within the cDNA of P-gp. Point mutations have been systematically introduced throughout TM segments 5,6, 11 and 12 of mouse, human and hamster P-gp as summarised in table 1.3 and illustrated in figure 1.10. Other membrane spanning segments have been also been

mutated, and the effects are summarised in a detailed review of residues involved in ligand specificity by Ambudkar *et al.* (4).

Realisation of the importance of residues in TM11 in ligand recognition originated from studies that showed that a single ser^{941} to phe^{941} substitution in mouse MDR1 and ser^{939} to phe^{939} in mouse MDR3 altered the drug-resistance profiles to a range of drugs, abrogated photoaffinity labelling with [^{3}H]-azidopine and [^{125}I]-IAAP and attenuated the chemosensitising effect of the modulatory drugs verapamil and progesterone (45, 46, 61). Replacement of serine with phenylalanine involves introduction of a large bulky group at the mutated position and may cause a gross perturbation of the region around the substitution. This kind of approach can be useful in determining regions sensitive to mutation and worthy of further examination using more conservative amino acid substitutions. In a subsequent study, all of the amino acid residues in predicted TM11 of mouse MDR3 were mutated to alanine (alanine scanning mutagenesis).

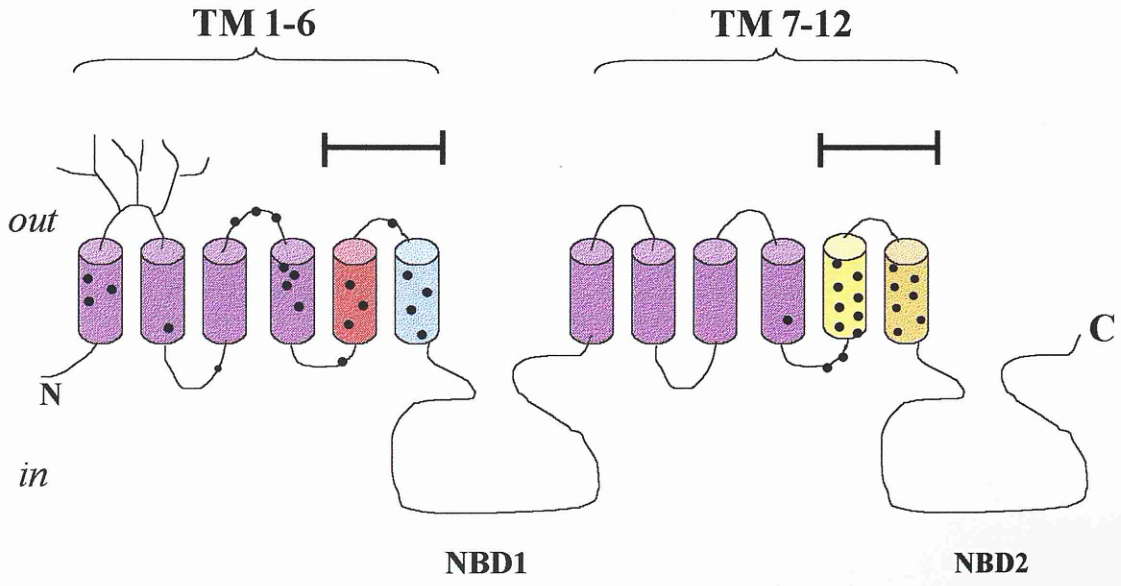

Figure 1.10 Location of membrane spanning regions of P-gp important in drug recognition. The positions of some point mutations that alter substrate specificity of P-gp are indicated by filled circles. Bars above model denote regions identified in photoaffinity labelling studies. TM segments 5, 6, 11 and 12 are highlighted in different colours and are purported to be directly involved in drug binding.

Substitutions of amino acid residues with alanine is commonly used, as it introduces modest perturbations due to the relatively small inert R group on alanine. The effect of the mutations on drug resistance profiles (vinblastine, adriamycin, colchicine and actinomycin D) were assessed in stable transfectants. More than half of the mutant proteins showed 2-10 fold reduction in the degree of resistance to one or two of the drugs investigated. However, the most deleterious effect was seen with mutants Y949A and F953A that were proposed by these authors to be essential for drug recognition (46).

Loo and Clarke have used cysteine-scanning mutagenesis (CSM) to determine amino acid residues involved in drug recognition. This was achieved by mutating the seven endogenous cysteines of human P-gp (MDR1) to alanines to create a cysteine-less P-gp template. Single cysteine residues were systematically introduced into TM segments 5, 6, 11 and 12. Interaction of the thiol-reactive reagent dibromobimane (dBBn) with the introduced cysteine residues results in inhibition of ATPase activity due to the formation of a cross-link by this probe. The ability of P-gp transport ligands vinblastine and colchicine and the modulator verapamil to block dBBn induced inhibition of ATPase activity is used to assess role of mutated residues in drug recognition. As shown in table 1.3, amino acid residues thought to be directly involved in drug binding, have been identified in all of the TM regions investigated using CSM analysis. Interestingly, two different mutagenic (CSM and ASM see table 1.3) approaches have each implicated three residues in TM12 as being directly involved in drug recognition (L^{975}, V^{982}, A^{985}).

In summary, slow progress has been made since the early photoaffinity labelling studies that first suggested a role for TM segments 5, 6, 11 and 12 in determining the ligand specificity of P-gp. The overall picture emerging from mutagenesis studies is that many amino acid residues located in each half of the P-gp molecule contribute to ligand

specificity. It has not been possible to determine from such studies whether there is a single binding pocket or discrete sites for ligand interaction. The effect of the introduced mutations have been assessed in a variety of ways, but no thorough characterisation of the introduced mutation on binding characteristics or ability of drug to stimulate ATP hydrolysis has been conducted. Many studies have used cytotoxicity assays to assess the effect of introduced mutations, but these assays merely report on the phenotype produced and not specific effects on drug binding. Assays of P-gp ATPase activity have commonly been used to analyse the effect of mutations on P-gp activity. However, in many cases only a single saturating concentration of drug has been used rather than complete dose-response analysis to look for changes in drug interaction and cannot be used to report changes in drug affinity, for example. Some of the reported changes in

Table 1.3 Mutations in P-gp that alter drug specificity

Mutated residue	*Region*	*Source*	*Functional effect*	*Reference*
Y949A F953A	TM11	MDR3 mouse	Altered drug resistance profiles Vinblastine, adriamycin, colchicine	Hanna *et al.*, 1996
S941F S939F	TM11	MDR1 mouse MDR3 mouse	Decreased labelling [^{125}I]-IAAP & [^{3}H]-azidopine; reduced resistance adriamycin, decreased reversal activity by verapamil	Kajiji *et al.*, 1993 Gros *et al.*, 1991
F942C T945C	TM11	MDR1 human	Verapamil, vinblastine & colchicine block inhibition ATPase by thiolreactive agent dibromobimane	Loo & Clarke, 1999
L339C A342C	TM6	MDR1 human	As above	Loo & Clarke, 1997
L975C V982C A985C	TM12	MDR1 human	As above	Loo & Clarke, 1997
I306C	TM5	MDR1 human	As above	Loo & Clarke, 2000
V982A F983A L975A	TM12	MDR1 human	No transport rhodamine 123 & daunomycin, decreased stimulation ATPase by verapamil, decreased [^{125}I]-IAAP labelling	Hafkemeyer *et al.*, 1998

drug specificity attributed to mutations introduced into P-gp may also reflect allosteric alteration of a drug binding site distant from the mutated residue. Furthermore, the use of photoactive drug analogues to detect alterations in drug binding is also fraught with difficulties due to the flexibility and high reactivity of the photoactive group that can sometimes cross-link to non-pharmacophoric regions of proteins (38). More refined studies need to be conducted on mutant P-gp isoforms. For example, the environment of the mutated residue could be examined using a range of cross-linking probes comprising differing chemical features and looking at the effect of high affinity ligands to interfere with labelling. Such an approach may help determine the distance of drug from any particular residue. However, the residues highlighted to date from site-directed mutagenesis and photoaffinity labelling studies, provide a good starting point from which to conduct more detailed analysis of the role of individual residues or TM segments in drug binding.

1.8 Mechanism of drug interaction by P-gp

Although there is convincing evidence from mutagenesis and photoaffinity labelling studies that the TMDs of P-gp are involved in ligand recognition, there was uncertainty surrounding how drugs access the binding domain(s) on P-gp. P-gp ligands can be defined by common features such as hydrophobicity, lipophilicity or the presence of aromatic rings (see table 1.1). These features allow P-gp ligands to readily partition across the membrane bilayer and enter the cytoplasm by passive diffusion (28, 121). Does ligand interact with P-gp from the cytoplasm or from the lipid bilayer? There are at present several lines of evidence suggesting that drugs do access P-gp from the lipid phase.

Raviv *et al.* (97) used the photoactive lipophilic probe 5-[^{125}I]-iodonaphthalene-1-azide ([^{125}I]-INA), which specifically cross-links membrane-spanning components of proteins, to show that drugs do interact with P-gp from the bilayer. The authors demonstrated energy transfer between the fluorescent ligands doxorubicin and rhodamine 123 and the membrane probe, which can only occur over a relatively short distance suggesting that the drugs must be interacting with P-gp in the bilayer. Other evidence has come from studies using acetoxy-methyl (AM) ester derivatives of fluorescent ligands such as the transported ligand calcein-AM. These compounds only fluoresce when the AM group has been cleaved by intracellular esterases. P-gp containing cells have no fluorescence unless the protein is inhibited. Addition of reversal agents has been shown to increase fluorescence, thereby demonstrating that drug-AM derivatives have not reached the cytoplasm, and must therefore be extracted from the bilayer (50). Evidence that P-gp transports drugs out of the lipid bilayer is also presented in a paper looking at transport of the lipophilic compound Hoechst 33342 in inside-out membrane vesicles prepared from P-gp over-expressing CH^{r}B30 cells. Hoechst 33342 is only fluorescent when membrane bound, and efflux was measured by following the reduction in fluorescence intensity due to the build up of Hoechst 33342 in the membrane vesicle interior (122, 126). These authors also further suggested in a subsequent study, that drugs are extracted from the inner leaflet of the bilayer. This was interpreted from studies where fluorescence resonance energy transfer (F.R.E.T) from donor Hoechst 33342 molecules to acceptor NBD-C6-HPC molecules located in the cytoplasmic leaflet of membrane vesicles was measured. Decreased fluorescence of Hoechst 33342 following addition of ATP was concomitant with decreases in energy-transfer related fluorescence of NBD-C6-HPC. Although initial rates were measured, the authors did not determine the percentage of vesicles in an inside-out orientation to determine (i) how much acceptor molecule was affected by actively transported Hoechst 33342 and (ii) had not distinguished between

F.R.E.T. due to passive Hoechst 33342 diffusion in vesicles in an 'outside-in' orientation. However, taken together the studies outlined above do provide strong evidence indicating that ligands most likely access the binding domain of P-gp from the lipid bilayer.

1.8.1 Models depicting ligand interaction with P-gp

Given that P-gp interacts with a wide range of ligands from undefined site(s) within the bilayer, different models have been proposed to describe the drug binding and efflux activities of P-gp. These include (i) the hydrophobic vacuum cleaner (ii) flippase (iii) multiple site and (iv) membrane potential ($\Delta\psi$)/intracellular pH (pH_i) alteration models. The hydrophobic vacuum cleaner model was first proposed to explain the broad substrate specificity of P-gp based on the hydrophobic nature of many P-gp ligands and the fact that drugs are extracted directly from the membrane (41). This model did not accommodate the presence of distinct drug interaction sites within the TMDs of P-gp, but rather suggested that the TMDs from each half contributed to a large central binding pocket of undefined specificity (refer to figure 1.11(a)).

A variation of the hydrophobic vacuum cleaner model is the flippase model for P-gp transport activity (see (48) for review). The underlying feature of this model is that P-gp interacts with drug from the inner leaflet of the bilayer mediating translocation of drug molecules to the outer leaflet, where the drug molecules dissociate to the extracellular space (figure 1.11(b)). However, flippase or more correctly bilayer-translocase activity is normally attributed to phospholipids. Phospholipid translocation performs an important role physiologically in maintaining membrane asymmetry which is necessary in many processes including endo- and exocytosis and cell signalling. Translocase activity was ascribed to the mechanism by which P-gp might mediate MDR based on the

suggestion that MDR1 should display functional similarity to the closely related MDR2 protein, which is known to mediate ATP dependent translocation of short-chain phosphatidylcholine (PC) lipids (108). A recent study demonstrated transport of MDR1 ligands such as paclitaxel and vinblastine in kidney cell monolayers transfected with MDR3 protein that was inhibited by a range of MDR1 reversal agents (135). However, MDR3/MDR2 protein has never been shown to be involved in the MDR phenomenon as is the case for MDR1 (P-gp). Conversely, efforts have focussed on establishing whether MDR1 protein can translocate lipids. Van Helvoort *et al* (150) investigated the translocation of membrane phospholipids and sphingolipids by addition of lipid precursors to epithelial cell lines transfected with human MDR1 or human MDR2(MDR3). There was an asymmetric distribution for PC phospholipids in MDR2 cells and for a range of phospholipids in MDR1 cells. However, this study was indirect as there was no unequivocal evidence for movement of phospholipids provided. A recent investigation using a direct assay on purified reconstituted hamster MDR1 displayed no lipid translocase activity (105).

In order for the flippase model of drug binding and transport by P-gp to work, drugs must be able to discriminate between the leaflets of the bilayer. The central tenet of this model states that drugs are extracted from the inner leaflet prior to movement to the extracellular leaflet. This has largely been based on a number of observations rather than direct measurement of 'flipping' activity. (i) As stated in the previous section, Shapiro and Ling (126) suggest that drug is extracted from the cytoplasmic leaflet of the bilayer. (ii) Other authors report that the cytotoxic drug doxorubicin partitions between the leaflets of the bilayer by a 'flip-flop' movement (28, 98). However, these authors did not clearly show that the 'flip-flop' movement observed was not due to rebinding of doxorubicin to the extracellular leaflet following diffusion across the bilayer. The

hydrophobicity of drugs transported by P-gp means that unlike phospholipids, they can readily diffuse across membranes, making it difficult to detect flipping.

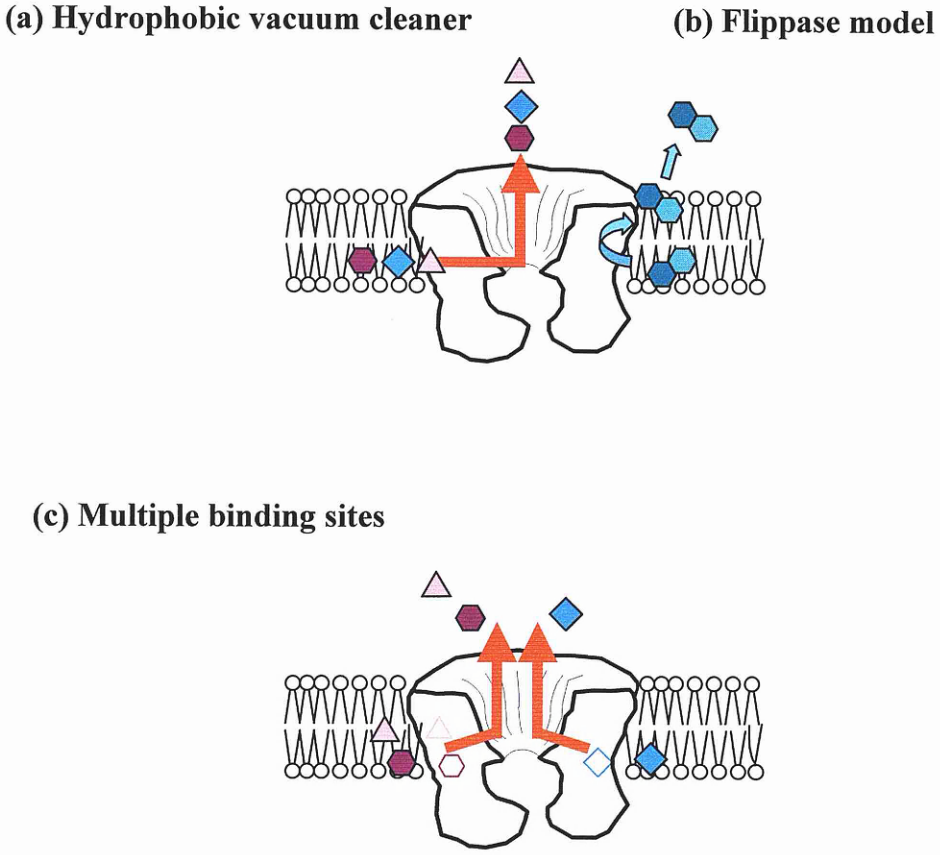

Figure 1.11 Proposed models depicting how drugs interact with and are effluxed by P-gp. P-gp is represented in cartoon form based on low resolution structure presented in Rosenberg et al., 1997 (a) Hydrophobic vacuum cleaner model where different drugs are extracted non-specifically from bilayer and extruded. (b) Flippase model where drug translocated from inner leaflet of bilayer to outer leaflet prior to release to extracellular milieu. (c) Multiple site model shows defined interaction sites for drug within the TMDs of P-gp.

The molecular basis of P-gp's broad substrate specificity has not been encompassed by either the hydrophobic vacuum cleaner or flippase models. Is there a single site of undefined specificity or distinct sites of interaction for ligand? The presence of multiple distinct sites for drug on the P-gp molecule was inferred from transport assays using combinations of drugs where the interactions were not consistent with a single binding site (6, 123, 127). For example, Shapiro and Ling (1997) showed that the transported

ligands Hoechst 33342 and rhodamine 123 bound at distinct sites and that these sites were co-operatively linked. Additionally, studies of ATP hydrolysis have shown that the maximal rate of activity of drug (e.g.vinblastine) was decreased in the presence of a second drug (e.g.verapamil) with no alteration in K_m. This is suggestive of non-competitive interaction between drugs and was interpreted to indicate distinct drug interaction sites on P-gp (93, 94).

Although investigation of drug effects on P-gp ATPase and transport activities suggested the presence of distinct drug binding sites they could not be taken as definitive proof. This is due to the fact that there are multiple stages in a transport and ATPase cycle making elucidation of the nature of drug:drug interactions difficult. Definitive proof for distinct drug binding sites could only result from direct measurement of drug binding. For this reason radioligand binding assays have been used to investigate the mechanisms contributing to the broad ligand specificity of P-gp. This may be achieved by looking at the effect of a drug on the dissociation rate of another (radiolabelled) drug. An alteration in the rate of dissociation of the radiolabelled drug-protein complex can only occur due to effects from an allosterically linked site(s). Using this kind of radioligand binding assay, Ferry *et al.* (29, 30) reported distinct sites of interaction for the transported drug [^{3}H]-vinblastine and the 1,4 dihydropyridine nicardipine, which acts as a modulator of P-gp transport activity. In a similar type of study, the sites of interaction for the modulators verapamil and SR33397 were found to be distinct from the [^{3}H]-vinblastine binding site (82). These studies were the first to directly show that there are distinct drug interaction sites on P-gp capable of communicating with each other through an allosteric mechanism. There is compelling evidence from both study of ATPase and transport activity and radioligand binding for the presence of distinct yet interacting drug binding

sites on P-gp. This has been termed the multiple binding site model for P-gp transport and may explain the broad ligand specificity exhibited by P-gp (figure 1.11(c)).

The three models presented above all imply a direct role for P-gp in the MDR phenomenon. An alternative model has been proposed that assigns an indirect role for P-gp in altering the distribution and accumulation of chemotherapeutic drugs. The tenets of this model are based on observations that over-expression of MDR proteins such as P-gp alters plasma membrane potential ($\Delta\psi$) and perturbs intracellular pH (ΔpH_i). These $\Delta\psi/pH_i$ effects have been proposed to cause (i) reduced rates of influx of chemotherapeutic agents (ii) perturbations in the plasma membrane perhaps by affecting lipid distribution which in turn modulates drug diffusion (iii) alterations in the trans-bilayer distribution of weakly basic drugs (iv) effects on signal transduction to reduce availability of cellular targets for cytotoxics (see (99-101) for reviews). Indeed, it has been demonstrated that that there is some perturbation of $\Delta\psi$ and pH_i in cells over-expressing MDR proteins. However, this cannot form the sole basis of MDR exhibited by P-gp expressing cells for a number of reasons. Firstly, there is a substantial body of evidence to show that P-gp directly interacts with a wide diversity of compounds. Secondly, mutations of residues within the drug binding region(s) alter the drug specificity exhibited by P-gp. Mutations within some of the intracellular loops connecting the energy generating NBDs and the TMDs also affect resistance profiles. None of these findings may be reasonably supported by an indirect effect of P-gp in the MDR phenomenon.

Given the weight of evidence from wide-ranging studies, I would favour the multiple drug interaction sites model over the hydrophobic vacuum cleaner or flippase models. However, it is not clear whether the drug binding sites can be classified according to

function i.e. sites from which transport occurs or sites that are regulatory only in activity. Are there sites at which both drugs that are normal substrates for transport and chemosensitisers that function to block P-gp activity interact? Knowledge of the classes of drug binding site on P-gp could then be used to design better strategies by which to inhibit P-gp extrusion of anticancer agents in chemotherapy. Elucidation of the classes of binding site on P-gp is a major focus of this thesis.

1.9 The kinetics of P-glycoprotein transport activity

P-gp is a membrane transporter that couples hydrolysis of ATP to the outward movement of ligand. There is a dearth of information concerning the kinetics of the P-gp transport process. How quickly are drugs transported by P-gp? Given that there is more than one drug binding site on P-gp, how many molecules of drug can be transported at any one time? The hydrolysis of ATP is coupled to drug translocation but it is still unclear as to the number of ATP molecules required per drug molecule effluxed.

The ability to determine the rate of P-gp mediated drug transport is dependent upon measures of initial rates of transport. Initial transport rates are driven by drug concentration and increase linearly over time, providing a direct measurement of the rate of P-gp mediated efflux activity. The rate of transport can then be expressed as a function of drug concentration to yield values for K_m of transport and maximal drug efflux rates. There are many technical problems that have thwarted efforts to measure the rate of drug transport by P-gp. This is borne out in the large discrepancies arising from transport assays of P-gp where vastly different values for drug turnover rates or the efficiency of coupling of ATP hydrolysis to drug translocation have been reported (130). The first major drawback relates to the largely hydrophobic nature of P-gp transport ligands. This feature allows these drugs to rapidly partition into the membrane bilayer

resulting in rapid initial rates of drug movement that are not P-gp mediated and difficult to accurately determine. Secondly, hydrophobic drugs also tend to be 'sticky' in nature and can bind to lipids and plastic-ware, which alters drug distribution in a manner unrelated to P-gp. This has precluded measurement of initial rates of P-gp mediated transport using radioligand binding assays regardless of the model system used (i.e. whole cells, membrane vesicles, purified reconstituted protein). Radioligand binding studies have been widely adopted to provide information concerning P-gp transport activity at steady-state. Transport activity at steady-state reflects P-gp activity when outward pumping by P-gp equals the rate of drug influx and therefore cannot be used to reliably determine kinetic parameters of the transport process.

Another important consideration in trying to measure transport kinetics of any protein is the model system. Many studies have been conducted in P-gp over-expressing whole cells. There are a number of problems associated with the use of whole cells in measuring drug transport kinetics as illustrated in figure 1.12(a). Passive influx and efflux processes (rates (1) and (3) respectively) can make it difficult to determine the P-gp component (rate (2)) of drug translocation. Intracellular distribution and metabolic modification of drug within the cell can also compound difficulties associated with such measurements (rate (4)). Experimentally, measurement of the P-gp component in whole cells is determined by either following the efflux of drug from preloaded cells, or looking at the uptake of drug into cells as depicted in figure 1.12(b). In using cells preloaded with drug, P-gp will be pumping drug down a drug concentration gradient and so passive efflux of drug will also contribute to efflux activity, making it difficult to determine precisely the P-gp contribution. Transport activity measured by looking at drug uptake relies on comparing intracellular accumulation in the presence or absence of inhibitors of

P-gp transport. Both methods rely on approximations to determine the actual rate of transport due to the presence of P-gp alone.

Numerous studies have attempted to directly measure the rate of P-gp transport activity, the number of ATP molecules hydrolysed per molecule of drug transported and the

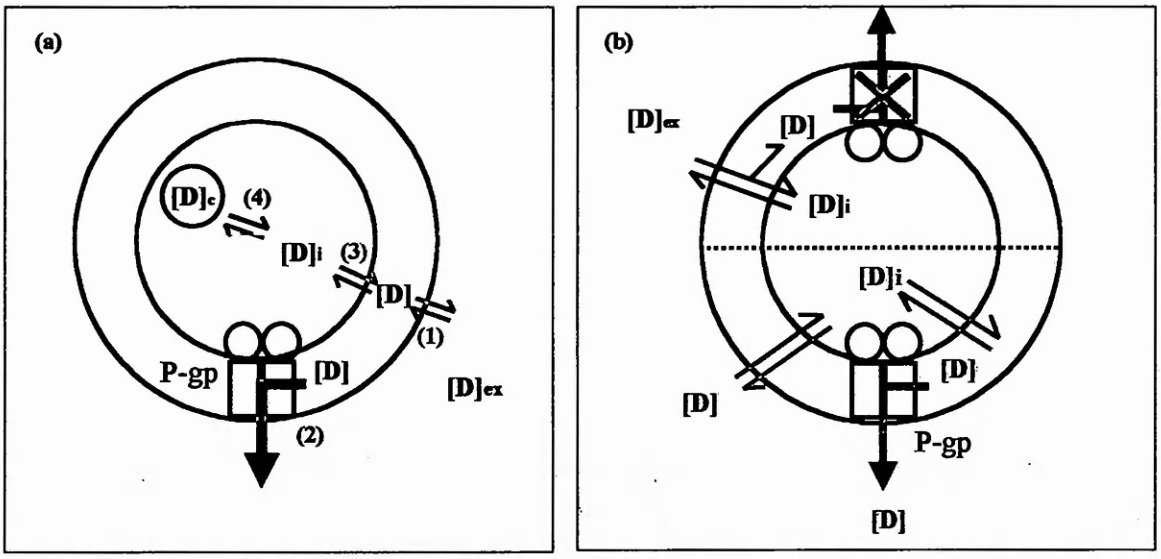

Figure 1.12 (a) Processes in whole cells that affect drug accumulation and kinetics. Passive influx and efflux denoted by rates (1) & (3) respectively. P-gp component of efflux is represented by (2). Rate (4) is due to compartmentalisation of drug. [D]c is concentration of drug in intracellular compartments. [D]ex and [D]i are extracellular and intracellular drug concentrations respectively. (b) Type of transport assays used to quantitate the P-gp component of transport. Top half of cell, uptake of drug is measured by using reversal agents to block P-gp activity. Lower half of cell, P-gp efflux activity measured by preloading cells with drug prior to transport measurements.

number of drug molecules transported when the pump is operating at maximal activity. Widely varying results have been reported and there is no consensus regarding the above parameters for P-gp transport activity. For example, estimates of the coupling ratio of drug transport to ATP hydrolysis vary between 0.02-1.0 mol drug transported per mol ATP hydrolysed. Ambudkar *et al.* (3) looked at [^{3}H]-vinblastine transport in NIH3T3 cells transfected with human P-gp, and found that 3 molecules of ATP were hydrolysed for every molecule of vinblastine transported. Initial rates were measured by (a) looking

at vinblastine uptake into P-gp expressing cells in the presence and absence of the modulator verapamil and (b) following efflux from cells preloaded with vinblastine. Turnover values for [^{3}H]-vinblastine transport of 1.1s^{-1} and 1.4s^{-1} were determined from the above assays. Calculation of turnover number or k_{cat} is dependent upon the system being at maximal activity (V_{max}) and the number of protein molecules ([R_t]) must be known ($k_{cat} = V_{max}/[R_t]$). An estimate for the number of P-gp molecules in the plasma membrane of NIH3T3 cells was derived from measurement of the binding of a fluorescently-conjugated antibody (UIC2) to an extracellular epitope on P-gp. When determining the number of ATP molecules hydrolysed per molecule of vinblastine transported, the authors only considered the vinblastine stimulated portion of the ATPase activity as being directly involved in the translocation of vinblastine molecules. In contrast to the results of this study, Shapiro and Ling (129) report, using plasma membrane vesicles, a coupling ratio of 1 mole of rhodamine 123 transported per mole of ATP hydrolysed. This represents tighter coupling of rhodamine 123 transport to ATP hydrolysis than was reported for vinblastine and may be a reflection of (a) different model system used, membrane vesicles versus whole cells, (b) using a fluorescent compound where changes can be monitored over short time intervals (sub second) (c) differences in relating turnover for transport to turnover for hydrolysis.

In a different study conducted by the same authors, the fluorescent lipophilic compound Hoechst 33342 was used to measure the apparent rate of transport of purified reconstituted P-gp (125). They reported a rate where one molecule of Hoechst 33342 was transported per minute per molecule of P-gp. This was in contrast to a turnover for ATPase activity, using the same system, of 50 molecules hydrolysed per minute per molecule of P-gp. This reflects very poor coupling of drug transport to ATP hydrolysis. The authors suggested that the slow rate of transport measured may be due to rapid re-

binding of Hoechst 33342 to the membrane following efflux. They also found that the proteoliposomes were leaky due to formation of Hoechst 33342 aggregates, therefore making it impossible to determine how much Hoechst 33342 was transported by P-gp. A combination of technical problems has probably led to an under-estimation of the rate of Hoechst 33342 transport in this study. Lu *et al.* (81) have used a derivative of the fluorescent compound rhodamine 123, tetramethylrosamine (TMR), to measure initial rates of efflux in purified reconstituted P-gp. Transport of TMR was ATP-dependent and followed Michaelis-Menten kinetics. The authors showed that the initial rate of TMR transport in proteoliposomes was dependent upon the concentrations of TMR and ATP, and they report K_m values of 0.3μM and 0.48mM for TMR and ATP respectively. The K_m for ATP to fuel transport of TMR is similar to reported values for the K_m of ATP hydrolysis. The fluorescent compound used in this study did not produce the high levels of background associated with the more lipophilic compound Hoechst 33342 due to rebinding to the lipid bilayer. Although the authors have been able to look directly at P-gp mediated transport of TMR, they have not been able to report on k_{cat} for TMR transport or the coupling ratio describing molecules ATP hydrolysed per molecule drug transported. This is due to the inherent difficulty associated with attempts to calculate the absolute number of drug molecules effluxed from relative fluorescence units.

The use of simpler model systems, such as membrane vesicles or purified P-gp reconstituted into proteoliposomes with defined lipid constituents, could circumvent some of the problems associated with direct measurement of P-gp mediated drug transport alluded to previously. For example, membrane vesicles and proteoliposomes are devoid of intracellular components that might interfere with drug pharmacokinetics. However, studies conducted in membrane vesicles and proteoliposomes with an inside-out orientation of P-gp are reliant on the formation of tightly sealed vesicles. This is

because transport rates are obtained by measuring the movement of drug from the bilayer into the vesicle interior, as depicted in figure 1.13 (a) and (b). However, transport assays that involve quantitation of P-gp related transport kinetics by following accumulation into the interior of membrane vesicles or proteoliposomes can also be fraught with difficulties.

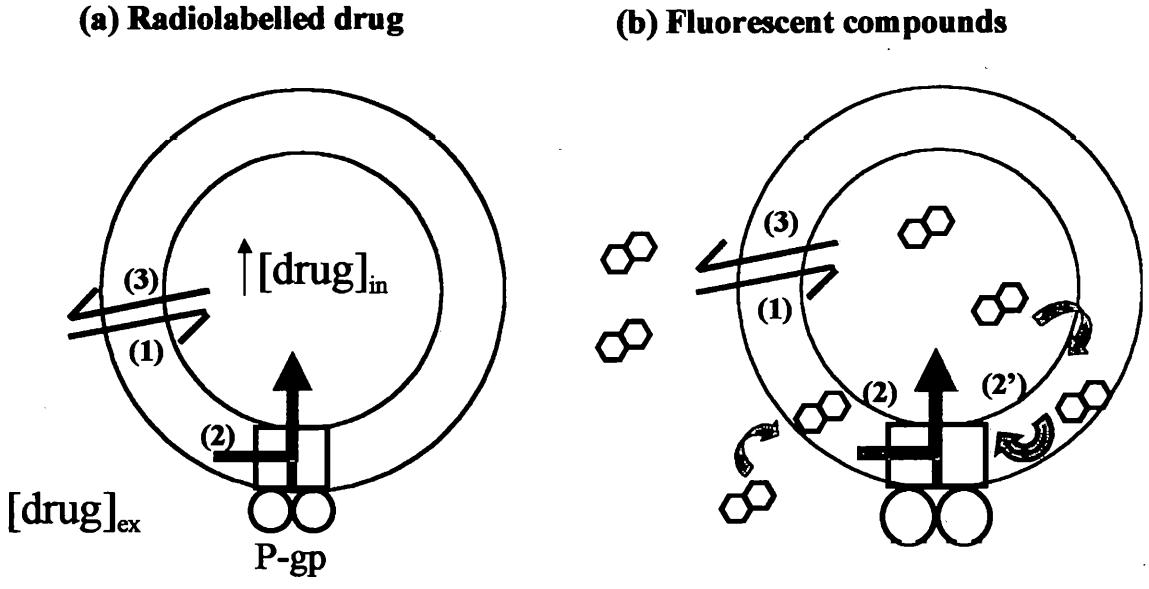

Figure 1.13 Model systems (membrane vesicles or proteoliposomes) used to measure kinetics of P-gp mediated drug transport. (a) Assay where transport detected by measuring accumulation of radiolabelled drug in vesicle/proteoliposome interior. (1) & (3) are passive influx and efflux respectively. (2) is drug influx due to P-gp. (b) Transport assays involving fluorescent ligands that are only fluorescent in the bilayer, measure reduction in fluorescence as ligand is moved to vesicle/proteoliposome interior. (1) & (3) represent passive influx and efflux. P-gp influx rate is represented by (2) & (2') where (2') arises from rebinding of drug from interior.

The interior of these systems is small and so high intracellular concentrations build up rapidly, leading to large passive efflux rates for drug (figure 1.13(a) and (b)). This is particularly problematic in fluorescence assays, which rely on high fluorescence in the bilayer and low levels in the aqueous interior. Rebinding of drug from the aqueous

interior of vesicles or proteoliposomes with the bilayer will lead to high fluorescence and under-estimation of P-gp transport kinetics (figure 1.13(b)). Additionally, P-gp reconstituted into liposomes will be transporting down a concentration gradient. Therefore, the assay system will have to measure the P-gp component of transport above the passive influx processes that will exist.

There is still quite a deficit in our knowledge of the mechanism of P-gp mediated transport and disagreement concerning the results that have been obtained to date from transport assays. Development of improved methods to purify and functionally reconstitute the protein into lipids at lower lipid:protein ratios may help reduce the problems of high background associated with assaying transport of hydrophobic P-gp ligands.

1.10 The catalytic cycle of P-gp

P-gp is similar to other active transporters in that its efflux and ATP hydrolytic activities are inextricably linked. Evidence for this has been derived using either membrane preparations or purified reconstituted P-gp that reveal P-gp mediated ATPase activity which is specifically stimulated by drugs that bind to the protein such as verapamil (1, 111, 124, 144). These studies showed that MgATP was the physiological substrate for the hydrolytic activity of P-gp, although it was capable of hydrolysing other nucleotide triphosphates at a slower rate. Maximal drug-stimulated turnover rates for MgATP hydrolysis of 10-20s^{-1} have been reported with a K_m value for MgATP in the range 0.15-1.4mM (117, 132). The ATPase activity was competitively inhibited by MgADP and the non-hydrolysable ATP analogue MgAMP-PNP with K_i values of 0.35-0.7mM (117). The ATPase activity of P-gp has a strict requirement for the presence of divalent cation and shows a particular preference for Mg^{2+} (1). Cations are thought to be necessary for

the stable co-ordination of the γ phosphate of the ATP molecule with an aspartate residue in the Walker B homology sequence within the catalytic site (145).

Although the ATPase activity of P-gp is stimulated by drug, P-gp displays a high level of intrinsic or 'basal' ATPase activity. This basal ATPase activity may indicate that the process of ATP hydrolysis is partially uncoupled from drug movement (69). Alternatively, the presence of an endogenous component within the plasma membrane or the lipid annulus surrounding purified P-gp has been postulated as the basis of this activity. This endogenous component may be a phospholipid(s) as a range of phospholipids have been shown to stimulate P-gp ATPase activity dose-dependently (132). This study demonstrated that there were endogenous phospholipids associated with purified P-gp, and they consisted largely of phosphatidylethanolamine and phosphatidylserine and a small amount of phosphatidylcholine. This prompted study of the effect of the lipid environment on P-gp ATP hydrolytic activity. It is well established that the lipid environment is influential in affecting both basal ATPase activity and the extent of drug stimulation of ATPase activity (16, 27, 102, 105, 144).

Measures of P-gp related ATPase activity have revealed only one value of K_m, even though there are two catalytic sites. This suggested that hydrolysis occurred from one site only. This was further investigated employing the technique of vanadate trapping which stabilises the protein in a stage of the catalytic cycle that immediately follows ATP hydrolysis but precedes dissociation of the resultant MgADP. The vanadate ion interacts with Mg.ADP with high affinity and dissociates slowly from the P-gp.Mg.ADP.Vi complex, allowing study of P-gp at this stage of the catalytic cycle (see figure 1.14). By using Mg-8-azido-[α^{32}P]-ATP to trap P-gp with vanadate, it was found that to achieve full inhibition there was only one molecule of nucleotide diphosphate

trapped per molecule of P-gp, with no preference exhibited for either the N- or C-terminal NBD. This result suggested that not only are both NBD sites capable of hydrolysing MgATP, but they interact closely as trapping of nucleotide in one catalytic site prevented hydrolysis of nucleotide at the other (144). This finding was corroborated in a later study in which vanadate trapped protein was photochemically cleaved and trapped nucleotide found at one NBD only (54).

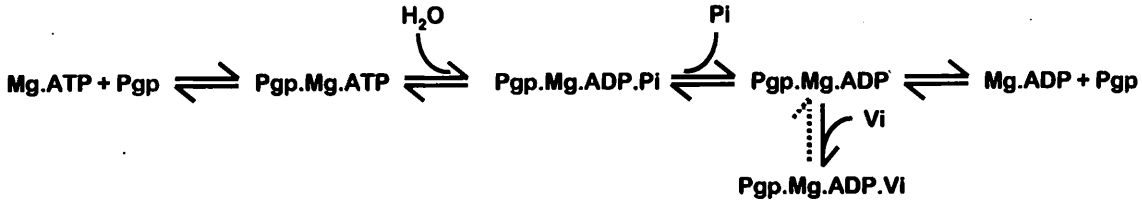

Figure 1.14 Scheme depicting ATP hydrolysis and vanadate-inhibition of P-gp ATPase activity.

The functional requirement for two nucleotide binding domains on P-gp is still puzzling and a combination of approaches, using either introduced mutations or catalytic inhibitors, have been used to probe their role in the catalytic cycle of P-gp. Studies employing the covalent reagent 7-Chloro-4-Nitrobenzo-2-Oxa-1,3-Diazole (NBD-Cl) showed that inhibition of ATP hydrolysis was complete when this compound covalently bound at a stoichiometry of 1 mol NBD-Cl mol^{-1} P-gp (2, 120). The inhibitory effect of NBD-Cl was reduced in the presence of ATP, indicating that this compound may be reacting at the catalytic site.

The strong interplay between the NBDs has also been demonstrated in mutational studies conducted by Loo & Clarke (76). They used a form of human P-gp from which the endogenous cysteines were removed following which single cysteine residues were systematically re-introduced into each NBD. Labelling of a cysteine residue within the

Walker A motif of either NBD (cys-431 and cys-1074 respectively) was sufficient to inactivate ATPase activity. These studies demonstrate the strong interdependence that exists between the NBDs of P-gp and illustrate an absolute requirement for two intact catalytic units.

The evidence from (i) vanadate inhibition (ii) stoichiometries for inhibiton by NEM and NBD-Cl and (iii) mutational analyses all imply that nucleotide hydrolysis by P-gp occurs by an alternating cycle. However, it is still unclear as to why two NBDs are required for function. Given that the NBDs of P-gp seem to alternate in ATP hydrolysis, does this indicate that they do not display equivalency of function? It was of interest to look at binding of the physiological substrate Mg.ATP to the NBDs and determine whether both domains could bind nucleotide with different affinities. Attempts to measure binding have been difficult due to the relatively low affinity with which nucleotide binds at the catalytic site. This has posed technical problems in attempts to measure binding stoichiometries or the K_d for nucleotide binding using radioligand binding assays, because of the high concentrations of [^{32}P]-ATP (mM) required to achieve saturable binding. In addition, trapping of bound complex is also difficult where binding affinities are low, due to rapid dissociation of bound complex. This problem was circumvented using a photoactivatable analogue of Mg.ATP, Mg-8-azido-[^{32}P]-ATP, to perform photolabelling studies. It was previously shown that 8-azido-ATP is a good hydrolysis substrate for P-gp with K_m values within the same range as those for Mg.ATP (144). Al-Shawi *et al.* (2) showed that Mg-8-azido-[^{32}P]-ATP labelled P-gp with a stoichiometry approaching 2mol mol^{-1} P-gp. Trypsin digestion of labelled P-gp revealed that label was evenly distributed between the N- and C-terminal NBDs illustrating that both NBDs are capable of binding Mg-8-azido-[^{32}P]-ATP and by extension Mg.ATP. However, it was not possible to determine the respective affinities of each NBD for Mg.ATP binding.

The fact that ATP can bind to either NBD and the observation from vanadate trapping experiments that both NBDs appear to be capable of ATP hydrolysis, has been taken as evidence that the NBDs of P-gp are indistinguishable in function. However, a recent study suggests that the catalytic domains of P-gp are functionally distinct. Hrycyna *et al.* (55) investigated nucleotide binding to P-gp, by looking at labelling of catalytic sites with Mg-8-azido-[α-^{32}P]-ATP under conditions where the protein can and cannot hydrolyse ATP. The C-terminal catalytic domain was preferentially labelled under hydrolysis conditions as shown in vanadate trapping experiments. On the other hand, the N-half was labelled with Mg-8-azido-[α-^{32}P]-ATP whether hydrolysis was possible or not. P-gp proteins containing point mutations that affect Mg^{2+} binding within the Walker B motif of the N- (D555N) and C- (D1200N) NBDs, were examined for their ability to bind nucleotide. The extent of labelling of C-terminal mutant was comparable to wild type, but binding of Mg-8-azido-[α-^{32}P]-ATP to mutant protein D555N was abrogated. This was taken as additional evidence for distinct functional roles of the two NBDs. It was suggested that binding of ATP to the N-terminal NBD may be necessary for hydrolysis of ATP to occur at the C-terminal catalytic site. This is the first study suggesting a non-equivalency in the role of the NBDs of P-gp.

There is evidence supporting distinct roles for the NBDs of other ABC proteins. The multidrug resistance associated protein (MRP1) also hydrolyses ATP effectively at the C-terminal NBD and displays preferential labelling of the N-terminal site (36, 53). Interestingly, the presence of Mg.ADP at NBD2 allosterically enhanced binding of Mg.ATP to the N-terminal site. A similar interplay between the NBDs was also reported for SUR1 (86) and TAP1/2, the transporter associated with antigen presentation (40). Non-equivalency in the role of the NBDs has also been reported for CFTR in an elegant

study conducted by Gadsby *et al.* (34). These authors demonstrated that hydrolysis of ATP at the N-site stimulated opening of the chloride channel whereas hydrolysis at the alternate NBD (C-site) brought about channel closure.

It is becoming clear that the NBDs of ABC proteins do possess distinct functional roles in catalysis and display strong interdependence in so doing. It is still unclear, particularly in the case of P-gp, what specific roles each individual NBD plays in drug transport. Do the NBDs transmit similar signals to the drug binding site during a transport cycle?

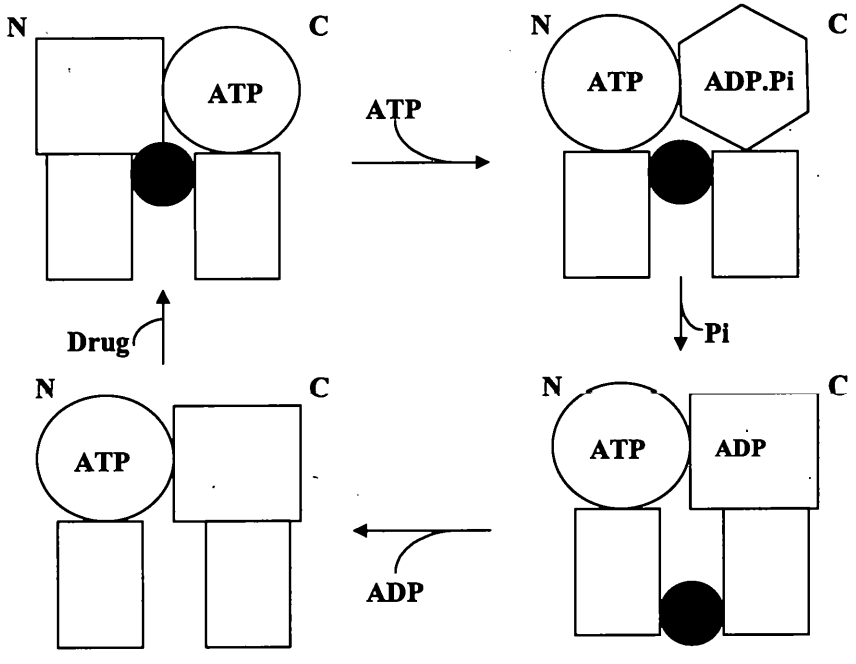

Figure 1.15 Proposed alternating catalytic sites cycle of ATP hydrolysis by P-glycoprotein. Rectangles represent the TMDs. Different conformations of the NBDs are represented by square, circle and hexagon (unfilled) Starting top left, N-site is empty. Binding of ATP to N-site NBD allows ATP hydrolysis at the C-site that induces a change preventing hydrolysis at the N-site. The ADP.Pi bound C-site is in a state of 'high chemical potential' (hexagon). Relaxation of C-site occurs upon release of Pi and is coupled to drug (filled circle) movement from inside facing high affinity site to outward low affinity site. Drug and ADP dissociate to end the cycle (adapted from (117)).

As outlined in figure 1.15, an alternating catalytic sites model relating the catalytic activity of P-gp to drug transport, has been proposed by Senior *et al.* (119). The model

of Senior and co-workers hypothesises that drug movement occurs post hydrolysis of ATP following release of Pi from the P-gp.ADP.Pi complex during the transport cycle. This hypothesis is still accepted but has not been rigorously tested. One of the aims of this thesis is to look at drug binding during different distinct stages of the catalytic cycle to determine when alterations in drug binding site are induced and elucidate the type of change wrought on the drug binding site.

1.11 How are signals transmitted between domains of P-gp?

To achieve active, vectorial transport, P-gp must transduce and couple signal between the drug binding domain(s) in the membrane and the cytoplasmically located catalytic domains. The signal transduction route adopted (figure 1.16) is unknown but the mechanism involved is via conformational alterations in the protein. Many different studies have looked at both intra- and inter-domain communication on P-gp using a variety of experimental approaches.

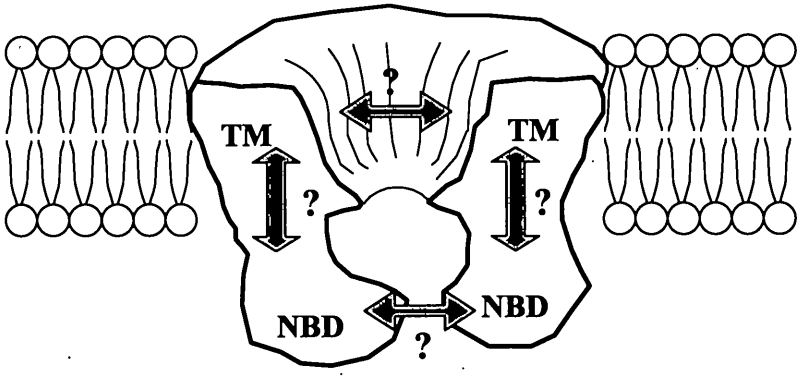

Figure 1.16 Communication within the P-gp molecule involves inter- and intra-domain signalling the routes of which are unknown.

1.11.1 Signalling between TMDs and NBDs

From study of drug transport and ATPase activity of P-gp it is known that communication exists between the TMDs and NBDs. Binding of drug does not affect nucleotide binding but does either stimulate or inhibit ATP hydrolysis by a process which must involve long-range communication. Communication between the TMDs and NBDs was further investigated by Sharom and co-workers who employed an elegant assay to investigate how the drug binding sites located at the TMDs communicate with the catalytic sites within the NBDs. They demonstrated that the sulfhydryl modifying agent 2-(4-maleimidoanilino)naphthalene-6-sulfonic acid (MIANS) covalently labelled the Walker A cysteines of NBD1 and 2 of P-gp purified and reconstituted from $CH^{r}B30$ cells (74). The fluorescence of MIANS was quenched and the rate of labelling of P-gp by the fluorescent probe was reduced by the addition of a range of cytotoxic drugs and modulators of P-gp. The authors concluded that this was indicative of long-range communication between drug binding sites, located in the membrane domain, and the catalytic sites within the NBDs.

1.11.2 Intra-domain communication on P-gp

Not only is there conformational signalling between the domains on P-gp, but there is also evidence for intra-domain communication. As discussed in a previous section in this introduction (1.8.1) there is a growing consensus that P-gp contains multiple distinct drug binding sites. However, although the binding sites are distinct they are linked as shown in radioligand binding studies where binding of the cytotoxic [^{3}H]-vinblastine, was allosterically modified by various modulatory compounds (29, 82). Such allosteric interaction is also indicative of domain:domain signalling within P-gp and will be explored further in chapters 4 and 6 of this thesis.

1.11.3 P-gp can exist in different conformations

A number of biochemical and biophysical studies have provided evidence suggesting that P-gp does undergo changes in conformation, particularly with respect to its catalytic cycle. This has been interpreted from studies designed to monitor changes in secondary and tertiary structures in the presence of nucleotide and drugs. Acrylamide quenching of tryptophan residues in purified reconstituted P-gp was investigated in the presence of nucleotide or a range of cytotoxic agents (138).. This study revealed that there was differential accessibility of tryptophan residues to quenching agent, which was dependent upon the nucleotide added, with more modest changes observed in the presence of drug. The same authors, by measuring the kinetics of $^{2}H/H$ exchange in the presence of MgATP and MgATP-verapamil, showed that there were major alterations in the tertiary structure of P-gp (137). Accessibility of the monoclonal antibody UIC2 to its extracellularly localised epitope, has also been used to monitor alterations in P-gp conformation. This antibody is conformationally sensitive and it was found that accessibility of UIC2 was decreased substantially due to binding of ATP. Binding of ATP conformationally reduced accessibility of the epitope for UIC2 and this effect was reversed in the presence of drugs such as cyclosporin A and vinblastine (87).

Similarly, study of proteolytic enzyme accessibility have been used to investigate the effect of different stages of the catalytic cycle on the conformation of P-gp. Wang *et al.* (154) investigated the proteolysis profiles of P-gp in the presence of Mg.ATP, Mg.AMP-PNP, Mg.ADP and Mg.ATP + vanadate. A total of four conformational states of P-gp were detected which were proposed to represent conformational cycling of P-gp during the catalytic cycle. In a later study this work was extended to investigate the trypsin sensitivity of mutants bearing single or double mutations in Walker A lysines or Walker B aspartate residues respectively, under conditions of vanadate trapping (60). The proteolysis profiles observed for the double mutants (both Walker A lysines) and the

single mutants (C-terminal Walker B aspartate) were significantly different to wild-type protein. This was due to the loss of ATP hydrolytic activity, but not ATP binding, in these mutants, as previously shown by Urbatsch *et al.,* (145). However, the trypsin digestion profile observed for the single mutant bearing an N-terminal aspartate substitution resembled that observed in wild-type, suggestive of a difference between homologous Walker B aspartate residues in NBD1 and 2. This result suggests that conformational cycling of P-gp during the catalytic cycle relies on the protein retaining full ATPase activity.

1.11.4 Functional relevance of conformational alterations in P-gp

Investigations highlighted in the preceding sections show that P-gp can adopt different conformations, particularly in response to the binding of nucleotides. How do the different conformations adopted by P-gp during the catalytic cycle affect drug binding? There have been few studies that have attempted to address this question directly, by looking at drug binding during the catalytic cycle. The binding of the photoaffinity prazosin analogue [^{125}I]-IAAP and [^{3}H]-azidopine with human P-gp, purified and reconstituted from insect cells, was significantly reduced in vanadate trapped protein (96). This abrogation in binding was only observed when protein was trapped under ATP hydrolysis conditions, indicating that ATP hydrolysis is required to induce a change in the drug binding sites. There was no effect of either ATP or ADP alone on drug binding properties. However, Ramachandra *et al.* did not directly investigate whether the abrogation in drug binding was due to altered affinity of [^{125}I]-IAAP and [^{3}H]-azidopine binding sites when the protein was vanadate trapped as only a single concentration of radioligand was used. The signal required to restore the drug binding site conformation during the catalytic cycle remains to be determined. Further investigation of conformationally driven alterations in drug binding site during the catalytic cycle will

provide insights into how drug binding and nucleotide interaction at the NBDs are coupled to generate transport. This will form a major portion of the work presented in this thesis.

1.11.5 Region(s) involved in transduction of signal between TMDs and NBDs

The question of signalling within and between domains is central to our understanding of the transport function of P-gp. However, what is not known are the regions on P-gp that are critical for signal transduction between the TMDs and the NBDs. There is some evidence suggesting a role for the intracellular loops that connect the TM helices in inter-domain signal transduction. In particular, a naturally occurring mutation in the first cytoplasmic loop (CL1) of P-gp from cells grown in high concentrations of colchicine, involving a glycine185 to valine substitution, has been associated with altered specificities for ligands. This was demonstrated by an alteration in the degree of resistance conferred by the mutant P-gp to the cytotoxic drugs colchicine, etoposide and adriamycin compared to wild type protein. The change in resistance was related to the ability of drug to interact with protein as demonstrated by altered drug stimulation of P-gp mediated ATP hydrolysis (92). Direct proof for altered drug handling by the G185V mutant was shown by Safa *et al.* (110) who demonstrated that decreased resistance to vinblastine was associated with increased binding of a photoactive analogue of vinblastine. In the same study, cells expressing mutant protein were more resistant to colchicine but had lower levels of colchicine binding compared to wild-type protein. Furthermore, glycine→valine substitutions at two additional positions in CL1 have also resulted in altered substrate specificity in MDR1 P-gp (75). These authors also introduced glycine mutations at several other intracellular loops and found altered resistance to colchicine and adriamycin with no alteration in resistance to vinblastine.

In a more recent study Kwan and Gros (70) used a random PCR mutagenesis method to introduce additional mutations into CL1 of mouse MDR3 P-gp (equivalent to human MDR1) and report a reduced ability of verapamil and valinomycin to stimulate ATPase activity in up to 70% of resultant mutants. This was also associated with loss of transport function in a smaller percentage of the mutants produced. In light of these studies it appears that CL1, and possibly other intracellular loops, do have a role to play in transmitting signals between the drug binding sites in the TMDs and the ATP hydrolysis sites at the NBDs. However, the nature of the change in drug specificities observed, as manifest by changes in drug stimulated ATPase activity or resistance profiles, is not known. It is not entirely clear whether altered drug resistance profiles or changes in drug stimulated ATPase activity is due to changes in (i) the binding affinity of drug or (ii) abrogation of the mechanism that couples drug binding to hydrolysis to effect drug transport. It is not inconceivable that the intracellular loops of P-gp may be actively involved in TMD:NBD communication. Interestingly, it has been shown in many prokaryotic ABC proteins that the intracellular loop connecting TM segments IV and V has a very highly conserved sequence, called the EAA-loop, that is essential for ligand transport (116). An EAA-loop has only been found in one eukaryotic ABC protein (a yeast orthologue of human ADLP) where mutations introduced into this loop abrogated transport activity (73). Mutations introduced in CFTR into the intracellular loop connecting TM segments IV and V, equivalent to the EAA-loop, disrupted opening and closing of the channel which may be dependent upon communication between the TMDs and NBDs (156). This observation suggests that the intracellular loops of ABC proteins in general may be important to mediate signal transduction between the membrane and cytoplasmic domains to elicit transport and lends support to the studies outlined above proposing a role for the intracellular loops of P-gp in signalling between the TMDs and NBDs.

1.11.6 Key residues in NBDs important for NBD:TMD signalling and drug specificity

Mutational analysis of the NBDs of P-gp has identified key residues that affect drug specificity and provides additional evidence that the NBDs can communicate with the TMDs. In studies of chimeric P-gp molecules where the NBD1 catalytic domain was replaced by the corresponding segments in NBD2, there was no loss of function except for a small segment (ERGA→DKGT (522-525)) located immediately upstream from the signature sequence and also at a single residue at position 578 (T→C) immediately downstream from the Walker B motif (7). The mutations completely disrupted verapamil stimulation of ATPase activity, but demonstrated that the protein still retained drug binding activity. All of the mutants displayed comparable levels of [^{125}I]-IAAP binding to wild type, that was displaced by a range of cytotoxic drugs and modulators (8). The mutations therefore seem to disrupt coupling of drug binding to hydrolysis of ATP. Another NBD mutation (K536R) has been shown to affect substrate specificity as manifested by enhanced resistance to colchicine. This mutation maps to a region upstream from the Walker B motif and immediately downstream from the ERGA/DKGT substitution mentioned above. The biochemical basis did not appear to involve abrogation of drug binding ability (51).

It has been postulated that the intracellular loops and the NBD residues highlighted in the above studies may be directly involved in transmission of signal between TMDs and NBDs. However, further study needs to be conducted in this regard to determine the location of putative signal transduction pathway(s) within the protein.

1.12 Objectives of thesis

In the absence of detailed structural information we are still very much heavily reliant on studies of P-gp function in order to obtain sufficient information to put together a working model of its transport activity. The clinical problem of MDR posed by the over-expression of P-gp in tumours is directly related to its ability to transport chemically diverse and functionally unrelated cytotoxics. Reversal agents or modulatory compounds have been used to overcome P-gp transport activity in the hope of re-sensitising tumour cells to cytotoxic agents. Indeed, the range of modulatory agents used is equally diverse.

The suggestion that P-gp lacks ligand specificity can now be refuted based on the results of studies suggesting the presence of distinct sites of interaction for ligand. The mechanism by which transport of ligand is mediated remains to be elucidated. However, it is known that drug binding at the TMD domain elicits a signal that is transduced to the NBDs to stimulate hydrolysis of ATP necessary for drug efflux to occur. The mechanism by which binding of modulators inhibits transport is not certain. Studies to date suggest that some modulators function by inhibiting ATPase activity or 'competing' for transport. Signalling between the TMDs and NBDs is via conformational signalling. Communication between these domains is a two-way process as decreases in drug binding have been observed when protein is trapped by vanadate immediately post-ATP hydrolysis. The region(s) on the protein involved in transduction of signal has not been identified.

The focus of this thesis is to use a pharmacological approach to characterise drug interaction with P-gp. I will be specifically concerned with elucidating further the mechanism by which multiple drugs can interact with P-gp. How many classes of site are there? For instance, do modulatory compounds interact at a site(s) that performs a

purely regulatory role and distinct from site(s) at which transport ligands may bind? Binding of drug at the TMDs does transduce a signal to the NBDs but is the signal transmitted dependent upon the molecule bound or the type of site occupied?

To address these questions I will use radioligand binding assays to directly characterise interaction of a range of cytotoxic drugs and modulatory agents with P-gp. The effect of drug interaction on P-gp activities such as ATPase and transport will be investigated in this initial characterisation. Then, using pairs of drugs, radioligand binding assays will be conducted to investigate the type of drug:drug interactions occurring on P-gp. This will yield information concerning whether drugs are interacting at the same site or not, particularly cytotoxic drugs and modulators. Studies of this kind have been lacking in the P-gp field to date.

A second major focus will be elucidation of how drug binding properties are altered as the protein undergoes a catalytic cycle and relating it to the transport cycle of P-gp. Again, radioligand binding assays are used to directly measure the binding parameters of the cytotoxic compound vinblastine at different discrete stages of the catalytic cycle. In terms of transport activity, binding sites for transported substances must cycle between low and high affinity conformations to facilitate transbilayer movement. I want to establish the stage in the cycle when the initial signal is transmitted from the NBDs to the vinblastine site to initiate transport. What is the nature of the change wrought on the vinblastine site and what triggers restoration of binding site to its pre-transport conformation?

Based on the pharmacological investigations conducted in this thesis models depicting (a) an interconnecting network of ligand interaction sites and (b) a molecular mechanism for P-gp transport activity have been devised.

Chapter 2

Materials and Methods

2.1 Introduction

In order to gain a clearer understanding of how drugs interact with P-gp it was necessary to develop a radioligand binding assay that would allow a direct and quantitative assessment of drug binding characteristics of this protein. Such an assay would provide important information concerning the potency of drug interaction, the binding site capacity on the protein, the type of site occupied by drug and the rate at which drug associates/dissociates. Although the range of compounds interacting with P-gp is extensive, they can be divided into two major classes a) transported ligands and b) modulators of the transport process. P-glycoprotein can be equated to a classic drug receptor and therefore is amenable to study using classical pharmacological techniques. Thus information can be obtained concerning the molecular pharmacology of drug interaction with P-gp in particular whether binding is to a single site or to multiple sites exhibiting high affinity for ligand. In addition, such studies may provide insight into the mode of modulator inhibition of transport function.

2.2 Drug Receptor Interaction

Simple occupation of receptor by ligand may be described by the Law of Mass Action. If P-gp is viewed as a receptor then binding of drug to P-gp can be described by the following;

$$[P] + [D] \underset{k_{-1}}{\overset{k_1}{\rightleftharpoons}} [PD] \qquad (2.1)$$

where k_{+1} and k_{-1} are the rate constants for association and dissociation reactions respectively. [P] denotes binding site on P-gp, [D] is drug and [PD] is the P-gp-drug complex. According to the law of mass action, the forward reaction rate is given by

$k_{+1}[P][D]$ and the reverse reaction by $k_{-1}[PD]$. At equilibrium, the forward and reverse reaction rates are equal

i.e. $$k_{+1}[P][D] = k_{-1}[PD] \quad (2.2)$$

By re-arrangement of this relationship the equilibrium dissociation constant for the reaction can be determined and it provides a measure of the affinity of ligand for its receptor

$$\frac{[P][D]}{[PD]} = \frac{k_{-1}}{k_{+1}} = K_d \quad (2.3)$$

A relationship representing the fraction of sites on P-gp occupied by drug can be derived from equation 2.3 by making the following substitutions;

$[P_t]$ denotes the total number of sites on P-gp available to ligand and can be represented as;

$[Pt] = [P] + [PD]$ and substituting in 2.3;

$$\frac{[Pt][D]}{[PD]} = K_d + [D] \quad (2.4)$$

thus the fraction of sites on P-gp that are occupied is represented by

$$\frac{[PD]}{[P_t]} = \frac{[D]}{[D] + K_d} \quad (2.5)$$

This equation derived from first principles is also known as the Langmuir adsorption isotherm, which was derived to model the binding of gas molecules to a surface (71) and can be used to describe binding of drug to receptor. This model assumes that binding is to a homogeneous class of non-interacting binding sites. The equation yields a hyperbolic curve relating fractional receptor occupancy ($[PD]/[P_T]$) to drug concentration. When this equation is plotted as a function of $\log_{10}[D]$, a sigmoidal curve is produced with a slope factor equivalent to a Hill number of 1. The Langmuir isotherm model assumes that the Hill slope will always be unity. The slope of the binding curve provides an indication of whether drug is binding independently to one or more sites, or whether there is co-operativity occurring whereby binding of a drug molecule affects the binding of other drug molecules. If there is positive co-operativity of binding, the curve will have $n>1$, whereas negative co-operativity manifests as a shallow sigmoidal curve with $n<1$.

To model binding of ligand to two sites on a receptor, an equation that is the sum of two Langmuir equations can be used as shown below;

$$Y = \frac{[D]}{[D]+K_{d1}} + \frac{[D]}{[D]+K_{d2}} \qquad 2.7a$$

where Y is the fraction of sites on P-gp bound and K_{d1} and K_{d2} are the equilibrium dissociation constants for binding to two sites of differing affinity.

An alternative pharmacological model to the Langmuir isotherm may also be considered.

$$[P] + [D] \underset{k_{-1}}{\overset{k_1}{\rightleftharpoons}} [PD]$$

$$[P] + [PD] \underset{k_{-2}}{\overset{k_2}{\rightleftharpoons}} [PD_2] \qquad (2.6)$$

Interaction of drug [D] with two sites on [P] can be described where an initial equilibrium may be established with association and dissociation rate constants of k_{+1} and k_{-1} respectively. The [PD] complex may then bind a further drug molecule with association and dissociation rate constants of k_{+2} and k_{-2} respectively. Adair used the pharmacological scenarios described in 2.6 to derive the following equation as outlined in appendix I;

$$Y = \frac{k_2[D] + 2[D]^2}{2\left(k_1 k_2 + k_2[D] + [D]^2\right)} \qquad (2.7)$$

where Y is the fraction of sites bound.

This is the equation formulated by Adair, which describes binding of ligand to two sites on its receptor in the absence of co-operativity (Adair, 1925). When modelling radioligand-binding data obtained in this thesis, these different pharmacological scenarios were used to assess the type of drug interaction observed.

2.2.1 Model testing.

An iterative process using the sum of squares is used to determine how experimentally produced data points fit the model parameters. This involves squaring the differences between the actual data points (y) and the calculated data point (yc) (for each different parameter) until the smallest difference is obtained using the following model;

$$SSq = \sum (y - yc)^2 \qquad (2.8)$$

The appropriateness of a particular model for a particular dataset can be tested by comparing data fitted with a more complex model to those fitted by a simpler model. This is achieved using the F statistic, which determines whether there is a significant difference between the complex model versus a simple model from the following equation;

$$F = \frac{((SSq(c) - SSq(s))(df_s - df_c))}{SSq(c)/df_c} \qquad (2.9)$$

where df refers to the degree of freedom of the model (number calculated from the difference between the number of data points and the number of fitting parameters in the model). If the value of F is not high enough to support a significant difference between these models, then the simpler model should be used to fit the data.

2.2.2 Standard saturation binding isotherms

Radioligand binding assays were conducted using P-gp containing CH^{r}B30 plasma membrane vesicles in all cases. The binding of the cytotoxic drugs [^{3}H]-vinblastine and [^{3}H]-paclitaxel and the modulatory drug [^{3}H]-XR9576 was characterised by measuring the amount bound as a function of radioligand concentration (i.e. saturation isotherm analysis).

Membrane vesicles were incubated in binding buffer (50mM Tris.HCl pH 7.4) with increasing concentrations of radiolabelled drug (added from 4X stock in binding buffer) in a total reaction volume of 100µl. The amount of membrane added to the reaction tubes varied depending upon the radioligand used. Tubes were set up in quadruplicate

for each concentration of radioligand. The non-specific binding component (nsb) of the reaction was determined at each concentration of radioligand. A 100-fold excess of an unrelated non-radiolabelled drug, which also interacts with P-gp, was added to two of the four tubes. The remaining two tubes gave a measure of total radioligand bound to the membrane vesicles. Samples were incubated in the dark for 2-3 hours at room temperature, to ensure binding equilibrium was reached (refer to Chapter 3). Stock solutions of non-radiolabelled drugs were usually made up in DMSO. The final concentration of DMSO never exceeded 1% (v/v) in any of the reactions, as higher concentrations interfere with drug binding. Due to the high degree of hydrophobicity of the radiolabelled drugs used in this thesis, all 4X stocks were made up in borosilicate glass test-tubes to minimise loss of drug due to binding to the glassware from aqueous solutions.

Following the appropriate incubation period, unbound radiolabel was separated from bound complex, by rapid filtration. A custom-made filtration box comprising 48 wells was used and was connected to a vacuum pump (KNF Neuberger, U.K. Ltd., type: PME0053 NO35 AN18). Samples were passed under vacuum (600mbar) through single GF/F glass fibre filters, which were pre-soaked in wash buffer (20mM Tris-HCl, pH 7.4, 20mM $MgSO_4$) containing 0.1%(w/v) BSA, followed by washing with 2 X 3ml wash buffer. Glass-fibre GF/F filters were used based on a screen previously conducted in our laboratory of different filter types. This type of filter offered the highest retention of radiolabelled-P-gp complex with minimal adsorption of unbound radiolabel. Filters were briefly pre-soaked with BSA to further reduce retention of unbound ligand.

The amount of radioactivity trapped on the filters was measured using liquid scintillation counting. The amount of radiolabel added to each tube was also measured by

scintillation counting by aliquoting the appropriate volume directly into scintillation vials. The results were displayed in disintegrations per minute (dpm) and using the specific activity of the radioligand, the dpm measured were converted to determine a) the molar amount of radioligand added to the assay tubes and b) the amount of drug bound to trapped membrane vesicles. Specific binding of radiolabel to P-gp was quantitated by subtracting the amount bound in the presence of an excess of unlabelled ligand, from the total amount bound (absence of unlabelled ligand). Specific binding (pmol mg^{-1} membrane protein) was plotted as a function of free radioligand concentration (nM) using the Langmuir binding isotherm, as described in section 2.2 from which parameters such as binding capacity (B_{max}) and K_d were obtained.

2.2.3 Homologous displacement of binding to extend saturation isotherm binding

Measuring binding parameters of a drug over a wider concentration range is often not possible using radiolabelled drugs, due to limits imposed by the stock concentration and the specific activity of radioligand. Strategies have been devised where this problem can be circumvented by combining two different types of binding assay (106). This can be achieved by performing a saturation binding assay over a range of radiolabelled drug concentrations and then extending the range by diluting the highest radioligand concentration, with increasing amounts of unlabelled ligand. It is possible to extend the range of ligand concentration over which binding is measured several fold. This approach was adopted to look at [^{3}H]-vinblastine binding to P-gp as follows.

Membranes (15μg) were incubated with increasing concentrations of [^{3}H]-vinblastine up to 100nM in the presence and absence of an excess of nicardipine (3μM) (which was sufficient to measure the n.s.b. component of binding). To measure binding over higher concentrations of vinblastine, membranes (15μg) were incubated with 100nM [^{3}H]-

vinblastine and increasing amounts of unlabelled vinblastine (up to 3000nM vinblastine) in the presence or absence of 3μM nicardipine. Unlabelled vinblastine was added from 100X DMSO stocks as 1μl aliquot in a total reaction volume of 100μl. Samples were incubated in the dark for 2-3 hours to reach equilibrium.

Bound ligand was separated from unbound by rapid filtration, and filter-entrapped radioactivity measured by liquid scintillation counting. The amount of ligand bound at the lower concentration range was calculated as outlined above for saturation binding. The amount of vinblastine bound in the homologous displacement assay was calculated by using the diluted specific activity of [^{3}H]-vinblastine at each added concentration of unlabelled vinblastine. The amount of bound dpm measured was then transformed to pmol vinblastine bound per mg membrane protein. The binding measured in the presence of nicardipine was subtracted from both the saturation binding data and the homologous displacement data to give specific vinblastine bound. Both data sets were combined and plotted as a function of ligand concentration.

2.2.4 Heterologous displacement of binding

Heterologous displacement of binding involves displacement of radioligand by an unlabelled drug distinct from the radioligand. These assays involved labelling of membranes with a single concentration of radioligand and using a range of concentrations of unlabelled drug to displace radiolabelling.

Membranes were incubated with either none or increasing concentrations of unlabelled competing drug and a fixed concentration of radiolabelled drug in binding buffer for 2-3 hours. Details concerning the amount of protein or concentration of radiolabelled drug employed, with respect to the various radioligands used in this thesis, are outlined in

Chapter 3. Bound ligand was separated from unbound by rapid filtration and filter-retained radioactivity measured by scintillation counting. Specific dpm were plotted as a function of the logarithm of displacing agent concentration and the effect of antagonist analysed using the dose-response relationship described by DeLean *et al.* (24)

$$Y = \{(a-b)/(1+(x/c)^{d})\}+b \qquad (2.10)$$

where Y is amount bound, a = initial binding, b = maximal binding, c = EC_{50} concentration (log M), d = slope factor and x = drug concentration (log M). EC_{50} denotes the concentration of antagonist that displaces 50% of the bound radioligand, and provides an estimate of the potency of the antagonism.

However, EC_{50} or IC_{50} values are not constants and are dependent upon the concentration of ligand displaced. A useful transformation of this parameter was devised by Cheng & Prusoff whereby IC_{50} values can be expressed as inhibition or antagonist affinity constants (K_i) using the equation below (19);

$$K_i = \frac{IC_{50}}{1+\frac{[L]}{K_d}} \qquad (2.11)$$

where K_i is antagonist affinity constant, IC_{50} is concentration of antagonist to displace 50% of bound radioligand, [L] = concentration of radioligand bound, K_d = equilibrium dissociation constant of radioligand. Estimates of K_i will only be valid where slopes of displacement curves are equal to or constrained to 1.

2.3 Drug-Receptor binding kinetics

In all studies of receptor-ligand interaction, knowledge of the kinetics of binding is essential. Investigation of the binding kinetics of drug with receptor provides

information concerning the onset and duration of drug action at a receptor. The rate of formation of drug receptor complex over time (d[PD]/dt) is dependent upon the difference between the rate at which drug associates with receptor and dissociation of drug receptor complex represented as follows;

$$\frac{d[PD]}{dT} = k_1[P][D] - k_{-1}[PD] \qquad (2.12)$$

The following function was derived from 2.12 as described in appendix II

$$\frac{[PD]}{[PD]_{eq}} = 1 - e^{-k_{obs}\, t} \qquad (2.13)$$

where $[PD]_{eq}$ is the amount of drug receptor complex at equilibrium; k_{obs} is the association rate for formation of $[PD]/[PD]_{eq}$ over time. But k_{obs} is a function of the drug concentration used and the dissociation and association rate constants as described below;

$$k_{obs} = k_1[D] + k_{-1} \qquad (2.14)$$

To determine the association rate constant, K_{obs} measured at different concentrations of radioligand is plotted as a function of ligand concentration. The slope of the linear relationship (equation 2.14) yields a value for k_1 the association rate constant (concentration^{-1}, time^{-1}).

2.3.1 Association kinetics of radioligand binding

The rate of onset of both [^{3}H]-vinblastine and [^{3}H]-XR9576 with P-gp was measured in CH^{r}B30 membranes. Membrane vesicles (2μg for [^{3}H]-XR9576 and 10μg for [^{3}H]-vinblastine) were incubated with a fixed concentration of tritiated drug (within the range 5-75nM) for fixed time intervals up to 2 hours. Binding reactions were set up in

quadruplicate by adding radiolabelled drug (75µl in binding buffer) to borosilicate glass test-tubes. The association reaction was begun with the addition of membrane protein (25µl) to the reaction tubes at timed intervals, in the presence or absence of an excess concentration of nicardipine (3µM). Reaction was stopped by rapidly filtering all of the samples together under vacuum, as previously described. Filter-entrapped radioactivity was measured and the amount of specifically labelled protein calculated. The association rate constant was determined from the binding data as described in the previous section.

2.3.2 Dissociation kinetics for drug-receptor complex

The rate of offset or the dissociation rate constant (k_{-1}) of either [^{3}H]-vinblastine or [^{3}H]-XR9567 was measured by labelling CH^{r}B30 membranes (10µg and 2µg respectively) with a fixed concentration of labelled drug (ususally K_d concentration) to equilibrium (2-3 hours at room temperature). The association reaction was stopped at timed intervals by adding a large excess of unlabelled drug vinblastine or XR9576 respectively (100-fold) from concentrated DMSO stocks. Dissociation of [^{3}H]-XR9567 was measured by adding unlabelled XR9576 (3µM) over the following time intervals, 0, 2, 4, 6, 8, 10, 15, 20, 30, 40, 50, 60 minutes to the [^{3}H]-XR9576-P-gp equilibrium complex. Dissociation of [^{3}H]-vinblastine was measured by adding unlabelled vinblastine (3µM) at intervals over 40 minutes (0, 2, 4, 6, 8, 10, 15, 20, 25, 30, 40). Different time courses were followed to accommodate differences in the off rate of the two radioligands. Samples were filtered sequentially at the end of the time-course.

In order to look at the effect of a second unrelated drug on the dissociation kinetics of radioligand as determined using the method outlined above, the assay was modified as follows. For example, dissociation of [^{3}H]-vinblastine was measured by adding excess unlabelled vinblastine, in the presence of an excess concentration of a second unrelated

drug, to the radioligand-P-gp complex for timed intervals. The concentrations of drug used in such experiments are detailed in Chapter 4.

2.4 Competitive & Non-competitive antagonism

Studies of antagonism of radioligand binding yield important information concerning (i) sites of interaction of drugs on P-gp, (ii) the effect of drug on the binding of other ligands and (iii) provide a measure of antagonist affinity. In general, antagonists may be classified into two broad groups namely, competitive and non-competitive. Competitive antagonism describes the binding of competing drug to the same site as the 'agonist'. This kind of competition manifests as a parallel shift to the right in the binding dose-response curves where increasing concentration of 'agonist' overcomes the effect of the competing drug to obtain maximal binding again. However, non-competitive drug interaction is due to binding of drug at an alternative site on P-gp. This inhibition of binding often manifests as a reduction in maximal binding and does not always cause a shift in the dose-response curve. In conducting studies to delineate the type of interaction occurring between drugs on a protein, it is important to use a range of antagonist concentrations in order to be able to fully assess the nature of the antagonism.

A mathematical equation to predict competitive effects of antagonist on interaction of agonist was first devised by Gaddum (33). If drug interacts with protein in a competitive manner then the following products will be produced;

$$[D] + [A] + [P] \rightleftharpoons [AP] + [DP] \tag{2.15}$$

As detailed in Appendix III, fractional saturation in the presence of antagonist is given by;

$$\frac{[DP]}{[P_T]} = \frac{[D']}{[D'] + K_d (1 + [A]/K_A)} \tag{2.16}$$

where $[D'] > [D]$ and represents the concentration of drug required to produce the same fractional saturation in the presence of antagonist.

Schild derived a useful equation based on the Gaddum model (equation 2.16), allowing a convenient means of estimating antagonist affinity (K_A) through linear regression of a series of dose ratios obtained over a range of antagonist concentrations (5):

$$\log (DR - 1) = n \log[A] - \log K_A \qquad (2.17)$$

DR refers to the ratio of equiactive concentrations of agonist, (usually defined as producing 50% occupation of receptor), in the presence and absence of antagonist. If the agonist-antagonist interaction is truly competitive, the above relationship will be linear over a wide concentration range with a slope of n=1. The x-intercept will then provide an estimate of K_A when the slope is equal to or constrained to 1. This type of analysis has been termed Schild analysis (see Kenakin, 1997). It is a powerful tool in pharmacology to differentiate between competitive and non-competitive interactions. This is particularly important as some non-competitive antagonists do produce parallel shifts in agonist dose-response curves but when Schild analysis is applied, fail to produce a linear curve with slope equal to unity.

Non-competitive drug interactions can also be investigated by following the effect of antagonist on the dissociation kinetics of agonist. If the rate of dissociation of an agonist is increased or decreased in the presence of antagonist, this is indicative of a non-competitive interaction according to the law of mass action. Such an effect can only be exerted through an allosteric interaction between the sites of interaction of the agonist and antagonist. Therefore interactions of drugs with P-gp were examined using

equilibrium binding or Schild Analysis in conjunction with kinetic analyses as detailed in Chapter 4.

2.5 Cell Culture

Drug resistant Chinese hamster ovary cells (CHOs) that over-expressed P-gp (CH^rB30) were used as the source of P-gp in this thesis. The cells were routinely grown at 37°C, 5% CO_2, in α-minimal essential medium (α-MEM) including 10% foetal bovine serum and supplemented with 30μg ml^{-1} colchicine to maintain selection of resistant cells. The CH^rB30 cells were originally derived from AuxB1 cells by step-wise selection in colchicine, as described in detail elsewhere (62). The parental AuxB1 cells were grown under the same conditions as CH^rB30 cells but without inclusion of colchicine in the media. All of the cells used in this thesis were grown at the ICRF tissue culture facility at Clare Hall except those used in steady-state drug accumulation assays.

2.5.1 Plasma membrane vesicle preparation

Plasma membrane vesicles were prepared by disruption of CH^rB30 cell membranes using nitrogen cavitation at a pressure between 1000-1500psi for 3 cycles of 15 minutes at 4°C. Protease inhibitors (leupeptin, 0.1mg ml^{-1}, pepstatin A, 0.1mg ml^{-1}, benzamidine, 1mM) were included in the disruption buffer (10mM Tris, 250mM sucrose, 0.2mM $CaCl_2$, pH 7.4). Membrane vesicles were collected from the lysed cell suspension following sucrose density centrifugation for 30 minutes at 30,000g on a 35% (w/v) sucrose cushion. Membranes at 0-35% sucrose interface were collected and pelleted at 100,000g over 45 minutes at 4°C. Pellets were resuspended at a protein concentration of approximately 20mg ml^{-1} in buffer (10mM Tris, pH 7.4, 250mM sucrose) containing protease inhibitors listed above and stored at –80°C for up to six months.

2.5.2 Purification of P-gp from CH^{r}B30 membrane vesicles.

Anion exchange chromatography was used to enrich P-gp from CH^{r}B30 membrane vesicles to 60% purity and the purification method is outlined in detail in Callaghan *et al.*, (16). In brief, P-gp containing membranes (protein content 5mg ml^{-1}) were solubilised in 1%(w/v) dodecyl-maltoside with 0.4% (w/v) crude lipid mixture (asolectin) in a low ionic strength buffer containing 10mM pipes, pH6.9, 1mM EDTA, 0.02% NaN_3 (w/v), 18%(v/v) glycerol. The soluble protein was passed down a 5ml bed volume anion-exchange column (Econo-pac High Q). All chromatography buffers contained 0.1%(w/v) dodecylmaltoside to maintain protein solubility. Protein was eluted with a continuous linear gradient of NaCl. P-gp containing fractions were identified by SDS-PAGE and concentrated to approximately 1mg ml^{-1} protein, using 50kDa membranes in an Amicon stirred cell concentrator.

2.5.3 Reconstitution of P-glycoprotein

2.5.3.1 Liposome preparation

The phospholipids phosphatidylcholine (PC) and phosphatidylethanolamine (PE) were used as the lipid system for the reconstitution of purified P-gp. PC and PE in the ratio 9:1 (w/w) were dried from chloroform stocks under N_2 onto glass test tubes. A trace amount of [^{3}H]-PC (0.1μCi/10mg lipid) was added to the lipid film to help detect lipids in analyses. The lipid films were suspended at 10mg ml^{-1} in buffer A containing 150mM NaCl, 1mM EDTA, 50mM Tris.HCl, pH7.4 by vortexing. The lipid suspensions were subjected to five freeze-thaw cycles to create larger liposomes that were predominantly multilamellar. These multilamellar vesicles were extruded through 200nm filters to produce unilamellar liposomes (see (16)).

2.5.3.2 Reconstitution procedure using SM-2 BioBeads

P-gp purified by anion-exchange chromatography is contained within protein/dodecylmaltoside (0.1%(w/v) detergent) micelles. Dodecylmaltoside (DDM) was the detergent of choice for the purification of functionally active P-gp (16). However, it was not possible to effectively reconstitute P-gp at low lipid/protein ratios using DDM. As described in Rothnie *et al.* (105) decylmaltoside (DM) was used to effectively reconstitute P-gp. Liposomes saturated with decylmaltoside were added to the solubilised protein at a ratio of 3:1 to ensure that (i) (DM) is the major detergent species present and (ii) the concentration of DDM is brought below its critical micellar concentration thereby facilitating its removal. The detergent/lipid/protein mixture is left to equilibrate on ice for a 40 minute period. Reconstitution is achieved by removal of detergent and the technique employed was detergent adsorption to SM-2 BioBeads. Bio-Bead additions (40mg ml^{-1}) were repeated at 40 minute intervals.

The efficiency of reconstitution was assessed by following the relative migration of protein and lipid through sucrose density gradients. Proteoliposomes (10µg) were diluted to a volume of 200µl and mixed with equal volume of 60% sucrose (w/v) in buffer A containing 0.05% (w/v) Triton-X-100. This was sequentially overlayed with 400µl each of 20, 10, 5 and 0% (w/v) sucrose solutions in buffer A. Samples were centrifuged at 150,000 X g for 8-10 hours at 4°C to reach equilibrium. Following centrifugation, 200µl fractions were taken throughout the gradient. Protein was precipitated from 150µl of each fraction using trichloroacetic acid. Pellets were resuspended in 20µl of solution containing 4% (w/v) SDS, 0.2M Tris.HCl pH 10, 0.15M NaOH and 5µl 5X Laemmli sample buffer (10%(w/v) SDS, 0.25%(w/v) DTT, 1.5M Tris.HCl pH 6.8, 18% glycerol, 0.5M EDTA, 0.01% (w/v) bromophenol blue). Samples were subjected to 8% SDS polyacrylamide electrophoresis (SDS-PAGE). Protein was located by silver-staining, using Rapid Ag Stain Kit (ICN) according to the

manufacturer's protocol. The location of phospholipid in the gradient was detected by taking 50µl of each fraction and subjecting to liquid scintillation counting.

2.6 Measurement of P-gp mediated ATPase activity of CH^{r}B30 membranes

P-gp-mediated ATPase activity was measured by following inorganic phosphate (Pi) release using a modification of a colorimetric assay developed by Chifflet (20). In brief, a microtitre plate assay has been developed to measure activity in the presence and absence of drugs that either stimulate or inhibit ATP hydrolysis. Membrane vesicles (1µg) were incubated in ATPase buffer (150mM NH_4Cl, 50mM Tris, pH 7.4, 5mM $MgSO_4$, 0.02% NaN_3) with either (i) 2mM Na_2ATP in the presence or absence of increasing concentrations of drug (see results Chapter 3) or (ii) a range of ATP concentrations (0-3mM) in the presence or absence of a single concentration of drug that produces a maximal effect on P-gp ATPase activity in a total volume of 50µl. Drugs were added as 1µl aliquots from concentrated DMSO stocks. Reactions were allowed to proceed at 37°C for 25 minutes (it had been previously determined in this laboratory that activity is linear up to 40 minutes at 37°C). Non-P-gp related ATPase activity of CH^{r}B30 membranes was accounted for by measuring activity in the presence of 200µM sodium vanadate. Sodium vanadate inhibits activity of P-type ATPase proteins including P-gp. The contribution of other ATPase proteins present in the membrane vesicles used, was also eliminated by omitting Ca^{2+}, Na^+ and K^+ ions from the ATPase buffer.

Hydrolysis was stopped with the addition of 40µl 12%(w/v) SDS solution to each well. To detect Pi released in the hydrolysis reaction, 100µl 1% (w/v) ammonium molybdate solution was added to form a complex with Pi. Samples were incubated at room temperature for 5 minutes to allow formation of phospho-molybdate complex. Samples were further incubated at 37°C for 15 minutes with 100µl 2%(w/v) sodium

citrate/arsenite/acetic acid solution to stabilise colour formation. Absorbance was read at λ = 750nm using a plate reader (Spectra Max 250, Molecular Devices). A standard curve was set up of known amounts of Pi (0.1-10nmoles) to quantitate nmoles Pi released in assays.

P-gp associated ATPase activity in CH^{r}B30 membrane vesicles was determined by subtracting nmoles of Pi released in the presence of 200μM sodium vanadate from all values, to eliminate contributions from non-vanadate-sensitive ATPase proteins as previously described (1). The vanadate-sensitive ATPase activity was expressed as nmoles Pi released minute^{-1} mg^{-1} membrane protein and was plotted as a function of drug or ATP concentration according to the experiment performed. In general, when experiments were conducted investigating the effect of a single concentration of drug on the kinetics of ATP hydrolysis i.e. V_{max} and K_m for ATP, results were plotted using the Michaelis-Menten equation below;

$$Y = \frac{V_{max}[S]}{K_m + [S]} \qquad 2.16$$

where Y is ATPase activity (nmol min^{-1}mg^{-1} membrane protein), V_{max} is maximal activity (nmol min^{-1}mg^{-1} membrane protein), [S] is ATP concentration (mM), K_m is the concentration of ATP which produces 50% maximal activity. In experiments designed to look at the ability and potency of drug to affect the ATPase activity of P-gp, data were plotted as fold change in basal activity as a function of drug concentration using the general dose-response equation (equation 2.10). Fold change in basal activity was calculated by expressing activity measured in the presence of drug as a fraction of that measured without drug present.

2.6.1 Vanadate-trapping of P-gp

As mentioned in the preceding section, sodium vanadate is a potent inhibitor of P-gp mediated ATPase activity. The mechanism of this inhibition is due to the ability of the vanadate ion to mimic Pi. Following hydrolysis of ATP, formation of nucleotide diphosphate/Pi complex results. This complex is transient and when Pi dissociates, vanadate can interact with the remaining bound ADP molecule to form a stable transition complex with P-gp. This feature of vanadate has been exploited to "conformationally restrict" P-gp and other ATPases to enable structural and functional studies.

Sodium orthovanadate stock solutions (100mM) were made up in water and adjusted to pH10 and subsequently boiled for 2-5 minutes to eliminate the presence of polymeric species prior to each use as described by Goodno (39). Trapping studies were conducted by first incubating $CH^{r}B30$ membrane vesicles (4μg μl^{-1}) with 2mM Na_2ATP or 8-azidoATP, 0.3mM $NaVO_3$, 50μM verapamil and ATPase buffer, in a total volume of 400μl over 25 minute period at 37°C. Verapamil was included in the reaction as it stimulates ATP hydrolysis and thus increases the rate of trapping by vanadate. Reactions were stopped by placing samples on ice. Components that were not used up by the reaction were removed by centrifuging 120μl aliquots through 1ml sephadex G-50 gel filtration spin columns at 300g for 4 minutes at 4°C as described in Urbatsch and Senior (147). Spin columns were pretreated with ATPase buffer prior to use. Where trapped samples were used in radioligand binding studies to measure the ability of drug to interact with trapped P-gp molecules, vanadate (300μM) was included in the spin-column equilibration buffer to prevent dissociation of Vi over the course of the binding experiment.

Some trapping experiments were conducted using 2mM 8-azidoATP as it was desirable to have P-gp molecules with ADP covalently bound (refer to Chapter 5). Identical trapping conditions were used except that 20%(v/v) glycerol was included in the ATPase buffer and the azido nucleotide was cross-linked to the protein following the trapping reaction. Cross-linking was achieved by placing samples on ice at a distance of 5cm from the U.V. lamp (Blak Ray, Model B 100 AP; from UPL, Upland, CA91786, USA) and exposed to U.V. light for 4 minutes. Unbound reaction components were removed using spin columns.

Removal of bound vanadate was achieved by incubating trapped protein at 37°C for up to 2 hours.

2.6.2 Photoaffinity labelling of reconstituted P-gp with 8-azido[α-^{32}P]ATP

Proteoliposomes (8μg) were incubated with 2μM 8-azido[α-^{32}P]ATP (2-10Ci mmol^{-1}) in ATPase buffer including 20% (v/v) glycerol, in the presence of increasing concentrations of unlabelled ATP (0.01-1mM). Reactions were made up in a final volume of 70μl and incubated for 15 minutes at 37°C. Labelling was stopped by placing the samples on ice. Bound nucleotide was cross-linked to the protein by U.V.-irradiating samples (100W) for 4 minutes on ice at a distance of 5cm. Unbound nucleotide was removed by trichloroacetic acid precipitation of P-gp, followed by electrophoresis on 8% SDS-PAGE gels. The relative labelling efficiency of the samples was measured by autoradiography of the gels.

2.7 Steady-state drug accumulation assay

AuxB1 and CH^{r}B30 cells were grown to confluent monolayers in 12-well (24mm) tissue culture dishes. Monolayers were washed with phosphate-buffered saline (PBS) and then

incubated in 1ml transport buffer (100mM NaCl, 10mM Tris, 25mM $NaHCO_3$, 5mM KCl, 2mM $CaCl_2$, 1mM $MgCl_2$ and 7mM glucose). Competing agents were added in the concentration range 10^{-9} to 10^{-5}M from DMSO stocks giving a final solvent concentration of 0.2%(v/v). The steady-state accumulation of either vinblastine or paclitaxel was started with the addition of 0.1μCi radiolabelled drug and up to 100nM unlabelled drug respectively. Samples were incubated over a 1 hour period at 37°C under 5%CO_2, to reach steady-state. This period of time has previously been shown to be sufficient to achieve steady-state accumulation of drug in Chinese Hamster Ovary cells (R.Callaghan personal communication). Monolayers were washed with 2 X 2ml ice-cold PBS. Cells were harvested with 0.4ml of 0.4M NaOH, and the cell extract neutralised with 0.8ml of 0.25M ammonium acetate (pH6.6). Radioactivity was measured using liquid scintillation counting and normalised for cell protein content. The general dose-response equation was used to plot [^{3}H]-vinblastine or [^{3}H]-paclitaxel accumulated (pmol mg^{-1} cell protein) as a function of modulator concentration. The amount of [^{3}H]-XR9576 accumulated (pmol mg^{-1} cell protein) was plotted as a function of [^{3}H]-XR9576 concentration using the same equation.

Experiments investigating accumulation of [^{3}H]-XR9576 in AuxB1 and CH^rB30 cells were essentially as described above. This was achieved by incubating cells with a range of radiolabelled XR9576 concentrations (1-300nM) in the presence and absence of 1μM GF120918.

2.8 Protein Assay

Protein content of all samples used in this thesis was measured using a DC Brad assay kit (BioRad, U.K.) that was based on the Lowry method for assaying protein concentration. Samples were diluted where necessary, and made up to 20μl with H_2O. A range of BSA

concentrations (in 20µl) were used to produce a linear standard curve (1-20µg). The assay was carried out according to the manufacturer's protocol.

2.9 Curve-fitting and statistical Analyses

All of the curve-fitting was carried out using Graphpad prism 2.0 (GraphPad Software, San Diego, CA).

All statistical analyses were conducted on sample means, using the parametric Students *t* test. P value below 0.05 was deemed significant.

2.10 Materials

Radiochemicals

[^{3}H]-vinblastine sulphate (12-18Ci mmol^{-1}), L-3-Phosphatidyl[N-methyl-^{3}H]choline, 1,2-dipalmitoyl (40-85Ci mmol^{-1}) Amersham Pharmacia Biotech (Amersham, UK),
[^{3}H]-paclitaxel (2.5-6 Cimmol^{-1}) Campro Scientific (Veenendaal, Netherlands),
[^{3}H]-XR9576 (32 Ci mmol^{-1}) gift from Xenova Ltd. (Slough, UK),
8-azido[α-^{32}P]ATP (2-10Ci mmol-1) ICN Pharmaceuticals BV, (Netherlands).

Drugs

Vinblastine sulphate, nicardipine hydrochloride, paclitaxel, verapamil hydrochloride, colchicine were purchased from Sigma, (Poole, U.K).
XR9576, XR9051 and GF120918 were synthesised and donated by Xenova Ltd. (Slough, UK).

Lipids

Egg phosphatidylcholine (PC), bovine liver phosphatidylethanolamine (PE), cholesterol were obtained from Sigma (Poole, U.K.). Soya-bean asolectin (50% pure) was obtained from Fluka (U.K.).

General chemicals

Adenosine 5'-triphosphate (ATP) disodium salt, adenosine 5'-diphosphate (ADP) disodium salt, adenosine 5'-monophosphate (AMP) disodium salt, 5'-adenylimidodiphosphate (AMP-PNP) lithium salt, sodium orthovanadate, N-ethylmaleimide (NEM), 7-chloro-4-nitrobenz-2-oxa-1,3-diazole (NBD-Cl), sodium azide (NaN_3), Tris-HCl, magnesium chloride, magnesium sulphate, sodium dodecylsulphate, sodium citrate, ammonium molybdate, sodium arsenite, phosphorous standard solution, benzamidine hydrochloride, ethylenediaminetetraacetic acid (EDTA), bovine serum albumin (BSA), PIPES (Piperazine-N,N'-bis[2-ethanesulfonic acid] 1,4-Piperazinediethanesulfonic acid), DL-Dithiothreitol (DL-DTT),sodium hydroxide, bromophenol blue (sodium salt), potassium chloride, calcium chloride, sodium bicarbonate, ammonium acetate, were all obtained from Sigma (Poole, U.K.).

Glycerol (Analar), dimethylsulphoxide (DMSO), BDH (U.K.)

8-azidoATP, ICN Pharmaceuticals BV (Netherlands).

Adenosine 5'-0-(3-thiotriphosphate) (ATP-γ-S), decyl- and dodecyl-β-maltoside, leupeptin hemisulphate, pepstatin A, Calbiochem (UK).
Maleimidylanilino-naphthalene-6-sulfonate (MIANS), Molecular Probes (Netherlands).

Ready Protein™ Scintillation fluid, Beckman (High Wycombe, U.K.)

Rapid-Ag Stain Kit, ICN (Thame, U.K.)

Detergent compatible protein assay kit , Bio Rad (U.K.)

Alpha Minimum Essential Medium (α-MEM), Foetal Bovine Serum, Gibco-BrL (U.K.)

Unless otherwise stated, all of the chemicals used were of the highest grade possible.

Materials

GF/F glass-fiber filters, Whatman (U.K.); Bio-spin disposable chromatography columns, Econo-pac High Q anion-exchange column, BioRad (Hemel Hempstead, U.K.); Sephadex™ G-50 Fine, Amersham Pharmacia Biotech (Sweden); Poly-Q mini scintillation vials, Beckman (High Wycombe, U.K.); borosilicate glass tubes, Samco (U.K.);

Instruments

LS6500 multipurpose scintillation counter, Beckman (High Wycombe, U.K.); Micro-titre Plate Reader, Spectra Max 250, Molecular Devices; U2010 spectrophotometer, Hitachi.

Chapter 3

Pharmacology of drug interaction with P-glycoprotein and its effect on ATPase function and drug efflux activities

3.1 Introduction

I have used a pharmacological approach to address the question of how P-gp can interact with diverse and often chemically distinct compounds. To achieve this, radioligand binding assays have been developed to allow direct measurement of drug binding to P-gp. These types of studies can provide quantitative information concerning the characteristics of drug binding, the sites of interaction and the affinity of drug for P-gp. Studies of this kind have been sadly lacking in the area of P-gp research.

Compounds that interact with P-gp can be classified as either transport ligands, as is the case for many cytotoxic drugs or, modulatory ligands, compounds that inhibit activity of the protein, but are not themselves transported. In this chapter the interaction of a range of transport and modulatory ligands with P-gp has been characterised in terms of their effect on P-gp drug efflux and ATP hydrolytic activities. The manner by which drug affects these activities of P-gp was characterised by directly assessing binding of the cytotoxic drugs [^{3}H]-vinblastine and [^{3}H]-paclitaxel and the modulator [^{3}H]-XR9567 with the protein. The ability of other unlabelled ligands to affect binding of radiolabelled drug provided the first direct measure of drug:drug interactions on P-gp. By fully characterising and comparing the interaction of agents that serve as transport substrates for P-gp, and those that are inhibitory in function, light may be shed on the mechanism of drug interaction with P-gp and also on the mechanism underlying inhibition of transport activity.

3.2 Drug efflux activity of P-gp

P-gp functions as a drug efflux pump preventing the intracellular accumulation of compounds such as many cytotoxic agents used in the chemotherapeutic treatment of cancer. I have characterised P-gp transport activity by looking at the accumulation

deficit of cytotoxic drug in P-gp over-expressing CH^{r}B30 cells as compared to the parental non-P-gp expressing AuxB1 cells. The effect of the modulatory compounds XR9576 and GF120918 on the efflux activity of P-gp has also been investigated. These drugs are third generation reversal agents as discussed in Chapter 1 section 1.3.2 and have been designed to specifically target P-gp.

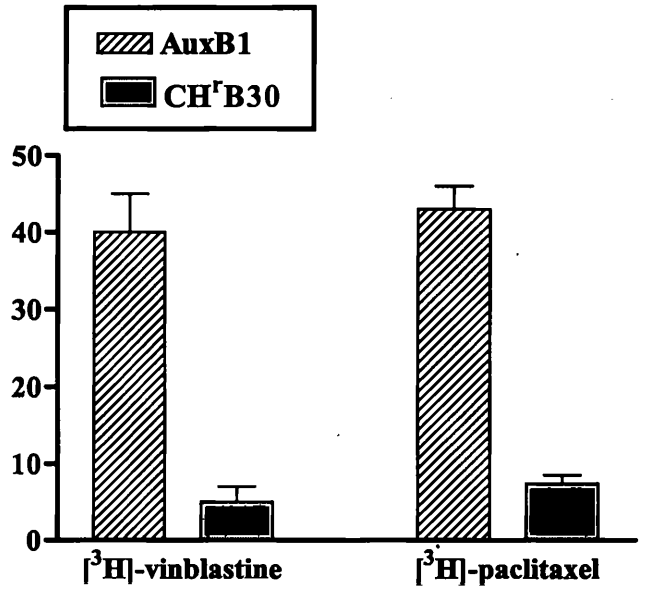

Figure 3.1 Steady-state accumulation of cytotoxic drug in AuxB1 cells versus CH^{r}B30s. Accumulation of [^{3}H]-vinblastine (0.1μM) and [^{3}H]-paclitaxel (1 μM) measured over 60 minute period at 37°C. Mean accumulation ± s.e.m. from at least three independent experiments are shown.

The ability of P-gp to mediate transport of [^{3}H]-vinblastine (0.1μM) and [^{3}H]-paclitaxel (1μM) was investigated by measuring steady-state accumulation of these cytotoxics in P-gp positive CH^{r}B30 cells and the AuxB1 controls. CH^{r}B30 cells reached a steady-state accumulation for [^{3}H]-vinblastine of 5 ± 2 pmol mg^{-1} ($n \geq 3$) and 7.4 ± 1.1 pmol mg^{-1} ($n \geq 3$) for [^{3}H]-paclitaxel. This is in contrast to steady-state concentrations of 40 ± 5 pmol mg^{-1} ($n \geq 3$) and 43 ± 3 pmol mg^{-1} ($n \geq 3$) reached in the parental AuxB1 cells, for [^{3}H]-vinblastine and [^{3}H]-paclitaxel respectively (figure 3.1). The presence of P-gp in

$CH^{r}B30$ cells reduces the accumulation of cytotoxic 5-8 fold as compared to control cells.

The effect of the modulators XR9576 and GF120918 on the accumulation deficit was investigated and compared to steady-state accumulation observed in the non-P-gp expressing control cells. This was achieved by measuring accumulation of a single concentration of [^{3}H]-vinblastine and [^{3}H]-paclitaxel in the presence and absence of a range of concentrations of modulator (10^{-9}-10^{-4} M). The accumulation of [^{3}H]-vinblastine was increased dose-dependently to levels observed in the drug-sensitive parental cells in the presence of both XR9576 and GF120918 (figure 3.2 (b)). Maximal accumulation of [^{3}H]-vinblastine of 44 $\pm$ 2 pmol mg^{-1} ($n \geq 3$) cell protein was achieved in the presence of XR9576 and the EC_{50} value to increase accumulation was 487 $\pm$ 50nM. The presence of GF120918 reversed the accumulation deficit for [^{3}H]-vinblastine to a similar extent as XR9576, with maximal accumulation at steady-state of 53 $\pm$ 2 pmol mg^{-1} ($n \geq 3$). The EC_{50} value for the GF120918 effect on [^{3}H]-vinblastine accumulation was 512 $\pm$ 25nM. Therefore both of these modulators displayed similar efficacy to reverse P-gp mediated transport of [^{3}H]-vinblastine.

The accumulation deficit seen for [^{3}H]-paclitaxel in $CH^{r}B30$ cells was also reversed in the presence of XR9576 to 69 $\pm$ 2.4 pmol mg^{-1} ($n \geq 3$) (EC_{50} = 25.4 $\pm$ 6.9nM) and by GF120918 to 56.4 $\pm$ 1.7 pmol mg^{-1} ($n \geq 3$) (EC_{50} = 109 $\pm$ 21nM) (figure 3.2 (a)). However, XR9576 and GF120918 each displayed greater potency in reversing the accumulation deficit of [^{3}H]-paclitaxel compared with their efficacy to restore accumulation of [^{3}H]-vinblastine. This may be due to the fact that 10 times more [^{3}H]-paclitaxel was used in accumulation assays than [^{3}H]-vinblastine reflecting poorer

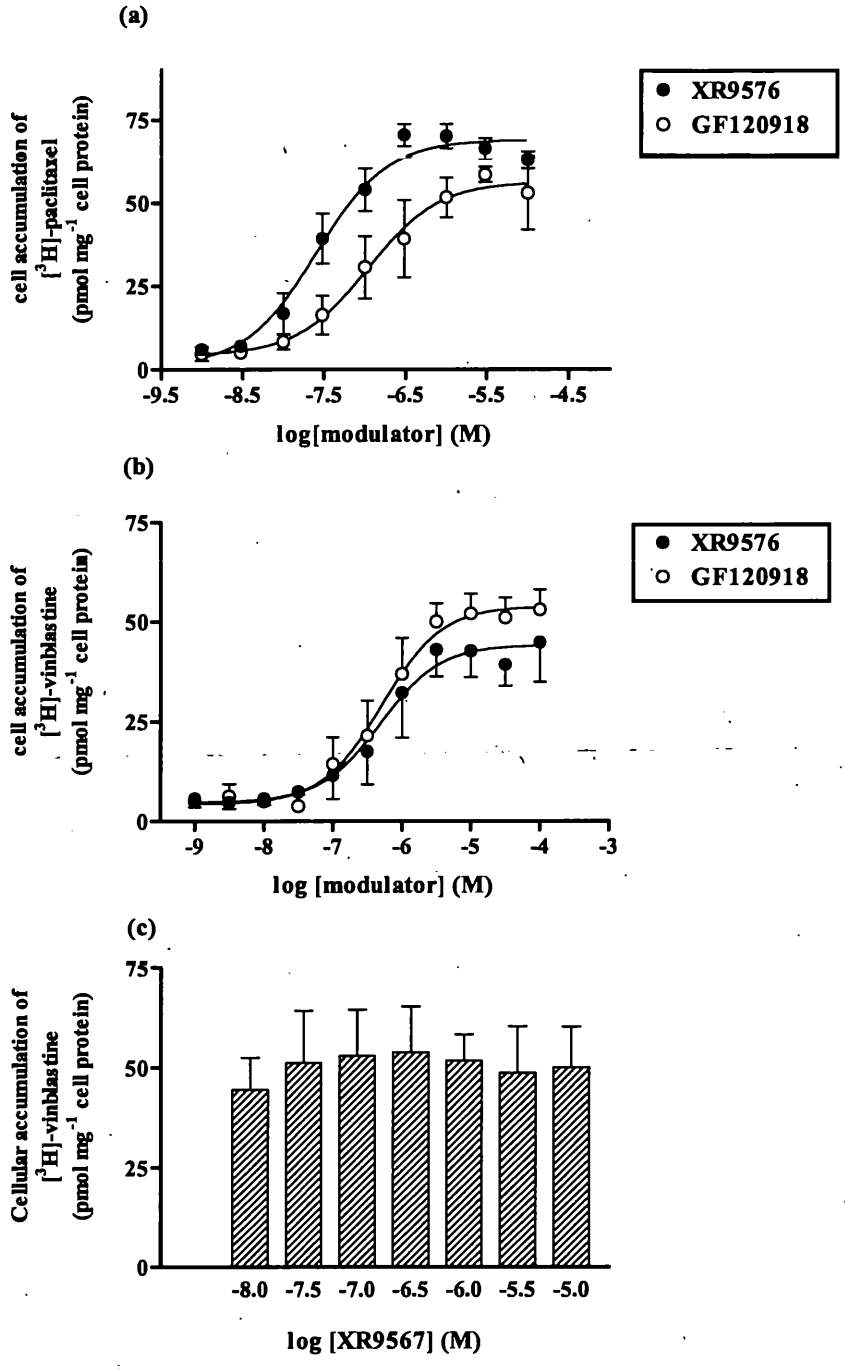

Figure 3.2 Effect of modulator on the steady-state accumulation of (a) [^{3}H]-paclitaxel (1μM) and (b) [^{3}H]-vinblastine (0.1μM) in CH^{r}B30 cells at 37°C as described in methods. (c) Cellular accumulation of [^{3}H]-vinblastine (0.1μM) in drug-senstitive AuxB1 cells in presence of XR9576 over the concentration range indicated. All values represent mean ± s.e.m. of at least three independent experiments. (a) and (b) published in Martin *et al.*, (84).

affinity of [^{3}H]-paclitaxel for transport by P-gp. XR9576 displayed 4-fold higher potency than GF120918 ($P< 0.05$) to restore accumulation of [^{3}H]-paclitaxel in CH^{r}B30 cells. This contrasts with the indistinguishable EC_{50} values for each of these compounds to affect accumulation of [^{3}H]-vinblastine.

The mechanism(s) by which modulatory compounds inhibit the drug efflux activity of P-gp is not known, although there are a number of possibilities. Inhibition could occur at the level of ATP hydrolysis, which is required to fuel transport, or through a direct competition for the transport process. As I had a radiolabelled version of [^{3}H]-XR9576 the latter possibility was investigated first. The accumulation of [^{3}H]-XR9576 in P-gp expressing CH^{r}B30 and the control AuxB1 cells was measured over a range of concentrations (2-300nM). As shown in figure 3.3(a) there was no difference between the cell lines in the level of [^{3}H]-XR9576 accumulated at any of the concentrations used. When [^{3}H]-XR9576 accumulation was measured in CH^{r}B30 cells in the presence of a high concentration of GF120918 (1μM), there was no effect of modulator on the levels of [^{3}H]-XR9576 accumulated (figure 3.3(b)). This is in contrast to the ability of GF120918 to affect the accumulation of the transported drugs vinblastine and paclitaxel, and suggests that P-gp is not involved. Finally, accumulation of [^{3}H]-XR9576 was linear over the entire concentration range used, in the presence and absence of GF120918. The lack of saturation in the levels of [^{3}H]-XR9576 accumulated within the cell, indicates that it was achieved by passive diffusion, rather than an active transport process. Taken together, these three lines of evidence suggest that XR9576 is not a transport substrate for P-gp. The mechanism underlying its ability to block drug efflux activity of P-gp most likely does not involve direct competition for transport with the transport ligands vinblastine and paclitaxel.

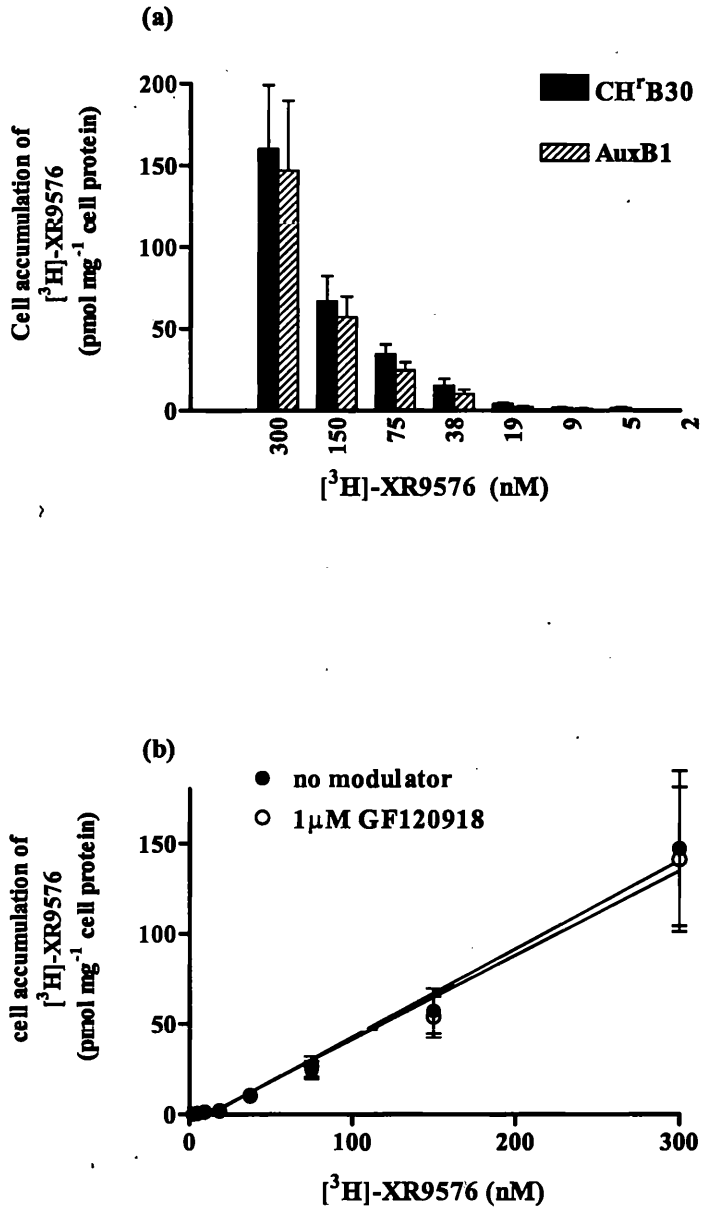

Figure 3.3 Cellular accumulation profiles for [^{3}H]-XR9576 in CH^{r}B30 and AuxB1 cells. (a) The relative accumulation of various concentrations of [^{3}H]-XR9576 in drug sensitive AuxB1 and drug-resistant CH^{r}B30 cells measured at 37°C over 60 minutes. (b) Effect of GF120918 (1μM) on the accumulation of [^{3}H]-XR9576 in CH^{r}B30 cells. All values represent the mean ± s.e.m. of at least three independent experiments. Published in Martin *et al.*, (84).

3.3 Effect of drug on P-gp ATPase function in CH^{r}B30 membrane vesicles

This section is concerned with characterising the consequence of drug interaction at the TMDs on P-gp related ATPase activity. P-gp transport activity cannot occur in the

absence of ATP hydrolysis. Therefore binding of drug at the TMDs must signal to the NBDs to generate transport. The ability of cytotoxic drugs and modulatory compounds to affect P-gp related ATPase activity has been investigated. In fact, inhibition of ATPase activity may be a mechanism employed by some modulators to reduce P-gp mediated transport especially since it was shown in section 3.2 that XR9576 does not inhibit P-gp transport activity via direct competition for transport. As discussed in the introduction to this thesis (Chapter 1 section 1.10) P-gp mediated ATPase activity has been detected in membrane vesicles from drug resistant $CH^{r}B30$ cells. ATP hydrolytic activity has been previously measured in $CH^{r}B30$ membranes in the absence of added drug and is described as 'basal' activity. The basal activity can be stimulated or inhibited in the presence of added drug. The ATPase activity measured in $CH^{r}B30$ membranes in the absence of drug may be due to endogenous lipid component in the membrane, but may also be due to contributions from non-P-gp ATPases. Although the buffer used in the ATPase assay is devoid of constituents that may be used by other ATPase proteins (no Ca^{2+}, or K^{+}) and contains NaN_3 to inhibit V-type ATPases, it may not be sufficient to block all non-P-gp ATPase activity. Therefore, ATPase activity was measured in the presence of 200μM vanadate, which inhibits all P-type ATPase proteins including P-gp. The vanadate inhibited portion of the basal ATPase activity is described as the vanadate-sensitive portion. ATPase activity detected in the presence of vanadate represents the proportion of the basal activity that is insensitive to vanadate and is attributable to non P-type ATPases. The contribution of non-P-gp ATPase activity to basal activity is corrected for by subtracting the vanadate-insensitive fraction.

The effect of drug binding on the ATPase activity in $CH^{r}B30$ membrane vesicles has been investigated as shown in figure 3.4 (a) & (b). It was surprising to find that the cytotoxic drugs paclitaxel and vinblastine, which were shown to be transported by P-gp

in the preceding section (3.2), exerted little effect on P-gp mediated ATPase activity in the membrane vesicles used. There was only a modest increase in the basal activity (1.33 fold) in the presence of paclitaxel (EC_{50} = 0.45 ± 0.2μM) (n≥3) (figure 3.4 (a)). There was no detectable alteration in basal ATPase activity of CH^rB30 membranes at any concentration of vinblastine used (data not shown). This lack of measurable effect of vinblastine has also been reported by other groups (132) and may be due to the high basal ATPase activity.

The modulatory compounds investigated had opposing effects on basal ATPase activity. There was a 1.8- and 2.2-fold increase in P-gp related ATPase activity above basal in the presence of verapamil (EC_{50} = 0.6 ± 0.13μM) (n≥3) and nicardipine (EC_{50} = 0.3 ± 0.0μM) (n≥3) respectively (figure 3.4 (a)). In contrast to the results observed with verapamil and nicardipine, the modulators XR9576, GF120918 and XR9051 all caused 60-70% inhibition of the P-gp related basal ATPase activity of CH^rB30 membranes. The IC_{50} values or potencies of this inhibition were 43 ± 9nM, 44 ± 5nM and 0.7 ± 0.09μM respectively (n≥3 in all cases) (figure 3.4(b)). The effect of vanadate on the basal activity of P-gp is also included in figure 3.4 (b). The extent of the vanadate induced inhibition of activity was approximately 85% of total basal activity measured and had a potency value or IC_{50} = 0.4 ± 0.02 μM (n≥3). This indicates that at least 15% of the activity measured in CH^rB30 membrane vesicles is not attributable to P-gp. However, the modulatory compounds mentioned above inhibited 60-70% of basal ATPase activity suggesting that not all of the vanadate sensitive portion of basal ATPase activity measured can be attributed to P-gp.

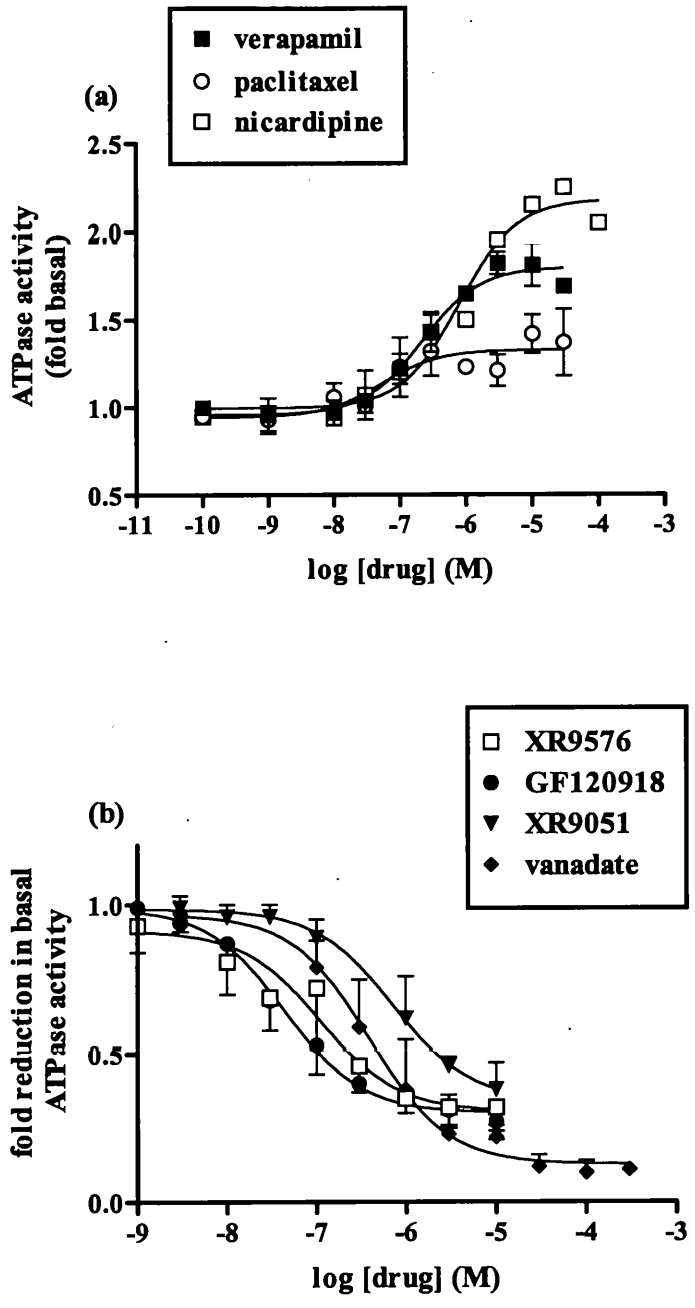

Figure 3.4 The effect of cytotoxic and modulatory compounds on the ATPase activity in CH^{r}B30 membrane vesicles. **(a) & (b) Membrane vesicles (1μg) were incubated with a range of drug concentrations (10^{-9} to 10^{-4} M) and 2mM ATP for 25 minutes at 37°C. Mean value ± s.e.m. from at least three independent experiments are plotted. Values for V_{max} and EC_{50} were derived as described in methods. (b) published in Martin *et al.*, (84).**

The fact that the modulators XR9576, XR9051 and GF120918, which are thought to specifically target P-gp, inhibited 60-70% of total basal ATPase activity provides evidence that they are specific for P-gp. The partial inhibition by these agents also

indicates that up to 25% of the vanadate-sensitive fraction of the total basal activity of CH^{r}B30 membranes may be attributable to non-P-gp ATPases. The data also indicate that inhibition of P-gp mediated transport by XR9576, XR9051 and GF120918 (reported in section 3.2) is through inhibition of ATP hydrolysis. It was not possible to determine the mechanism through which the modulators verapamil and nicardipine inhibit drug transport. It may be through competition for transport, but in the absence of tritiated versions of these compounds, it has not been possible to pursue this possibility.

In subsequent sections of this chapter, radioligand binding assays were devised to further characterise the nature of drug interaction with P-gp, and to investigate how the protein deals with the presence of multiple ligands.

3.4 Characterisation of the binding of [^{3}H]-vinblastine to CH^{r}B30 membrane vesicles

3.4.1 Saturation binding isotherm

A rapid filtration radioligand binding assay was used to characterise the interaction of [^{3}H]-vinblastine sulphate with CH^{r}B30 membrane vesicles which was based on a method developed by Ferry *et al.* (30). As outlined in Chapter 2 (2.2.3) when designing a radioligand binding assay a number of criteria must be adhered to. The ligand used must display selectivity for the target, it is important to measure specific interaction with P-gp and eliminate contributions due to non-specific drug interactions.

It is therefore essential that the concentration of free ligand in the binding system is not depleted so that it does not become rate-limiting. This can be avoided by using the lowest possible concentration of receptor. The first experiment was designed to look at [^{3}H]-vinblastine binding to CH^{r}B30 membrane vesicles using 8μg membrane protein over a range of radioligand concentrations (1-120nM). The specificity of [^{3}H]-

vinblastine binding for P-gp has previously been demonstrated by the lack of binding of vinblastine to membranes from the parental AuxB1 cells (R.Callaghan, personal communication) and the fact that there was no transport of vinblastine in AuxB1 cells as shown in section 3.2. The degree of non-specific binding (nsb) occurring at each concentration of radiolabelled drug was determined by adding an excess of an unrelated drug, which also displays selectivity and high affinity for P-gp. Specific [^{3}H]-vinblastine binding was determined by subtracting binding measured in the presence of 10μM unlabelled verapamil from total [^{3}H]-vinblastine bound. Figure 3.5 is a representative plot depicting specific, total and nsb [^{3}H]-vinblastine binding to P-gp containing membrane vesicles as a function of free [^{3}H]-vinblastine concentration. Specific binding was fitted using the Langmuir adsorption isotherm. From this equation the maximal [^{3}H]-vinblastine bound or B_{max}, was estimated at 95pmol mg^{-1} membrane protein and the dissociation constant, K_d, a measure of binding affinity, was 20nM. There was a linear relationship between the degree of non-specific binding occurring and the concentration of free radioligand. The nsb component of [^{3}H]-vinblastine binding to CH^{r}B30 membranes never exceeded 25% of total binding measured, and total binding was <15% of radioligand added. Therefore, specific binding of [^{3}H]-vinblastine to CH^{r}B30 membranes comprised at least 75% of the total radiolabel bound. The effect of receptor concentration on [^{3}H]-vinblastine (50nM) binding was determined by varying the amount of CH^{r}B30 membranes added (5-40μg). Figure 3.6 shows specific [^{3}H]-vinblastine binding as a function of the amount of membrane protein.

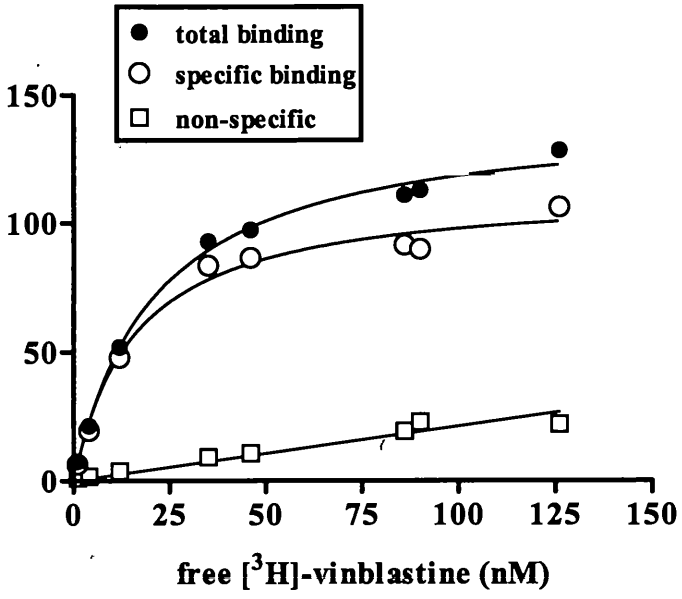

Figure 3.5 Saturation binding isotherm for binding of [^{3}H]-vinblastine to CH^{r}B30 membrane vesicles. Membranes (8μg) were incubated with [^{3}H]-vinblastine (1-120nM) over 2 hour period at 22°C. Non-specific binding was determined in the presence of 10μM unlabelled verapamil. A representative saturation binding isotherm is shown illustrating total, specific and nsb [^{3}H]-vinblastine binding as a function of free radioligand concentration. Values for maximal binding capacity (B_{max}) and potency of interaction (K_d) were derived as described in methods.

The specific binding of [^{3}H]-vinblastine was linear up to 20μg, illustrating that there is no excessive depletion of the free ligand occurring within this range of membrane protein. As illustrated in the inset to figure 3.6, when the amount of receptor added was in excess of 20μg, total binding measured represented > 20% depletion of added radioligand. This reduction in the concentration of free radioligand caused a loss of linearity of binding, at higher amounts of receptor. All future binding experiments with [^{3}H]-vinblastine were conducted with < 15μg CH^{r}B30 membrane vesicles.

By conducting a series of [^{3}H]-vinblastine binding assays the mean value for the B_{max} of binding was 93 ± 10 pmol mg^{-1} membrane protein with K_d = 21 ± 5nM (n=4).

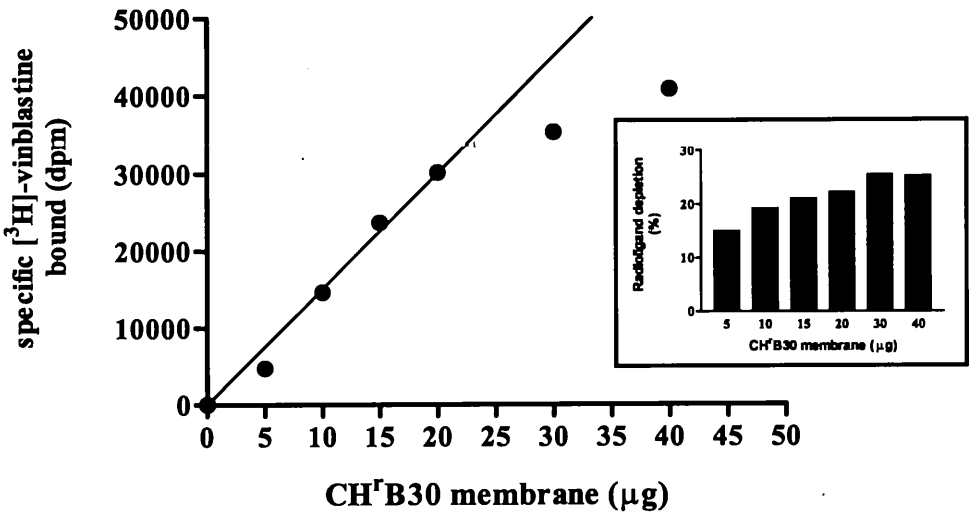

Figure 3.6 Effect of protein concentration on specific [^{3}H]-vinblastine binding to CH^{r}B30 membrane vesicles. Membrane vesicles (5-40µg) were incubated with [^{3}H]-vinblastine (50nM) for 2 hours at 22°C. Non-specific binding was determined in the presence of 10µM unlabelled verapamil. *Inset* % depletion of radioligand added as a function of membrane protein.

3.4.2 Kinetics of [^{3}H]-vinblastine interaction with CH^{r}B30 membrane vesicles

The previous section has been concerned with measuring the binding of [^{3}H]-vinblastine to P-gp containing membrane vesicles at equilibrium. The kinetics of drug-P-gp interaction were also studied in order to provide information concerning the onset and duration of drug action. The off-rate for [^{3}H]-vinblastine from its binding site was determined by labelling CH^{r}B30 membrane vesicles with 20-30nM [^{3}H]-vinblastine until equilibrium was attained, following which the association reaction for [^{3}H]-vinblastine was blocked by the addition of 100-fold excess unlabelled vinblastine. The unlabelled vinblastine competed with [^{3}H]-vinblastine for binding to P-gp, and the reduction in [^{3}H]-vinblastine binding observed provides a measure of vinblastine dissociation. In figure 3.7 the natural logarithm of the proportion of [^{3}H]-vinblastine remaining as a function of time is shown. The linear logarithmic plot demonstrates that dissociation of

[^{3}H]-vinblastine from its binding site is monophasic suggesting that the dissociation is from a single class of site. The dissociation rate constant (k_{-1}) was obtained from the slope of the relationship and a mean value for k_{-1} of 0.027 $\pm$ 0.001 min^{-1} was obtained from at least three independent experiments (refer to table 3.1).

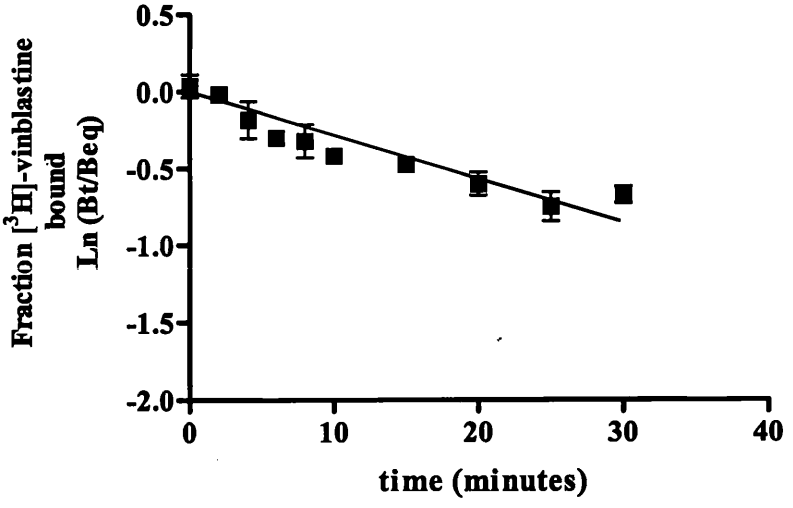

Figure 3.7 Measurement of the dissociation rate constant for [^{3}H]-vinblastine binding to CH^{r}B30 membrane vesicles. CH^{r}B30 membrane vesicles (8µg) were incubated with [^{3}H]-vinblastine (20-30nM) and allowed to bind to equilibrium over 2hrs at 22°C. Association was blocked by adding 3µM unlabelled vinblastine and dissociation of [^{3}H]-vinblastine measured over 40 minutes at 22°C. Bt is binding remaining at time *t* and Beq represents amount bound at equilibrium prior to dissociation. Dissociation rate constant determined as described in methods. Data plotted represent the mean $\pm$ s.e.m. of at least three independent experiments.

The rate of onset or the association rate for the formation of the P-gp-[^{3}H]-vinblastine complex, was measured by allowing a range of concentrations of [^{3}H]-vinblastine to associate with P-gp for various periods of time. The amount of [^{3}H]-vinblastine specifically bound (nM), was plotted as a function of time as shown in figure 3.8. Using equation 2.13, a value for K_{obs} was obtained for the data shown in figure 3.8 that defines the rate of association of [^{3}H]-vinblastine with P-gp. However, K_{obs} is defined by the following relationship $K_{obs} = k_1[L] + k_{-1}$ (equation 2.14) and is therefore a function of

the sum of the association and dissociation rate constants and the concentration of ligand used. Therefore, values for K_{obs} were measured at different concentrations of [^{3}H]-vinblastine to determine the association rate constant for [^{3}H]-vinblastine binding using the above relationship. The experimentally determined value for k_{-1} (see above) was used to determine k_1, the association rate constant, for [^{3}H]-vinblastine binding. A mean value for k_1 of 0.00048 $\pm$ 0.00013 (nM^{-1} min^{-1}) ($n \geq 4$) was obtained for [^{3}H]-vinblastine binding (summarised in table 3.1)

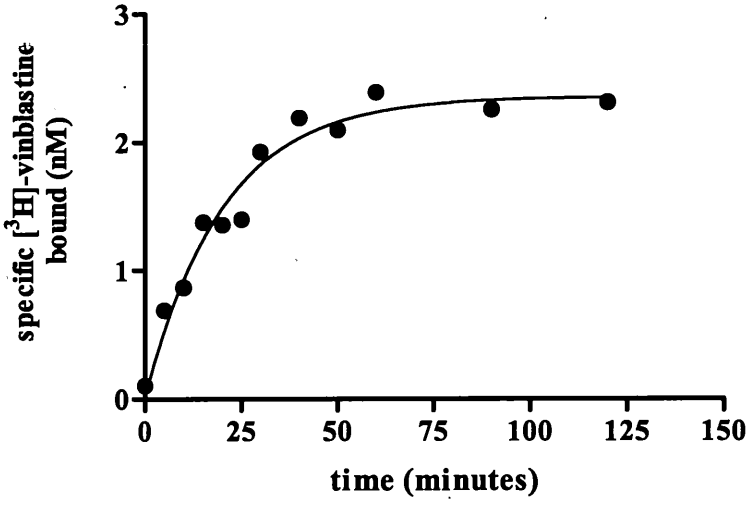

Figure 3.8 To determine the K_{obs} for the binding of [^{3}H]-vinblastine to CH^{r}B30 membrane vesicles. Membrane vesicles (8μg) were incubated with [^{3}H]-vinblastine (17nM) over the time period shown. Data was plotted using an exponential function and value for K_{obs} derived as described in methods.

3.5 Radioligand binding assay to measure the binding of [^{3}H]-paclitaxel to P-gp containing membrane vesicles.

Paclitaxel is a natural product cytotoxic drug and has been shown to be transported by P-gp resistant cells (section 3.2). A radioligand binding assay based on that used to measure [^{3}H]-vinblastine binding was established to directly assess the affinity of [^{3}H]-paclitaxel binding to P-gp. Membrane vesicles (20μg) were incubated with a broad range of [^{3}H]-paclitaxel concentrations (10-600nM) and the nsb component was

measured in the presence of an excess of unlabelled vinblastine (10μM). Higher amounts of membrane vesicles were used in the binding assays for [^{3}H]-paclitaxel compared to assays of [^{3}H]-vinblastine, in order to reproducibly obtain high levels of binding. The specific binding of [^{3}H]-paclitaxel was saturable with respect to free radioligand concentration, as illustrated in figure 3.9. The B_{max} for [^{3}H]-paclitaxel binding was 25 pmol mg^{-1} membrane protein with a K_d value of 85nM, as determined using the Langmuir adsorption isotherm. There was no specific binding of radioligand to membranes produced from the parental AuxB1 cell line, suggesting that binding measured in CH^{r}B30 membranes was due to the presence of P-gp (data not shown). What is apparent from figure 3.9 is that the nsb binding component of [^{3}H]-paclitaxel constitutes more than 50% of the total binding to CH^{r}B30 membranes. However, there was no significant depletion of free radioligand concentration (< 5%) by total binding of ligand to membrane vesicles.

The effect of varying the amount of receptor (P-gp containing membranes) added to the binding assay was investigated to see if this had any effect on the amount of specific [^{3}H]-paclitaxel binding measured. As shown in figure 3.10 specific binding of [^{3}H]-paclitaxel was linear with up to 100μg membrane protein indicating that binding can be measured over a wide range of protein concentration without affecting the reaction kinetics. By conducting a series of radioligand binding assays the specific binding of [^{3}H]-paclitaxel to CH^{r}B30 membranes was characterised by a mean value for B_{max} of binding of 26 ± 4 pmol mg^{-1} (n=3) and K_d of 102 ± 17nM (n=3). This agrees with the studies of Woodhouse (155) who report values for B_{max} and K_d for binding of [^{3}H]-

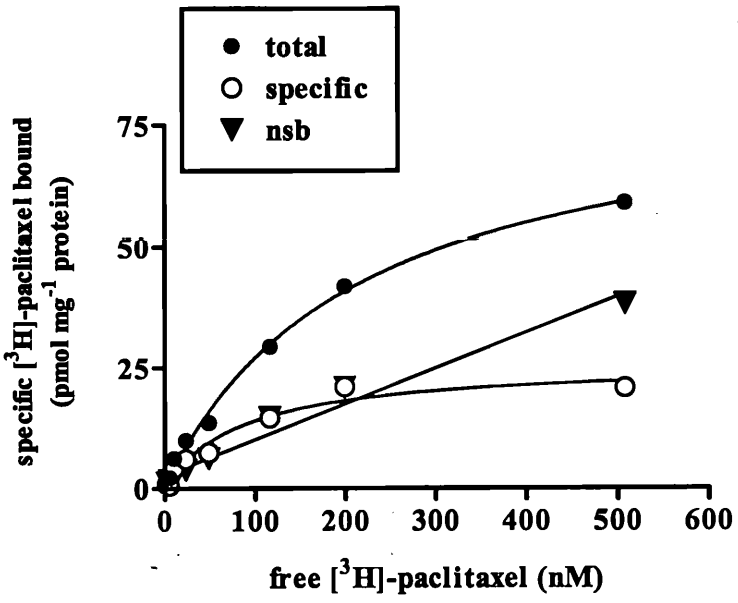

Figure 3.9 Saturation binding isotherm for [^{3}H]-paclitaxel interaction with CH^{r}B30 membrane vesicles. Membranes (20μg) were incubated with [^{3}H]-paclitaxel (1-600nM) for 2 hours at room temperature. Non-specific binding was measured in the presence of 10μM unlabelled vinblastine. A representative binding isotherm is shown with total, specific and non-specific binding as a function of free radioligand. Values for B_{max} and K_d were derived as described in methods.

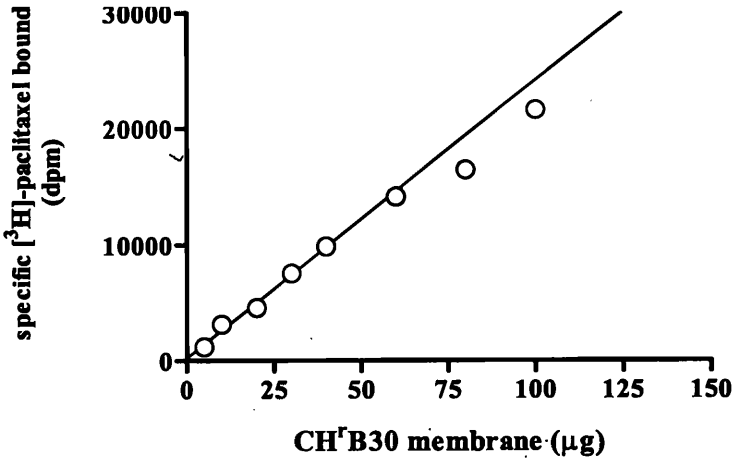

Figure 3.10 Effect of amount of CH^{r}B30 membrane protein on [^{3}H]-paclitaxel binding. [^{3}H]-paclitaxel (100nM) was incubated with membrane vesicles (1-100μg) for two hours at 22°C. Non-specific binding was measured in the presence of 10μM unlabelled vinblastine.

paclitaxel of 48 ± 5 pmol mg^{-1} and 81 ± 25nM respectively. The binding of [^{3}H]-paclitaxel to P-gp displays 3-4-fold lower affinity than [^{3}H]-vinblastine binding. Unfortunately, it was not possible to extend the radioligand binding studies to investigate the binding kinetics of [^{3}H]-paclitaxel because of the relatively low levels of specific [^{3}H]-paclitaxel binding measured in CH^{r}B30 membranes (see figure 3.9).

3.6 Radioligand binding assay to assess interaction of [^{3}H]-XR9576 with P-gp containing CH^{r}B30 membrane vesicles.

XR9576 is an anthranilic acid derivative and was generated from a chemical screening programme to identify novel but selective modulators of P-gp action as reviewed in the introduction to this thesis (1.3.2). It has been established in sections 3.2 and 3.3 that XR9576 can potently inhibit transport and ATPase activities of P-gp. However, there was little knowledge concerning the affinity of its interaction with P-gp. A radioligand binding assay was developed to directly and quantitatively measure the interaction of XR9576 with P-gp containing membrane vesicles.

Initially, membrane vesicles (10μg) were incubated with a broad range of [^{3}H]-XR9576 concentrations (1-60nM) and the non-specific binding component measured in the presence of 1μM GF120918 at each concentration of radioligand. Specific, total and non-specific binding of [^{3}H]-XR9576 were plotted as a function of free [^{3}H]-XR9576 concentration and curve-fitting performed using the Langmuir adsorption isotherm (figure 3.11).

It was possible to measure specific binding of [^{3}H]-XR9567 to CH^{r}B30 membrane vesicles whilst there was no binding of this compound to membranes from the parental drug sensitive AuxB1 cells (data not shown). Upon examination of all of the components of [^{3}H]-XR9576 binding to CH^{r}B30 membranes, it was found that there

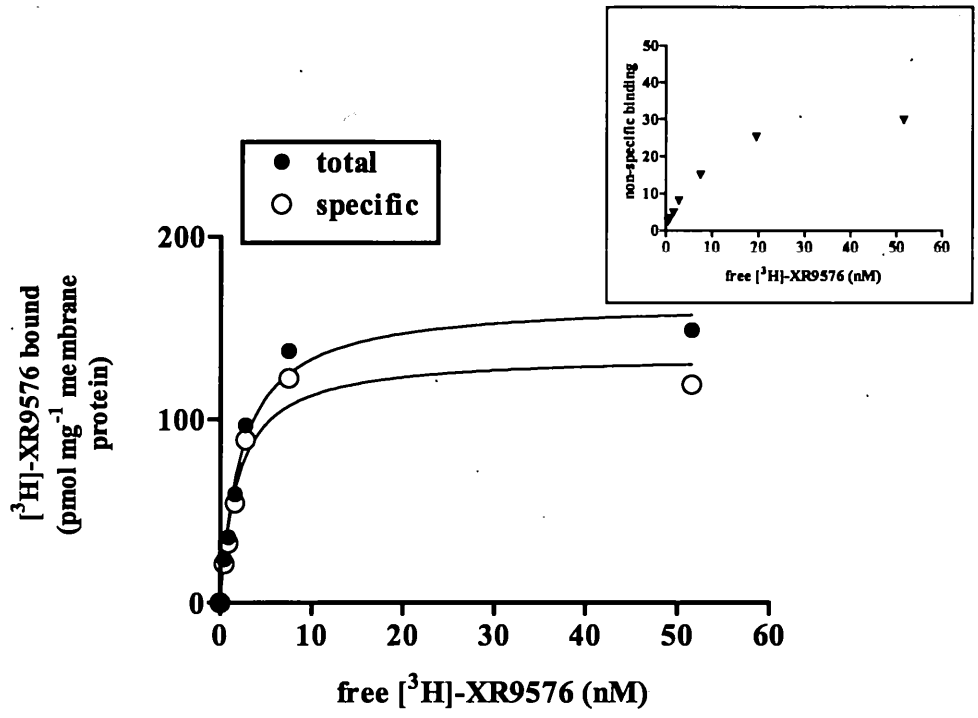

Figure 3.11 Interaction of [^{3}H]-XR9576 with CH^{r}B30 membrane vesicles. Membranes (10µg) were incubated with a range of concentrations of [^{3}H]-XR9576 (1-60nM) for three hours at 22°C. Non-specific binding was determined in the presence of 1µM unlabelled GF120918. Binding is plotted as a function of free radioligand concentration. Values for B_{max} and K_d were derived as described in methods. ***Inset:*** **nsb component of binding is shown as a function of free radioligand concentration.**

was a loss in linearity of the non-specific binding component at concentrations of radioligand > 7-10nM, as shown in the inset to figure 3.11. There was also significant depletion of radioligand (up to 60%) for concentrations up to 10nM. Such a reduction in the concentration of free drug available will alter the kinetics of drug-receptor interaction. The loss in linearity of the nsb component and the reduction in the amount of free radiolabel available for binding, suggested that the amount of receptor in the assay system may be excessive. Therefore, the effect of varying the amount of membrane protein on [^{3}H]-XR9576 binding was investigated as shown in figure 3.12.

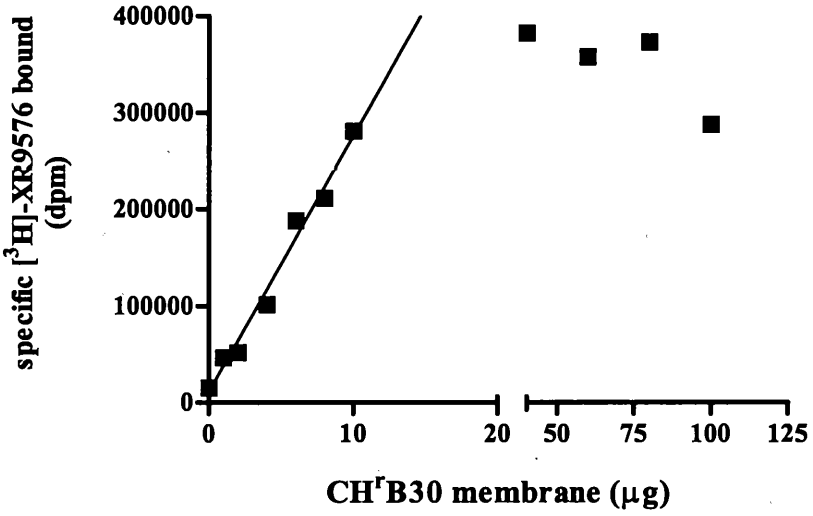

Figure 3.12 Effect of protein concentration on the specific binding of [^{3}H]-XR9576. Membrane vesicles (1-20μg) were incubated with 50nM [^{3}H]-XR9576 for three hours at 22°C. Specific binding is plotted as a function of protein.

Specific binding was linear up to 10μg of membrane protein added, and all future binding experiments with [^{3}H]-XR9576 were conducted using 2μg of membrane protein.

[^{3}H]-XR9576 binding was then measured using 2μg membrane protein per assay tube in the concentration range 0.5-50nM. Using the Langmuir adsorption isotherm, the B_{max} for [^{3}H]-XR9576 binding was calculated to be 350pmol mg^{-1} and the K_d value for binding was 3nM using the representative data shown in figure 3.13. The nsb component was linear and did not exceed 10% of total [^{3}H]-XR9576 bound. By conducting a series of radioligand binding studies, mean values for B_{max} and K_d of 275 ± 15 pmol mg^{-1} and 5.1 ± 0.9 nM (n=7) respectively were determined for binding of [^{3}H]-XR9576 to CH^{r}B30 membranes. The low value for K_d indicated that this modulator interacts with P-gp with high affinity displaying 4-fold and 20-fold higher affinity of binding than [^{3}H]-vinblastine and [^{3}H]-paclitaxel respectively.

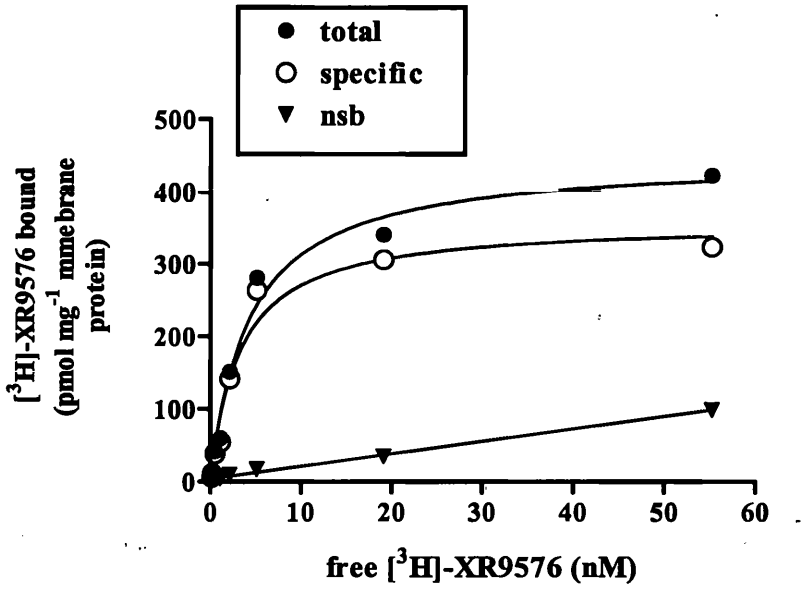

Figure 3.13 Saturation binding isotherm for [^{3}H]-XR9576 binding to CH^{r}B30 membrane vesicles. Membrane vesicles (2μg) were labelled with [^{3}H]-XR9576 (0.5-50nM) for three hours at 22°C. Non-specific binding was determined in the presence of 1μM unlabelled GF120918. Specific, total and non-specific components of binding are shown. B_{max} and K_d were obtained as described in methods.

3.6.1 Kinetics of [^{3}H]-XR9576 binding to CH^{r}B30 membrane vesicles

Dissociation of the [^{3}H]-XR9576-P-gp complex was followed over time to assess the duration of action of this modulator with P-gp. Membrane vesicles (2μg) were allowed to equilibrate with 12nM [^{3}H]-XR9576 in the dark for at least three hours. The association reaction was stopped by the addition of 1μM unlabelled XR9576 and a monophasic linear plot relating fraction of [^{3}H]-XR9576-P-gp complex remaining over time was produced (figure 3.14). The dissociation rate constant (k_{-1}) of 0.0166 ± 0.0004 min^{-1} was derived from the slope of this relationship. This corresponds to a half-life of 42 minutes for [^{3}H]-XR9576 dissociation as compared to $t_{1/2}$ = 26 minutes for [^{3}H]-vinblastine.

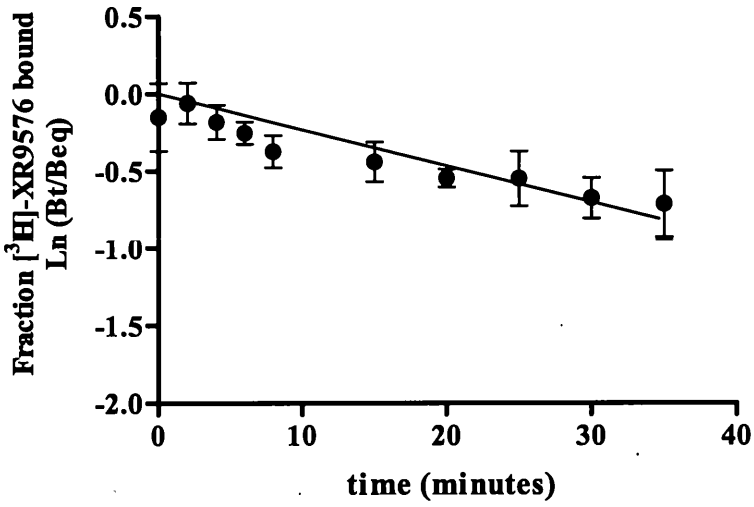

Figure 3.14 Measurement of the dissociation rate constant for binding of [^{3}H]-XR9576 to CH^{r}B30 membrane vesicles. Membrane vesicles (2μg) were incubated with [^{3}H]-XR9576 (12nM) and allowed to bind to equilibrium over 3 hrs at room temperature. The association reaction was blocked by the addition of 1μM unlabelled XR9576 at timed intervals. Bt is binding remaining at time *t* and Beq represents amount bound at equilibrium prior to dissociation. Dissociation rate constant (k_{-1}) was derived as described in methods. Data are the mean ± s.e.m. of at least three independent experiments.

The rate of formation of the [^{3}H]-XR9576-P-gp complex was measured by allowing varying concentrations of [^{3}H]-XR9576 (7-60nM) to associate with membrane vesicles (2μg) over time. The rate constant, or K_{obs}, for association of each concentration of [^{3}H]-XR9576 with P-gp, was derived from plots of specific [^{3}H]-XR9576 bound (nM) as a function of time (an example is shown in figure 3.15). Equation 2.13 was used to derive a value for K_{obs}. The value for K_{obs} is dependent upon the concentration of radioligand and is not strictly a measure of the association rate constant (k_1). The k_1 for [^{3}H]-XR9576 association with CH^{r}B30 membranes was derived from equation 2.14, where K_{obs} is expressed as a function of ligand concentration and the on and off rate for ligand interaction.

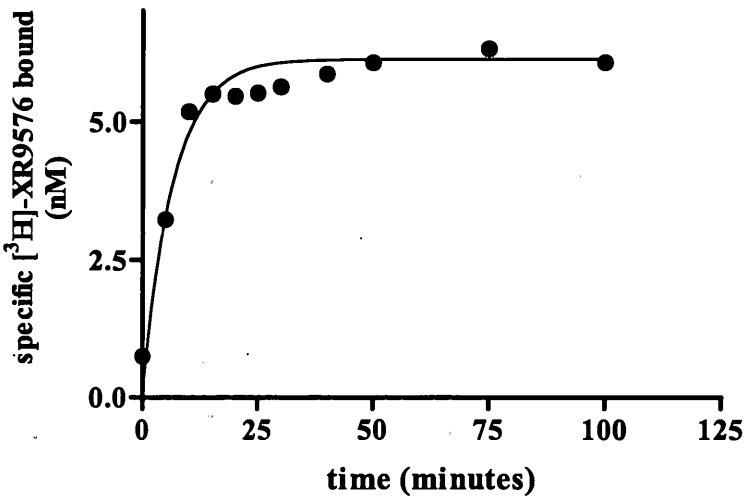

Figure 3.15 Measurement of K_{obs} for [^{3}H]-XR9576 association with CH^{r}B30 membrane vesicles. Membrane vesicles (2μg) were incubated with [^{3}H]-XR9576 (40nM) at 22°C over the time period indicated. Value for K_{obs} was derived as described in methods.

The experimentally derived value for k_{-1} (see above) was used to determine k_1. The rate constant for [^{3}H]-XR9576 association was 0.00421 ± 0.00043 nM^{-1} min^{-1} (mean value ± s.e.m. from at least 7 independent experiments) see table 3.1. This is approximately 10-fold greater than the rate measured for [^{3}H]-vinblastine association. From these kinetic studies it was found that the modulator XR9576 displays a faster rate of onset, and longer duration of interaction with P-gp, by comparison with the cytotoxic agent vinblastine. Interestingly, the K_d for interaction of drug with its receptor is a function of k_{-1}/k_1. Using the values for k_{-1} and k_1 measured in [^{3}H]-XR9576 and [^{3}H]-vinblastine kinetic assays, K_d values of 3.9 and 56nM respectively were obtained for these radioligands. These correlate well with the values obtained in equilibrium binding assays reported earlier in this chapter.

Table 3.1 Kinetics of [^{3}H]-XR9576 and [^{3}H]-vinblastine binding to P-gp in CH^{r}B30 membranes.

Ligand	Association rate constant k_1 (nM^{-1} min^{-1})	Dissociation rate constant k_{-1} (min^{-1})
[^{3}H]-vinblastine	0.00048 ± 0.00013	0.027 ± 0.001
	(n = 3)	(n = 3)
[^{3}H]-XR9576	0.00421 ± 0.00043	0.0166 ± 0.0004
	(n = 7)	(n = 4)
P	<0.05	<0.05

The association (k_1) and dissociation (k_{-1}) rate constants for binding of [^{3}H]-XR9576 and [^{3}H]-vinblastine to CH^{r}B30 membrane vesicles were measured at room temperature as described in methods. All values represent means ± s.e.m. for the number of observations indicated. P values obtained from Student's t test comparing [^{3}H]-XR9576 with [^{3}H]-vinblastine (Published in Martin *et al.*, (84))

3.7 Displacement equilibrium binding assays to investigate relative affinities of ligand interaction with P-gp

As stated in the introduction to this thesis a distinctive feature of P-gp function is its broad substrate specificity, whereby it interacts with a myriad of chemically and functionally distinct compounds. This feature was evident during the course of refining and establishing radioligand binding assays to investigate the binding parameters of the anticancer drugs [^{3}H]-vinblastine and [^{3}H]-paclitaxel and the resistance modulator [^{3}H]-XR9576. In this section, I shall present data on the ability of a range of P-gp ligands to displace binding of radiolabelled drug. This provides evidence for (i) a direct interaction of drug with P-gp (ii) an indication of the potency of drug interaction particularly where drugs are not available in radiolabelled form. Radioligand binding assays of this type are a first step towards direct investigation of drug:drug interactions on P-gp.

The assays involve labelling of CH^{r}B30 membrane vesicles with a single concentration of radiolabelled drug in the presence of increasing concentrations of 'antagonist' (generally 10^{-9} to 3.10^{-4}M). The amount of radioligand chosen was usually the K_d concentration. Essentially, an important criterion was to ensure that a concentration was chosen whereby the level of specific binding was sufficient to provide adequate displaceable counts, so that drug effects could be detected. Membrane vesicles (2μg, 8μg, 20μg respectively) were bound to equilibrium with [^{3}H]-XR9576 (12nM), [^{3}H]-vinblastine (30nM) and [^{3}H]-paclitaxel (100nM) respectively, in the presence of displacing drug for a 2-3 hour period at room temperature. The fraction of specific radioligand bound as a function of 'antagonist' concentration was plotted using the general dose-response equation (2.10). Displacement equilibrium binding curves were obtained for each radioligand as shown in figure 3.16(a-c). Information concerning the extent of radioligand displaced and the IC_{50} of the displacing agent were obtained from these curves. The IC_{50} for displacing agent is a measure of the ability of drug to displace 50% of specific binding observed in the absence of antagonist, and also provides an index of the potency of displacing agent. However, this value is not a constant and is dependent upon the concentration of radioligand used in the binding assay. The IC_{50} can be converted to a K_i value or inhibition constant using the Cheng-Prusoff transformation as described in methods (chapter 2 section 2.2.4). The value of K_i for antagonist may be equated to the antagonist affinity constant only if the interaction with antagonist and radioligand is competitive in nature. Data obtained from displacement curves are summarised in table 3.2.

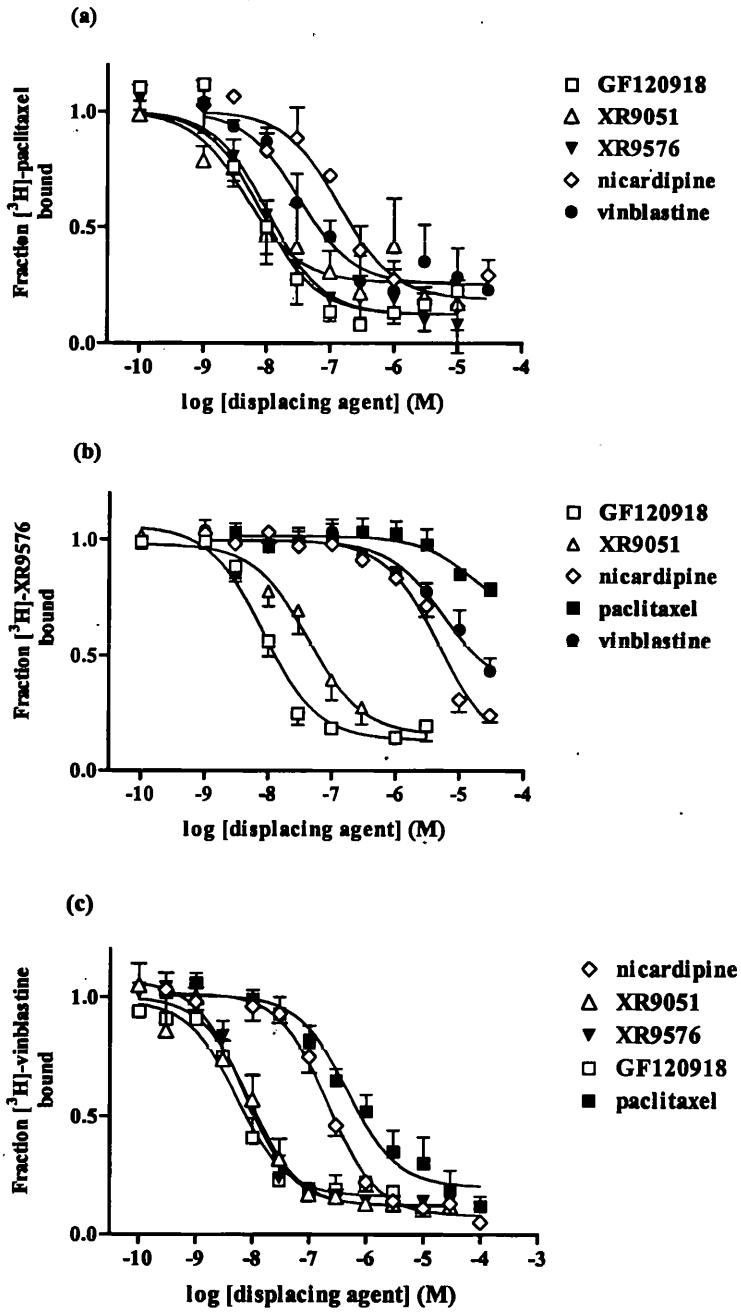

Figure 3.16 Drug displacement of equilibrium binding of [^{3}H]-paclitaxel, [^{3}H]-XR9576 and [^{3}H]-vinblastine to CH^{r}B30 membrane vesicles. (a) Membrane vesicles (20μg) were labelled with [^{3}H]-paclitaxel (100nM) in the presence of displacing agent (10^{-10}M to 10^{-5} M) for 2hrs at room temperature. (b) [^{3}H]-XR9576 (12nM) was used to label CH^{r}B30 membrane vesicles (2μg) to equilibrium for 3 hrs at 22°C in the presence of displacing agent over the concentration range indicated. (c) Membrane vesicles (8μg) were labelled with [^{3}H]-vinblastine (20-30nM) for 2 hrs at room temperature in the presence of increasing concentrations of displacing agent as shown. All values represent the mean ± s.e.m. of at least four independent experiments.

Most of the drugs examined were able to displace at least 85% of the specifically bound radioligand. The transport substrate paclitaxel could only displace 18% of bound [^{3}H]-XR9576 with an estimated K_i value of 1640 $\pm$ 270nM. However, these values are estimates only as higher concentrations of paclitaxel could not be used to extend the displacement curve due to precipitation of solutions of paclitaxel at concentrations in excess of 1mM. Nonetheless, this value deviates significantly from the experimentally derived K_d for [^{3}H]-paclitaxel binding of 100nM. The fractional displacement and different affinities suggest that these drugs are not interacting at the same site on P-gp. The K_i (1250 $\pm$ 510nM) obtained for displacement of [^{3}H]-XR9576 binding by vinblastine which is also a transport ligand for P-gp, also differed from its measured K_d (25nM) and vinblastine was also only able to exert fractional displacement of XR9576 binding (70%). However, as was the case with paclitaxel, these values are estimated values due to limitations on the concentration of vinblastine used in the [^{3}H]-XR9576 displacement assays.

The P-gp modulators XR9576, XR9051 and GF120918 were all able to displace at least 90% of bound [^{3}H]-vinblastine, [^{3}H]-paclitaxel and [^{3}H]-XR9576 and the K_i values for this antagonism were all in the low nM range (<20nM), indicating that these agents have high affinity interaction with P-gp. Such high affinity interaction has facilitated the use of these modulators in clinical trials for MDR reversal (see introduction 1.3.2). The 1,4,-dihydropyridine nicardipine, which is also modulatory in function, displaced most of the bound [^{3}H]-paclitaxel and [^{3}H]-vinblastine with K_i value in the low nM range. However, the potency with which nicardipine displaced the binding of [^{3}H]-XR9576 was shown by a K_i value of 885 $\pm$ 52nM. It is difficult to reconcile the different values for K_i observed for nicardipine with competitive interaction with displaced drug, as the K_d for binding of nicardipine with P-gp is not known. However, differences observed in the value for K_i to

displace radiolabelled drug may be indicative of non-competitive interactions between different pairs of drugs for binding to P-gp.

Table 3.2 The relative affinities of drug interaction with P-gp in CH^{r}B30 membrane vesicles.

	[^{3}H]-XR9576			[^{3}H]-paclitaxel			[^{3}H]-vinblastine		
Displacing agent	**Fraction displaced**	**IC_{50} (nM)**	**K_i (nM)**	**Fraction displaced**	**IC_{50} (nM)**	**K_i (nM)**	**Fraction displaced**	**IC_{50} (nM)**	**K_i (nM)**
Vinblastine	0.7±0.1	7120±281	1250±510	0.77±0.13	28.5±6.4	19.9±7.5	—	—	—
Paclitaxel	0.18±0.02	5310±110	1640±270	—	—	—	0.9±0.05	486±59	335±6
Nicardipine	0.88±0.05	5120±88	885±52	0.92±0.04	110±40	10.8±1.4	0.99±0.01	172±21	82±9
XR9576	—	—	—	0.86±0.07	7.1±0.6	4.2±1.4	1.0	4.4±0.9	2.6±0.8
GF120918	0.93±0.02	8.5±0.75	1.5±0.2	0.94±0.03	7.1±4.3	2.5±0.2	0.99±0.07	5.4±0.7	1.4±0.4
XR9051	0.91±0.03	29±10	11±4.2	0.86±0.04	21±2.8	10.6±1.4	1	3.6±0.6	1.8±0.3

Displacement drug equilibrium binding studies were used to look at the ability of various substrates and modulators to displace the binding of [^{3}H]-XR9576 (12nM), [^{3}H]-paclitaxel (100nM) and [^{3}H]-vinblastine (20-30nM) from CH^{r}B30 membrane vesicles. IC_{50} values for antagonist activity were obtained from displacement binding curves (see figure 3.16). K_i values were derived from the IC_{50} values as described in methods. The extent of [^{3}H]-ligand displacement has also been shown. The data represent the means ± s.e.m. of 3-5 independent experiments. (Published in Martin *et al.*, (84))

3.8 Summary

1. P-gp over-expressing CH^{r}B30 cells transport the cytotoxic drugs vinblastine and paclitaxel as shown by the accumulation deficit of these drugs in a whole cell assay.

2. The transport of vinblastine and paclitaxel by P-gp was inhibited in the presence of the modulatory compounds XR9576 and GF120918, in the sub-micromolar range. This is in contrast to the relatively low efficacy of the modulatory compound verapamil, which is only able to effectively block vinblastine transport at micromolar concentrations (Martin *et al.*, (82)).

3. The mechanism by which XR9576 modulated the transport activity of P-gp was shown to be due to inhibition of ATP hydrolysis.

4. Steady-state accumulation assays showed that XR9576 is not a transport ligand for P-gp.

5. Radioligand binding assays provided a direct measurement of ligand interaction with P-gp. The affinity of the cytotoxic agents [^{3}H]-vinblastine and [^{3}H]-paclitaxel to bind to P-gp was described by K_d values of 21 $\pm$ 3.2nM (n=4) and 102 $\pm$ 17nM (n=3) respectively. The third generation reversal agent [^{3}H]-XR9576 displayed higher affinity binding for P-gp with a K_d for binding of 5 $\pm$ 0.9nM (n=7). The amount of drug specifically bound to P-gp containing membranes also varied. The B_{max} for [^{3}H]-XR9576 binding was 275 $\pm$ 15pmol mg^{-1} (n=7) membrane protein. This is higher than the values for B_{max} obtained for binding of [^{3}H]-vinblastine and [^{3}H]-paclitaxel, 93 $\pm$ 10pmol mg^{-1} (n=4) and 26 $\pm$ 4 pmol mg^{-1} (n=3) respectively.

6. Study of the binding kinetics of [^{3}H]-vinblastine and [^{3}H]-XR9576 showed that XR9576 has a faster rate of onset (10-fold) and slower rate of dissociation than

vinblastine, and this is probably reflected in the higher affinity of XR9576 for P-gp, since K_d is a function of off and on rates for binding.

7. The displacement equilibrium binding studies have provided an initial insight into drug:drug interactions on P-gp. The results of these studies reveal that binding of drug X can affect the binding of drug Y, but the nature of this effect was not determined. However, discrepancies observed in K_i values indicates that not all drug:drug interactions with P-gp are competitive.

Chapter 4

Investigation of drug interaction sites on P-glycoprotein and the inter-site communication network

4.1 Introduction

The preceding chapter was concerned with characterising the interaction of drug with P-gp in terms of binding kinetics, the affinity and capacity of drug interaction sites and the ability of ligands to displace drug binding. The consequence of drug interaction on P-gp function was investigated by examining the drug efflux and ATP hydrolytic activities. As outlined in chapter 1 (section 1.8.1) the apparent lack of ligand specificity displayed by P-gp arises because of the presence of multiple drug binding sites. However, there is no information concerning the number of sites, their location within the TMDs or the nature of the communication that may exist between binding sites. Are there distinct sites for drugs that are transported by P-gp and those that are purely inhibitory? The focus of this chapter is to investigate drug interactions with and between drugs on P-gp in order to address some of these issues.

4.2 Effects of XR9576, XR9051, GF120918 and nicardipine on the equilibrium and kinetic binding of [^{3}H]-vinblastine.

The first stage of our investigation into drug:drug interactions on P-gp was to conduct a more indepth analysis of [^{3}H]-vinblastine binding in the presence of known inhibitors of P-gp transport activity. As mentioned earlier, drugs that interact with P-gp can be broadly classified as either modulators of, or ligands for, the transport activity of P-gp. Previous studies have shown that XR9576, XR9051 and GF120918 can inhibit P-gp transport function through a mechanism other than direct competition for transport (22, 57, 84). The other inhibitor used was the 1,4,-dihydropyridine nicardipine, but it is not known whether it is transported by P-gp or not.

To fully assess interaction between [^{3}H]-vinblastine and modulatory compounds on P-gp, complete saturation isotherms for [^{3}H]-vinblastine binding were measured in the

presence of several different concentrations of added modulator (10^{-9} to 10^{-5}M). Equilibrium binding isotherms for [^{3}H]-vinblastine were plotted for each concentration of modulator added and the individual B_{max} values determined. In figure 4.1 a representative plot is shown illustrating saturating [^{3}H]-vinblastine binding dose-response curves at different concentrations of nicardipine (only three concentrations are shown for clarity). The reduction in the B_{max} for [^{3}H]-vinblastine binding was dependent upon the concentration of modulator used. In fact there was a dose-dependent decrease in the B_{max} for [^{3}H]-vinblastine binding in the presence of each modulator. In order to determine the potency of modulator to elicit a reduction in the

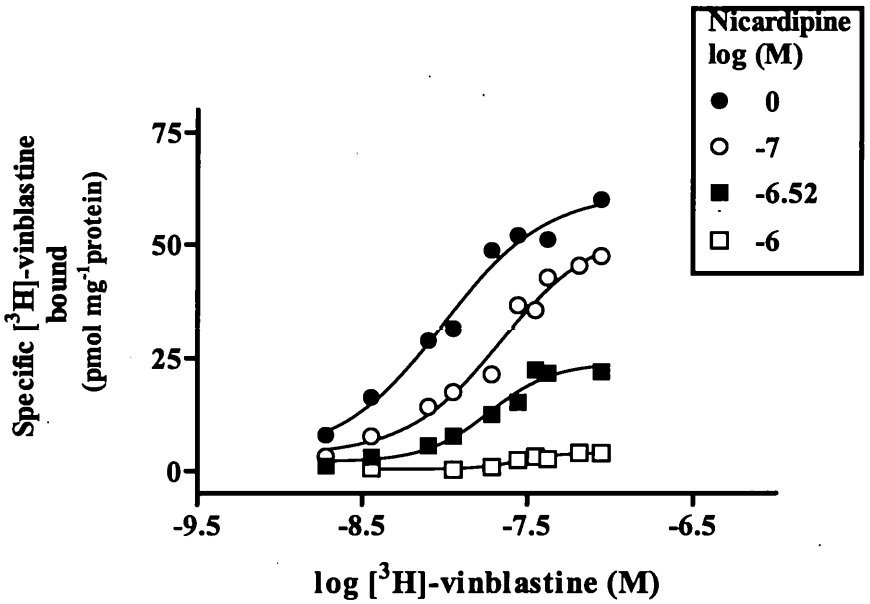

Figure 4.1 Effect of nicardipine on the binding of [^{3}H]-vinblastine. Dose-response curves for [^{3}H]-vinblastine (1-100nM) binding to CH^{r}B30 membrane vesicles (8μg) were measured in the presence of different concentrations of nicardipine. Values for B_{max} and K_d were determined from dose-response equation as described in methods.

B_{max} for [^{3}H]-vinblastine binding, secondary plots of the type of data shown in figure 4.1 were produced. The value for B_{max} of [^{3}H]-vinblastine binding determined in the presence of modulator was expressed as a fraction of that in the absence of modulator,

and plotted as a function of modulator concentration (figure 4.2 (a)-(d)). Figure 4.2(a) demonstrates that nicardipine reduced the B_{max} for [^{3}H]-vinblastine binding to less than 5% of that observed in the absence of nicardipine with EC_{50} = 459nM ± 12nM (n=3). The modulators XR9576 (EC_{50} = 11.8 ± 0.3nM (n=3)), XR9051 (EC_{50} = 19.2 ± 0.4nM (n=3)) and GF120918 (EC_{50} = 11.2 ± 0.2nM (n=3)) had a similar effect on B_{max} but displayed higher potency of action than nicardipine. The affinity or the K_d for [^{3}H]-vinblastine binding was not altered in the presence of any of the modulatory compounds investigated. The fact that binding of modulator resulted in a reduction in the B_{max} for [^{3}H]-vinblastine binding, but had no effect on the K_d of binding, is indicative that these agents are interacting non-competitively. Therefore, it can be concluded that the reversal agents tested are interacting at a site(s) distinct from the site of interaction for [^{3}H]-vinblastine. The most likely method by which modulator can diminish vinblastine binding is via an allosteric effect. To corroborate the existence of an allosteric interaction between binding sites, the effect of modulator on the dissociation kinetics of [^{3}H]-vinblastine was investigated.

As discussed in methods the rate of dissociation of a drug from its binding site can only be altered by a second unrelated drug through an allosteric mechanism. Therefore, the dissociation kinetics of [^{3}H]-vinblastine was measured in the presence and absence of up to a 100-fold excess of modulatory compound (chapter2, 2.3.2). The effect of nicardipine on the rate of dissociation of [^{3}H]-vinblastine is illustrated in figure 4.3 (a). A logarithmic plot of the amount of [^{3}H]-vinblastine remaining bound at time *t* (B_t), as a

PICCIE IN THIS PAGE (FIGURE 4.2)

fraction of amount bound at equilibrium (B_{eq}), was plotted as a function of time. Monophasic plots for vinblastine dissociation were produced and the dissociation rate constant derived from the slope of the relationships in figure 4.3(a). The presence of nicardipine elicited a dose-dependent increase in the rate of dissociation of [^{3}H]-vinblastine from its binding site. This reduced accessibility of [^{3}H]-vinblastine to its site is indicative of a negative heterotropic effect induced by binding of nicardipine. To quantitate the allosteric potency of modulator, the mean value for k_{-1} measured at each concentration of modulator was plotted as a function of modulator concentration (figure 4.3(b)). By conducting non-linear regression of the data in figure 4.3 (b), (i) the potency or EC_{50} for nicardipine to increase k_{-1} and (ii) the maximal k_{-1} in the presence of nicardipine were derived. The maximal value for k_{-1} of [^{3}H]-vinblastine binding in the presence of nicardipine was compared to the value for k_{-1} measured in the presence of unlabelled vinblastine, to quantify fold increase in the dissociation rate constant due to modulator. The dissociation rate constant for [^{3}H]-vinblastine binding, as determined by following dissociation in the presence of 3μM unlabelled vinblastine, was 0.093 minute^{-1}. From figure 4.3(b) the dissociation rate constant was found to be maximally increased to 0.452 min^{-1} in the presence of nicardipine, representing a 4.9-fold increase in the rate of dissociation of [^{3}H]-vinblastine from its binding site. The potency of the allosteric effect of nicardipine was described by an EC_{50} value of 1.2 μM. This value is similar to the efficacy of nicardipine (0.459 $\pm$ 0.012μM) to reduce the B_{max} for [^{3}H]-vinblastine demonstrated earlier. Indeed all of the modulatory agents investigated caused a dose-dependent increase in the dissociation rate constant for [^{3}H]-vinblastine binding. The allosteric potencies for modulator and the maximal change in the dissociation rate constant for [^{3}H]-vinblastine were determined as described for nicardipine and are summarised in table 4.1.

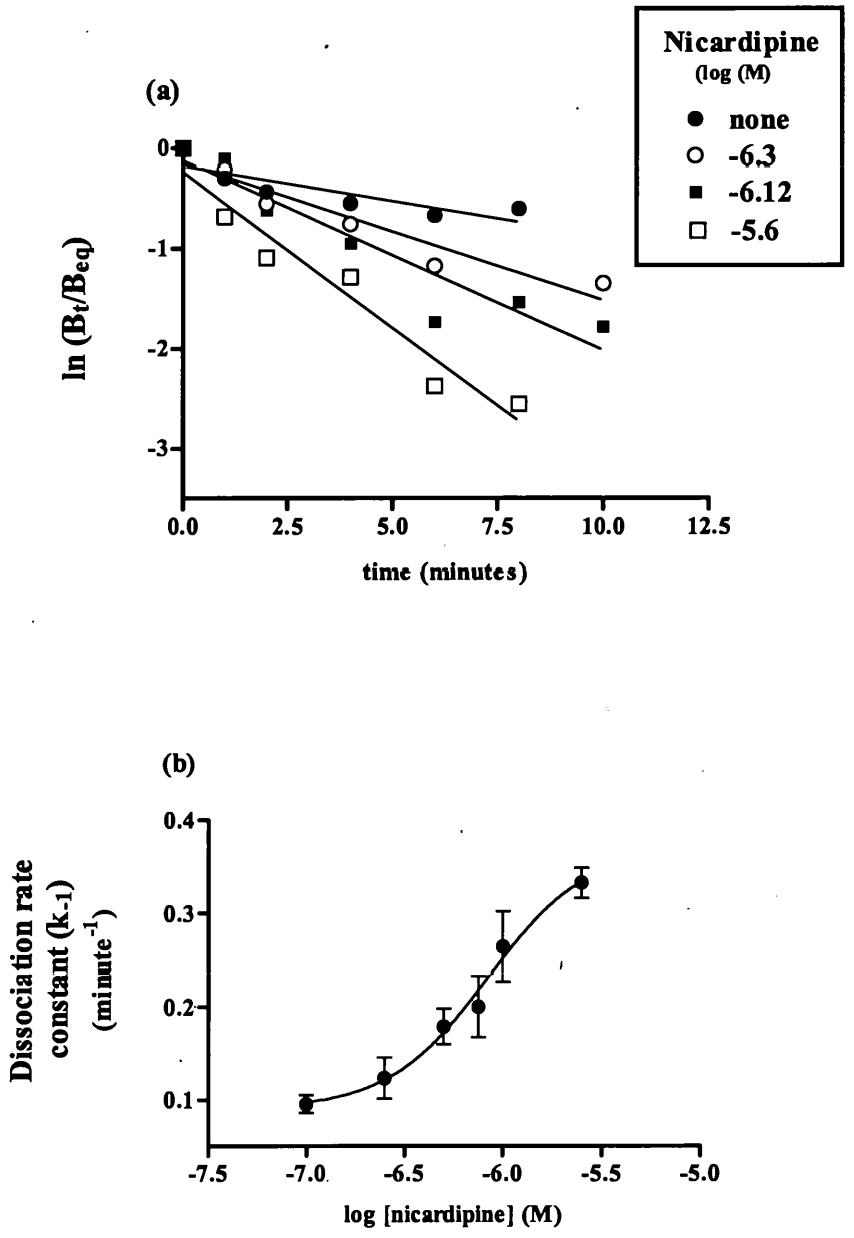

Figure 4.3 Effect of modulator on the dissociation rate constant for [^{3}H]-vinblastine binding. (a) Dissociation rate constant for [^{3}H]-vinblastine binding was measured in the absence and presence of increasing concentrations of nicardipine. A representative plot is shown depicting the logarithm of the fraction of [^{3}H]-vinblastine-Pgp complex remaining as a function of time. Dissociation rate constants (k_{-1}) were determined from the slope of the relationship. (b) The allosteric potency to affect [^{3}H]-vinblastine dissociation rate was determined by plotting k_{-1} values as a function of nicardipine concentration. Values represent the mean $\pm$ s.e.m. of at least four independent experiments.

The third generation modulators XR9576, GF120918 and XR9051 all increased the dissociation rate constant for [^{3}H]-vinblastine binding several fold as shown. However, the efficacy of these agents to increase the k_{-1} for [^{3}H]-vinblastine were up to 40-fold less than their EC_{50} values to reduce the B_{max} for [^{3}H]-vinblastine binding. This most likely reflects a difference in the experiments conducted. In order to follow dissociation kinetics of [^{3}H]-vinblastine, unlabelled vinblastine must be added in a large molar excess to compete effectively with radiolabelled drug to stop the association reaction. In order to ascertain the effect of a second unrelated drug on the dissociation rate, it too needs to be in a large molar excess.

Table 4.1 Effect of modulators on the dissociation kinetics of [^{3}H]-vinblastine.

Drug (n≥3)	Maximal rate (k_{-1}) (min.$^{-1}$)	Fold change	Potency (μM)
Vinblastine	0.093	N/A	N/A
XR9576	0.493	5.3	0.46
GF120918	0.293	3.2	0.17
Nicardipine	0.452	4.9	1.2
XR9051	0.370	4	0.29

The effect of drug on the dissociation rate constant (k_{-1}) for [^{3}H]-vinblastine binding was measured as described in methods. The dissociation rate constants were determined at a number of drug concentrations and the maximal rate constant was estimated from non-linear regression of the general dose-response equation. The potency of each drug to increase the dissociation rate constant is shown as an EC_{50} value.

In summary, two different assays have been used to look at how modulatory drugs interact with the transport ligand vinblastine on P-gp. It was found that each modulator was able to abrogate B_{max} for [^{3}H]-vinblastine binding in the absence of any alteration in the affinity (K_d) of binding. This finding strongly suggested that the modulatory agents used were interacting at a site distinct from the vinblastine site. The mechanism by

which they affected vinblastine binding was thought to involve conformational alteration of the vinblastine drug binding site. The effect of modulator on the dissociation rate constant for vinblastine was used to corroborate such an allosteric interaction. All of the modulators caused between a 3- to 5-fold increase in the k_{-1} for vinblastine, providing definitive proof that the modulatory compounds were interacting at a distinct but allosterically linked site(s) from that of vinblastine.

4.3 [^{3}H]-vinblastine binding parameters assessed in the presence of Paclitaxel, Hoechst 33342 and Rhodamine 123

In the preceding section it was shown that a range of different classes of modulatory agent interacted with the [^{3}H]-vinblastine site non-competitively, suggesting distinct sites of action for vinblastine and modulator. How then do compounds that are substrates for transport by P-gp interact with the vinblastine binding site? Is there a common site on P-gp for transport? The drugs paclitaxel, Hoechst 33342 and Rhodamine 123, have previously been shown to be transported by P-gp, and are not used as modulators of P-gp function. It is on this basis that they are referred to as transport ligands for P-gp in order to distinguish them from compounds that play a purely modulatory role.

To assess how drugs that are transport ligands for P-gp interact with each other for binding to P-gp, a series of [^{3}H]-vinblastine equilibrium binding assays were carried out in the presence of different concentrations of transport ligand, and the effect on the B_{max} and K_d of binding was determined. From the saturation isotherms obtained, the B_{max} for [^{3}H]-vinblastine binding at different concentrations of added drug was determined. As in section 4.2, this information was used to construct secondary plots of the binding data to relate fractional alteration in the B_{max} for [^{3}H]-vinblastine binding as a function of

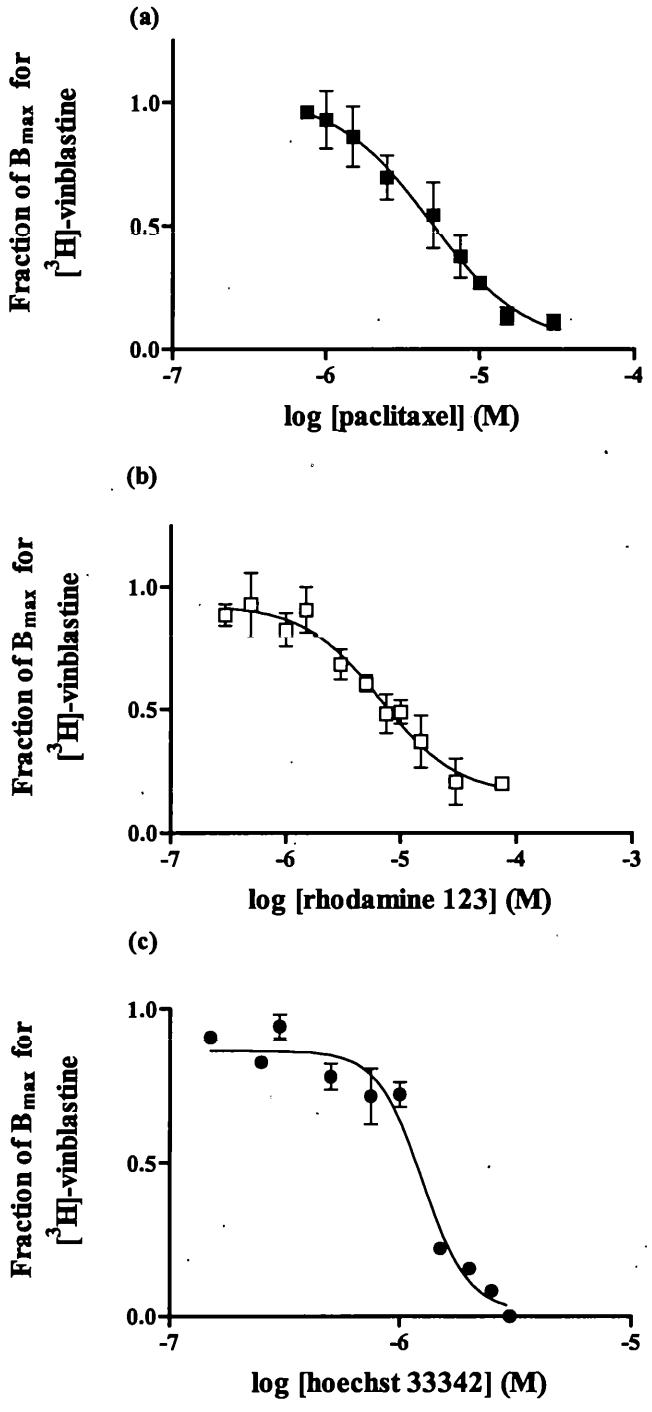

Figure 4.4 Effect of transport ligands on [^{3}H]-viblastine binding in CH^{r}B30 membrane vesicles. The effects of (a) paclitaxel, (b) rhodamine 123 and (c) Hoechst 33342 on the B_{max} for [^{3}H]-vinblastine binding were determined. Data are presented as the fractional reduction in B_{max} as a function of antagonist concentration. Values represent the mean ± s.e.m. of at least three independent experiments.

transport ligand concentration. As shown in figure 4.4 (a to c), all of the transport substrates investigated abrogated the B_{max} for [^{3}H]-vinblastine binding in a similar dose-dependent fashion to the modulatory compounds. The potency or EC_{50} value of drug to reduce the maximal binding capacity for [^{3}H]-vinblastine was similar for all three of the transport ligands examined (paclitaxel $EC_{50} = 4.8 \pm 0.1\mu M$ (n=3); rhodamine 123 $EC_{50} = 9.0 \pm 0.4\mu M$ (n=3); Hoechst 33342 $EC_{50} = 1.26 \pm 0.01\mu M$ (n=3)). On close examination of the relationship depicting the reduction in the B_{max} for [^{3}H]-vinblastine as a function of Hoechst 33342 concentration (figure 4.4(c), a slope factor of 3 for this relationship was measured. This deviation in the slope of the dose-response curve from a value of one suggests that vinblastine and Hoechst 33342 are interacting co-operatively with P-gp. It may indicate that Hoechst 33342 is interacting at more than one site. This is in contrast to a slope factor of 1 which best described the relationships for paclitaxel and rhodamine123 (*F* test , $P<0.01$). There was no observed effect of any of the transport ligands on the affinity (K_d) of [^{3}H]-vinblastine binding. Since there was a reduction in the maximal binding capacity for [^{3}H]-vinblastine by transport ligand in the absence of an alteration in the K_d for binding, it was concluded that paclitaxel, Rhodamine 123 and Hoechst 33342 are interacting non-competitively with the vinblastine binding site.

Non-competitive interactions between drugs must involve allosteric mechanisms. The nature of the non-competitive interaction observed between the transport ligands and the vinblastine site was investigated by looking at the effect of drug on the dissociation kinetics of [^{3}H]-vinblastine. As in the previous section, the dissociation rate constant (k_{-1}) for vinblastine was measured following addition of 3μM unlabelled vinblastine to pre-equilibrated P-gp-[^{3}H]-vinblastine complexes. The measured dissociation rate constant for [^{3}H]-vinblastine was 0.093 min^{-1} as shown in table 4.2. The effect of increasing

concentrations of paclitaxel, rhodamine 123 or Hoechst 33342 (10^{-9} to 10^{-5}M) on this rate was investigated.

Dose-response curves relating changes in k_{-1} to concentration of transport ligand were produced (data not shown). From non-linear regression analysis of dose-response curves the potency (EC_{50}) and the maximal effect of drug on the dissociation kinetics of [^{3}H]-vinblastine were determined (table 4.2). There was a 3.4-fold increase in the dissociation rate constant for [^{3}H]-vinblastine in the presence of Hoechst 33342 with an EC_{50} value of 18μM. In contrast, paclitaxel was only able to cause a modest increase in k_{-1} (1.2-fold) and there was no measurable effect of rhodamine 123 on the [^{3}H]-vinblastine dissociation rate constant. Therefore, it can be concluded that Hoechst 33342 is able to reduce the B_{max} for [^{3}H]-vinblastine binding via an allosteric mechanism that promotes dissociation of the P-gp-[^{3}H]-vinblastine complex. The lack of effect seen with paclitaxel and rhodamine 123 may simply be due to the poorer

Table 4.2 Effect of transport ligands on the dissociation kinetics of [^{3}H]-vinblastine

Drug (n>3)	Maximal rate (k_{-1}) (min^{-1})	Fold change	Potency (μM)
Vinblastine	0.093	N/A	N/A
Paclitaxel	0.114	1.2	0.024
Hoechst 33342	0.317	3.4	18
Rhodamine 123	0.095	1.0	N/A

Effect of drug on the dissociation rate constant for [^{3}H]-vinblastine was determined as described in methods. The k_{-1} for [^{3}H]-vinblastine was determined at a number of drug concentrations. Maximal change in k_{-1} and the potency of drug allosteric effect (EC_{50}) were estimated from non-linear regression of dose-response equations. n refers to number of independent experiments conducted to obtain parameters shown in table.

allosteric efficacy of these drugs by comparison with the modulators investigated in the previous section. Due to problems with drug solubility it was not possible to use higher concentrations of either paclitaxel or rhodamine 123 to test this possibility. However, it is clear from the experiments conducted thus far that P-gp does not contain a single site from which transport is mediated.

4.4 Investigation of [^{3}H]-XR9567 binding parameters in the presence of transport ligands

The preceding sections have demonstrated that some modulator compounds interact at a site(s) distinct from the site of interaction of the transport ligand [^{3}H]-vinblastine. In addition, the binding of vinblastine is modulated in the presence of MDR reversal agents through a negative allosteric mechanism. It has also been shown in the previous section that not all transport ligands interact at a common site. In this section experiments have been conducted to investigate:

a) the mechanism by which transport ligands affect modulator binding, and

b) whether modulatory compounds, some of which may not be transported, share a common site of interaction?

In chapter 3 (3.6), a radioligand binding assay was developed to quantitatively characterise the interaction of the third generation modulator [^{3}H]-XR9576 with P-gp. It was found that this modulator binds P-gp containing CH^{r}B30 membranes with high affinity (2-4nM). I have also demonstrated (refer to chapter 3, (3.7)) that the transport ligands vinblastine and paclitaxel could displace binding of [^{3}H]-XR9576 by 70% and 18% respectively. However, the type of antagonism produced could not be determined in these experiments. It has been shown in this chapter that vinblastine and XR9576 interact non-competitively and that XR9576 can communicate with the vinblastine

binding site via an allosteric mechanism. Is there two-way communication between these sites, that is can binding of vinblastine elicit an allosteric effect on the XR9576 binding site? It was also of interest to investigate how other transport ligands such as rhodamine 123, Hoechst 33342 and paclitaxel interact with [^{3}H]-XR9576, particularly as it has been established that they interact at site(s) distinct from the vinblastine site.

To address these issues, the effect of the transport ligands vinblastine, Hoechst 33342, rhodamine 123 and paclitaxel on the complete binding isotherms for [^{3}H]-XR9576 were investigated. Saturation isotherms for [^{3}H]-XR9576 were measured in the presence of different concentrations of transport ligand as described in methods. There was no reduction of the B_{max} for [^{3}H]-XR9576 binding to CH^{r}B30 membrane vesicles in the presence of either vinblastine or Hoechst 33342 at any of the concentrations used. However, there was a dose-dependent shift in the saturation isotherms for [^{3}H]-XR9576 binding in the presence of different concentrations of vinblastine and Hoechst 33342 (10^{-6}-10^{-4} M). Data for Hoechst 33342 are shown in figure 4.5(a) and for vinblastine in figure 4.6(a). The observed reduction in the apparent affinity of [^{3}H]-XR9576 binding in the absence of any diminution of B_{max}, was suggestive of competitive interaction between either vinblastine or Hoechst 33342, with [^{3}H]-XR9576. However, I had previously shown that XR9576 non-competitively affects [^{3}H]-vinblastine binding. Therefore the alterations in the apparent K_d for [^{3}H]-XR9576 binding observed with both vinblastine and Hoechst 33342, required further investigation to determine whether it was due to competitive interaction.

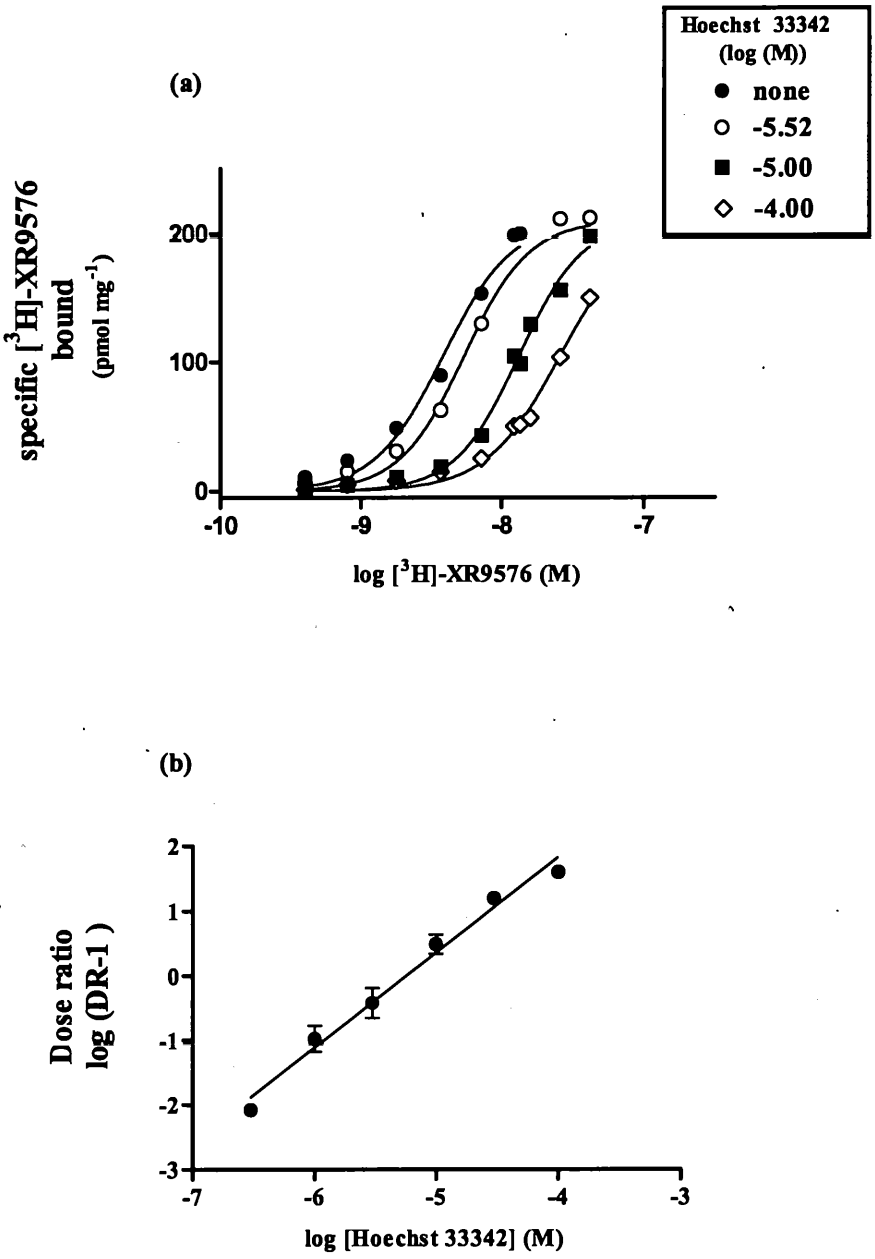

Figure 4.5 Effect of Hoechst 33342 on the binding parameters of [^{3}H]-XR9576. (a) [^{3}H]-XR9576 saturation binding isotherms measured in the presence of different concentrations of unlabelled Hoechst 33342 (a representative plot is shown). (b) Schild plots were derived from saturation isotherms to describe the interaction of Hoechst 33342 with [^{3}H]-XR9576 binding. The shift in the apparent K_d for [^{3}H]-XR9576 binding in the presence of Hoechst 33342 was used to derive a dose ratio (DR). The DR was plotted as a function of unlabelled antagonist. The slope of this relationship and the *x*-axis intercept are used to delineate the type of interaction occurring between compounds on P-gp. Each value represents the mean ± s.e.m. from four independent experiments. Published in Martin *et al.*, (83).

Competitive interactions involve specific quantifiable changes in the apparent K_d which can be assessed using Schild analysis. The shift in K_d apparent at each concentration of antagonist was expressed as a ratio of K_d measured in the absence of antagonist to produce a dose ratio (DR). The logarithm of the dose ratio is plotted as a function of logarithmic antagonist concentration. According to Schild, if there is a competitive interaction occurring the relationship between dose ratio and antagonist concentration will be linear, and the slope of that relationship must equal 1. Figure 4.5(b) is a Schild plot of the data shown in figure 4.5 (a) where dose ratio or alteration in K_d for [^{3}H]-XR9576 binding was related to concentration of Hoechst 33342. The slope of this relationship was 1.14 $\pm$ 0.2 (n=3) and was not significantly different from 1 (*F* test, P> 0.05). This result strongly suggests that Hoechst 33342 competitively interacts with [^{3}H]-XR9576 for binding to P-gp. The antagonist affinity constant (K_b) obtained from the Schild plot was 5.3 $\pm$ 0.076μM (n=3). Where competitive interactions exist the value for K_b of antagonist equals the K_d for binding of antagonist. The value for the affinity of Hoechst 33342 obtained from Schild analysis, agrees with the previously reported affinity of Hoechst 33342 to interact with P-gp, as reported by Shapiro and Ling (122).

The effect of Hoechst 33342 on the rate of dissociation of the [^{3}H]-XR9576-P-gp complex was also investigated. There was no effect of Hoechst 33342 measured over a range of concentrations (up to a 1000-fold molar excess) on the dissociation rate constant for [^{3}H]-XR9576. This result supports the findings from Schild analysis, and thus it was concluded that the transport substrate Hoechst 33342 and the modulator XR9576 interact at the same site on P-gp. This important result provides direct evidence that the same binding site on P-gp can elicit either a transport role or act as a regulator of activity, depending upon the drug bound.

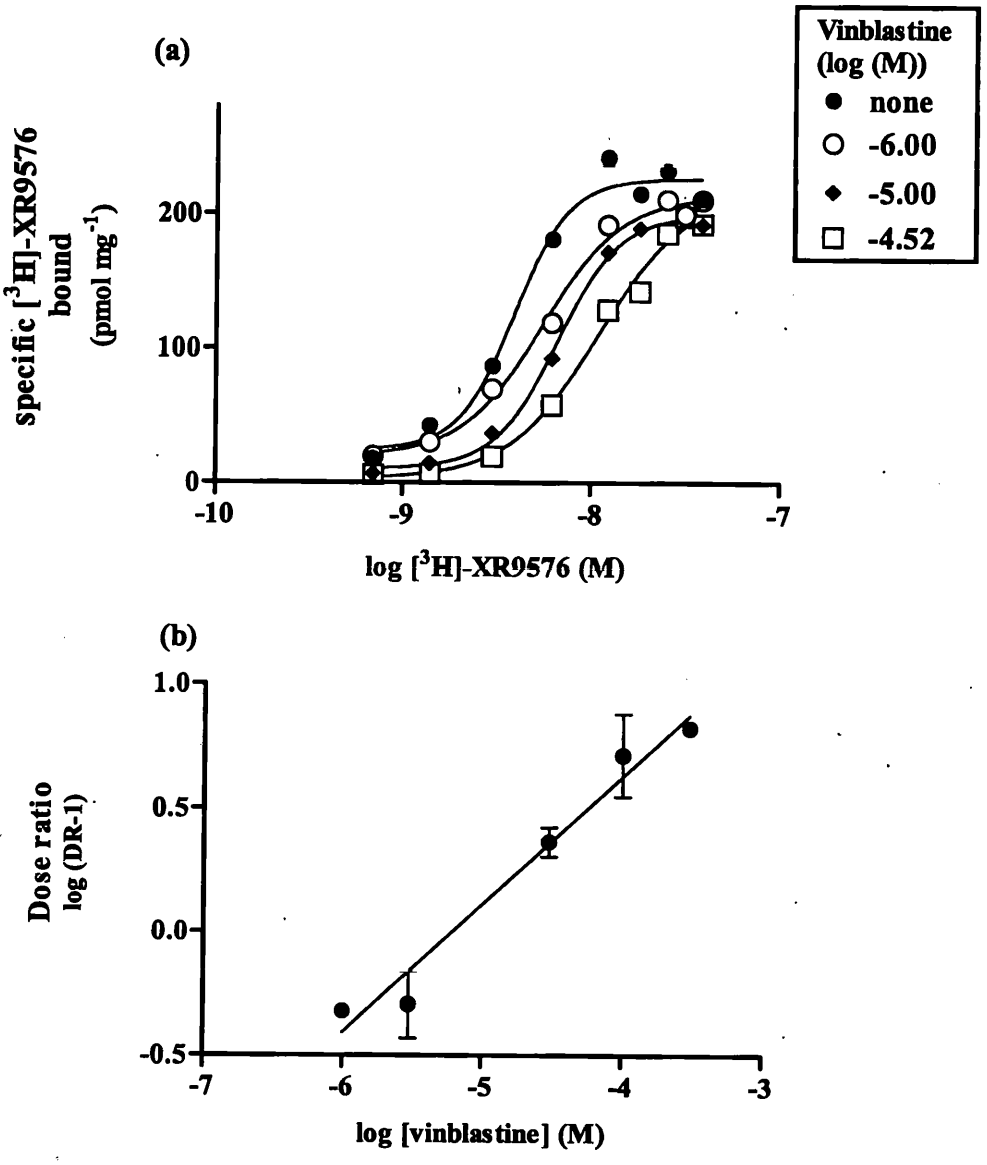

Figure 4.6 **Effect of vinblastine on the binding of [^{3}H]-XR9576. (a) [^{3}H]-XR9576 saturation binding isotherms measured in the presence of different concentrations of unlabelled vinblastine (a representative plot is shown). (b) Schild plot relating dose ratio as a function of vinblastine concentration. The slope of this relationship and the *x*-axis intercept are used to delineate the type of interaction occurring between compounds on P-gp. Each value represents the mean ± s.e.m. from four independent experiments. Published in part in Martin *et al.*, (83).**

A Schild plot relating alterations in the apparent K_d for [^{3}H]-XR9576 due to vinblastine, is shown in figure 4.6(b). The resultant relationship yielded a slope of 0.52 ± 0.05 and a value for K_b = 6.56 ± 0.56μM (n=4). Since the slope was significantly different from 1.0

($P < 0.01$), this strongly indicated that vinblastine and [^{3}H]-XR9576 are interacting non-competitively on P-gp. The fact that the value for K_b (antagonist affinity constant) deviated from the measured K_d for vinblastine binding by more than 300-fold, is further evidence for non-competitive interaction. This finding agrees with the results obtained in section 4.2 and also substantiates the power of Schild analysis to prove the existence of competitive antagonism.

Unfortunately there was no effect of the transport substrates rhodamine 123 and paclitaxel on any of the binding parameters for [^{3}H]-XR9576 binding at any concentration used which is probably due to the relatively low affinity of these agents to bind P-gp (data not shown).

4.5 Is there a common site of interaction for modulators on P-gp?

The modulators XR9576, XR9051, GF120918 and nicardipine have been shown to non-competitively interact with the [^{3}H]-vinblastine site by reducing the maximal binding capacity via an allosteric mechanism. Is this effect on the vinblastine binding site mediated from a common site of interaction for modulatory agents on P-gp, or from separate and pharmacologically distinct sites? To address this question, a series of complete [^{3}H]-XR9576 binding curves were produced in the presence of unlabelled modulator (XR9051 10^{-8} to 10^{-6} M; GF120918 10^{-8} to 10^{-6} M; Nicardipine 10^{-7} to 10^{-4} M) to elucidate the type of interaction occurring between [^{3}H]-XR9576 and other modulatory compounds on P-gp. XR9051 elicited a dose-dependent alteration in the affinity of [^{3}H]-XR9576 binding, as evidenced by a rightward shift in [^{3}H]-XR9576 binding curves (see figure 4.7(a)). Representative binding curves obtained in the

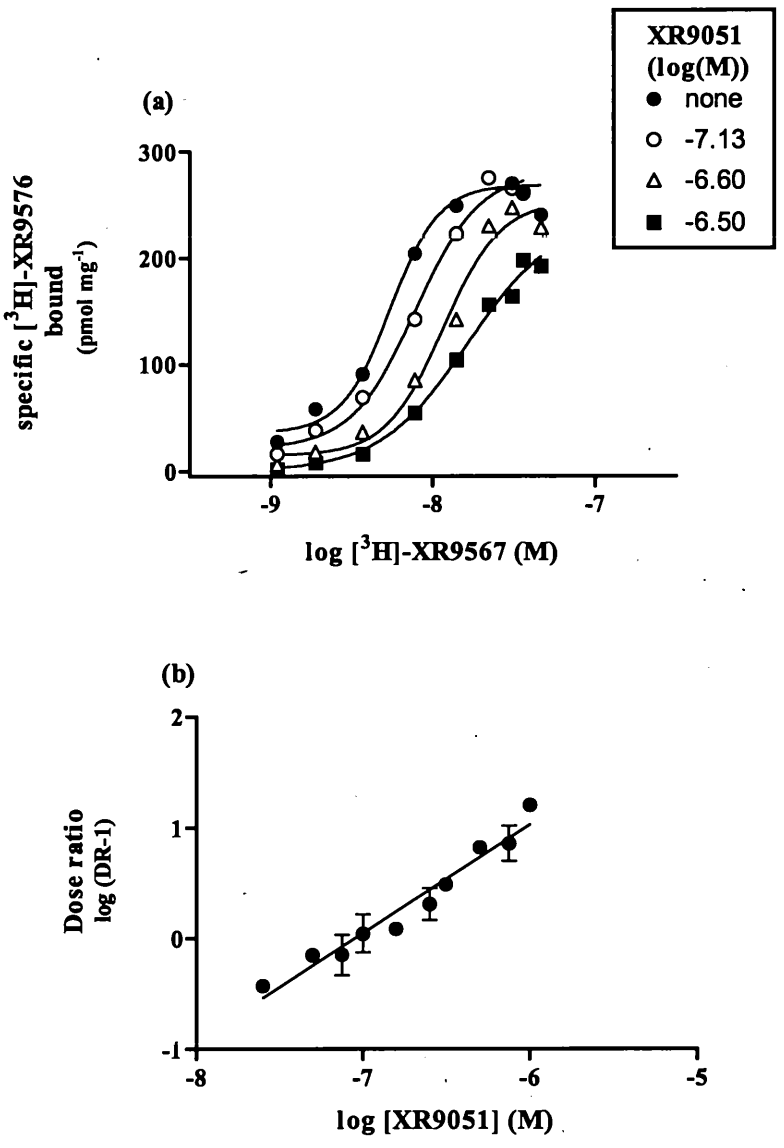

Figure 4.7 Effect of XR9051 on the binding of [^{3}H]-XR9576 to CH^{r}B30 membranes. (a) [^{3}H]-XR9576 binding curves conducted in the presence of different concentrations of unlabelled XR9051 (a representative plot is shown). (b) Schild plot was derived from type of data shown in (a) relating change in affinity (DR) as a function of antagonist concentration. The slope of this relationship and the *x*-axis intercept are used to determine the type of interaction occurring between compounds. Each value is the mean±s.e.m. of at least three independent experiments. Published in part, in Martin *et al.*, (83).

presence of antagonist are shown for clarity. A shift in the binding curve with no diminution in B_{max} is indicative of a competitive interaction, but not proof as such, as was the case with the effect of vinblastine on the saturation binding curves for [^{3}H]-

XR9576 in section 4.4. To unequivocally determine the existence of competitive interaction, Schild plots relating the change in the apparent K_d for [^{3}H]-XR9576 binding as a function of antagonist concentration, were produced (figure 4.7(b)). The Schild plot describing the interaction between XR9051 and [^{3}H]-XR9576 on P-gp yielded a slope value of 0.981 $\pm$ 0.075 (n=3) that was not significantly different from 1.0 (*F* test, P > 0.05). The value for K_b, a measure of antagonist affinity, was 89.3 $\pm$ 9.3nM (n=3). This value for K_b, agrees with the previously reported potency of XR9051 binding to P-gp (22) and is similar to its IC_{50} value to displace [^{3}H]-XR9576 binding (chapter 3, 3.7). This result shows that XR9051 and [^{3}H]-XR9576 have a common site of interaction on P-gp, which is not surprising, given their structural similarity (refer to figure 1.3 chapter 1, 1.3.2).

The effect of unlabelled XR9051 on the dissociation rate constant (k_{-1}) for [^{3}H]-XR9576 binding was also investigated as another means of identifying how XR9051 and XR9576 interact with each other for binding to P-gp. As illustrated in previous sections, the dissociation rate constant for drug can only be altered by a second unrelated drug via an allosteric interaction that only arises from binding at a distinct site. The presence of XR9051 did not have any effect, even at concentrations up to 1000-fold excess, upon the dissociation kinetics of [^{3}H]-XR9576 (data not shown). This provides further support for the findings of the Schild analysis demonstrating a competitive interaction between these two agents on P-gp.

The saturation binding curves for [^{3}H]-XR9576 binding obtained in the presence of different concentrations of the 1,4-dihydropyridine nicardipine also display a rightward shift as shown by the representative plots in figure 4.8(a).

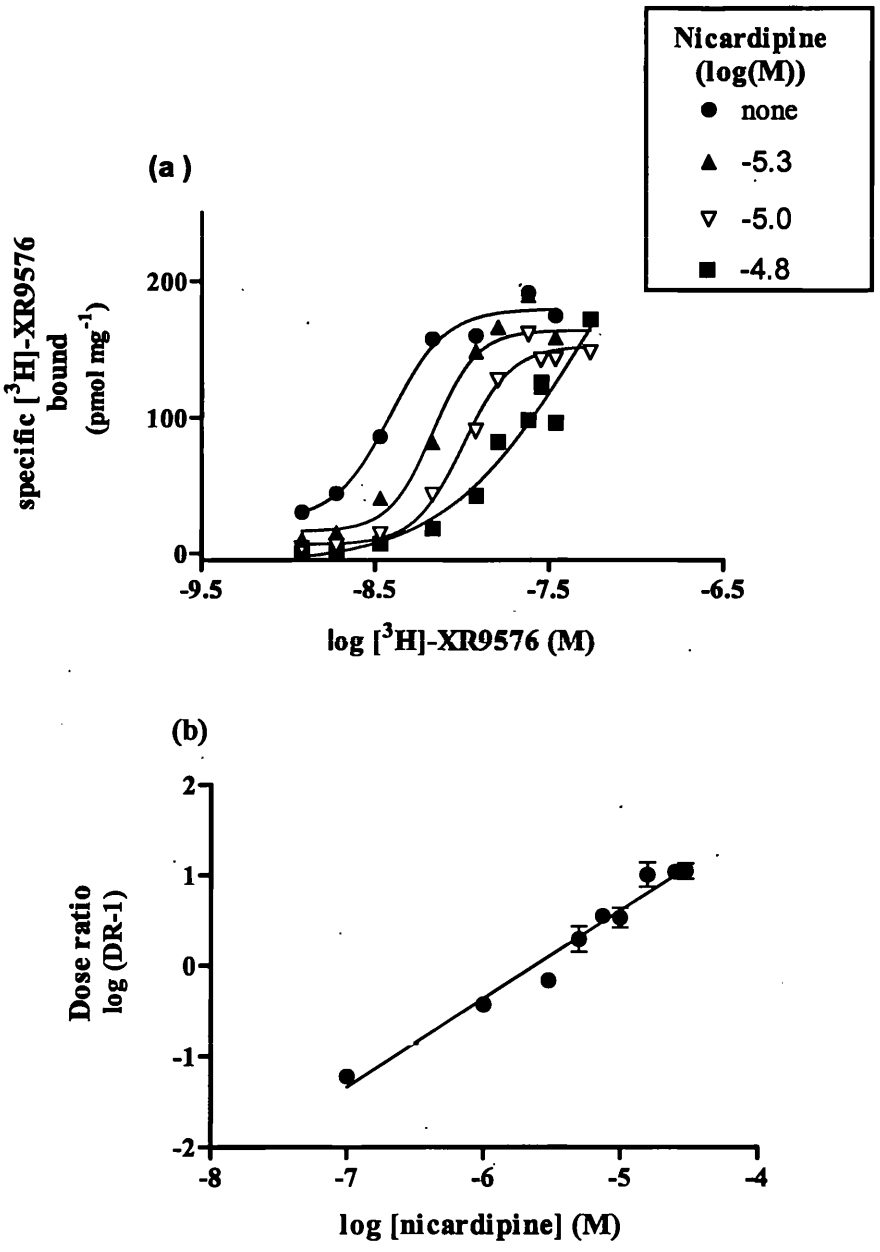

Figure 4.8 **Investigating the binding parameters of [^{3}H]-XR9576 in the presence of nicardipine. (a) effect of different concentrations of nicardipine on binding curves for [^{3}H]-XR9576 (representative plot shown). (b) Schild plot derived from binding data relating alteration in K_d to antagonist concentration. The type of interaction occurring between drugs is determined by the slope and *x*-axis intercept of this relationship. Each value is the mean ± s.e.m. of at least three independent experiments. Published in Martin *et al.*, (83).**

To determine whether the displacement of binding curves by nicardipine was due to a competitive interaction, Schild analysis of the binding data was conducted. A Schild plot depicting alterations in the affinity of [^{3}H]-XR9576 binding due to the presence of

increasing concentrations of nicardipine, is shown in figure 4.8(b). The slope of this relationship did not deviate significantly from 1.0 (0.945 $\pm$ 0.066) (*F* test, $P<0.05$). However, the affinity constant (K_b) for nicardipine derived from the *x*-axis intercept of this relationship was higher than expected (K_b = 4.89 $\pm$ 0.34μM), given its 10-fold greater potency (see section 4.2) to modulate [^{3}H]-vinblastine binding. This suggested that the interaction occurring between nicardipine and [^{3}H]-XR9576 on P-gp may not be competitive in nature. To determine whether this was the case, the effect of nicardipine on the dissociation kinetics for [^{3}H]-XR9576 binding was examined. There was a 2.1-fold increase in the dissociation rate constant for [^{3}H]-XR9576 in the presence of 1000-fold molar excess of unlabelled nicardipine (see table 4.3). This alteration in the dissociation rate constant of a drug by another drug can only be exerted via an allosteric mechanism. When considered in combination with the aberrant value for K_b observed, it provides proof for non-competitive interaction.

In contrast to the effects of XR9051 and nicardipine on the binding of [^{3}H]-XR9576, inclusion of different concentrations of the acridonecarboxamide GF120918 in binding assays of [^{3}H]-XR9567 elicited a reduction in the B_{max} for binding. The degree by which the maximal binding capacity was reduced was dependent upon the concentration of GF120918 present. A secondary plot depicting fractional reduction in the B_{max} as a function of GF120918 concentration is shown in figure 4.9. There was a 75% reduction in the B_{max} for [^{3}H]-XR9576 binding in the presence of GF120918. The potency (EC_{50}) of this antagonistic effect was derived from non-linear regression of the dose-response curve in figure 4.9. GF120918 reduced the binding of [^{3}H]-XR9576 with an EC_{50} value of 85.9 $\pm$ 0.9nM (n=3). There was no measurable alteration in the K_d of binding. A reduction in B_{max} in the absence of any changes in the K_d is indicative of non-competitive interactions.

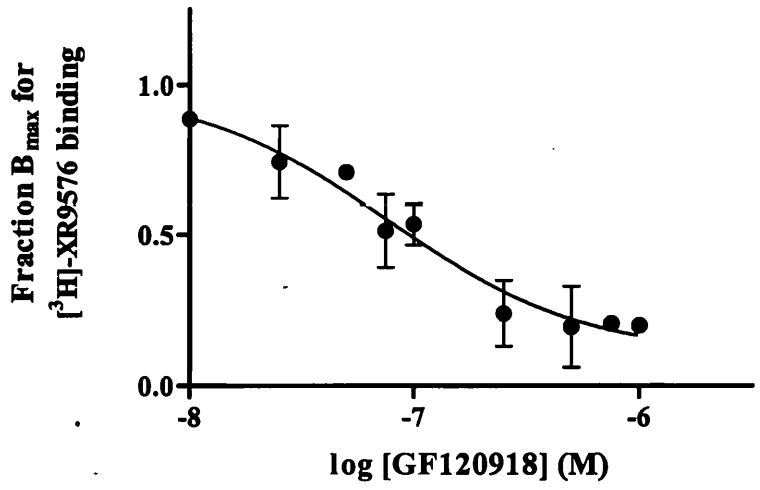

Figure 4.9 Effect of GF120918 on B_{max} for [^{3}H]-XR9567 binding to P-gp. Data presented are fractional reduction in B_{max} for [^{3}H]-XR9576 obtained from binding dose-response curves produced at different concentrations of GF120918. All values are the mean ± s.e.m. from at least three independent experiments. Published in Martin *et al.*, (83).

To corroborate that XR9576 and GF120918 interact non-competitively on P-gp, the effect of increasing concentrations of GF120918 on the dissociation rate constant for [^{3}H]-XR9576 was investigated. There was a dose-dependent increase in the dissociation rate constant for [^{3}H]-XR9576 in the presence of GF120918 (increased maximally 1.4-fold) as shown in table 4.3. This finding provided unequivocal evidence that XR9576 and GF120918 interact at distinct, but allosterically linked sites. The results obtained in this section indicate that there is not a common site on P-gp at which modulatory compounds bind, as GF120918 and nicardipine interact at a site(s) distinct from the XR9567 site. Due to the unavailability of radiolabelled versions of GF120918 or nicardipine, it was not possible to determine whether these modulators share a common site on P-gp or not.

Table 4.3 Effect of modulatory compounds on dissociation kinetics [^{3}H]-XR9576

Drug (n>3)	Maximal k_{-1} (min^{-1})	Fold change	EC_{50} (μM)
XR9576	0.023	N/A	N/A
GF120918	0.0315	1.4	0.08
Nicardipine	0.049	2.1	1.7

Effect of drug on the dissociation rate constant for [^{3}H]-XR9576 was determined as described in methods. The k_{-1} for [^{3}H]-XR9576 was determined at a number of drug concentrations. Maximal change in k_{-1} and the potency of drug allosteric effect (EC_{50}) were estimated from non-linear regression of dose-response equations.

4.6 Summary

A number of radioligand binding studies have been conducted to investigate competitive and non-competitive interactions between drugs on P-gp. These studies have identified four distinct classes of drug interaction site on P-gp. Two distinct sites of interaction for transport ligands were found. A third site was identified capable of binding either modulator or transport ligand, and a fourth was found that appears to be purely modulatory in role. Not only are there distinct sites of drug interaction on P-gp, but these sites interact via an allosteric communication network. A model depicting a multiple inter-connecting binding site network on P-gp has been proposed based on these findings, and will be discussed at length in chapter 6.

Chapter 5

Drug binding at discrete stages of the catalytic cycle of P-glycoprotein

5.1 Introduction

As P-glycoprotein is a primary active transporter, the binding of drug at the transmembrane domains must be intimately linked, or coupled, to its catalytic activity at the cytoplasmic nucleotide binding domains. Presumably, to achieve transmembrane translocation, the drug binding sites must cycle between high and low affinity conformations in response to signals from the NBDs. However, the stages of the catalytic cycle involved in inducing such alterations in drug binding site affinity have not been fully delineated. The purpose of the studies reported in this chapter is to examine drug binding parameters during discrete stages of the catalytic cycle to determine (i) when the initial signal is transmitted to instigate a transport event and (ii) the point in the cycle at which transport is completed and the binding site has returned to its "pre-transport" conformation.

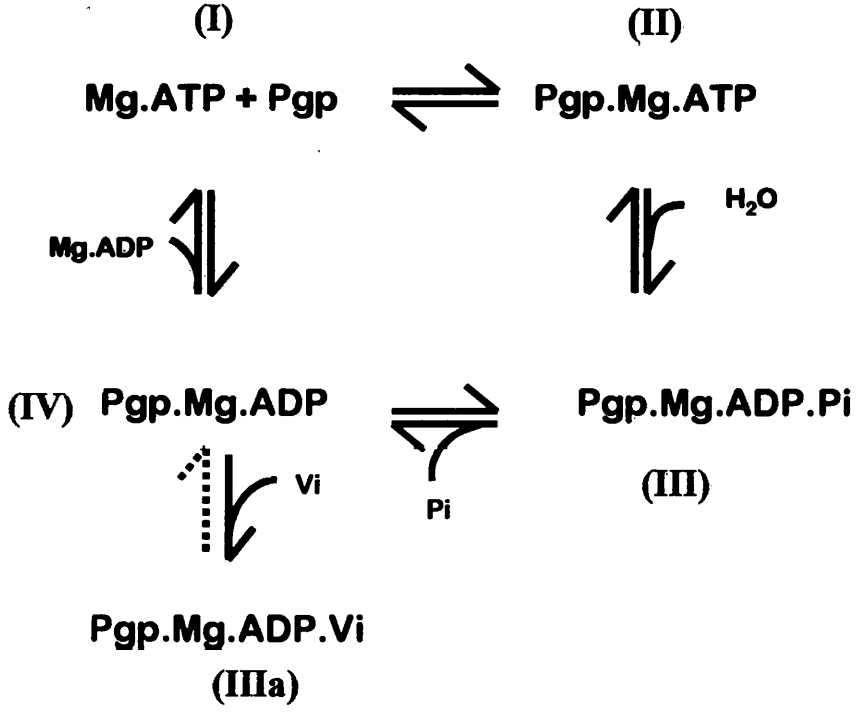

Figure 5.1 Discrete stages in the catalytic cycle of P-gp

A catalytic cycle refers to the events involved in the hydrolysis of a single molecule of ATP and a scheme depicting discrete stages of a catalytic cycle of P-gp is shown in figure 5.1, as proposed by Senior *et al.* (117), and discussed in section 1.10 of this thesis. Catalysis can only occur at a single NBD at any one time, as it has been previously shown that the NBDs of P-gp do not hydrolyse ATP simultaneously (146). The NBDs of P-gp are proposed to alternate in ATP hydrolysis, exhibiting strong co-operativity as both NBDs must be intact to permit even a single round of hydrolysis. How drug interacts with the protein as it undergoes a catalytic cycle has not been fully elucidated. In this chapter, I want to investigate the ability of drug to bind at all of the stages outlined in figure 5.1. Radioligand binding studies will be used to directly measure the binding parameters of the transport ligand vinblastine and the modulatory compound XR9576. This will provide information regarding signalling between the NBDs and two different classes of drug binding site, at different steps in the catalytic cycle.

In order to examine specific stages of a catalytic cycle, a number of experimental tools will be used as outlined in the scheme presented in figure 5.2. To look at drug binding to P-gp at an early or pre-hydrolysis stage (stage II) a technique is required to investigate the ATP bound form of the protein. The molecules ATP-γ-S and AMP-PNP, which are non-hydrolysable analogues of ATP, have been chosen to mimic binding of intact ATP by P-gp. It is not technically possible to directly assess the type of signal transmitted to the drug binding sites at the next stage of the cycle (III/IIIa in figure 5.2), which follows ATP hydrolysis but precedes dissociation of Pi. This is due to the instability of the P-gp.Mg.ADP.Pi complex (147). To circumvent this problem the technique of vanadate trapping can be used to mimic stage III (refer to stage IIIa of figures 5.1 and 5.2). The vanadate ion has higher affinity than Pi for the P-gp.Mg.ADP complex, which is reflected in a much slower rate of dissociation and thereby functions to 'stabilise' the

protein in the Mg.ADP.Vi bound form. Finally, it was of interest to investigate whether conformational changes are wrought on drug binding sites following dissociation of Pi. To investigate this stage, it was important to be able to measure drug binding to P-gp with bound nucleotide diphosphate, but without Pi (see stage IV of figures 5.1 and 5.2).

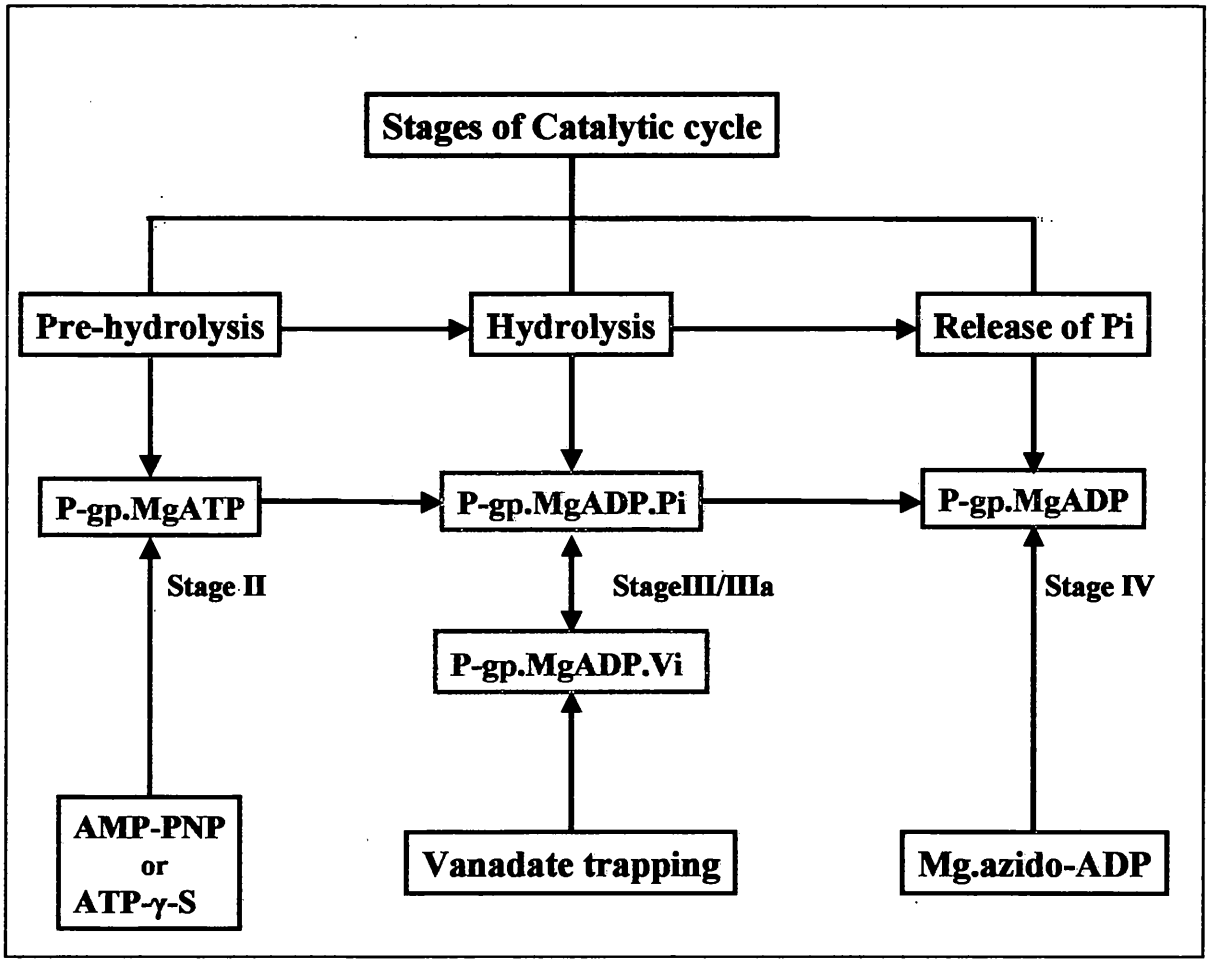

Figure 5.2 Scheme outlining the stages in the catalytic cycle to be investigated. The experimental tools used to isolate each stage are shown in red.

However, this is difficult due to the inherently low affinity of ADP to bind P-gp. To achieve this, P-gp was vanadate-trapped using 8-azido-ATP, an azido analogue of P-gp, which has previously been shown to be hydrolysed by P-gp (1). Following vanadate trapping, the samples are irradiated with U.V. light to covalently cross-link 8.azido.ADP to P-gp. Vanadate was removed as described in Chapter 2, 2.6.1.

5.2 The effect of nucleotide analogues and vanadate trapping on ATPase activity in CH^rB30 membranes

Prior to proceeding with investigation of drug binding during the catalytic cycle using the tools outlined above, the effect of these agents on the ability of P-gp to hydrolyse ATP was investigated. Measurement of ATPase activity is a convenient means by which to assess the effectiveness of the compounds used to interact with and affect the activity of P-gp. The ability of the non-hydrolysable ATP analogues ATP-γ-S and AMP-PNP to interact with P-gp was assessed by measuring basal ATPase activity in the presence of a range of concentrations of these nucleotides (0.01mM to 10mM). The ATPase activity of P-gp was inhibited in the presence of ATP-γ-S with a potency of IC_{50} = 0.31 ± 0.01mM ($n \geq 3$). It was not possible to determine the effect of AMP-PNP on the ATPase activity of P-gp using a Pi release assay due to the high free Pi content of the commercially available AMP-PNP.

The effect of vanadate on basal ATPase activity in CH^rB30 membranes has been reported on in Chapter 3, 3.3. Vanadate could inhibit up to 85% of basal activity measured at a single concentration of ATP in CH^rB30 membranes with IC_{50} = 0.7 ± 0.09μM ($n \geq 3$). CH^rB30 membranes were incubated with ATP and 300μM vanadate, a concentration that is significantly greater than its IC_{50} value above, and was thus sufficient to achieve full inhibition of activity. Trapped protein nucleotide complex was separated from unincorporated nucleotide and vanadate using gel filtration chromatography. Isolated trapped protein was examined to ascertain (i) whether protein was sufficiently trapped with vanadate to inhibit activity, (ii) if activity was recoverable, (iii) the conditions required to achieve recovery of activity. The V_{max} of basal ATPase activity in vanadate trapped protein, prior to separating unbound components, was reduced from 177 ± 30 nmol min^{-1} mg^{-1} membrane protein to 29 ± 4 nmol min^{-1} mg^{-1} (n=3). This represents an 85% reduction in the V_{max} for ATP hydrolysis. Activity

remaining in CH^{r}B30 membranes may be due to contributions from non-P-gp ATPases. The reversibility of the vanadate effect was investigated by looking at conditions required to dissociate bound vanadate ion. Following separation of unbound reaction components, recovery of ATPase activity was monitored by incubating trapped protein

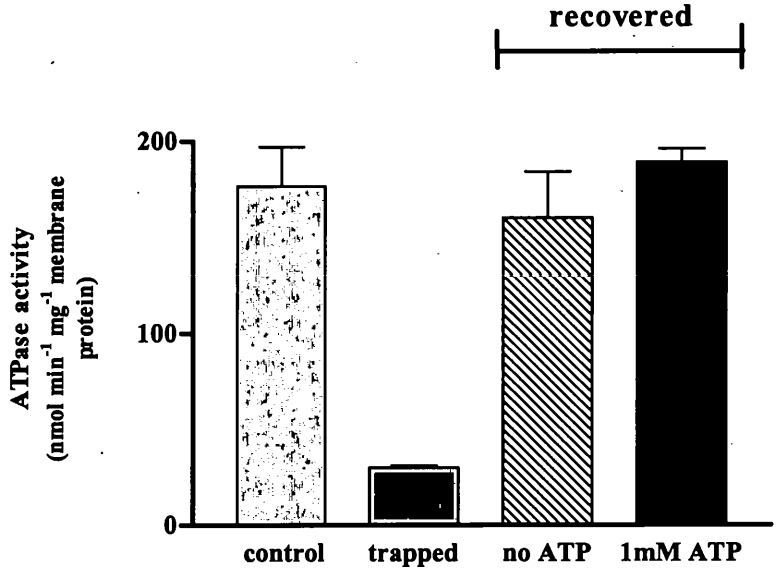

Figure 5.3 CH^{r}B30 membrane vesicles were incubated with 2mM ATP and 300μM vanadate at 37°C for 25 minutes. Unbound nucleotide and vanadate were removed by sephadex G50 centrifuge columns and recovery of ATPase measured by incubating at 37°C in the presence or absence of 1mM ATP. Data are the mean ± s.e.m. from at least three independent experiments.

at 37°C in buffer with or without 1mM ATP and devoid of vanadate, for up to 2 hours. As shown in figure 5.3, there was full recovery of ATPase activity after incubation at 37°C, and recovery was complete by 120 minutes post-incubation. The presence of ATP did not influence the extent to which activity could be recovered, indicating that ATP hydrolysis is not required to restore activity post-vanadate trapping. This is in agreement with the previously published study of Urbatsch *et al.*, (144). Trapping of P-gp with vanadate produces a stable catalytic cycle intermediate, which is more long-lived at

22°C, thus enabling study of the characteristics of drug binding at this step (III/IIIa) of the cycle.

As stated in the previous section, in order to isolate stage IV of the catalytic cycle (see figures 5.1 and 5.2), an azido nucleotide diphosphate (8-azido-ADP) will be covalently cross-linked to the protein using U.V. light. However, it was important to determine (i) the efficiency with which the azido-nucleotide diphosphate was crosslinked to the protein and (ii) that there was no effect of the cross-linking procedure on the activity of P-gp. This was achieved by looking at the ability of verapamil to stimulate basal ATPase activity of 8-azido-ADP bound P-gp.

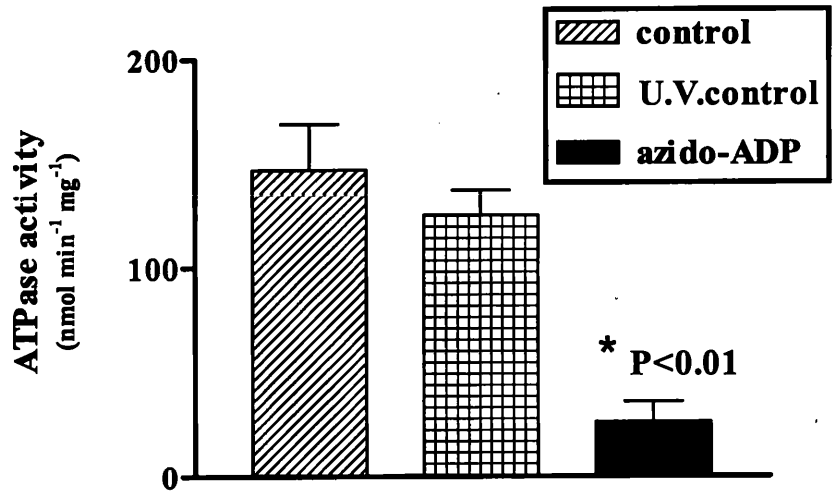

Figure 5.4 CH^{r}B30 membrane vesicles (1μg) that were either untreated, exposed to U.V. light or U.V. cross-linked with 8-azidoADP were incubated with 0-2.5mM Na_2ATP in the presence of 50μM verapamil over a 20 minute period at 37°C. Dose-response curves plotting drug stimulated ATPase activity as a function of ATP concentration were produced from which values for V_{max} of activity were derived. Values presented represent mean V_{max} ± s.e.m. from at least three independent experiments. * Significant reduction in activity versus untreated control (Student's *t* test P < 0.01)

There was significant reduction in the level of drug-stimulated ATPase activity measured in CH^{r}B30 membranes treated with azido-nucleotide and U.V. cross-linking, as compared to untreated membranes (P< 0.01) (figure 5.4). There was a small decrease

(10%) in the ATPase activity of CH^{r}B30 membranes exposed to cross-linking conditions, but this was not statistically significant (P>0.05). This suggests that inhibition of ATPase activity was due to the presence of azido-nucleotide covalently bound at the catalytic site, and not by a detrimental effect of the cross-linking procedure on verapamil binding or ATP hydrolysis.

The effect of the sulphydryl-reactive agents NBD-Cl, NEM and MIANS on basal ATPase activity of CH^{r}B30 membranes was also investigated. These compounds can covalently label cysteine residues located within the Walker A motif of each nucleotide binding domain. I wanted to examine the ATPase activity of P-gp in the presence of

Table 5.1 Potencies of 'catalytic' inhibitors to affect the ATPase activity of P-gp.

compound	**Inhibition of ATPase activity IC_{50} (μM)**
NBD-Cl	17.8 ± 3.6
NEM	3.2 ± 0.6
MIANS	1.9 ± 0.3
ATP-γ-S	311 ± 99
Vanadate	0.7 ± 0.1

The potencies (IC_{50}) of vanadate, covalent inhibitors and nucleotide analogues on the ATP hydrolytic activity of P-gp were measured using 2mM ATP at 37°C with 1μg CH^{r}B30 membrane vesicles. Values represent the mean+s.e.m. of at least three independent experiments. (Published in Martin *et al.*, (85).

molecules, other than nucleotide analogues, which bind within the catalytic pockets of P-gp. All three sulfhydryl-reactive compounds caused a dose-dependent decrease in basal ATPase activity as shown in table 5.1. MIANS (IC_{50} = 1.9 ± 0.3μM) (n=3) and NEM (IC_{50} = 3.2 ± 0.6μM) (n=3) abolished activity with similar potency, whilst NBD-Cl

displayed slightly lower potency to inhibit activity (IC_{50} = 17.8 ± 3.6μM) (n=3). The effect of these agents on drug binding will be investigated in the next section.

Having developed various procedures to inhibit P-gp activity and 'freeze' it at specific stages of the catalytic cycle, the ability of drug to interact at discrete steps of this cycle was investigated.

5.3 Drug binding in the presence of nucleotide.

Signalling between the TMDs and NBDs underlies transport activity of P-gp. Numerous studies using a variety of assays, including measurements of ATPase activity, have demonstrated that drug binding sites are capable of communicating with the NBDs. There is little information concerning the reverse, i.e. the effect of events at the catalytic sites on drug binding. In this section, I have directly measured drug binding in the presence of different nucleotides, as a first step towards elucidating the effect of signals originating at the NBDs on the ability of drug to bind at the TMDs. The relative effects of the nucleotides ATP-γ-S, AMP-PNP, ADP and AMP (0.01-10mM) on the binding of [^{3}H]-vinblastine and [^{3}H]-XR9576 were measured. As shown in figure 5.5, the binding of [^{3}H]-vinblastine (15-20nM) was reduced by 60% in a dose-dependent fashion in the presence of ATP-γ-S (IC_{50} = 0.14 ± 0.05mM) (n≥3). The presence of AMP-PNP displaced 70% of bound [^{3}H]-vinblastine and the potency to reduce binding was reflected in an IC_{50} value of 0.37 ± 0.09mM (n≥3). Binding of [^{3}H]-vinblastine measured in the presence of increasing concentrations of ADP displayed less than 30% displacement of bound drug, whilst there was a modest (<10%) reduction of binding in the presence of AMP. In contrast to the nucleotide-induced changes in [^{3}H]-vinblastine binding, there was no effect of any of the nucleotides used on the binding of the modulatory compound [^{3}H]-XR9576 (data not shown). This initial investigation of the effect of nucleotide on

the ability of drug to interact with P-gp shows that binding of nucleotide, particularly nucleotide triphosphate, transmits a signal to the TMDs that alters the vinblastine drug binding site. However, the lack of effect seen with [^{3}H]-XR9576 indicates that perhaps not all binding sites are coupled to binding of nucleotide. The specificity of the effect seen with nucleotide on [^{3}H]-vinblastine binding was investigated further by

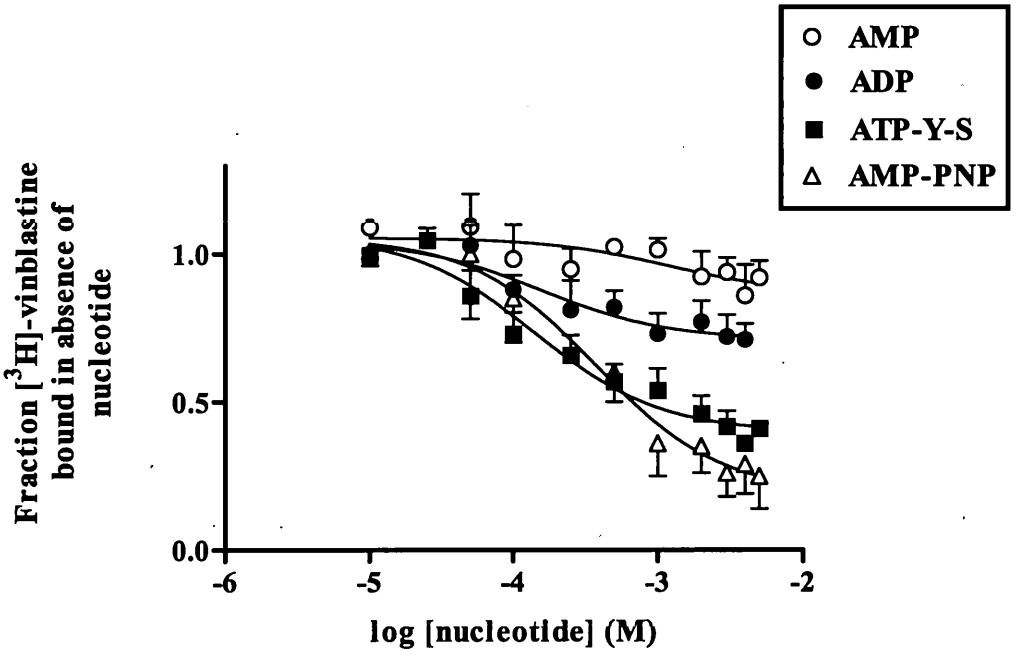

Figure 5.5 Nucleotide displacement of [^{3}H]-vinblastine binding. CH^{r}B30 membrane vesicles (8μg) were incubated with [^{3}H]-vinblastine (15-20nM) in the presence of nucleotides (0.01-5mM). The amount bound was expressed as a fraction of the total specific binding obtained in the absence of nucleotide and plotted as a function of nucleotide concentration. The extent of displacement and the IC_{50} values were obtained from general dose-response curves. Data presented are the mean ± s.e.m. from three to five independent experiments. (Published in Martin *et al.*, (85).

looking at the ability of the sulphydryl-reactive compounds MIANS, NEM and NBD-Cl to alter drug binding. There was no reduction of [^{3}H]-vinblastine binding in the presence of these agents (data not shown). This demonstrates that signalling from the NBDs to the TMDs is specifically dependent upon the molecule bound in the catalytic pocket. This initial investigation of drug binding in the presence of nucleotide has provided the first direct evidence that the drug binding site receives specific communication from the

NBDs. The fact that binding of the transport ligand [^{3}H]-vinblastine was effectively displaced by non-hydrolysable analogues of ATP suggests that binding of ATP provides a signal early in the catalytic cycle to alter [^{3}H]-vinblastine binding. The nature of the change induced on the vinblastine binding site in the presence of non-hydrolysable ATP analogues could not be ascertained from the displacement equilibrium binding assays conducted. Therefore, to characterise the effect of ATP binding on the vinblastine site, full saturation binding isotherms for [^{3}H]-vinblastine were conducted in the presence of different concentrations of ATP-γ-S or AMP-PNP. These assays are more informative than displacement binding experiments as they provide information concerning the effect of nucleotide on the affinity and extent of drug binding by P-gp.

Full saturation binding assays for [^{3}H]-vinblastine and [^{3}H]-XR9576 were conducted in the presence of different concentrations of either ATP-γ-S (0-5mM) or AMP-PNP (0-3mM). Investigation of the effect of AMP-PNP on [^{3}H]-XR9576 saturation binding curves was not possible due to lack of continued availability of this radiochemical. The B_{max} for [^{3}H]-vinblastine binding measured at each concentration of nucleotide was used to produce a secondary plot (as shown in figure 5.6) relating effects on B_{max} to nucleotide concentration. As shown in figure 5.6 (a), there was a dose-dependent decrease in the B_{max} for [^{3}H]-vinblastine binding in the presence of ATP-γ-S to 40% of that observed in the absence of nucleotide. The potency of ATP-γ-S to alter [^{3}H]- vinblastine binding was described by an IC_{50} value of 0.14 $\pm$ 0.05mM (n=3). AMP-PNP, on the other hand, caused more than 90% reduction in the B_{max} for [^{3}H]-vinblastine binding and a maximal effect was seen at 2-3mM. The IC_{50} value (0.2mM) to inhibit binding was similar to that determined for ATP-γ-S, and these values are within the range of values reported for the K_m of ATP hydrolysis (see chapter 1, section 1.10).

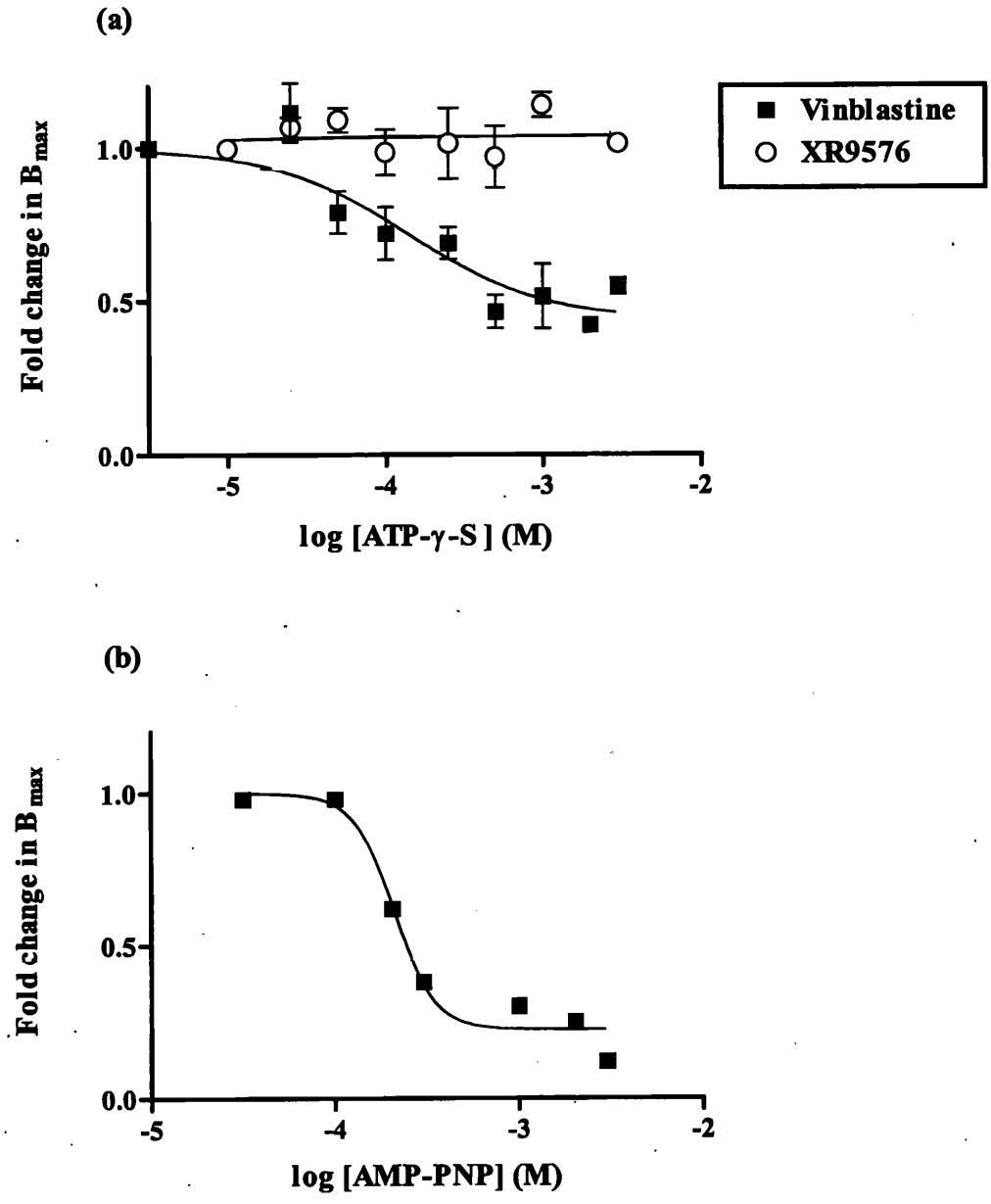

Figure 5.6 (a) Effect of ATP-γ-S on the binding capacity of [^{3}H]-vinblastine and [^{3}H]-XR9576. Saturation isotherms for [^{3}H]-vinblastine (1-100nM) and [^{3}H]-XR9576 (0.1-40nM) were conducted in the presence and absence of different concentrations of nucleotide. A secondary plot relating B_{max} at each concentration of nucleotide is shown and data fitted using the general dose-response equation. Data are mean±s.e.m. from 3 to 5 independent experiments. (b) Effect of AMP-PNP on B_{max} for [^{3}H]-vinblastine binding. Saturation isotherms were conducted in the presence of different concentrations of AMP-PNP (0-3mM). A secondary plot showing B_{max} as a function of nucleotide concentration is shown. Data represent single observations from full isotherms at each concentration of nucleotide used. Note data in (a) published in Martin *et al.*, (85).

By using two different non-hydrolysable analogues of ATP, it was shown that binding of ATP in the absence of hydrolysis causes a reduction in the B_{max} for [^{3}H]-vinblastine binding. However, the difference in the extent to which binding is reduced by these nucleotide analogues may be due to the fact that ATP-γ-S is very slowly hydrolysed at 22°C and AMP-PNP is not. This slow hydrolysis was confirmed by conducting a coupled enzyme assay as described in Al-Shawi *et al.* (1), data not shown. Therefore, AMP-PNP was used in all subsequent investigations of nucleotide effects on drug binding. Nonetheless, the decrease in the B_{max} for [^{3}H]-vinblastine due to binding of ATP analogues suggests that vinblastine cannot readily access its binding site, and is indicative of conformational alteration of the high affinity site.

In contrast, there was no effect of ATP-γ-S on the binding of [^{3}H]-XR9576 (figure 5.6(a)) which confirmed the result seen from displacement binding assays conducted earlier. The lack of effect of nucleotide on the binding of [^{3}H]-XR9576, which is a modulatory compound and not transported by P-gp, (shown in chapter 3, 3.2.) may suggest either (i) binding of nucleotide transmits a different signal to different sites or (ii) the signal transmitted by nucleotide is dependent upon the drug bound.

5.3.1 Further characterisation of nucleotide-induced alteration of [^{3}H]-vinblastine binding

5.3.1.1 Modification of radioligand binding assay to detect changes in affinity

The results in the previous section have shown that the binding site for the transport ligand vinblastine is altered at a stage of the catalytic cycle (stage II in figure 5.1) that occurs prior to nucleotide hydrolysis. The alteration in the binding site was manifest as a reduction in the B_{max} and indicates an altered affinity of the protein for vinblastine. The reduced binding capacity could be due to either a complete conformational shift in the high affinity drug binding site to a low affinity conformation, or complete occlusion of

the high affinity drug binding site. It has not been possible to directly measure vinblastine binding to the low affinity site due to the technical limitations of the existing radioligand binding assay. The highest concentration of [^{3}H]-vinblastine used in radioligand binding assays is 150nM and is clearly not high enough to measure low affinity binding. To circumvent this problem, the radioligand binding assay for [^{3}H]-vinblastine was modified to enable measurements to be made over a range of concentrations up to 3μM vinblastine, which is 150-fold higher than its measured K_d for binding. This was achieved by performing homologous displacement binding (refer to chapter 2, section 2.2.4) and was based on methods described by Rovati (106).

This type of analysis could also provide detailed information relating to whether there was a single class of site for vinblastine, or two classes of site that alternated between high and low affinity conformations. This was of particular interest as it had been suggested from study of the effect of vinblastine binding on (a) the fluorescence of MIANS bound at the NBDs and (b) accessibility of UIC2 for its extracellularly located epitope, that there were two vinblastine binding sites on P-gp. Two models were chosen to test these possible pharmacological scenarios on the experimentally produced [^{3}H]-vinblastine binding data. As shown in figure 5.7 (a), theoretical binding data that was best-fitted by the dose response equation (equation 2.10), indicated binding to a single class of binding site, whilst data best described by the Adair equation (equation 2.7) or the sum of two Langmuir equations (equation 2.7a) was indicative of drug interaction at two sites of different affinity (figure 5.7 (b) and (c)). If vinblastine interacted at a single class of site, a reduction in affinity would be represented as a parallel shift to the right in the binding curve (figure 5.7 (a)). In contrast, if vinblastine interacted with two sites, one of which was altered during the catalytic cycle, the binding curve would become biphasic as illustrated in figure 5.7(b) & (c).

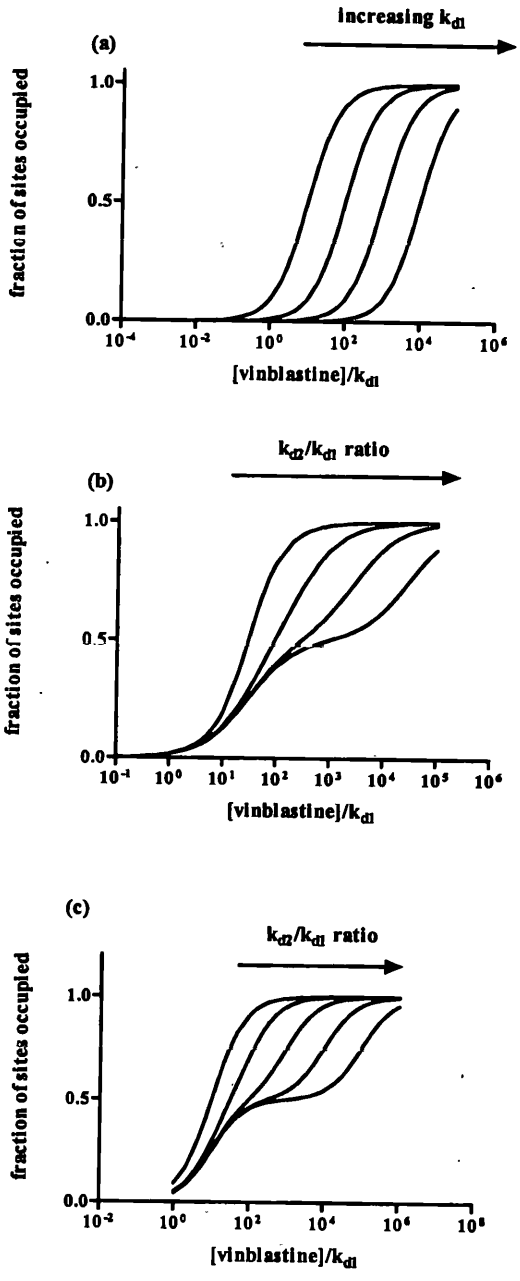

Figure 5.7 Theoretical binding curves were generated to demonstrate the characteristics of binding to a single site or to two sites of different affinity. (a) Dose-response curves as first described by Gaddum, simulating fraction of ligand bound to a single site over a range of ligand concentrations having arbitrary affinity (k_{d1}) between 1 and 1000. (b) & (c) Fraction bound to two independent sites determined over a range of ligand concentrations where the ratio of affinity of two sites (k_{d2}/k_{d1}) is increased from 1-up to 10000. This data was modelled using the Adair equation (b) or the sum of two Langmuir isotherms (c) as described in methods.

The experimentally produced [^{3}H]-vinblastine binding data, measured in the absence of nucleotide, was plotted as a function of vinblastine concentration and fitted by both equation 2.7 and 2.10.

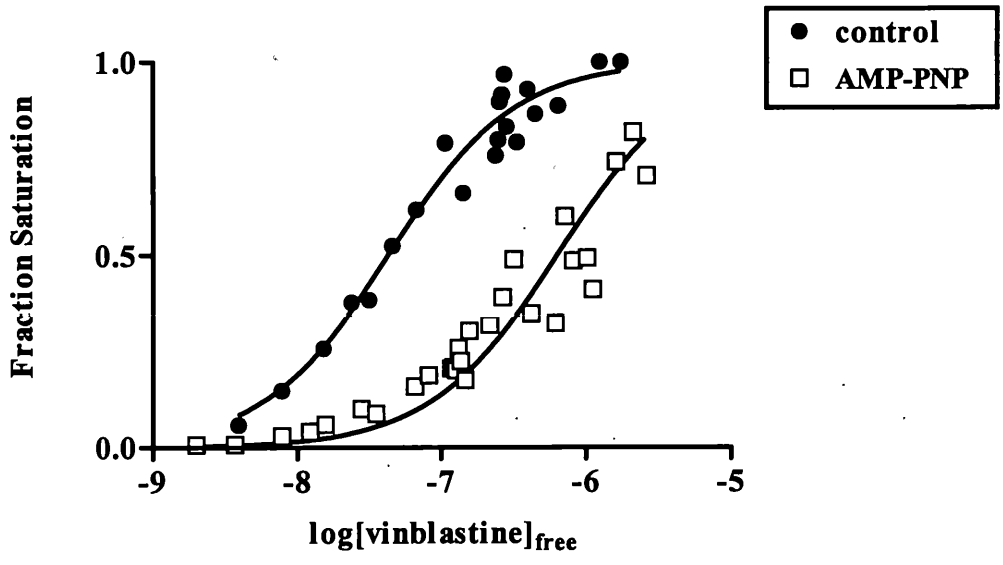

Figure 5.8 Binding of [^{3}H]-vinblastine in the presence of AMP-PNP. CH^{r}B30 membrane vesicles (15μg) were labelled with 1-100nM [^{3}H]-vinblastine and ligand range extended by supplementing 100nM [^{3}H]-vinblastine with unlabelled vinblastine (up to 3μM). Non-specific binding was measured in the presence of 10μM nicardipine. Representative semi-logarithmic plots depicting specific binding (fraction of saturable binding) as a function of vinblastine concentration (M). Values for B_{max} and K_d determined from dose-response equation as described in methods.

The goodness of fit was determined using the *F*-test and equation 2.7, which describes binding to a single class of binding site, best fitted the data produced (*F*-test, $P<0.05$) (figure 5.8 refer to 'control' data). [^{3}H]-vinblastine binding to P-gp in the absence of nucleotide was described with a single K_d of 59 ± 7nM (n=7) and a binding capacity (B_{max}) of 62 ± 2 pmol mg^{-1} membrane protein (figure 5.8 & table 5.3).

5.3.1.2 Homologous displacement of vinblastine binding in the presence of AMP-PNP

In the previous section, an abrogation in the B_{max} for [^{3}H]-vinblastine was observed at 2-3mM AMP-PNP. However, this was only measured over concentrations of vinblastine up to 150nM. By using an extended range of vinblastine concentrations, it was apparent that the binding was not abrogated, as a parallel shift to the right in the vinblastine isotherm was detected in the presence of AMP-PNP. Vinblastine binding in the presence of nucleotide was described by a K_d value of 856 $\pm$ 165nM (n=3) (table 5.3), which represents a 20-fold decrease in the affinity of binding. There was no diminution in the binding capacity. The more simple dose-response curve provided the best fit for the binding data as compared to the Adair equation (F-test, $P<0.05$), illustrating that vinblastine binding was still to a single class of site. This strongly suggested that the binding of nucleotide, prior to a hydrolytic event, conformationally alters the vinblastine site from high to low affinity. This also demonstrated that there were not multiple sites for vinblastine present that were alternating in affinity. Subsequent steps in the catalytic cycle were examined next in order to determine when the binding site re-adopts a high affinity conformation again.

5.4 The binding of drug to CH^{r}B30 membranes at post-hydrolytic stages of the catalytic cycle

5.4.1 The ability of drug to bind to 'vanadate trapped' P-gp

As outlined in section 5.1 of this chapter, the technique of vanadate trapping can be used to mimic stage III of the catalytic cycle (figure 5.1). This step immediately follows hydrolysis of ATP, but precedes dissociation of the P-gp.MgADP.Pi complex from the catalytic site. As mentioned earlier, the vanadate ion mimics Pi and can stabilise the protein in the 'transition state' conformation (stage IIIa, figure 5.1) that precedes dissociation of the products of hydrolysis from the catalytic site. It has been established

that the binding site for [^{3}H]-vinblastine is conformationally altered by binding of nucleotide. Does this alteration persist post-hydrolysis of nucleotide? In contrast, the binding site for [^{3}H]-XR9576 is 'resistant' to nucleotide induced alterations in conformation. Can the energy of nucleotide hydrolysis provide a signal that will conformationally alter this drug binding site? To address these issues the ability of [^{3}H]-vinblastine and [^{3}H]-XR9576 to bind vanadate trapped protein was investigated.

An initial characterisation of drug binding was conducted by performing saturation binding isotherms on vanadate-trapped protein. There was a significant effect of vanadate trapping on the equilibrium binding of [^{3}H]-vinblastine and [^{3}H]-XR9576 as shown in the representative saturation isotherms in figure 5.9 (a) & (b). The vanadate-trapped P-gp displayed a markedly reduced binding capacity (B_{max}) for [^{3}H]-vinblastine (15.2 $\pm$ 2.1 pmol mg^{-1} membrane protein) (n>3) as compared to the non-trapped state (58.7 $\pm$ 8.3 pmol mg^{-1}) (n>3) with no *apparent* effect on the affinity of ligand binding. This reduction in the binding capacity of [^{3}H]-vinblastine was completely reversed upon removal of unbound vanadate and subsequent incubation of treated membranes at 37°C for up to 120 minutes (71.7 $\pm$ 16.1 pmol mg^{-1}) (n$\geq$3). This complete recovery demonstrates that the low affinity binding is occurring because the protein is in a transition state complex, rather than a detrimental effect of the treatment on P-gp activity. The addition of nucleotide or drug to the 'recovery' sample was not required to restore [^{3}H]-vinblastine binding.

In a similar fashion, there was a reduced ability of vanadate-trapped P-gp to bind [^{3}H]-XR9576, as manifest by a reduced value for B_{max} (63.9 $\pm$ 6.8 pmol mg^{-1}) (n>3) as compared to untreated P-gp (211 $\pm$ 37 pmol mg^{-1}) (n$\geq$3), with no apparent alteration in

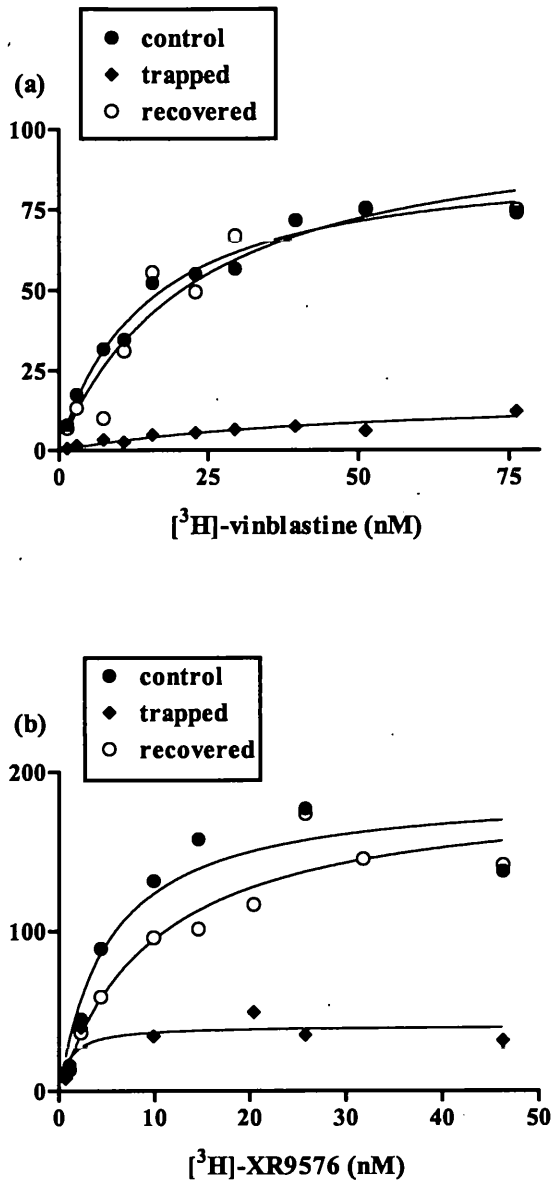

Figure 5.9 **The effect of vanadate-trapping on the equilibrium binding of (a) [^{3}H]-vinblastine and (b) [^{3}H]-XR9576 to CH^{r}B30 membrane vesicles. Plasma membrane vesicles were treated with 300μM vanadate and allowed to recover at 37°C for 2 hours prior to radioligand binding. The equilibrium binding of [^{3}H]-vinblastine (1-100nM) and [^{3}H]-XR9576 (0.1-40nM) was measured by a rapid filtration method following 2-3 hour incubation at 22°C. Representative saturation isotherms are shown for each radioligand. Values for B_{max} and K_d were obtained from the hyperbolic relationships and are summarised elsewhere (table 5.2).**

the K_d of the binding reaction. Binding of [^{3}H]-XR9576 to P-gp was fully restored following recovery of trapped protein, illustrating that the effect of vanadate treatment was reversible, as was the case for [^{3}H]-vinblastine binding (data summarised in table

5.2). The reduced ability of [^{3}H]-XR9576 to bind to trapped protein contrasts with the lack of effect of nucleotide binding on the binding site for XR9576. This indicates that binding of nucleotide and hydrolysis of nucleotide elicit different conformational outcomes with respect to the binding site for XR9576. However, it cannot be determined whether the different signalling to the XR9576 site is due to the nature of this site or the specific drug bound.

Table 5.2 Effect of vanadate trapping on the binding of [^{3}H]-vinblastine and [^{3}H]-XR9576

	[^{3}H]-vinblastine		[^{3}H]-XR9576	
n≥3	**B_{max} (pmol mg^{-1})**	**K_d (nM)**	**B_{max} (pmol mg^{-1})**	**K_d (nM)**
control	58.7±8.3	16.1±2.2	211±37	4.6±0.5
trapped	15.2±2.1	23.6±5.4	63.9±6.8	1.5±0.1
recovered	71.5±16.1	23.0±4.7	179±35	7.2±2.1

Equilibrium binding of [^{3}H]-vinblastine (1-100nM) and [^{3}H]-XR9576 (0.1-40nM) was conducted at 22°C for 2-3hrs on CH^{r}B30 membranes that had undergone the treatments indicated. The mean values ± s.e.m. for B_{max} and K_d from at least three independent experiments are presented. (Published in Martin *et al.*, (85).

These results show that the initial alterations wrought on the vinblastine binding site by nucleotide binding persist post-hydrolysis when protein is trapped in the MgADP.Vi bound conformation. However, the alterations in binding site have presented as a reduction in the B_{max} for binding over the low concentration range of [^{3}H]-vinblastine used (1-150nM). Homologous displacement equilibrium binding over a wider concentration range of radiolabel was conducted to quantitate the change in affinity, and to determine whether binding was still to a homogeneous population of sites. When binding of vinblastine to MgADP.Vi bound P-gp was measured over a broad range of concentrations, it was found that binding was still to a single class of low affinity site.

Binding data was best fitted by the dose-response equation for a single site (F-test, $P < 0.05$) and a value for K_d of 337 ± 60nM (n=3) was determined (representative plot shown in figure 5.10). This value for K_d was 'intermediate' between that observed for control and nucleotide bound P-gp. It could not be shown whether this represents the same low affinity conformation obtained in the presence of nucleotide.

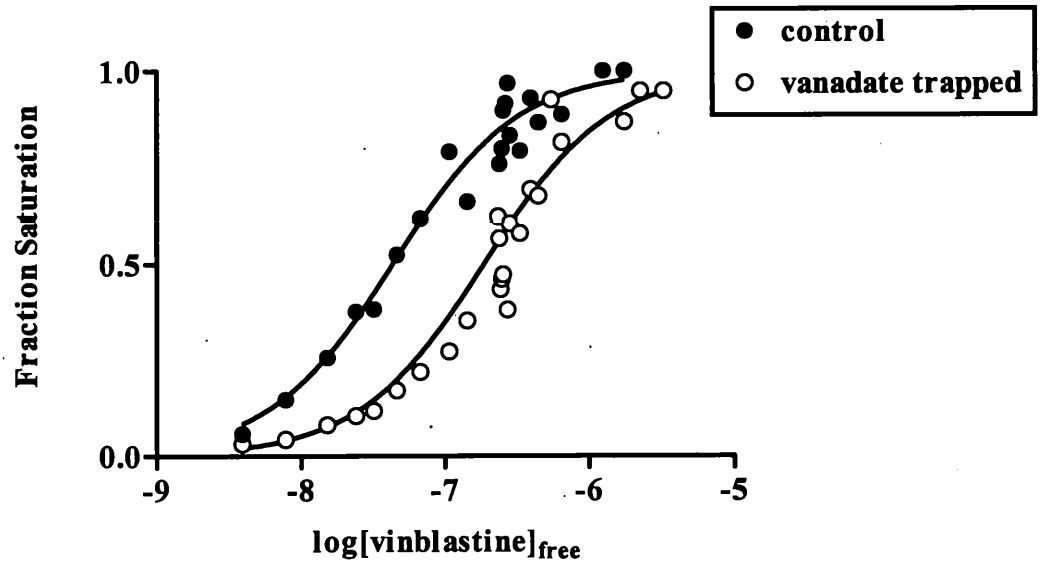

Figure 5.10 Effect of vanadate-trapping on binding parameters of [^{3}H]-vinblastine. CH^{r}B30 membrane vesicles (15μg) were labelled with 1-100nM [^{3}H]-vinblastine and ligand range extended by supplementing 100nM [^{3}H]-vinblastine with unlabelled vinblastine up to 3μM. Non-specific binding was measured in the presence of 10μM unlabelled nicardipine. Representative logarithmic plot is shown. B_{max} and K_d for binding determined as described in methods.

However, it can be concluded that the [^{3}H]-vinblastine binding sites on vanadate-trapped P-gp constitute a homogeneous population of low affinity sites. This experiment was not conducted with [^{3}H]-XR9576 as there was not a radiolabelled version of this compound available at the time.

5.5 Restoration of the high-affinity drug binding site conformation during the catalytic cycle

Characterisation of the binding of [^{3}H]-vinblastine to vanadate trapped P-gp revealed that at stage III of the catalytic cycle (figure 5.1) the vinblastine binding site is still in a low affinity conformation for substrate. This demonstrated that hydrolysis of nucleotide did not trigger restoration of the high affinity conformation. The next stage of the cycle involves dissociation of Pi from the MgADP.Pi-Pgp complex (see stage IV, figure 5.1). The effect of dissociation of Pi from the post-hydrolytic nucleotide complex was investigated to determine whether this provides the signal necessary to 'reset' the binding site again (stage IV, figure 5.1). The MgADP bound form of P-gp was mimicked by vanadate trapping P-gp with Mg-8-azido-ATP, following which the resultant azido-ADP was cross-linked to the protein and bound vanadate dissociated following gel filtration chromatography.

The binding of vinblastine to azido-nucleotide diphosphate bound P-gp was measured over a broad concentration range of vinblastine using the homologous displacement assay. Vinblastine binding was best described by the dose-response equation for binding to a single class of site. The K_d value of 81 $\pm$ 39nM (n=5) showed that the vinblastine binding site had been restored to a high affinity conformation. As shown in table 5.3, the value for K_d post-dissociation of Pi/Vi was not significantly different to the K_d for binding to protein under basal conditions ($P>0.05$). However, it was significantly lower than K_d observed under nucleotide binding or vanadate-trapping conditions. This result suggests that the release of Pi from the post-hydrolytic nucleotide diphosphate complex transmits a signal to the TMDs that restores high affinity binding of vinblastine.

Table 5.3 The effect of distinct stages of the catalytic cycle on the affinity of [^{3}H]-vinblastine binding

Stage in catalytic cycle	I	II	IIIa	IV	V
	control	AMP-PNP	ATP + Vanadate	ADP	ADP + AMP-PNP
K_d (nM)	59±7	856±165	337±60	81±39	85±13
n	7	3	3	5	3
P		<0.001	<0.01	NS	NS

Radioligand binding assays were conducted over a wide range of ligand concentration (0-3000nM) to compare the binding characteristics of [^{3}H]-vinblastine in the absence of nucleotide with pre- and post-nucleotide hydrolysis stages of the catalytic cycle. Dose-response curves were generated from which a single value for K_d (nM) was determined for each condition investigated, as described in methods. Mean values for K_d ± s.e.m. are presented. P values relate changes to untreated control (Student's *t* test). NS are non-statistically significant.

5.6 Role of non-catalytically active NBD in catalytic cycle

The investigations conducted thus far have identified stages in the catalytic cycle at which drug binding site parameters are altered. I have shown that a single round of catalysis is sufficient to cycle the binding site for the transport ligand vinblastine between high and low affinity conformations. This suggests that hydrolysis of a single molecule of ATP may be sufficient to support a single transport event. As discussed in chapter 1, 1.10, the NBDs of P-gp are proposed to alternate in hydrolysis, with only one NBD actively participating in a single round of the catalytic cycle (146, 147). This was borne out in vanadate trapping experiments conducted by Urbatsch *et al.* who showed trapping of one mol of nucleotide diphosphate per mol of P-gp. However, given the strong interplay that has been demonstrated to exist between the NBDs of P-gp, is there a role for the non-active NBD in signal transmission to the TMDs during catalysis and transport?

The nucleotide occupancy of the NBDs as the protein undergoes a cycle of catalysis is not known. I wanted to establish whether the non-active NBD was occupied during a catalytic cycle. This was achieved by comparing binding of ATP to untreated control membranes and those that were subjected to vanadate trapping. A displacement binding assay in which a range of concentrations of unlabelled ATP (0.01-1mM) was used to prevent photolabelling with a single concentration of 8-azido[α-^{32}P]ATP (2μM) was used to measure the affinity of ATP binding. Displacement assays were conducted, as it was not possible to use concentrations of 8-azido[α-^{32}P]ATP high enough to produce a saturation binding isotherm for ATP binding. Photo-affinity labelling experiments were carried out with P-gp purified and reconstituted from CH^{r}B30 membranes, to avoid possible contributions from other ATPases found in the CH^{r}B30 membranes.

Densitometric analysis of photolabelled P-gp containing proteoliposomes showed that ATP was able to completely displace 8-azido[α-^{32}P]ATP labelling of untreated protein (basal state) with an EC_{50} of 16μM (figure 5.11). More significantly, there was also labelling of protein that had previously been trapped with nucleotide at a single NBD by treatment with vanadate. However, the extent of labelling of trapped protein was approximately 50% of that measured under basal or non-trapped conditions. The 50% reduction in the extent of 8-azido[α-^{32}P]ATP labelling of fully trapped protein versus untreated control is indicative that binding is to one NBD. This finding demonstrated that the NBD, not actively involved in a catalytic cycle, could be labelled with nucleotide.

Having demonstrated that ATP can bind at the non-catalytically active NBD during a catalytic cycle, I wanted to ascertain whether this NBD can transmit a signal to the

TMDs. I have already shown that binding of non-hydrolysable ATP analogues at the 'active' NBD triggers the switch in the high affinity vinblastine binding site to low affinity. If binding of ATP at the 'non-active' site transmitted a similar signal, then the binding site may never regain its high affinity conformation prior to the next catalytic cycle! To discount this possibility, we wanted to examine the effect of AMP-PNP binding to the Mg-8-azido-ADP bound form of P-gp on drug binding. Binding of [^{3}H]-vinblastine to Mg-8-azido-ADP bound P-gp was conducted using homologous displacement binding assays in the presence and absence of 2mM AMP-PNP. The presence of the non-hydrolysable ATP analogue, AMP-PNP, did not alter vinblastine binding to MgADP-bound P-gp (table 5.3). The K_d (85 $\pm$ 13 nM) (n=3) for vinblastine binding to MgADP-bound P-gp when AMP-PNP was present at the 'non-active' NBD, was not significantly different to that observed for MgADP-bound P-gp alone (K_d = 81 $\pm$ 39nM, (n=5)). The K_d for binding measured under both conditions did not differ significantly from binding to nucleotide free protein. The lack of effect of AMP-PNP on the binding of vinblastine is in stark contrast to the previously measured 15-fold increase in the K_d for [^{3}H]-vinblastine binding measured in the presence of AMP-PNP alone. This finding suggests therefore that the 'non-active' NBD does not signal to the TMDs during a round of the catalytic cycle. If the alternating catalytic sites model for P-gp function holds true then it may be hypothesised that the alternate NBD becomes 'active' in a subsequent round of catalysis, following dissociation of MgADP. A second molecule of drug may bind prior to dissociation of MgADP as we have shown that the drug binding site is in a high affinity conformation at this stage and ATP bound at the 'non-active' NBD is not yet capable of transmitting a signal to the TMDs. The dissociation rate of Mg.ADP may be critical in propagation of coupled drug transport.

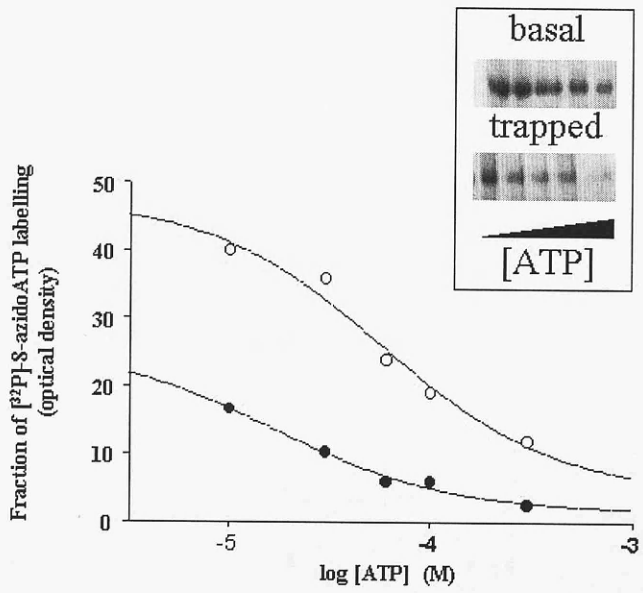

Figure 5.11 Displacement of 8-azido[α-^{32}P]ATP photo-labelling of P-gp, purified and reconstituted from CH^{r}B30 membranes, by increasing unlabelled ATP. Proteoliposomes (8μg) were incubated with 2μM 8-azido[α-^{32}P]ATP in the presence of increasing ATP (0.01-1mM) at 37°C for 15 minutes. Nucleotide trapping by vanadate was carried out as described in methods. Labelling of nucleotide was measured in trapped P-gp (•) versus untreated P-gp (O). *Inset*; SDS-PAGE illustrating displacement of 8-azido[α-^{32}P]ATP labelling of proteoliposomes in trapped versus untrapped (basal) protein.

5.7 Summary

1 Signalling from the NBDs to the TMDs has been investigated in terms of drug binding as P-gp undergoes a catalytic cycle. The binding of ATP triggers the initial change in the conformation of the [^{3}H]-vinblastine binding site as shown by low affinity binding measured in the presence of AMP-PNP.

2 The low affinity conformation produced in the presence of nucleotide consisted of a complete shift in the conformation of a single class of high affinity binding site.

3 Nucleotide-induced alteration of drug binding displayed specificity for the drug binding site occupied or perhaps the drug bound, as there was no effect of nucleotide binding on the [^{3}H]-XR9576 binding site.

4 Vanadate-trapping experiments demonstrated that the low affinity conformation of the [^{3}H]-vinblastine binding site persisted immediately post-hydrolysis of nucleotide. The affinity of [^{3}H]-XR9576 binding to vanadate trapped P-gp was altered as manifest by abrogation in the B_{max} for binding.

5 The release of Pi from the post-hydrolysis nucleotide diphosphate complex was sufficient to restore the conformation of the [^{3}H]-vinblastine binding site to high affinity.

6 It was concluded that hydrolysis of a single molecule of ATP is sufficient to support cycling of the [^{3}H]-vinblastine between high and low affinity conformations during a catalytic cycle. It was hypothesised that one molecule of vinblastine may be transported per molecule of ATP hydrolysed.

Chapter 6

General Discussion

6.1 Introduction

The ability of P-gp to interact with and transport numerous different compounds has been a puzzling feature of P-gp activity. Does this imply that P-gp is in violation of the classic 'lock and key' hypothesis for enzyme-substrate interaction? There is ample evidence from investigations of drug interaction with P-gp suggesting the presence of more than one binding site for drug on this protein. A primary objective of this thesis was to develop pharmacological probes to investigate further the molecular mechanism underlying P-gp's ability to interact with, and mediate translocation of, multiple different compounds.

6.2 Characterisation of P-gp activity in CH^{r}B30 membranes

A molecular pharmacological approach has been adopted in this thesis to directly investigate the mechanism of drug transport by P-gp. The transport activity of P-gp is dependent upon (i) the ability of drug to interact with the protein (ii) hydrolysis of ATP to provide the energy required for active translocation of drugs and (iii) transbilayer movement of drug to facilitate dissociation of drug to the extracellular milieu. When the studies carried out in this thesis were embarked upon, there was a dearth of information concerning how multiple drugs interact with P-gp or the affinity of such interactions. Therefore a primary aim was to develop radioligand binding assays to directly and quantitatively measure drug interaction with P-gp. P-gp ligands were broadly classified as transported ligands (usually anticancer agents) or modulators of P-gp activity, some of which may also be transported by P-gp.

Radioligand binding assays demonstrated that the anticancer agents [^{3}H]-vinblastine and [^{3}H]-paclitaxel could directly interact with P-gp containing CH^{r}B30 membranes with high affinity, as shown by K_d values in the low nanomolar range. The high affinity

binding measured in CH^{r}B30 membranes was shown to be specifically related to P-gp expression, as there was no measurable binding to membranes prepared from parental AuxB1 cells. The high affinity binding observed for [^{3}H]-vinblastine and [^{3}H]-paclitaxel to hamster P-gp is in agreement with radioligand binding studies conducted on human P-gp in membranes from MCF7 cells by Ferry *et al.* (30, 155). The low value for the K_d of vinblastine binding measured in the radioligand binding experiments alluded to above, contrasts with the studies of Romsicki and Sharom (102) who report values for the K_d of vinblastine interaction, in the micromolar range. The discrepancy between this study and the radioligand binding studies is due to the indirect nature of the assay used. The latter study, unlike radioligand binding assays, did not derive the true value for K_d but rather the potency of vinblastine to allosterically quench the fluorescence of MIANS, which was covalently bound within the catalytic pocket of the NBDs.

Having established that the anticancer agents vinblastine and paclitaxel can bind to P-gp with high affinity, I wanted to investigate whether binding of these drugs could transmit a signal to the energy generating NBDs, to affect ATP hydrolytic activity. Given the fact that P-gp positive tumours are resistant to these agents and together with evidence from cytotoxicity assays, it has been suggested that these compounds are transported by P-gp. Therefore, as P-gp transport activity only occurs under ATP hydrolysis conditions, it was expected that ATP hydrolysis activity might be increased in the presence of either vinblastine or paclitaxel. However, there was no measurable effect of vinblastine on basal ATPase activity and only a modest stimulation of activity by paclitaxel (1.3-fold) in CH^{r}B30 membrane vesicles. The lack of effect of vinblastine, on basal ATPase activity in CH^{r}B30 membranes has previously been reported by others (1, 132). Does this then imply that binding of vinblastine or paclitaxel is not tightly coupled to ATP hydrolysis? Interestingly, it has recently been proposed that P-gp behaves like an

uncoupled active transporter (69). This classification has been based on a number of observations from the P-gp literature including (i) a lack of variation in the extent to which different drugs alter the V_{max} for ATP hydrolysis, even though the affinity of drug binding might vary several fold (ii) the lack of effect, or in some cases, inhibition of ATPase activity by drugs that are translocated by P-gp and (iii) the presence of a basal ATPase activity in purified and reconstituted P-gp. However, ATPase activity of human P-gp in insect cells does display a low degree of stimulation by vinblastine (111). The difference may be related to the lipid environment encountered by P-gp in CH^rB30 cells versus insect cells. There is evidence to suggest that the basal activity of P-gp is related to the presence of an endogenous lipid component, which may be transported by P-gp (132).

To investigate the ATP dependent transport of vinblastine and paclitaxel by P-gp, a whole cell assay was used to measure steady-state accumulation of these compounds in P-gp expressing versus parental cells. There was 8-fold less accumulation of [^{3}H]-vinblastine or [^{3}H]-paclitaxel in CH^rB30 cells compared to parental AuxB1 cells. It was not possible to measure the transport kinetics of either of these cytotoxics using the whole cell assay for reasons outlined in Chapter 1, section 1.9. Therefore, the K_m or V_{max} for the transport of vinblastine or paclitaxel by P-gp was not determined. However, the extent of the accumulation deficit for [^{3}H]-vinblastine, measured in the multidrug resistant CH^rB30 cells, was similar to that demonstrated by Cano-Gauci and Riordan, (17).

This first series of experiments conducted to investigate the binding of cytotoxics with P-gp and the consequences of drug interaction for P-gp ATPase and transport functions show that (i) cytotoxics directly and specifically bind to P-gp with high affinity and (ii)

drug binding results in ATP-dependent transport of these compounds. The fact that there was no measurable stimulation of the basal ATPase activity in $CH^{r}B30$ membrane vesicles by the cytotoxics, poses interesting questions concerning the coupling of drug binding to ATP hydrolysis to mediate transport, and will provide a focus for future studies of P-gp transport activity.

As stated in the introduction to this discussion, if reversal of P-gp transport activity is to be used effectively to overcome MDR in the clinic, a greater understanding of how modulators interact with P-gp is required. As discussed in Chapter 1, section 1.3.2, many of the early modulatory compounds failed to effectively block P-gp transport activity due to the relatively poor potency of interaction of these compounds, relative to the more potent anticancer agents. A newer generation of modulatory compound emerged that was more efficacious in restoring sensitivity of resistant tumour cells to anticancer agents. However, no studies were conducted to directly measure interaction of these modulators with P-gp and compare the functional consequence of modulator binding on P-gp activity and the binding of cytotoxics.

I have shown that the third generation modulator [^{3}H]-XR9576 directly binds with P-gp displaying high affinity (K_d in low nanomolar range). Binding was specific for P-gp, as there was no binding to membranes from the parental cell line. This was the highest affinity reported to date for any modulatory compound, and contrasts with the 1000-fold lower affinity reported for the first generation modulator, verapamil (81, 158). The affinity of [^{3}H]-XR9576 interaction with P-gp was also 5- and 20-fold more potent than that observed for the cytotoxics vinblastine and paclitaxel, respectively.

High affinity binding is an important factor underlying the effectiveness of XR9576 to reverse P-gp mediated MDR, reported in both *in vitro* and *in vivo* resistance models (89). But what consequence does binding of XR9576 have on the activity of P-gp? This question was addressed by measuring the ATPase activity of P-gp containing CH^{r}B30 membrane vesicles in the presence of XR9576. XR9576 potently inhibited the P-gp related ATPase activity, as did the other third generation modulators GF120918 and XR9051, investigated in this thesis. This is the first report showing that drugs can potently inhibit the ATPase activity of P-gp. The effect of these modulators on ATPase activity is in stark contrast to the ability of the first generation modulators verapamil and nicardipine to increase hydrolysis. The potent inhibition of P-gp mediated ATPase activity by the new generation high affinity modulators, implied that they were not ligands for P-gp transport activity. This was confirmed in transport assays where there was no difference in the extent of [^{3}H]-XR9576 accumulated in CH^{r}B30 cells, compared to parental cells. Furthermore, there was no saturability in drug accumulated over a wide range of concentrations, indicating that XR9576 distribution was passive, rather than carrier mediated. Thus it was concluded, that the newer generation modulators could directly bind P-gp with equal or greater affinity than cytotoxic drugs, but the signal transmitted to the NBDs was different leading to inhibition of ATPase activity. This difference in signalling possibly underlies the reason why cytotoxic drugs are transported by P-gp, and compounds such as XR9576, are not.

Inhibition of ATPase activity rather than competition for transport, may represent the mechanism by which XR9576 and GF120918 effectively reversed the accumulation deficit observed for [^{3}H]-vinblastine and [^{3}H]-paclitaxel in CH^{r}B30 cells. The mechanism employed by first generation modulators, such as verapamil and nicardipine, to block P-gp transport activity is not known. These compounds can stimulate ATPase

activity and are proposed to be transport ligands for P-gp. However, there is as yet, no unequivocal evidence that verapamil or nicardipine are transported by P-gp (see review by Stein, (139)). As there were no radiolabelled versions of these compounds available, this possibility could not be tested in this thesis. An alternative hypothesis proposes that these agents modulate P-gp mediated transport by uncoupling the ATPase activity. Thereby the hydrolysis activity may be recruited by modulator, and is no longer available to transmit signal to the binding site(s) for transport ligands.

Additional information concerning the interaction of cytotoxic drug and modulator was obtained from study of the kinetics of drug binding. [^{3}H]-XR9576 had a faster rate of onset, and a slower rate of offset, from P-gp than vinblastine. This observation is in agreement with the findings of a recent study conducted by Mistry *et al.* (89), who demonstrate that XR9576 could potently modify MDR in human and murine cancer cell lines, and was active up to 24 hours post administration. This is in contrast to the several-fold poorer efficacy, and shorter duration of action of CsA and verapamil, to reverse cellular drug resistance. The action of these two drugs is short-lived, since they were only effective for up to 60 minutes post-administration. The difference in the duration of action of these compounds on P-gp, may be due to the fact that CsA and verapamil are ligands for transport by P-gp, and are therefore transported out of the cell.

In summary, this characterisation of the interaction of the modulatory compound [^{3}H]-XR9576 with P-gp, has shown the potential benefits of specifically designing pharmaceutical agents to target P-gp. XR9576 directly interacts with P-gp with high affinity and has a long duration of action. In fact, these features have been translated *in vivo,* as XR9576 is currently undergoing Phase II clinical trials to determine its efficacy in restoring cancer resistance to chemotherapy (89).

The radioligand binding studies described thus far, have provided a direct measure of the affinity of P-gp to bind the cytotoxic drugs vinblastine and paclitaxel, and the modulatory compound XR9576. Where drugs are not available in radiolabelled form, study of the antagonistic effect of drug on the binding of radiolabelled drug, is often used to determine the relative affinity of antagonist interaction. Inhibition of drug binding has been a methodology adopted by many investigators in the P-gp field to measure either drug interaction with P-gp, or as an estimate antagonist 'affinity' (25, 30, 109). Displacement binding experiments provide IC_{50} values that denote the concentration of antagonist that produces 50% inhibition of binding. However, as this value is not a constant and is dependent on experimental factors such as the concentration of radioligand to be displaced and the amount of membranes used, it has been common practice to transform this parameter to provide an inhibition constant for antagonist action. One such transformation is that derived by Cheng-Prusoff (19), where the IC_{50} value is converted to an inhibition constant or antagonist affinity constant (K_i value). However, the K_i value for antagonist action can only be equated with the K_d for binding of antagonist, where antagonist-drug interaction is competitive.

I performed a series of displacement binding experiments to measure the antagonistic potency of a range of drugs, both cytotoxic and modulatory on P-gp, as summarised in table 3.2 (Chapter 3, 3.7). IC_{50} values obtained from displacement binding curves were converted to K_i values to assess the potency of antagonist binding. Interestingly, the validity of the Cheng-Prusoff transformation was called in to question as there were a number of discrepancies between the K_i values for the antagonistic effect of some drugs, and their measured K_d values to interact with P-gp. In particular, vinblastine displaced the binding of [^{3}H]-XR9576 with a K_i value of 1.25μM and this deviated significantly from its measured K_d for binding to P-gp of 21nM (Chapter 3 (3.4.1)). There was also a

discrepancy between the K_i value for inhibition of [^{3}H]-XR9576 binding by paclitaxel, which was 16-fold higher than its previously determined K_d of binding. Additionally, the K_i values describing interaction of nicardipine with each of the radioligand drugs investigated, ranged between 10 and 885nM. Taken together, these findings suggested that the Cheng-Prusoff transformation may not provide a valid estimate for the affinity of antagonist to bind P-gp. Moreover, this suggests that there are non-competitive interactions between drugs on P-gp, which in turn means there is more than one drug binding site on the protein.

6.3 Communication between multiple distinct sites on P-gp

This provided the impetus to determine how many binding sites there were on the protein, and what kind of interaction occurs between the sites. From the binding studies outlined in chapter 4, a multiple drug binding site model for P-gp has been produced depicting the presence of at least four distinct sites of drug interaction on P-gp that are allosterically linked (figure 6.1).

As discussed in Chapter 2 (2.4), examination of the effects of antagonist binding on the B_{max} and K_d of drug, can yield important information concerning the type of interaction occurring between pairs of drugs at a receptor. This pharmacological principle was used to determine the number of binding sites (depicted in figure 6.1) and the kind of interactions occurring between them. An exhaustive series of radioligand binding experiments was therefore carried out, where complete saturation isotherms for either [^{3}H]-vinblastine or [^{3}H]-XR9576 were conducted in the presence of a range of concentrations of antagonist. Schild analysis was applied to the binding data to rigorously test for competitive interactions between drugs. The validity of using Schild analysis to discriminate between competitive and non-competitive antagonism has been

discussed at length by Kenakin (66) and demonstrated to be applicable to the study of antagonist interaction at receptors (72). Decreases in the B_{max} of binding were observed in many cases, strongly indicating non-competitive interactions. Measurement of the off-rate of radioligand in the presence of antagonist was used to verify these non-competitive effects (as discussed in Chapter 2 (2.4)).

Based on the results from Schild analysis and measurement of dissociation kinetics of drug, it was possible to identify distinct sites and to classify them according to the type of drug bound. Therefore as shown in figure 6.1, sites I and II have been assigned to vinblastine and paclitaxel respectively, and are clearly capable of being involved in transport. Site IV of the model has been classified as a regulatory or modulatory site, although it has not been determined whether transport occurs from this site or not. This site was designated as a possible site common to the modulators nicardipine and GF120918, based on their ability to non-competitively inhibit binding of [^{3}H]-vinblastine and [^{3}H]-XR9576. However, due to the unavailability of radiolabelled versions of nicardipine and GF120918, it was not possible to determine whether these compounds interact competitively or not. Due to the relatively poor binding of [^{3}H]-paclitaxel to CH^{r}B30 membranes, the type of interaction occurring between paclitaxel and these modulators could not be determined. However, these compounds were assigned to a site other than the paclitaxel site, based on the results of a study by Woodhouse (155). This work showed that nicardipine binding elicited a 3-5 fold increase in the dissociation rate constant for [^{3}H]-paclitaxel binding, which is indicative of a non-competitive interaction between these drugs.

The existence of more than one drug binding site on P-gp has been demonstrated in numerous studies, employing either measures of ATPase or transport activity, or from

direct measurement of drug binding using photo-affinity or radioligand binding methods. For instance, Tamai and Safa (142) showed that vinblastine and CsA non-competitively inhibited the equilibrium binding of [^{3}H]-azidopine.

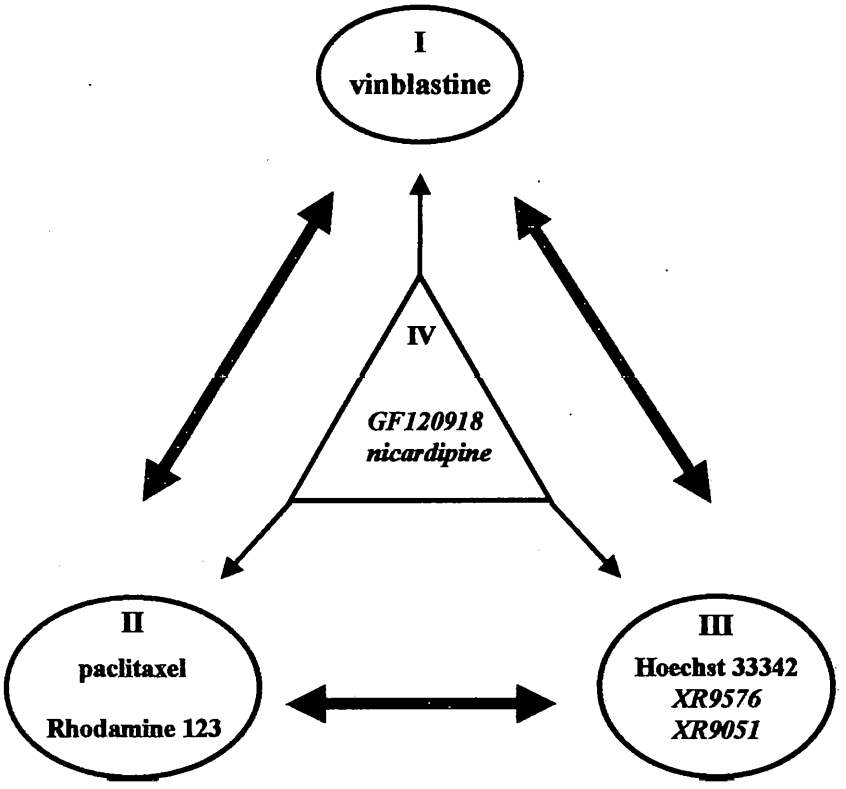

Figure 6.1 Classification of four distinct drug binding sites on P-gp. Sites I, II and III have a role in transport as a consequence of drug binding, although site III can have a modulatory role depending upon ligand bound. Site IV has been designated as modulatory only. Solid arrows indicate that the sites identified can communicate with each other. (Published in Martin *et al.* (83)).

By investigating the effect of drugs on the dissociation kinetics of [^{3}H]-vinblastine, Ferry *et al.* (29, 30) report the presence of at least two distinct binding sites for drug; a vinblastine selective site and one at which 1,4-dihydropyridine reversal agents bind. This result agrees with the non-competitive interaction observed between vinblastine and the 1,4-dihydropyridine nicardipine, reported in this thesis.

A common site on P-gp can elicit either transport or modulatory roles. The sites identified thus far in this thesis have been classified as eliciting either transport or

modulatory roles. Therefore, the observation that the modulatory drugs XR9576 and XR9051 interacted competitively was not surprising (site III, figure 6.1). More especially, a competitive interaction between these agents was expected, given the structural similarity of these compounds as illustrated in Chapter 1 (1.3.2). This is related to the fact that XR9051 was a precursor molecule for XR9576, in a medicinal chemistry programme to develop high affinity inhibitors of P-gp activity.

There is evidence from the literature suggesting that drugs that are transported and those that are modulatory can interact at a common site on P-gp. For example, Tamai and Safa (141) showed that the modulator CsA could competitively inhibit the uptake of vinca alkaloids. However, the presence of a common site of interaction for vinca alkaloids and CsA was inferred from transport assays, and not through direct measurement of binding. Using radioligand binding studies I have unequivocally shown that site III displayed a dual function in terms of transport and modulatory activity. A competitive interaction between [^{3}H]-XR9576 and Hoechst 33342 was observed from Schild analysis, and was confirmed by the lack of effect of Hoechst 33342 on the dissociation rate constant for [^{3}H]-XR9576. This result clearly demonstrates that a common site on P-gp can elicit either a transport or modulatory role. Therefore, it seems that the functional consequence of drug binding is not strictly dependent upon the site occupied, but is also related to the type of drug bound. For instance, binding of Hoechst 33342 at site III (figure 6.1) results in transport of the Hoechst 33342 molecule, and has been shown to have no measureable effect on ATPase activity (125). Conversely, XR9576 binding does not result in translocation of the XR9576 molecule, but rather inhibition of P-gp transport activity, which may be related to its ability to inhibit P-gp related ATPase activity. Does this then imply that these molecules transmit different signals to the energy-generating NBDs? Translocation of a drug molecule must involve alteration in the affinity and 're-

orientation'of, the drug binding site. The signal to induce changes in the binding site must originate at the NBDs, because of the requirement for ATP hydrolysis to support transport. Why is there a different functional outcome arising from occupation of site III by XR9576 compared to Hoechst 33342? One possibility is that when XR9576 is bound, the site is unable to undergo 're-orientation' to face the 'opposite side' of the membrane. This scenario is quite likely in view of the potent inhibition of ATPase activity observed in the presence of XR9576. Alternatively, XR9576 may dissociate very slowly from the binding site following 're-orientation'. However, a more in-depth discussion of signalling between the drug binding domain and the NBDs during a transport cycle will be dealt with later.

Classification of the site for interaction of the transport ligand rhodamine 123 has been problematic for a number of reasons. There was no effect of rhodamine 123 on the binding parameters of [^{3}H]-XR9576, and this may reflect the relatively poorer affinity of rhodamine 123 to interact with P-gp compared to [^{3}H]-XR9576. However, it was deduced that rhodamine 123 does not interact with the [^{3}H]-XR9576 binding site, since this site is shared by Hoechst 33342, and it has been previously shown that Hoechst 33342 and rhodamine 123 interact at distinct sites (127). Non-competitive interactions observed between [^{3}H]-vinblastine and rhodamine 123, excluded this compound from interaction at site I. Due to the poor binding affinity of [^{3}H]-paclitaxel to P-gp demonstrated in chapter 3, it has not been possible to examine the binding parameters of this drug in the presence of antagonist. Therefore I would tentatively suggest that rhodamine 123 interacts at the paclitaxel site as illustrated in figure 6.1, given that both ligands are transported by P-gp.

Do multiple ligands simultaneously bind to P-gp? The presence of multiple distinct drug binding sites within the drug binding domain of P-gp, has been established by the work conducted in this thesis. Does this observation imply that P-gp can bind different drug molecules simultaneously? By studying the effect of 'antagonist' on the dissociation kinetics of either [^{3}H]-vinblastine or [^{3}H]-XR9576, it was established that all of the binding sites were linked by a communication network, as depicted by inter-connecting arrows between the binding sites in figure 6.1. The nature of the allosteric effect observed between the drugs tested in chapter 4, involves a negative heterotropic effect that manifests as an increase in the dissociation rate constant for drug. By analogy, this could be likened to drug being 'pushed' off its binding site by the binding of another unrelated drug at an alternative site. Therefore, drugs would not simultaneously bind to P-gp but would be governed by allosteric regulation. A model is presented in figure 6.2 to illustrate how binding of multiple drugs to distinct sites on P-gp might be regulated.

Molecular mechanism for the binding of multiple drugs to P-gp. The central tenet of the model in figure 6.2, suggests that the binding sites on P-gp can exist in either high or low affinity conformations for their specific ligand. The presence of high and low affinity sites for ligand has been demonstrated for other transport proteins. Drug binding studies of the L-type calcium channel revealed the presence of distinct but interacting sites for verapamil, 1,4,-dihydropyridines and cis-diltiazem. Each site could exist in either high or low affinity conformations due to either alterations in temperature or the binding of ions or drugs (37). The existence of high and low affinity sites for ligand on a receptor or protein molecule has also been demonstrated for the cholecystokinin receptor (90) and bilitranslocase, a carrier protein involved in the uptake of bilirubin at the sinusoidal domain of the liver cell plasma membrane (95). The model in figure 6.2 details the

movement of drug binding sites on P-gp between various states of occupancy with, and

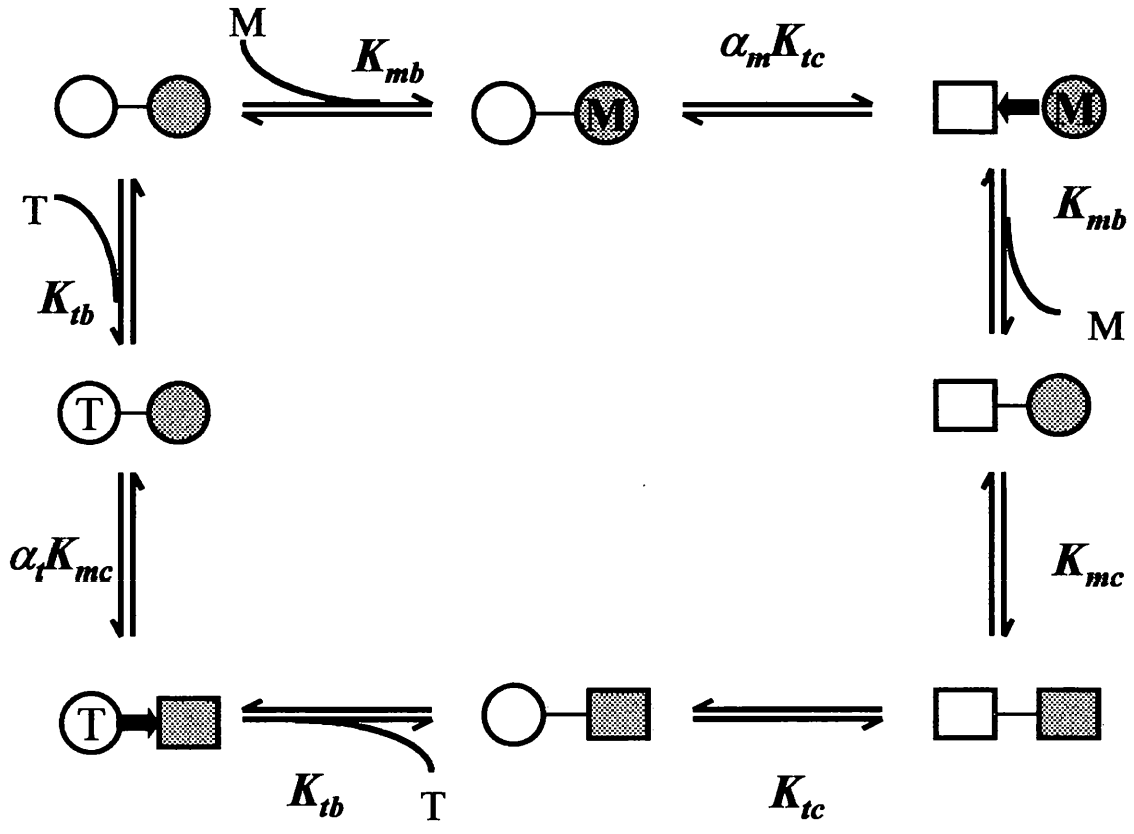

Figure 6.2 'Multiple site transition model' depicting possible molecular mechanism of drug binding to P-gp. Only two classes of site are shown for clarity and are connected by a line to depict interacting sites. Circles represent high affinity binding sites for T and M respectively. Rectangles depict low affinity conformation of the T and M sites. K_{th} and K_{mb} are the equilibrium constants for binding of T and M to their high affinity sites. The switch in conformation of linked site due to drug binding is represented by a solid arrow. Conformational change in binding site due to drug binding is governed by either $\alpha_t K_{mc}$ (in the case of T altering M) and $\alpha_m K_{tc}$ for alteration of T by M where α is the allosteric potency of drug to induce conformational change and K_{mc} and K_{tc} are the equilibrium constants describing shift between high and low affinity conformation. Published in Martin *et al.*, (83)).

affinity for, their respective ligands. Only two of the sites identified on P-gp are shown for clarity, and are designated T and M. These sites are depicted as distinct but interacting drug binding sites. The binding site for drug T or M, can exist in either high or low affinity conformations, and the equilibrium between the conformations is governed by the constants K_{tc} and K_{mc} respectively (see bottom right hand corner of

figure 6.2). The top left hand corner of figure 6.2 depicts high affinity binding sites for both T and M on a single molecule of P-gp, and binding of T or M, is governed by the equilibrium constant for their respective binding reaction i.e. K_{tb} or K_{mb}. From the dissociation kinetic experiments conducted in chapter 4, it is known that the drug binding sites on P-gp are allosterically linked. For example, binding of T to its high affinity site will drive the conformation of the M site to low affinity (represented by switch from circle to rectangle). This conformational alteration is described by the equilibrium constant $\alpha_t K_{mc}$ where α_t represents the allosteric potency of drug molecule T, to increase the propensity of the M site to exist in a low affinity conformation. The ability of drugs to interact with their respective high affinity binding sites will be dependent upon the relative affinities of the two drugs to bind, but also, and more especially, on the relative allosteric potencies of these drugs. The inter-connecting network of allosterically linked sites suggests that two molecules of drug may not simultaneously access their respective high affinity sites. Thus it is possible to conceptualise a mechanism for the binding of multiple ligands by P-gp, which is allosterically regulated via conformational signalling between binding sites, to facilitate ligand interactions at multiple sites.

Evidence for conformational signalling between drug binding sites has also come from studies of the transport activity of P-gp, conducted by Shapiro and Ling (123, 127). They suggested that binding of Hoechst 33342 and rhodamine 123 at their respective sites, resulted in positive co-operativity in the transport of each. Do these observations in transport studies disagree with the drug binding interactions of figure 6.2? This model provides information on the initial interaction of drugs with P-gp and cannot predict the functional outcome in terms of transport kinetics. Likewise, it is difficult to determine whether the positive co-operativity seen in the transport of Hoechst 33342 and rhodamine 123, is due to the nature of the allosteric communication that exists between

the binding sites of these compounds. One could speculate that positive co-operativity in the transport of drug molecules from two different sites, could arise if they were linked by negative allosteric communication. If the low affinity state actually corresponded to the "outward" facing orientation of a drug binding site, then the negative allosteric interaction could manifest as a co-operative transport process. Using this scenario, binding of drug could 'push' the binding site for the other drug to low affinity, leading to 're-orientation' and simultaneous transport of both.

Does specificity for multiple ligands make P-gp an atypical transporter? The fact that P-gp, a primary active transporter, contains multiple sites for drug recognition is an apparent contradiction of the classic 'lock and key' hypothesis for enzyme-substrate interaction. Other primary active transporters such as the Ca^{2+}- and Na^{+}, K^{+}-ATPases display strong substrate specificity and tight coupling of ligand binding to ATP hydrolysis. However, other members of the ABC super-family of membrane transport proteins to which P-gp belongs, are also capable of interacting with and transporting multiple ligands. The multidrug resistance associated protein (MRP1) has a broad specificity for conjugated drugs and has been implicated as playing a role in MDR (reviewed by Borst *et al.*, (12)). LmrA, an ABC transporter found in *Lactococcus lactis,* also mediates transport of multiple drugs (151). Other ABC proteins including Pdr5p and Yor1p in yeast, Cdr1p of *C.albicans* and Pfmdr1 in *P. falciparum* are each able to interact with and transport many different classes of drug.

Poly-specificity, a feature of multidrug transporters. The concept of 'poly-specificity' in ligand interaction is not only restricted to members of the ABC superfamily, but also to proteins of the major-facilitator (MFS), small-multidrug resistance (SMR) and resistance-nodulation (RND) transport families. The drugs transported by multidrug

transporters are structurally and chemically dissimilar, but they share common features such as lipophilicity, planarity and many contain a quaternary nitrogen group. How do multidrug transporters such as P-gp accommodate multiple binding sites on a single protein molecule? To accommodate the multi-site model depicted in figure 6.1, a large binding pocket can be visualised that most likely has contributions from both N- and C-terminal TMDs. The binding pocket may contain specific drug recognition elements that will become exposed or hidden dependent upon the ligand present. Allosteric regulation of binding as outlined in figure 6.2, will most likely involve conformational alteration in the availability of specific transmembrane elements required for high affinity interaction of ligand. Photoaffinity-labelling studies using analogues of different P-gp ligands, detected labelling of different membrane spanning segments located in each half of the protein (42, 91), suggesting contribution of TM elements from each half of the P-gp molecule in drug binding. In addition, the cross-linking studies of Loo and Clarke have produced a cyclone model proposing that TM segments 4,5,6 and 10,11,12 are directly involved in drug interaction (78-80). The only low-resolution structure available for P-gp to date, described in Rosenberg *et al.*, (104), indicates that the P-gp molecule is toroidal in shape with a central membrane spanning pore that narrows towards the cytoplasmic face which could accommodate a large binding pocket comprising both halves of the protein molecule.

Study of the crystal structure of the unrelated transcriptional activator (BmrR) of Bmr, a multidrug transporter in *B.subtilis,* has been used as a model to provide a structure-based mechanism for interaction of a single transporter with multiple drugs The crystal structure data revealed the presence of a large binding pocket that contained flexible elements, allowing ligands of differing structures to access their appropriate binding residues (159). Although BmrR is not a transporter, it does interact with ligands that are

transported by P-gp such as the hydrophobic cationic dyes rhodamine, ethidium and acridine and may help to shed light on how P-gp interacts with multiple drugs. The 'induced fit' model for BmrR, in the absence of high resolution structural data for P-gp, could be used to explain how different drugs might access their respective sites on P-gp, within a large flexible binding domain.

6.4 Binding of drug at discrete stages of the catalytic cycle

The studies conducted in chapter 3 and 4 have yielded important information concerning the molecular mechanism of multi-ligand binding by P-gp. The focus of chapter 5 has been elucidation of how drug binding events at the TMDs are linked to ATP hydrolysis at the NBDs to mediate translocation of drug. Conceptually, transport of a drug molecule can only occur following a sequence of events encompassing both (i) 're-orientation' of a binding site to the opposite side of the membrane and (ii) a switch in binding site from high to low affinity. P-gp has a strong requirement for ATP hydrolysis in order to transport drugs across the plasma membrane against a concentration gradient. Therefore, signalling must occur between the TMDs and the NBDs during a transport cycle. Radioligand binding assays were used to investigate drug binding at discrete stages of the catalytic cycle to (i) determine when the initial change is wrought on the drug binding site to initiate transport (ii) elucidate the kind of changes conferred on the drug binding site(s) and (iii) ascertain the signal required to restore the drug binding site to a 'pre-transport' conformation. A model has been devised putting forward a molecular mechanism that describes how the binding site for transport ligand adopts high and low affinity conformations during a catalytic cycle and by extension, a transport cycle of P-gp (figure 6.3).

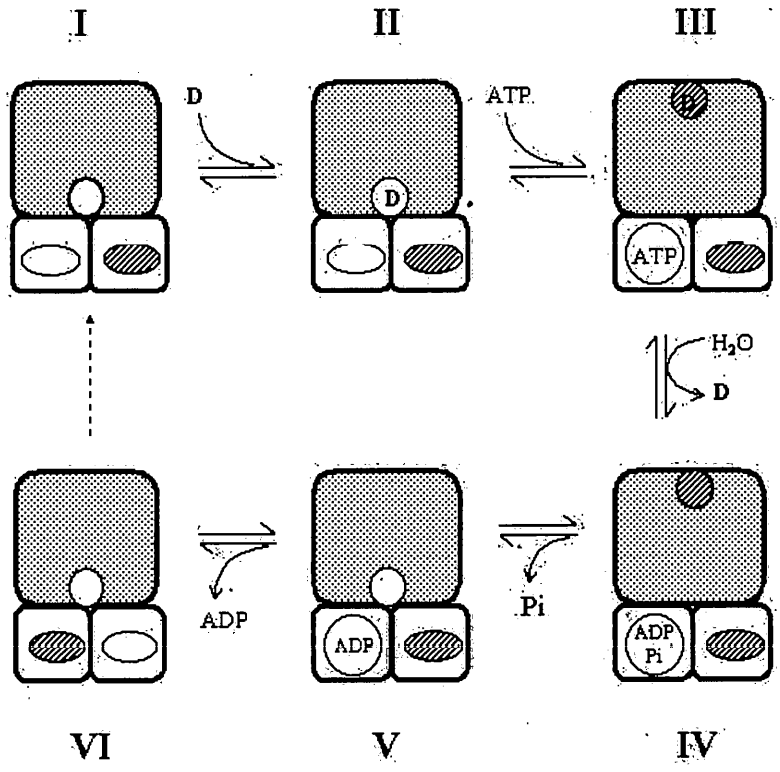

Figure 6.3 Based on study of the characteristics of [^{3}H]vinblastine binding at discrete stages of the catalytic cycle, a model for P-gp mediated drug transport is presented. The two transmembrane domains are represented by one large shaded square and the NBDs by two small clear squares. The catalytic sites within each NBD are depicted by ellipses, open represents 'active' catalytic site conformation and shaded ellipse 'passive' conformation. Upon nucleotide binding the'active' catalytic site is depicted by a circle to indicate that this NBD is actively participating in a catalytic cycle. Stage I depicts the pre-nucleotide binding state of P-gp where both NBDs are devoid of nucleotide and the drug binding site has a high affinity inward-facing conformation. ATP-bound or pre-hydrolysis state for P-gp is illustrated at stage III and the drug binding site is now in a low affinity outward-facing orientation. Stage IV depicts protein following hydrolysis of ATP. Subsequent dissociation of phosphate restores drug binding to inward facing high affinity conformation prior to release of ADP as represented in V. Stage VI depicts P-gp following release of ADP from the active catalytic site with possible switching of this site to a passive conformation before entering a new catalytic cycle.

The model depicted in figure 6.3 was produced from direct measurement of drug binding, at each stage of the catalytic cycle of P-gp. In order to quantitate changes in the drug binding site as P-gp undergoes a catalytic cycle, the radioligand binding assay for [^{3}H]-vinblastine was modified to enable measurements to be made over a wider

concentration range of ligand. In fact, the concentration range of vinblastine used was increased 30-fold as described in methods (chapter 2, 2.2.3). Therefore, interaction of vinblastine could be measured at concentrations up to 150-fold greater than its previously measured K_d of binding, enabling large alterations in the affinity of binding to be detected in binding assays.

At stage I→II of the model presented in figure 6.3, the binding of [^{3}H]-vinblastine was measured in the absence of nucleotide using the refined radioligand binding assay alluded to above. A model describing binding of vinblastine to a single class of high affinity binding site best described the experimental data obtained. This confirmed the findings of previous radioligand binding studies that show binding of [^{3}H]-vinblastine to a single class of high affinity site on hamster (16) and human P-gp (30). Given that binding sites on transporters cycle between high and low affinity conformations, it was necessary to unequivocally establish that there was a single class of vinblastine site present under 'basal' conditions. This clarification was also required given the suggestion that there are two classes of vinblastine site of opposite affinity, on the related transporter LmrA (152). The authors report that interaction of vinblastine at a low affinity site promotes binding at a linked site of high affinity. LmrA is often described as a bacterial homologue of P-gp. However, differences observed in the binding of [^{3}H]-vinblastine to P-gp versus LmrA, may be due to the fact that LmrA is a homodimer, whereas the functional unit for P-gp is believed to be monomeric. Each dimer subunit may contain a site of interaction for vinblastine accounting for the differences observed between LmrA and P-gp.

Indeed, the evidence presented in this thesis for binding of vinblastine to a single class of site is also at variance with some studies of P-gp concerned with measurement of

vinblastine binding. Romsicki and Sharom (102) reported that vinblastine was interacting at a high and low affinity site on P-gp. This was interpreted from study of the ability of vinblastine to quench fluorescence of the sulfhydryl-reactive probe MIANS, bound at the Walker A cysteines. However, this is an indirect method with which to assess drug binding. Vinblastine quenching of bound MIANS produced a biphasic curve, interpreted to represent binding of vinblastine to two classes of binding site. It is quite likely that a biphasic quenching curve could have arisen due to quenching of MIANS molecules bound at each NBD, a possibility not addressed by these authors.

Binding of nucleotide triggers the first major conformational change in the vinblastine binding site. The ability of the catalytic cycle to influence [^{3}H]-vinblastine interaction with P-gp at an early pre-hydrolysis stage was investigated by measuring binding in the presence of a non-hydrolysable analogue of ATP (stage II→III). Preliminary experiments demonstrated that the non-hydrolysable ATP analogues ATP-γ-S and AMP-PNP, had a pronounced effect on [^{3}H]-vinblastine binding with up to 70% inhibition observed. The fact that there was no alteration in the binding of vinblastine when the NBDs were occupied with either NBD.Cl or MIANS, confirmed that signalling to the TMDs was specifically related to the binding of nucleotide. The type of change wrought on the [^{3}H]-vinblastine binding site in the presence of nucleotide analogues was further investigated using complete binding curves for vinblastine binding. Analysis of the binding data produced at stage III of the model in the presence of AMP-PNP, showed that (i) there was a 15-fold reduction in the affinity of binding (ii) a model describing interaction of vinblastine at a single class of site best fitted the data. Together these observations were taken as evidence that the binding of ATP induced a complete shift in the conformation of the vinblastine binding site from high to low affinity. If vinblastine was interacting at two sites of distinct affinities, a biphasic binding curve would have

resulted as determined from the theoretical modelling studies reported in chapter 5 (5.3.1.1). This is the first direct evidence to show that binding of ATP at the NBDs, prior to hydrolysis, was sufficient to provide the initial signal required to instigate a transport event.

The observation that binding of ATP can elicit conformational changes in the P-gp molecule is not unprecedented. There is evidence from numerous studies, using a variety of different techniques, to demonstrate that binding of nucleotide induces conformational changes in the P-gp molecule. For example, Urbatsch and Senior (148) reported decreased photoaffinity labelling of [^{3}H]-azidopine to purified reconstituted hamster P-gp, in the presence of AMP-PNP. It has been shown that the accessibility of the UIC2 antibody for its extracellularly located epitope on P-gp is reduced in the presence of bound ATP (87). Acrylamide quenching of endogenous tryptophan residues showed changes in tertiary structure upon binding of nucleotide (138) while non-hydrolysable analogues of ATP increased resistance of P-gp to trypsin digestion (60).

What is the role of ATP hydrolysis in a transport cycle? The novel observation that the binding of ATP is sufficient to instigate the initial alterations in the binding site during a transport/catalytic cycle, goes against the proposition that hydrolysis of ATP is necessary to bring about an initial significant change in the drug binding sites. Therefore, it was important to elucidate any consequence of ATP hydrolysis for P-gp-drug interactions. This was achieved using the technique of vanadate trapping to stabilise the protein in the MgADP.Vi bound form, to mimic the step in the catalytic cycle that immediately follows ATP hydrolysis, but precedes dissociation of Pi. The low affinity vinblastine site detected in the presence of bound nucleotide persisted post hydrolysis of ATP (stage IV). However, the low affinity conformation observed at stage IV was different to that

observed in the presence of bound AMP-PNP. This was reflected in a value for the K_d of binding to trapped protein that was significantly lower than the K_d measured in the presence of AMP-PNP. Thus the low affinity vinblastine binding site detected post-hydrolysis of ATP was 'intermediate' in affinity between the high affinity site measured under 'basal' conditions and the low affinity site induced by the binding of nucleotide. This observation agrees with the low resolution structural data produced from crystals grown with P-gp under 'basal', vanadate trapping and AMP-PNP bound states. Three different conformations were observed and the vanadate trapped protein had a conformation that was 'intermediate' between the control and nucleotide bound proteins (Rosenberg *et al.* (103)). The functional relevance of the low/intermediate affinity conformation observed post-hydrolysis of ATP is not known. The lower value for K_d obtained is not due to 'recovery' of the vanadate trapped protein over the course of the binding assay, as vanadate was included in all of the binding buffers to prevent dissociation of bound species.

The presence of low affinity binding sites for ligand, when P-gp is in a vanadate trapped conformation, is in agreement with photoaffinity labelling studies that demonstrate reduced labelling of the prazosin analogue [^{125}I]-IAAP (96, 113, 115). However, there was no effect of ATP binding on [^{125}I]-IAAP labelling, which is contrary to the effect of nucleotide on the binding of [^{3}H]-vinblastine reported in this thesis. Interestingly, I found that the binding of nucleotide was also without effect on the interaction of [^{3}H]-XR9576 with P-gp, whilst there was reduced binding of this modulator to vanadate trapped protein (chapter 5, 5.3-5.4). This implies that changes in drug binding site induced by ATP binding may be specific for the class of drug bound at the drug binding domain. I have previously demonstrated that the binding site occupied by drug may not be the prime determinant for the specificity of signalling between drug binding sites and

the NBDs. As shown in the multi-site model depicted in figure 6.1, the same binding site (site III) can elicit either transport or modulatory roles. Can the lack of effect of nucleotide on the binding of [^{3}H]-XR9576 and [^{125}I]-IAAP be related to fact that these compounds are not transported by P-gp? It has been established that XR9576 is not transported by P-gp (Chapter 3 (3.2)), whereas vinblastine is. There is no published data to show whether or not prazosin is a transport ligand of P-gp. The fact that the binding of [^{3}H]-XR9576 and [^{125}I]-IAAP was only affected by ATP hydrolysis, might indicate that conformational signals arising from ATP binding and hydrolysis of nucleotide have different functional outcomes, in terms of drug binding, that may be related to the class of drug bound.

What signal restores the binding site to high affinity during a transport cycle? Thus far, I have demonstrated the stage of the catalytic cycle that induces the first major conformational change in the drug binding site to instigate transport (stage II→III). The low affinity conformation of the drug binding site persisted post-nucleotide hydrolysis at stage IV. In order to complete a transport cycle the drug binding site must regain a high affinity conformation once more. Subsequently, the trigger required to 'reset' the binding site was investigated. Therefore, vinblastine binding was measured at the next stage of the catalytic cycle that occurs immediately following release of Pi from the post-hydrolytic complex. P-gp was covalently labelled with 8-azido-ADP (section 2.6.1) to mimic the MgADP.P-gp transition state. As shown in stage V of the model in figure 6.3, dissociation of Pi from the post-nucleotide diphosphate complex induced a major conformational change in the vinblastine binding site that enabled restoration of the high affinity state. Dissociation of Pi from the post-hydrolytic complex is proposed to be accompanied by a large release in free energy, (117) that may be harnessed to 'reorient'

the low affinity site to a high affinity orientation following release of translocated drug. This will enable the binding site to participate in a second round of transport.

One molecule of ATP may be sufficient to support transport of a single molecule of drug.

The transport model devised from the binding studies conducted at distinct steps of the catalytic cycle demonstrates that binding and hydrolysis of a single molecule of ATP is sufficient to completely cycle the vinblastine binding site between high→low→high affinity conformations. It is on this basis that one might speculate that hydrolysis of a single molecule of ATP is sufficient to support transport of one drug molecule. The expenditure of one molecule of ATP per molecule of drug transported has been reported in assays of P-gp mediated transport of rhodamine 123 (128) and valinomycin (28). This is further supported by a complete recovery of ATPase activity and drug binding in vanadate trapped P-gp in the absence of a further round of nucleotide hydrolysis (Chapter 5, (5.3.4); (147)). In contrast, the studies of Sauna *et al.* (113, 114) demonstrate a requirement for the hydrolysis of a second molecule of ATP, to bring about restoration of the high affinity site for [^{125}I]-IAAP following vanadate trapping of P-gp. These authors performed sequential vanadate trapping of P-gp, and although recovery of ATPase activity was achieved after the first round of hydrolysis/trapping upon dissociation of ADP and vanadate, hydrolysis of a second molecule of ATP was required to regain high affinity drug binding (114). A major criticism of this study lies in the use of a single concentration of [^{125}I]-IAAP that was 150-fold lower than the value for the K_d of [^{125}I]-IAAP binding to P-gp, that they had reported previously. Therefore, the ability of [^{125}I]-IAAP to bind during a catalytic cycle of P-gp was investigated using a concentration of drug where there was only fractional occupation of the drug binding sites. It is also known that the association of drug with its receptor is driven by the concentration of free

drug and therefore the amount of free drug in the assay system could be of importance for the kinetics of drug binding to 'recovering' protein.

Does the 'non-catalytic' NBD participate in a catalytic/transport cycle? The participation of both NBDs during a catalytic cycle has been the subject of conjecture in studies of P-gp function and this topic has been touched upon in chapter 1 (1.10). The alternating catalytic sites model of Senior *et al.*, (117) states that although there is a strict requirement for two intact NBDs in hydrolysis, the NBDs do not simultaneously hydrolyse ATP. This was borne out in vanadate trapping experiments where Urbatsch *et al.* (147) demonstrate trapping of only one molecule of nucleotide post-hydrolysis. Therefore during a single catalytic cycle, only one of the NBDs is 'active'. The NBD that is not hydrolysing ATP will be referred to as the 'passive' NBD. Given the strong interplay that has been demonstrated by many studies to exist between the NBDs of P-gp, what role does the 'passive' NBD play in catalysis? I looked at the ability of ATP to bind to the 'passive' NBD by measuring ATP binding to P-gp that was previously trapped with vanadate. It was found that when ADP/Vi is bound at the 'active' NBD, ATP is able to access and bind to the catalytic site within the 'passive' NBD. There is communication between the NBDs of P-gp during catalysis, as the presence of mutations or inhibitors at either NBD disrupts hydrolysis. Therefore it seems reasonable to assume that the 'passive' NBD does transmit a signal to the active NBD during catalysis. Can the 'passive' NBD transmit a signal to the drug binding domain? Having established that ATP can bind to the 'passive' NBD it was imperative to ascertain whether binding of nucleotide at this NBD could also affect drug binding. If this were the case, the model produced in figure 6.3 would require revision; as the protein would never regain a high affinity conformation for drug, since ATP bound at the 'passive' NBD would not support this binding site conformation. Therefore, stage V of the cycle was further investigated

by measuring binding of vinblastine when ADP was bound at the 'active' NBD, in the presence of saturating concentrations of AMP-PNP. The presence of AMP-PNP did not alter the conformation of the vinblastine site. This was an important finding as it demonstrated that the 'passive' NBD, whilst being essential for catalysis to occur at the 'active' NBD, did not transmit a signal to the TMDs. If the alternating catalytic sites model is correct, I hypothesise that the NBDs switch roles before commencing another round of catalysis, after ADP has dissociated from the 'active' NBD, as depicted at stage VI of figure 6.3. However, it is not known whether hydrolysis can occur until ATP is bound at both NBDs. According to the alternating catalytic sites model of Senior, it is hypothesised that both of the NBDs must be occupied by ATP, before hydrolysis can occur at a single NBD. This assumption has been based on the co-operativity that has been shown to exist between the NBDs of P-gp (118) Direct evidence for allosteric communication between the NBDs of ABC proteins was shown for MRP1 a transporter that is also involved in MDR. Hou *et al.*, (53) demonstrated that binding of ATP at the passive NBD allosterically promoted hydrolysis of nucleotide at the alternate active NBD. Perhaps the role of the 'passive' NBD during a cycle of catalysis is to allosterically promote hydrolysis at the 'active' NBD as it has been shown in this thesis that the 'passive' NBD does not transmit a signal to the binding domain.

At what stage does drug bind to begin a second cycle of transport? It has been established that the binding site for vinblastine has been 'reset' to a high affinity conformation for ligand at stage V of the model in figure 6.3 and is ready to bind an additional molecule of drug to commence the next round of transport. But when does the protein bind the next molecule of vinblastine? Theoretically, a second molecule of drug could bind at stage V, prior to dissociation of ADP, as the binding site is in a high affinity orientation. Alternatively, release of ADP may take place before another

molecule of vinblastine can interact with the protein. It has been suggested by a recent study investigating the effect of drug on ATP hydrolysis and vanadate trapping, that the release of ADP is the rate-limiting step in the catalytic cycle of P-gp (67). However if the 'passive' NBD, which already has ATP bound, becomes 'active' following release of ADP, then the binding site may be switched to a low affinity state before a second molecule of drug can bind. Therefore, it seems more likely that a second molecule of drug binds prior to dissociation of ADP (stage V) as bound ADP may function to 'anchor' the protein in a high affinity conformation for drug, before the NBDs undergo another round of catalysis.

In summary, the work conducted in this thesis has both confirmed and augmented studies of P-gp-drug interaction and transport activity. Different drugs were used as pharmacological probes in radioligand binding assays to produce models for drug binding and transport processes:

- It has been shown that P-gp directly interacts with a diverse range of drugs including cytotoxics used in chemotherapy and compounds that inhibit P-gp activity.

- The molecular basis of this apparent lack of ligand specificity is the presence of at least four distinct drug interaction sites.

- A model has been put forward depicting allosteric regulation governing binding of multiple ligands at distinct sites on P-gp.

The binding studies were extended to investigate communication between the NBDs and TMDs during catalysis to elucidate further the mechanism of P-gp transport activity.

- The binding site for the transport ligand vinblastine, cycled between high and low affinity conformations during a catalytic cycle.

- Binding of ATP, prior to hydrolysis, elicited the initial major change in the conformation of the binding site from high to low affinity to initiate drug transport.

- The trigger to restore the binding site to its high affinity conformation was provided post-hydrolysis of nucleotide following release of Pi, but prior to release of ADP from the catalytic site.

- It has been proposed that hydrolysis of a single molecule of ATP is sufficient to support transport of one molecule of drug

APPENDIX I

The Adair Equation: description of binding to two sites on a receptor.

In the scenario described below the receptor protein [P] contains two drug [D] binding sites. An initial equilibrium may be established with association and dissociation rate constants of k_1 and k_{-1} respectively.

$$[P] + [D] \underset{k_{-1}}{\overset{k_1}{\rightleftharpoons}} [PD] \qquad 2.1$$

The [PD] complex may then bind a further drug with association and dissociation rate constants of k_2 and k_{-2} respectively.

$$[P] + [PD] \underset{k_{-2}}{\overset{k_2}{\rightleftharpoons}} [PD_2] \qquad 2.2$$

The dissociation rate constants for the two binding reactions may be expressed as:

$$K_1 = \frac{[P]\bullet[D]}{[PD]} \qquad K_2 = \frac{[PD]\bullet[D]}{[PD_2]}$$

These may be re-arranged as follows:

$$[P] = \frac{[PD]\bullet k_1}{[D]} \qquad [PD_2] = \frac{[PD]\bullet[D]}{k_2}$$

The fraction of total receptor bound (f) may be expressed as:

$$f = \frac{[PD] + 2[PD_2]}{2([P] + [PD] + [PD_2])}$$

And by substituting for [P] and $[PD_2]$ the fraction bound can be described as:

$$f = \frac{[PD] + 2\left(\frac{[PD]\bullet[D]}{k_2}\right)}{2\left(\frac{[PD]\bullet k_1}{[D]} + [PD] + \frac{[PD]\bullet[D]}{k_2}\right)}$$

Simplifying this relationship yields the Adair Equation:

$$f = \frac{k2 \bullet [D] + 2[D]^2}{2\left(k1 \bullet k2 + k2 \bullet [D] + [D]^2\right)}$$

APPENDIX II

Determination of the association rate constant for drug binding to a receptor.

The rate of formation of a drug receptor complex [PD] over time is dependent upon the difference between the rate at which drug associates with receptor and the dissociation of drug receptor complexes:

$$[P] + [D] \underset{k_2}{\overset{k_1}{\rightleftharpoons}} [PD]$$

To follow this reaction we require a relationship between the amount of bound protein as a function of time.

$$\frac{d[PD]}{dT} = k_1 \bullet [P] \bullet [D] - k_2[PD]$$

Let $[P_T] = [P] + [PD]$ and $[P] = [P_T] - [PD]$

Substituting;

$$\frac{d[PD]}{dT} = k_1 \bullet [D]([P_T] - [PD]) - k_2 \bullet [PD]$$

$$\frac{d[PD]}{dT} = k_1 \bullet [D] \bullet [P_T] - k_1 \bullet [D] \bullet [PD] - k_2[PD]$$

$$\frac{d[PD]}{dT} = k_1 \bullet [D] \bullet [P_T] - [PD] \bullet (k_1 \bullet [D] + k_2)$$

Integrating this function with time;

$$\int \frac{d[PD]}{dT} = k_1 \bullet [D][P_T] \bullet \left(e^{-(k1[D]+k2) \bullet t}\right)$$

therefore;

$$k_1 \bullet [D] \bullet [P_T] - [PD] \bullet (k_1 \bullet [D] + k_2) = k_1 \bullet [D] \bullet [P_T] \bullet \left(e^{-(k1 \bullet [D] + k2) \bullet t}\right)$$

rearranging and simplifying this relationship;

$$-[PD] \bullet (k_1 \bullet [D] + k_2) = -k_1 \bullet [D] \bullet [P_T] \bullet \left(e^{-(k1 \bullet [D] + k2) \bullet t}\right)$$

since $$\frac{k_2}{k_1} = K_D$$

$$[PD] = \frac{[D] \bullet [P_T]}{[D] + K_D} \bullet \left(1 - e^{-(k1 \bullet [D] + k2) \bullet t}\right)$$

the amount bound at equilibrium $[PD]_{eq}$ is;

$$[PD]_{eq} = \frac{[D] \bullet [P_T]}{[D] + K_D}$$

therefore fractional saturation is;

$$\frac{[PD]}{[PD]_{eq}} = 1 - e^{-(k1 \bullet [D] + k2) \bullet t}$$

let $$K_{obs} = k_1 \bullet [D] + k_2$$

therefore the fraction of protein bound at any time prior to equilibrium is;

$$\frac{[PD]}{[PD]_{eq}} = 1 - e^{-Kobs \bullet t}$$

APPENDIX III

Schild Analysis to investigate competitive binding inhibition

The receptor may bind a specific drug [D] or a competitive inhibitor [A] as follows;

$$[P] + [D] \underset{k_2}{\overset{k_1}{\rightleftharpoons}} [PD]$$

$$[P] + [A] \underset{k_{2a}}{\overset{k_{1a}}{\rightleftharpoons}} [PA]$$

At equilibrium

$$k_1 \bullet [D] \bullet [P] = k_2 \bullet [PD] \qquad \text{and} \qquad k_{1a} \bullet [A] \bullet [P] = k_{2a} \bullet [PA]$$

therefore

$$\frac{k_2}{k_1} = \frac{[D] \bullet [P]}{[PD]} \qquad \frac{k_{2a}}{k_{1a}} = \frac{[A] \bullet [P]}{[PA]}$$

$$\frac{[P]}{[PD]} = \frac{K_D}{[D]} \qquad \frac{[P]}{[PA]} = \frac{K_A}{[A]}$$

$$[P] = \frac{K_D \bullet [PD]}{[D]} \qquad [PA] = \frac{[A] \bullet [P]}{K_A}$$

the total number of receptors is given by;

$$[P_T] = [P] + [PD] + [PA]$$

therefore;

$$[P] = [P_T] - [PD] - [PA]$$

and dividing by [PD];

$$\frac{[P]}{[PD]} = \frac{[P_T]}{[PD]} - \frac{[PD]}{[PD]} - \frac{[PA]}{[PD]}$$

substituting from above for [PA] with $\frac{[A] \bullet K_D \bullet [PD]}{K_A \bullet [D]}$

and with $\frac{K_D}{[D]}$ for $\frac{[P]}{[PD]}$

$$\frac{K_D}{[D]} = \frac{[P_T]}{[PD]} - 1 - \frac{[A] \bullet K_D \bullet [PD]}{[PD] \bullet K_A \bullet [D]}$$

rearranging gives;

$$\frac{[P_T]}{[PD]} = \frac{K_D}{[D]} + 1 + \frac{[A] \bullet K_D}{K_A \bullet [D]}$$

$$\frac{[P_T]}{[PD]} = \frac{K_D \bullet K_A}{[D] \bullet K_A} + \frac{[D] \bullet K_A}{[D] \bullet K_A} + \frac{[A] \bullet K_D}{[D] \bullet K_A}$$

$$\frac{[P_T]}{[PD]} = \frac{K_D \bullet K_A + K_A \bullet [D] + [A] \bullet K_D}{[D] \bullet K_A}$$

inverting to express as fractional saturation of binding;

$$\frac{[PD]}{[P_T]} = \frac{K_A \bullet [D]}{K_A \bullet [D] + K_A \bullet K_D + [A] \bullet K_D}$$

$$\frac{[PD]}{[P_T]} = \frac{[D]}{[D] + K_D \bullet (1 + [A]/K_A)}$$

The fractional saturation of receptor at a drug concentration [D], in the absence of antagonist, is given by:

$$\frac{[PD]}{[P_T]} = \frac{[D]}{[D] + K_D}$$

A concentration of [D'] is required to give the same fractional saturation at an antagonist concentration of [A] (where [D'] > [D]);

i.e. $$\frac{[PD]}{[P_T]} = \frac{[D']}{[D'] + K_D \bullet (1 + [A]/K_A)}$$

therefore;

$$\frac{[D]}{K_D \bullet [D]} = \frac{[D']}{[D'] + K_D \bullet (1 + [A]/K_A)}$$

which simplifies to;

$$[D] \bullet K_D \bullet (1 + [A]/K_A) = [D'] \bullet K_D$$

the ratio of drug concentrations to give equivalent fractional saturation of the receptor ([D']/[D]) is known as the dose-ratio (DR);

$$DR = 1 + \frac{[A]}{K_A}$$

$$(DR - 1) = \frac{[A]}{K_A}$$

which may be transformed into the linear Schild relationship with a slope of n;

$$\log(DR - 1) = n \bullet \log[A] - \log K_A$$

REFERENCES

1. Al-Shawi, M. K., Senior, A. E. 1993. Characterization of the adenosine triphosphatase activity of chinese hamster P-glycoprotein. *J Biol. Chem.* 268: 4197-4206

2. Al-Shawi, M. K., Urbatsch, I. L., Senior, A. E. 1994. Covalent inhibitors of P-glycoprotein ATPase Activity. *J Biol. Chem.* 269: 8986-8992

3. Ambudkar, S. V., Cardarelli, C. O., Pashinsky, I., Stein, W. D. 1997. Relation between the turnover number for vinblastine transport and for vinblastine-stimulated ATP hydrolysis by human P-glycoprotein. *J Biol Chem* 272: 21160-6.

4. Ambudkar, S. V., Dey, S., Hrycyna, C. A., Ramachandra, M., Pastan, I., Gottesman, M. M. 1999. Biochemical, cellular, and pharmacological aspects of the multidrug transporter. *Annu. Rev. Pharmacol. Toxicol.* 39: 361-398

5. Arunlakshana, O., Schild, H. O. 1959. Some quantitative uses of drug antagonists. *Br. J. Pharmacol.* 14: 48-58

6. Ayesh, S., Shao, Y.-M., Stein, W. D. 1996. Co-operative, competitive and non-competitive interactions between modulators of P-glycoprotein. *Biochim. Biophys. Acta* 1316: 8-18

7. Beaudet, L., Gros, P. 1995. Functional dissection of P-glycoprotein nucleotide binding domains in chimeric and mutant proteins. *J. Biol. Chem.* 270: 17159-17170

8. Beaudet, L., Urbatsch, I. L., Gros, P. 1998. Mutations in the nucleotide binding sites of P-glycoprotein that affect substrate specificity modulate substrate induced adenosine triphosphatase activity. *Biochemistry* 37: 9073-9082

9. Benson, A. B., 3rd, Trump, D. L., Koeller, J. M., Egorin, M. I., Olman, E. A., Witte, R. S., Davis, T. E., Tormey, D. C. 1985. Phase I study of vinblastine and verapamil given by concurrent iv infusion. *Cancer Treat Rep* 69: 795-9.

10. Boesch, D., Gaveriaux, C., Jachez, B., Pourtier-Manzanedo, A., Bollinger, P., Loor, F. 1991. In vivo circumvention of P-glycoprotein-mediated multidrug resistance of tumor cells with SDZ PSC833. *Cancer Res* 51: 4226-4233

11. Boote, D. J., Dennis, I. F., Twentyman, P. R., Osborne, R. J., Laburte, C., Hensel, S., Smyth, J. F., Brampton, M. H., Bleehen, N. M. 1996. Phase I study of etoposide with SDZ PSC 833 as a modulator of multidrug resistance in patients with cancer. *J Clin Oncol* 14: 610-8.

12. Borst, P., Zelcer, N., van Helvoort, A. 2000. ABC transporters in lipid transport. *Biochim Biophys Acta* 1486: 128-44.

13. Bosch, I., Croop, J. 1996. P-glycoprotein multidrug resistance and cancer. *Biochimica et Biophysica Acta* 1288: F37-F54

14. Brophy, N. A., Marie, J. P., Rojas, V. A., Warnke, R. A., McFall, P. J., Smith, S. D., Sikic, B. I. 1994. MDR1 gene expression in acute childhood lymphoblastic leukemias and lymphomas: a critical evaluation by four techniques. *Leukemia* 8 (2): 327-335

15. Bruggeman, E. P., Germann, U. A., Gottesman, M. M., Pastan, I. 1989. Two different regions of phosphoglycoprotein are photoaffinity labeled by azidopine. *J Biol. Chem.* 264: 15483-15488

16. Callaghan, R., Berridge, G., Ferry, D. R., Higgins, C. F. 1997. Activity of purified, reconstituted P-glycoprotein requires maintenance of a lipid-protein interface. *Biochim. Biophys. Acta* 1328: 109-124

17. Cano-Gauci, D. F., J.R., R. 1987. Action of calcium antagonists on multidrug resistant cells. *Biochem.Pharmacol.* 36: 2115-2123

18. Chen, C., Chin, J. E., Ueda, K., Clark, D. P., Pastan, I., Gottesman, M. M., Roninson, I. B. 1986. Internal duplication and homology with bacterial transport

proteins in the mdr1/P-glycoprotein gene from multidrug resistant human cells. *Cell* 47: 381-389

19. Cheng, Y., Prusoff, W. H. 1973. Relationship between the inhibition constant (Ki) and the concentration of inhibitor which causes 50 per cent inhibition (I_{50}) of an enzymatic reaction. *Biochem Pharmacol* 22: 3099-3108

20. Chifflet, S., Chiesa, U. T. R., Tolosa, S. 1988. A method for the determination of inorganic phosphate in the presence of labile organic phosphate and high concentrations of protein: application to lens ATPases. *Anal. Biochem.* 168: 1-4

21. Croop, J. M. 1993. P-glycoprotein structure and evolutionary homologies. *Cytotechnology* 12: 1-32

22. Dale, I. L., Tuffley, W., Callaghan, R., Holmes, J. A., Martin, K., Luscombe, M., Mistry, P., Ryder, H., Stewart, A. J., Charlton, P., Twentyman, P. R., Bevan, P. 1998. Reversal of P-glycoprotein-mediated multidrug resistance by XR9051, a novel diketopiperazine derivative. *British Journal of Cancer* 78: 885-892

23. Dalton, W. S., Grogan, T. M., Meltzer, P. S., Scheper, R. J., Durie, B. G., Taylor, C. W., Miller, T. P., Salmon, S. E. 1989. Drug resistance in multiple myeloma and non-Hodgkins lymphoma: detection of P-glycoprotein and potential circumvention by addition of verapamil to chemotherapy. *J. Clin. Oncol.* 7: 415-424

24. De Lean, A., Munson, P. J., Rodbard, D. 1978. Simultaneous analysis of families of sigmoidal curves: applications to bioassay, radioligand assay, and physiological dose-response curves. *Am. J. Physiol.* 235: E97-E102

25. Dey, S., Ramachandra, M., Pastan, I., Gottesman, M. M., Ambudkar, S. V. 1997. Evidence for two non-identical drug-interaction sites in human P-glycoprotein. *Proc. Natl. Acad. Sci. USA* 94: 10594-10599

26. Diederichs, K., Diez, J., Greller, G., Muller, C., Breed, J., Schnell, C., Vonrhein, C., Boos, W., Welte, W. 2000. Crystal structure of MalK, the ATPase subunit of the trehalose/maltose ABC transporter of the archeon *Thermococcus litoralis*. *EMBO J.* 19: 5951-5961

27. Doige, C. A., Yu, X., Sharom, F. J. 1992. ATPase activity of partially purified P-glycoprotein from multidrug-resistant Chinese hamster ovary cells. *Biochim. Biophys. Acta* 1109: 149-160

28. Eytan, G. D., Regev, R., Assaraf, Y. G. 1996. Functional reconstitution of P-glycoprotein reveals an apparent near stoichiometric drug transport to ATP hydrolysis. *The Journal of Biological Chemistry* 271: 3172-3178

29. Ferry, D. R., Malkhandi, J. P., Russell, M. A., Kerr, D. J. 1995. Allosteric regulation of [^{3}H]vinblastine binding to P-glycoprotein of MCF-7 Adr cells by dexniguldipine. *Biochem. Pharmacol.* 49: 1851-1861

30. Ferry, D. R., Russell, M. A., Cullen, M. H. 1992. P-glycoprotein possesses a 1,4-dihydropyridine selective drug acceptor site which is allosterically coupled to a vinca alkaloid selective binding site. *Biochem. Biophys. Res. Commun.* 188: 440-445

31. Fields, A., Hochster, H., Runowicz, C., Speyer, J., Goldberg, G., Cohen, C., Dottino, P., Wadler, S., Berk, G., Gretz, H., Mandeli, J., Holland, J., Letvak, L. 1998. PSC833: initial clinical results in refractory ovarian cancer patients. *Curr Opin Oncol* 10 Suppl 1: S21.

32. Fisher, G. A., Lum, B. L., Hausdorff, J., Sikic, B. I. 1996. Pharmacological considerations in the modulation of multidrug resistance. *Eur J Cancer* 32A: 1082-8.

33. Gaddum, J. H. 1937. The quantitative effects of antagonistic drugs. *Journal of Physiology (London)* 89: 7P-9P

34. Gadsby, D. C., Dousmanis, A. G., Nairn, A. C. 1998. ATP hydrolysis cycles and the gating of CFTR Cl- channels. *Acta Physiol Scand Suppl* 643: 247-56.

35. Gadsby, D. C., Hwang, T. C., Baukrowitz, T., Nagel, G., Horie, M., Nairn, A. C. 1994. Regulation of CFTR channel gating. *Jpn J Physiol* 44: S183-92.

36. Gao, M., Cui, H. R., Loe, D. W., Grant, C. E., Almquist, K. C., Cole, S. P., Deeley, R. G. 2000. Comparison of the functional characteristics of the nucleotide binding domains of multidrug resistance protein 1. *J Biol Chem* 275: 13098-108.

37. Glossmann, H., Ferry, D. R., Goll, A., Rombusch, M. 1984. Molecular pharmacology of the calcium channel, evidence for sub-types, multiple drug receptor sites, channel sub-units, and the development of a radioiodinated 1,4-dihydropyridine calcium channel label, [^{125}I]Iodipine. *J. Cardiovascular Pharmacology* 6: S608-S621

38. Glossmann, H., Ferry, D. R., Striessnig, J., Goll, A., Moosburger, K. 1987. Resolving the structure of the Ca^{2+} channel by photoaffinity labeling. *TIPS* 8: 95-100

39. Goodno, C. C. 1982. Myosin active site trapping with vanadate ion. *Methods Enzymol.* 85: 116-123

40. Gorbulev, S., Abele, R., Tampe, R. 2001. Allosteric crosstalk between peptide-binding, transport, and ATP hydrolysis of the ABC transporter TAP. *Proc Natl Acad Sci U S A* 98: 3732-7.

41. Gottesman, M. M., Pastan, I. 1993. Biochemistry of multidrug resistance by the multidrug transporter. *Ann. Rev. Biochem.* 62: 385-427

42. Greenberger, L. M. 1993. Major photoaffinity labeling sites for iodoaryl azidoprazosin in P-glycoprotein are within or immediately C-terminal to transmembrane domains 6 and 12. *J Biol. Chem.* 268: 11417-11425

43. Grogan, T. M., Spier, C. M., Salmon, S. E., Matzner, M., Rybski, J., Weinstein, R. S., Scheper, R. J., Dalton, W. S. 1993. P-glycoprotein expression in human plasma cell myeloma: correlation with prior chemotherapy. *Blood* 81 (2): 490-495

44. Gros, P., Croop, J., Houseman, D. E. 1986. Mammalian multidrug resistance gene: complete cDNA sequence indicates stong homology to bacterial transport proteins. *Cell* 47: 371-380

45. Gros, P., Dhir, R., Croop, J., Talbot, F. 1991. A single amino acid substitution strongly modulates the activity and substrate specificity of the mouse mdr1 and mdr3 drug efflux pumps. *Proc Natl Acad Sci U S A* 88: 7289-93.

46. Hanna, M., Brault, M., Kwan, T., Kast, C., Gros, P. 1996. Mutagenesis of transmembrane domain 11 of P-glycoprotein by alanine scanning. *Biochemistry* 35: 3625-35.

47. Higgins, C. F. 1992. ABC transporters; from microorganisms to man. *Annu. Rev. Cell. Biol.* 8: 67-113

48. Higgins, C. F., Gottesman, M. M. 1992. Is the multidrug transporter a flippase? *Trends in Biochem. Sci.* 17: 18-21

49. Holland, I. B., Blight, M. A. 1999. ABC-ATPases, adaptable energy generators fuelling transmembrane movement of a variety of molecules in organisms from bacteria to humans. *J Mol Biol* 293: 381-99.

50. Homolya, L., Hollo, Z., Germann, U., Pastan, I., Gottesman, M. M. 1993. Fluorescent cellular indicators are extruded by the multidrug resistance protein. *J. Biol. Chem.* 268: 21493-21496

51. Hoof, T., Demmer, A., Hadam, M. R., Riordan, J. R., Tummler, B. 1994. Cystic fibrosis-type mutational analysis in the ATP-binding cassette transporter signature of human P-glycoprotein MDR1. *J Biol Chem* 269: 20575-83.

52. Hopfner, K. P., Karcher, A., Shin, D. S., Craig, L., Arthur, L. M., Carney, J. P., Tainer, J. A. 2000. Structural biology of Rad50 ATPase: ATP-driven conformational control in DNA double-strand break repair and the ABC-ATPase superfamily. *Cell* 101: 789-800.

53. Hou, Y., Cui, L., Riordan, J. R., Chang, X. 2000. Allosteric interactions between the two non-equivalent nucleotide binding domains of multidrug resistance protein MRP1. *J Biol Chem* 275: 20280-7.

54. Hrycyna, C. A., Ramachandra, M., Ambudkar, S. V., Ko, Y. H., Pedersen, P. L., Pastan, I., Gottesman, M. M. 1998. Mechanism of action of human P-glycoprotein ATPase activity. Photochemical cleavage during a catalytic transition state using orthovanadate reveals cross-talk between the two ATP sites. *J Biol Chem* 273: 16631-4.

55. Hrycyna, C. A., Ramachandra, M., Germann, U. A., Cheng, P. W., Pastan, I., Gottesman, M. M. 1999. Both ATP sites of human P-glycoprotein are essential but not symmetric. *Biochemistry* 38: 13887-99.

56. Hung, L.-W., Wang, I. X., Nikaido, K., Ardeshir, F., Garcia, G., Ames, G. F.-L. 1998. Crystal structure of the ATP-binding subunit of an ABC transporter. *Nature* 396: 703-707

57. Hyafil, F., Vergely, C., Du Vignaud, P., Grand-Perret, T. 1993. *In Vitro* and *in Vivo* Reversal of Multidrug Resistance by GF120918, an Acridonecarboxamide Derivative. *Cancer Research* 53: 4595-4602

58. Jones, P. M., George, A. M. 1998. A new structural model for P-glycoprotein. *J Membr Biol* 166: 133-47.

59. Juliano, R. L., Ling, V. 1976. A surface glycoprotein modulating drug permeability in Chinese hamster ovary cell mutants. *Biochim Biophys Acta* 455: 152-62.

60. Julien, M., Gros, P. 2000. Nucleotide-induced conformational changes in P-glycoprotein and in nucleotide binding site mutants monitored by trypsin sensitivity. *Biochemistry* 39: 4559-4568

61. Kajiji, S., Talbot, F., Grizzuti, K., Van Dyke-Phillips, V., Agresti, M., Safa, A. R., Gros, P. 1993. Functional analysis of P-glycoprotein mutants identifies predicted transmembrane domain 11 as a putative drug binding site. *Biochemistry* 32: 4185-94.

62. Kartner, N., Riordan, J. R., Ling, V. 1983. Cell surface P-glycoprotein associated with multidrug resistance in mammalian cell lines. *Science* 221: 1285-8.

63. Kast, C., Canfield, V., Levenson, R., Gros, P. 1995. Membrane topology of P-glycoprotein as determined by epitope insertion: transmembrane organization of the N-terminal domain of mdr3. *Biochemistry* 34: 4402-11.

64. Kast, C., Canfield, V., Levenson, R., Gros, P. 1996. Transmembrane organization of mouse P-glycoprotein determined by epitope insertion and immunofluorescence. *J Biol Chem* 271: 9240-8.

65. Kast, C., Gros, P. 1997. Topology mapping of the amino-terminal half of multidrug resistance-associated protein by epitope insertion and immunofluorescence. *J Biol Chem* 272: 26479-87.

66. Kenakin, T. 1997. *Pharmacologic Analysis of Drug-Receptor Interaction*, p. Chapter 13 page 449: Lippincott-Raven

67. Kerr, K. M., Sauna, Z. E., Ambudkar, S. V. 2001. Correlation between steady-state ATP hydrolysis and vanadate-induced ADP trapping in Human P-glycoprotein. Evidence for ADP release as the rate-limiting step in the catalytic cycle and its modulation by substrates. *J Biol Chem* 276: 8657-64.

68. Krishna, R., Mayer, L. D. 2000. Multidrug resistance (MDR) in cancer. Mechanisms, reversal using modulators of MDR and the role of MDR modulators

in influencing the pharmacokinetics of anticancer drugs. *Eur. J. of Pharm. Sci.* 11: 265-283

69. Krupka, R. M. 1999. Uncoupled active transport mechanisms accounting for low selectivity in multidrug carriers: P-glycoprotein and SMR antiporters. *J Membr Biol* 172: 129-43.

70. Kwan, T., Gros, P. 1998. Mutational analysis of the P-glycoprotein first intracellular loop and flanking transmembrane domains. *Biochemistry* 37: 3337-50.

71. Langmuir, I. 1916. The constitution and fundamental properties of solids and liquids. *J. Am. Chem. Soc.* 38: 2221-2229

72. Larazeno, S., Birdsall, N. J. M. 1993. Estimation of competitive antagonist affinity from functional inhibition curves using the Gaddum, Schild and Cheng-Prusoff equations. *Br. J. Pharmacol.* 109: 1110-1119

73. Ligtenberg, M. J., Kemp, S., Sarde, C. O., van Geel, B. M., Kleijer, W. J., Barth, P. G., Mandel, J. L., van Oost, B. A., Bolhuis, P. A. 1995. Spectrum of mutations in the gene encoding the adrenoleukodystrophy protein. *Am J Hum Genet* 56: 44-50.

74. Liu, R., Sharom, F. J. 1996. Site-directed fluorescence labeling of P-glycoprotein on cysteine residues in the nucleotide binding domains. *Biochemistry* 35: 11865-11873

75. Loo, T. W., Clarke, D. M. 1994. Functional consequences of glycine mutations in the predicted cytoplasmic loops of P-glycoprotein. *J Biol. Chem.* 269: 7243-7248

76. Loo, T. W., Clarke, D. M. 1995. Covalent modification of human P-glycoprotein mutants containing a single cysteine in either nucleotide binding fold abolishes drug stimulated ATPase activity. *J Biol. Chem.* 270: 22957-22961

77. Loo, T. W., Clarke, D. M. 1995. Membrane topology of a cysteine-less mutant of human P-glycoprotein. *J. Biol. Chem.* 270: 843-848

78. Loo, T. W., Clarke, D. M. 1999. Identification of residues in the drug-binding domain of human P-glycoprotein. Analysis of transmembrane segment 11 by cysteine-scanning mutagenesis and inhibition by dibromobimane. *J Biol Chem* 274: 35388-92.

79. Loo, T. W., Clarke, D. M. 2000. Identification of residues within the drug-binding domain of the human multidrug resistance P-glycoprotein by cysteine-scanning mutagenesis and reaction with dibromobimane. *J Biol Chem* 275: 39272-8.

80. Loo, T. W., Clarke, D. M. 2001. Defining the drug-binding site in the human multidrug resistance P-glycoprotein using a methanethiosulfonate analog of verapamil, MTS-verapamil. *J Biol Chem* 276: 14972-9.

81. Lu, P., Liu, R., Sharom, F. J. 2001. Drug transport by reconstituted P-glycoprotein in proteoliposomes. Effect of substrates and modulators, and dependence on bilayer phase state. *Eur J Biochem* 268: 1687-97.

82. Martin, C., Berridge, G., Higgins, C. F., Callaghan, R. 1997. The multi-drug resistance reversal agent SR33557 and modulation of vinca alkaloid binding to P-glycoprotein by an allosteric interaction. *Br. J. Pharmacol.* 122: 765-771

83. Martin, C., Berridge, G., Higgins, C. F., Mistry, P., Charlton, P., Callaghan, R. 2000. Communication between multiple drug binding sites on P-glycoprotein. *Molecular Pharmacol* 58: 624-632

84. Martin, C., Berridge, G., Mistry, P., Higgins, C. F., Charlton, P., Callaghan, R. 1999. The molecular interaction of the high affinity reversal agent XR9576 with P-glycoprotein. *Br. J. Pharmacol.* 128: 403-411

85. Martin, C., Berridge, G., Mistry, P., Higgins, C. F., Charlton, P., Callaghan, R. 2000. Drug binding sites on P-glycoprotein are altered by ATP binding prior to nucleotide hydrolysis. *Biochemistry* 39: 11901-11906

86. Matsuo, M., Tanabe, K., Kioka, N., Amachi, T., Ueda, K. 2000. Different binding properties and affinities for ATP and ADP among sulfonylurea receptor subtypes, SUR1, SUR2A, and SUR2B. *J Biol Chem* 275: 28757-63.

87. Mechetner, E. B., Schott, B., Morse, B. S., Stein, W. D., Druley, T., Davis, K. A., Tsuruo, T., Roninson, I. B. 1997. P-glycoprotein function involves conformational transitions detectable by differential immunoreactivity. *Proc. Natl. Acad. Sci. USA* 94: 12908-12913

88. Mistry, P., Bootle, D., Liddle, C., Loi, R., Templeton, D. 1998. Reversal of P-glycoprotein mediated multidrug resistance *in vivo* by XR9576. *Annals of Oncology* 9: Abstract 568

89. Mistry, P., Stewart, A. J., Dangerfield, W., Okiji, S., Liddle, C., Bootle, D., Plumb, J. A., Templeton, D., Charlton, P. 2001. In vitro and in vivo reversal of P-glycoprotein-mediated multidrug resistance by a novel potent modulator, XR9576. *Cancer Res* 61: 749-58.

90. Molero, X., Miller, L. J. 1991. The gall bladder cholecystokinin receptor exists in two guanine nucleotide-binding protein-regulated affinity states. *Mol Pharmacol* 39: 150-6.

91. Morris, D. I., Greenberger, L. M., Bruggemann, E. P., Cardarelli, C., Gottesman, M. M., Pastan, I., Seamon, K. B. 1994. Localization of the forskolin labeling sites to both halves of P-glycoprotein: similarity of the sites labeled by forskolin and prazosin. *Molecular Pharmacology* 46: 329-337

92. Muller, M., Bakos, E., Welker, E., Varadi, A., Germann, U. A., Gottesman, M. M., Morse, B. S., Roninson, I. B., Sarkadi, B. 1996. Altered drug-stimulated

ATPase activity in mutants of the human multidrug resistance protein. *J Biol Chem* 271: 1877-83.

93. Orlowski, S., Mir, L. M., Belehradek, J., Garrigos, M. 1996. Effects of steroids and verapamil on P-glycoprotein ATPase activity: progesterone, desoxycorticosterone and verapamil are mutually non-exclusive modulators. *Biochem. J.* 317: 515-522

94. Pascaud, C., Garrigos, M., Orlowski, S. 1998. Multidrug resistance transporter P-glycoprotein has distinct but interacting binding sites for cytotoxic drugs and reversing agents. *Biochem. J.* 333: 351-358

95. Passamonti, S., Battiston, L., Sottocasa, G. L. 1998. Bilitranslocase can exist in two metastable forms with different affinities for the substrates--evidence from cysteine and arginine modification. *Eur J Biochem* 253: 84-90.

96. Ramachandra, M., Ambudkar, S. V., Chen, D., Hrycyna, C. A., Dey, S., Gottesman, M. M., Pastan, I. 1998. Human P-glycoprotein exhibits reduced affinity for substrates during a catalytic transition state. *Biochem.* 37: 5010-5019

97. Raviv, Y., Pollard, H. B., Bruggemann, E. P., Pastan, I., Gottesman, M. M. 1990. Photosensitized labeling of a functional multidrug transporter in living drug resistant tumor cells. *J Biol. Chem.* 265: 3975-3980

98. Regev, R., Assaraf, Y. G., Eytan, G. D. 1999. Membrane fluidization by ether, other anesthetics, and certain agents abolishes P-glycoprotein ATPase activity and modulates efflux from multidrug-resistant cells. *Eur. J. Biochem.* 259: 18-24

99. Roepe, P. D. 1995. The role of the MDR protein in altered drug translocation across tumor cell membranes. *Biochim Biophys Acta* 1241: 385-405.

100. Roepe, P. D. 1998. The P-glycoprotein efflux pump: how does it transport drugs? *J Membr Biol* 166: 71-3.

101. Roepe, P. D. 2000. What is the precise role of human MDR 1 protein in chemotherapeutic drug resistance? *Curr Pharm Des* 6: 241-60.

102. Romsicki, Y., Sharom, F. J. 1999. The membrane lipid environment modulates drug interactions with the P-glycoprotein multidrug transporter. *Biochemistry* 38: 6887-96.

103. Rosenberg, M. F., Callaghan, R., Berridge, G., Kerr, I. D., Linton, K. J., Velarde, G., Ford, R. C., Higgins, C. F. 2001. Projection structure of an ABC transporter, the multidrug resistance P-glycoprotein, determined to 10A resolution by electron cryo-microscopy. *EMBO J* submitted

104. Rosenberg, M. F., Callaghan, R., Ford, R. C., Higgins, C. F. 1997. Structure of the multidrug resistance P-glycoprotein to 2.5nm resolution. *J. Biol. Chem.* 272: 10685-10694

105. Rothnie, A. R., Soceneantu, L., Theron, D., Martin, C., Berridge, G., Deveaux, P., Higgins, C. F., Callaghan, R. 2000. The importance of cholesterol to maintain activity of P-glycoprotein and modify its membrane perturbing influence. *Eur. J. Biophys.* Submitted

106. Rovati, G. E. 1998. Ligand-binding studies: old beliefs and new strategies. *TIPS* 19: 365-369

107. Rowinsky, E. K., Smith, L., Wang, Y. M., Chaturvedi, P., Villalona, M., Campbell, E., Aylesworth, C., Eckhardt, S. G., Hammond, L., Kraynak, M., Drengler, R., Stephenson, J., Jr., Harding, M. W., Von Hoff, D. D. 1998. Phase I and pharmacokinetic study of paclitaxel in combination with biricodar, a novel agent that reverses multidrug resistance conferred by overexpression of both MDR1 and MRP. *J Clin Oncol* 16: 2964-76.

108. Ruetz, S., Gros, P. 1994. Phosphatidylcholine translocase: A physiological role for the *mdr2* gene. *Cell* 77: 1071-1081

109. Safa, A. R. 1988. Photoaffinity labelling of the multidrug resistance related P-glycoprotein with photoactive analogs of verapamil. *Proc. Natl. Acad. Sci. USA* 85: 7187-7191

110. Safa, A. R., Stern, R. K., Choi, K., Agresti, M., Tamai, I., Mehta, N. D., Roninson, I. B. 1990. Molecular basis of preferential resistance to colchicine in multidrug resistant human cells conferred by Gly185 - Val185 substitution in P-glycoprotein. *Proc. Natl. Acad. Sci. USA* 87: 7225-7229

111. Sakardi, B., Price, E. M., Boucher, R. C., Germann, U. A., Scarborough, G. A. 1992. Expression of the human multidrug resistance cDNA in insect cells generates a high activity drug stimulated membrane ATPase. *J Biol. Chem.* 267: 4854-4858

112. Sauerbrey, A., Zintl, F., Volm, M. 1994. P-glycoprotein and glutathione-S-transferase p.i. in childhood acute lymphoblastic leukaemia. *Br. J. Cancer* 70 (6): 1144-1149

113. Sauna, Z. E., Ambudkar, S. V. 2000. Evidence for a requirement for ATP hydrolysis at two distinct steps during a single turnover of the catalytic cycle of human P-glycoprotein. *Proc Natl Acad Sci U S A* 97: 2515-20.

114. Sauna, Z. E., Ambudkar, S. V. 2001. Characterization of the catalytic cycle of ATP hydrolysis by human P-glycoprotein. The two ATP hydrolysis events in a single catalytic cycle are kinetically similar but affect different functional outcomes. *J Biol Chem* 276: 11653-61.

115. Sauna, Z. E., Smith, M. M., Muller, M., Ambudkar, S. V. 2001. Functionally similar vanadate-induced 8-azidoadenosine 5'. *J Biol Chem* 276: 21199-208.

116. Saurin, W., Koster, W., Dassa, E. 1994. Bacterial binding protein-dependent permeases: characterization of distinctive signatures for functionally related integral cytoplasmic membrane proteins. *Mol Microbiol* 12: 993-1004.

117. Senior, A. E., Al-Shawi, M. K., Urbatsch, I. L. 1995. The catalytic cycle of P-glycoprotein. *FEBS Letters* 377: 285-289

118. Senior, A. E., Bhagat, S. 1998. P-glycoprotein shows strong catalytic cooperativity between the two nucleotide sites. *Biochemistry* 37: 831-6.

119. Senior, A. E., Gadsby, D. C. 1997. ATP hydrolysis cycles and mechanism in P-glycoprotein and CFTR. *Semin Cancer Biol* 8: 143-50.

120. Senior, A. E., Gros, P., Urbatsch, I. L. 1998. Residues in P-glycoprotein catalytic sites that react with the inhibitor 7-chloro-4-nitrobenzo-2-oxa-1,3-diazole. *Arch. Biochem. Biophys* 357: 121-125

121. Seydel, J. K., Coats, E. A., Cordes, H. P., Wiese, M. 1994. Drug membrane interaction and the importance for drug transport, distribution, accumulation, efficacy and resistance. *Arch Pharm (Weinheim)* 327: 601-10.

122. Shapiro, A. B., Corder, A. B., Ling, V. 1997. P-glycoprotein-mediated Hoechst 33342 transport out of the lipid bilayer. *Eur J Biochem* 250: 115-21.

123. Shapiro, A. B., Fox, K., Lam, P., Ling, V. 1999. Stimulation of P-glycoprotein-mediated drug transport by prazosin and progesterone. Evidence for a third drug-binding site. *Eur J Biochem* 259: 841-50.

124. Shapiro, A. B., Ling, V. 1994. ATPase activity of purified and reconstituted P-glycoprotein from Chinese hamster ovary cells. *J Biol Chem* 269: 3745-54.

125. Shapiro, A. B., Ling, V. 1995. Reconstitution of drug transport by purified P-glycoprotein. *J Biol Chem* 270: 16167-75.

126. Shapiro, A. B., Ling, V. 1997. Extraction of Hoechst 33342 from the cytoplasmic leaflet of the plasma membrane by P-glycoprotein. *Eur J Biochem* 250: 122-9.

127. Shapiro, A. B., Ling, V. 1997. Positively cooperative sites for drug transport by P-glycoprotein with distinct drug specificities. *Eur J Biochem* 250: 130-7.

128. Shapiro, A. B., Ling, V. 1998. Stoichiometry of coupling of rhodamine 123 transport to ATP hydrolysis by P-glycoprotein. *Eur J Biochem* 254: 189-93.

129. Shapiro, A. B., Ling, V. 1998. Stoichiometry of coupling of rhodamine 123 transport to ATP hydrolysis by P-glycoprotein. *European Journal of Biochemistry* 254: 189-193

130. Sharom, F. J. 1997. The P-glycoprotein efflux pump: how does it transport drugs? *J Membr Biol* 160: 161-75.

131. Sharom, F. J., Liu, R., Qu, Q., Romsicki, Y. 2001. Exploring the structure and function of the P-glycoprotein multidrug transporter using fluorescence spectroscopic tools. *Semin Cell Dev Biol* 12: 257-65.

132. Sharom, F. J., Yu, X., Chu, J. W., Doige, C. A. 1995. Characterization of the ATPase activity of P-glycoprotein from multidrug-resistant Chinese hamster ovary cells. *Biochem J* 308: 381-90.

133. Sikic, B. I., Fisher, G. A., Lum, B. L., Halsey, J., Beketic-Oreskovic, L., Chen, G. 1997. Modulation and prevention of multidrug resistance by inhibitors of P-glycoprotein. *Cancer Chemother Pharmacol* 40 (suppl:S13-S19)

134. Smit, J. J. M., Schinkel, A. H., Oude Elferink, R. P. J., Groen, A. K., Wagenaar, E., van Deemter, L., Mol, C. A. A. M., Ottenhoff, R., van der Lugt, N. M. T., van Roon, M. A., van der Valk, M. A., Offerhaus, G. J. A., Berns, A. J. M., Borst, P. 1993. Homozygous disruption of the murine mdr2 P-glycoprotein gene leads to a complete absence of phospholipid from bile and to liver disease. *Cell* 75: 451-462

135. Smith, A. J., van Helvoort, A., van Meer, G., Szabo, K., Welker, E., Szakacs, G., Varadi, A., Sarkadi, B., Borst, P. 2000. MDR3 P-glycoprotein, a phosphatidylcholine translocase, transports several cytotoxic drugs and directly interacts with drugs as judged by interference with nucleotide trapping. *J Biol Chem* 275: 23530-9.

136. Sonnenveld, P., Durie, B. G., Lokhorst, H. M., Frutiger, Y., Schoester, M., Vela, E. E. 1993. Analysis of multidrug-resistance (MDR-1) glycoprotein and CD56 expression to separate monoclonal gammopathy from multiple myeloma. *Br. J. Haematol.* 83 (1): 63-67

137. Sonveaux, N., Shapiro, A. B., Goormaghtigh, E., Ling, V., Ruysschaert, J. M. 1996. Secondary and tertiary structure changes of reconstituted P-glycoprotein. A Fourier transform attenuated total reflection infrared spectroscopy analysis. *J Biol Chem* 271: 24617-24.

138. Sonveaux, N., Vigano, C., Shapiro, A. B., Ling, V., Ruysschaert, J. M. 1999. Ligand-mediated tertiary structure changes of reconstituted P-glycoprotein. A tryptophan fluorescence quenching analysis. *J Biol Chem* 274: 17649-54.

139. Stein, W. D. 1997. Kinetics of the multidrug transporter (P-glycoprotein) and its reversal. *Physiol Rev* 77: 545-90.

140. Stewart, A. J., Mistry, P., Dangerfield, W., Okiji, S., Templeton, D. 1998. XR9576, a potent modulator of P-glycoprotein mediated resistance. *Annals of Oncology* 9: Abstract 556

141. Tamai, I., Safa, A. R. 1990. Competitive interaction of cyclosporins with the Vinca alkaloid-binding site of P-glycoprotein in multidrug-resistant cells. *J Biol Chem* 265: 16509-13.

142. Tamai, I., Safa, A. R. 1991. Azidopine noncompetitively interacts with vinblastine and cyclosporin A binding to P-glycoprotein in multidrug resistant cells. *J Biol. Chem.* 266: 16796-16800

143. Tsuro, T., Iida, H., Tsukagoshi, S., Sakurai, J. 1981. Overcoming of vincristine resistance in P388 leukemia *in vivo* and *in vitro* through enhanced cytotoxicity of vincristine and vinblastine by verapamil. *Cancer Research* 41: 1967-1972

144. Urbatsch, I. L., Al-Shawi, M. K., Senior, A. E. 1994. Characterization of the ATPase activity of purified Chinese Hamster P-glycoprotein. *Biochemistry* 33: 7069-7076

145. Urbatsch, I. L., Beaudet, L., Carrier, I., Gros, P. 1998. Mutations in either nucleotide binding site of P-glycoprotein (Mdr3) prevent vanadate trapping of nucleotide at both sites. *Biochemistry* 37: 4592-4602

146. Urbatsch, I. L., Sankaran, B., Bhagat, S., Senior, A. E. 1995. Both P-glycoprotein nucleotide binding sites are catalytically active. *J Biol. Chem.* 270: 26956-26961

147. Urbatsch, I. L., Sankaran, B., Weber, J., Senior, A. E. 1995. P-glycoprotein is stably inhibited by vanadate induced trapping of nucleotide at a single catalytic site. *J. Biol. Chem.* 270: 19383-19390

148. Urbatsch, I. L., Senior, A. E. 1995. Effects of lipids on ATPase activity of purified Chinese hamster P-glycoprotein. *Arch Biochem Biophys* 316: 135-40.

149. van den Heuvel-Eibrink, M. M., Sonneveld, P., Pieters, R. 2000. The prognostic significance of membrane transport-associated multidrug resistance (MDR) proteins in leukemia. *Int. J. Clin. Pharmacol. Ther.* 38 (3): 94-110

150. van Helvoort, A., Smith, A. J., Sprong, H., Fritzsche, I., Schinkel, A. H., Borst, P., van Meer, G. 1996. MDR1 P-glycoprotein is a lipid translocase of broad specificity, while MDR3 P-glycoprotein specifically translocates phosphatidylcholine. *Cell* 87: 507-17.

151. Van Veen, H. W., Konings, W. N. 1997. Multidrug transporters from bacteria to man: similarities in structure and function. *Seminars in Cancer Biol.* 8: 183-191

152. Van Veen, H. W., Margolles, A., Muller, M., Higgins, C. F., Konings, W. N. 2000. The homodimeric ATP Binding Cassette transporter LmrA mediates multidrug transport by an alternating (two cylinder engine) mechanism. *EMBO J.* 19: 2503-2514

153. Walker, J. E., Runswick, M. J., Saraste, M. 1982. Subunit equivalence in Escherichia coli and bovine heart mitochondrial F1F0 ATPases. *FEBS Lett* 146: 393-6.

154. Wang, G., Pincheira, R., Zhang, M., Zhang, J.-T. 1997. Conformational changes of P-glycoprotein by nucleotide binding. *Biochemical Journal* 328: 897-904

155. Woodhouse, J. R. 1998. In *The pharmacology of P-glycoprotein mediated multidrug resistance*. Birmingham: University of Birmingham

156. Xie, J., Drumm, M. L., Ma, J., Davis, P. B. 1995. Intracellular loop between transmembrane segments IV and V of cystic fibrosis transmembrane conductance regulator is involved in regulation of chloride channel conductance state. *J Biol Chem* 270: 28084-91.

157. Zhang, J. T., Ling, V. 1993. Membrane orientation of transmembrane segments 11 and 12 of MDR- and non-MDR-associated P-glycoproteins. *Biochim Biophys Acta* 1153: 191-202.

158. Zhang, W., Ling, V. 2000. Cell-cycle-dependent turnover of P-glycoprotein in multidrug-resistant cells. *J Cell Physiol* 184: 17-26.

159. Zheleznova, E. E., Markham, P. N., Neyfakh, A. A., Brennan, R. G. 1999. Structural basis of multidrug recognition by BmrR, a transcription activator of a multidrug transporter. *Cell* 96: 353-62.

160. Zhou, D. C., Hoang-Ngoc, L., Delmer, A., Fausset, A. M., Russo, D., Zittoun, R., Marie, J. P. 1994. Expression of resistance genes in acute leukemia. *Leukem. Lymphoma.* 13 (Suppl 1:27-30): 27-30